Universidade de Aveiro Departamento de Engenharia Civil
Ano 2016

SANDRA MARISA SILVA COSTA

Sedimentos em suspensão na Ria de Aveiro: Dinâmica atual e futura

Suspended sediments in Ria de Aveiro: Present and future dynamics

Dissertação apresentada à Universidade de Aveiro para cumprimento dos requisitos necessários à obtenção do grau de Doutor em Engenharia Civil, realizada sob a orientação científica do Doutor Carlos Daniel Borges Coelho, Professor Auxiliar do Departamento de Engenharia Civil da Universidade de Aveiro, do Doutor Luís Ivens Ferraz Saavedra Portela, Investigador Auxiliar do Laboratório Nacional de Engenharia Civil e do Doutor João Miguel Sequeira Silva Dias, Professor Auxiliar com Agregação do Departamento de Física da Universidade de Aveiro.

O autor foi financiado pela Fundação para a Ciência e a Tecnologia através da bolsa de doutoramento SFRH/BD/77599/2011, no âmbito do Quadro de Referência Estratégico Nacional (QREN) e do Programa Operacional de Potencial Humano (POPH), comparticipado pelo Fundo Social Europeu.

Dedico este trabalho à memória dos meus avós António e Adélia.

o júri/ the jury

president/ president

Doutora Ana Isabel Couto Neto da Silva Miranda
Professora Catedrática, Universidade de Aveiro

vogais/examiners committee

Doutor António Alexandre Trigo Teixeira
Professor Associado, Instituto Superior Técnico, Universidade de Lisboa

Doutora Maria Isabel Rola Abrantes
Professora Coordenadora, Escola Superior de Educação de Viseu

Doutor João Miguel Sequeira Silva Dias
Professor Auxiliar com Agregação, Universidade de Aveiro

Doutora Inês Osório de Castro Meireles
Professora Auxiliar, Universidade de Aveiro

Doutor Carlos Daniel Borges Coelho
Professor Auxiliar, Universidade de Aveiro

Doutora Paula Maria dos Santos Freire
Investigadora Auxiliar, Laboratório Nacional de Engenharia Civil

Doutor Paulo Miguel Chambel Filipe Lopes Teles Leitão
Consultor, Hidromod – Modelação e Engenharia Lda.

acknowledgments

This work was supported by the FCT - Fundação para a Ciência e a Tecnologia through a PhD grant - SFRH/BD/77599/2011.

In the first place, a special thanks to my supervisors Professor Carlos Coelho, Luís Portela and João Miguel Dias for the scientific support and their criticism and encouragement during this work.

To the Aveiro harbour Administration, especially to Eng. Carla Garrido, for the support and provided information, essential for the development of the work, and to the Ria Azul boat crew, for their support in the field campaigns.

To the LAGOONS and BioChangeR project teams for the fluvial discharges and suspended sediment concentrations data provided.

To Fernando Brito by his support and help in carrying out the laboratory tests at Estuaries and Coastal Zones Division – National Laboratory of Civil Engineering.

To my colleagues from the Estuarine and Coastal Modeling Division of University of Aveiro, especially Carina Lopes, Nuno Vaz, João Rodrigues, Magda Sousa and Leandro Vaz by the way they welcomed me, and helped to overcome my numerical modelling difficulties.

To Ana Picado, I have no words to thank her help, support and encouragement!

To my colleagues Carla Pereira and Ana Dinis from the Civil Engineering Department by good daily mood, having been essential to face each day with a big smile!

To my family and friends which always supported me in the difficult times!

A special thanks to my mother and Paulo, by the love and words of encouragement.

To all my thank you!

palavras-chave

Sedimentos coesivos, Concentração, Levantamentos batimétricos, Velocidade de queda, Modelação numérica, Ações antropogénicas, Alterações climáticas.

resumo

Ao longo do tempo a Ria de Aveiro foi sujeita a modificações geomorfológicas, resultantes da combinação de ações naturais e humanas, que levaram a alterações na dinâmica da maré, e consequentemente no balanço sedimentar e no seu potencial para exportar os sedimentos. Desta forma, o objetivo deste trabalho é avaliar a influência de alterações climáticas e humanas futuras na dinâmica dos sedimentos em suspensão na Ria de Aveiro. A metodologia seguida foi a análise da evolução passada dos caudais em suspensão do rio Vouga, com recurso a curvas de caudal sólido em suspensão, e da evolução morfológica da área portuária e entrada dos principais canais, através de levantamentos batimétricos, entre 2001 e 2012. Adicionalmente analisou-se a influência da salinidade e da concentração inicial na velocidade de queda dos sedimentos finos, através de ensaios em coluna de sedimentação. Foi também implementado e validado um modelo de transporte de sedimentos em suspensão para a Ria de Aveiro. A sua validação foi efetuada através da comparação das previsões numéricas com dados *in situ* da concentração de sedimentos em suspensão. Esta implementação foi usada para investigar a evolução do transporte sedimentar em suspensão do passado (1987/88) para o presente (2012), tendo ainda sido usada no estudo da influência de ações antropogénicas e alterações climáticas. Os resultados evidenciaram que o caudal em suspensão do rio Vouga apresentou uma tendência de decréscimo no passado. A área portuária e a entrada dos principais canais apresentaram um aprofundamento devido às operações de dragagem realizadas decorrentes das obras de expansão do Porto de Aveiro. Ensaios laboratoriais em coluna de sedimentação mostraram que a velocidade de queda é influenciada pela salinidade, concentração inicial e dimensão das partículas. O modelo numérico implementado reproduz satisfatoriamente a dinâmica dos sedimentos em suspensão na Ria de Aveiro. Os resultados da modelação revelaram que o aprofundamento dos canais verificado desde o passado até ao presente intensificou os fluxos sedimentares. As operações de dragagem planeadas no futuro nos canais de Mira e Ílhavo poderão levar ao aumento do transporte sedimentar nestes canais, sobretudo no de Ílhavo. A redução do caudal do rio Vouga devido à barragem de Ribeiradio-Ermida poderá levar à acentuada diminuição dos fluxos sedimentares em todos os canais. O efeito das alterações climáticas nos caudais fluviais acentuará a assimetria sazonal, sendo esperado o aumento/diminuição do transporte sedimentar em condições de caudal máximo/médio. Em oposição, a subida do nível médio do mar (NMM) poderá conduzir à intensificação dos fluxos sedimentares em todos os canais. A combinação do efeito das alterações climáticas nos caudais fluviais com a subida do NMM apresenta as mesmas tendências observadas para o cenário de alterações nos caudais fluviais, mas com menores diferenças relativamente ao presente, em condições de caudal máximo e médio. Por outro lado, em condições de caudal mínimo são esperadas as mesmas tendências previstas nos cenários de subida do NMM, mas com maiores diferenças relativamente ao presente.

keywords

Fine sediment, Concentration, Bathymetric data, Settling velocity, Numerical modelling, Anthropogenic actions, Climate change effects.

abstract

Over time, Ria de Aveiro has experienced geomorphological changes, result of natural and anthropogenic pressures, which have led to changes in tidal dynamics. Tidal changes influence the lagoon sediment budgets and modify its potential to export sediments. Therefore, the main aim of this work is to study the influence of future anthropogenic actions and climatic change effects on the lagoon suspended sediment transport. The methodology followed was the analysis of the evolution of the Vouga river suspended sediment load, by the application of sediment rating curves, and the morphodynamic characterization of the harbour area and the main lagoon channels downstream areas, through bathymetric data. In addition, the influence of salinity and initial suspended sediment concentration on the settling velocity of fine sediments was examined, through tests performed in a settling column. Afterwards, a suspended sediment numerical model was implemented and validated for the study area. Validation was performed through the comparison of numerical predictions with observations of suspended sediment concentrations (SSC). This implementation was then used to investigate the evolution of suspended sediment transport from past (1987/88) to present (2012) conditions and the influence of future anthropogenic actions and climate change effects on suspended sediment dynamics. Results indicate that suspended sediment loads in the Vouga river have shown a decreasing trend in the past. The harbour area and the main lagoon channels have experienced deepening, mainly associated to dredging operations. Experiments with the settling column showed that the settling velocity of fine sediments is influenced by salinity, initial concentration and particle size. The numerical model showed the capability to reproduce accurately the SSC of the study area. The modelling results reveal that the deepening of the main lagoon channels has led to suspended sediment transport increase. Regarding future anthropogenic actions, planned dredging operations at Mira and Ílhavo channels will have higher impact at Ílhavo channel, with an increase in the sediment fluxes being expected. The reduction of the Vouga river discharge and suspended sediment loads due to the construction of Ribeiradio-Ermida dam, is expected to decrease suspended sediment fluxes at all main lagoon channels, with higher impact for mean fluvial discharge conditions. Climate change effects on fluvial discharges will accentuate the seasonal asymmetry, with an increase/decrease in sediment fluxes being predicted at the main lagoon channels for high/mean and low fluvial discharge conditions. For mean sea level rise (MSLR) scenarios an intensification of sediment fluxes is predicted at the main channels. On the other hand, for a combination of climate change effects on fluvial discharges and MSL, the trends found for climate change effects on fluvial discharges are expected to be reduced for high and mean fluvial discharge conditions. Finally, for low fluvial discharge conditions suspended sediment is expected to decrease as predicted for MSLR, but with higher differences comparing to the present lagoon conditions.

Contents

List of Figures

List of Tables

List of Symbols

A_j	Cross sectional area at location *j*
C	Suspended sediment concentration
C^t	Vertically averaged concentration of suspended sediment at time *t*
C^{t+1}	Vertically averaged concentration of suspended sediment at time *t+1*
C_D	Bottom drag coefficient
C_{pi}	Predicted suspended sediment load
C_{ei}	Estimated suspended sediment load
d_{10}	Diameter for which 10% of the particles in the sediment sample are finer
d_{50}	Diameter for which 50% of the particles in the sediment sample are finer
d_{90}	Diameter for which 90% of the particles in the sediment sample are finer
D	Deposition rate
E	Erosion rate
g	Gravity
h	Water depth
H	Height of the water column
H^t	Height of the water column after sample collection at time *t*
H_{min}	Minimum height
K_1, K_2	Parameters depend on sediment mineralogy
m_1, m_2	Parameters depend on sediment size and shape
M_D	Mass deposited
M_E	Mass eroded
n	Manning coefficient
p_{atm}	Atmospheric pressure
q	Water flux
q_{sj}	Suspended sediment flux at vertical profile *j*
q_s	Suspended sediment flux
Q	River water discharge
Q_s	River sediment load
R_i	Discrepancy ratio
$\overline{R}$	Mean discrepancy ratio

S	Salinity
t	Time
v_j	Velocity projected in the channel direction at location j
w_s	Settling velocity
w_s^n	Vertically averaged settling velocity
w_{50}	Median settling velocity
x_i	Cartesian directions
z	Vertical coordinate
Δt	Time interval
ε	Diffusion coefficients
τ	Bed shear stress
τ_D	Critical bed shear stress for deposition
τ_E	Critical bed shear stress for erosion
u_i	Velocity vector components
η	Free surface level
υ	Turbulent viscosity
ρ	Specific mass
ρ'	Specific mass anomaly
ρ_0	Reference specific mass
$\rho(\eta)$	Specific mass at free surface
Ω	Earth's velocity of rotation
ε	Alternate tensor
$\breve{\xi}_p(t)$	Predicted value
$\breve{\xi}_o(t)$	Observed value

List of Acronyms

APA	Aveiro Harbour Administration
BD	Bathymetric differences volume
CD	Chart datum
CFP	Coastal fishing port
DV	Dredged volume
EC	Espinheiro channel
GIS	Geographic Information System
HFP	High-sea fishing port
IH	Hydrographic Institute of Portuguese Navy
INE	Statistics of Portugal
IST	Instituto Superior Técnico
LBT	Liquid bulk terminal
LNEC	National Laboratory of Civil Engineering
MARETEC	Marine and Environmental Technology Research Center
MC	Main channel
MSL	Mean sea level
MSLR	Mean sea level rise
NB	Net balance volume
NT	North terminal
PIK	Potsdam Institute for Climate Impact Research
RE	Relative error
RMSE	Root mean squared error
SJAB	S. Jacinto air base
SJC	S. Jacinto channel
SNIRH	National Information System of Water Resources
SRC	Sediment rating curves
SSC	Suspended sediment concentration
ST	South terminal
SWIM	Soil and Water Integrated Model
Vel.	Velocity magnitude

1D	One dimensional
2D	Two dimensional
3D	Three dimensional

1 Introduction

1.1 Motivation

Estuaries and coastal lagoons are present in many coastal areas worldwide. They are important to mankind as places of navigation, recreation and commerce, as well as unique marine environments that support highly productive ecosystems (Morton *et al.*, 2000; Karunaratha *et al.*, 2008; Beer and Joyce, 2013). Generally, these ecosystems present a significant percentage of cohesive sediments, which are mixtures of fine sediment fractions and in contrast to non-cohesive sediments are transported mainly in suspension (Soulsby *et al.*, 2013).

Suspended sediment transport can induce economic problems, since suspended sediments movement may cause siltation at harbour docks and navigation channels, creating difficulties for local port facilities that require safe and navigable channels, leading to expensive dredging operations (Soulsby *et al.*, 2013; Shen and Maa, 2015). Cohesive sediments may carry adsorbed heavy minerals and contaminants, making their management more complex, especially at industrialized areas (Pereira *et al.*, 1998; Pereira *et al.*, 2009; Martins *et al.*, 2015). Heavy metals, mineral oils and other toxic contaminants may be adsorbed into fine sediments, and thus be available for resuspension by strong tidal currents and dredging

operations. Desorption of the contaminants and nutrients can have a significant impact in the ecological balance. Furthermore, high suspended sediment concentrations inhibit photosynthesis since they attenuate sunlight penetration into water column (Leupi *et al.*, 2008). Therefore, suspended sediment dynamics plays a major role in the biomass primary productivity, biogeochemical cycling and pollutant transfer at coastal systems, being determinant for local water quality (Cancino and Neves, 1999; Lopes *et al.*, 2006; Son Le *et al.*, 2006; Chao *et al.*, 2008; Volpe *et al.*, 2011).

Ria de Aveiro is located in the north-western Portuguese coast (Figure 1.1). This ecosystem is of enormous social-economical value to the surrounding area, by the services that it provides for the population, which includes nutrient retention, fisheries resources, habitat and food resources for terrestrial, aquatic and marine fauna, biomass and biodiversity, and recreation and tourism services.

Ria de Aveiro bottom sediments present a high local variability, being a mixture of sand (2-90%), silt (10-80%) and clay (0-30%) (Abrantes, 2005; Lopes *et al.*, 2006). Sediments where clay fraction varies in the range 5-10% present cohesive properties (van Ledden *et al.*, 2004). Surface and near-surface Ria de Aveiro bottom sediments trap relatively large quantities of metals partially adsorbed (*e.g. Cu*, *Pb*, *Co*, *Ni*, *Cd*, *Zn*, *Fe*, *Mn* and *Cr*), particularly on silty and clayey particles (Rocha *et al.*, 2005).

Moreover, in the lagoon is located the Aveiro harbour, which is one of major Portuguese seaports. Harbour facilities occupy the inlet area, which for several years was subjected to major modifications, as a consequence of the port development and expansion. The artificial opening of the inlet in 1808 was decisive to the actual lagoon configuration. Several studies have showed that changes in the inlet characteristics followed the deepening of navigation channels had an impact on the local tidal dynamics, with tidal amplitude and prism increase (Araújo *et al.*, 2008; Dias and Mariano, 2011; Dias and Picado, 2011).

Moreover, Ria de Aveiro is one of the Portuguese coastal regions that is forecasted to be most affected by mean sea level rise (MSLR). Some studies have evaluated MSLR influence in the lagoon hydrodynamics and have concluded that it will lead to residual circulation and tidal wave distortion decrease and tidal prism, tidal asymmetry, currents and fluxes between the lagoon and ocean increase (Silva and Duck, 2001; Lopes *et al.*, 2011; Valentim *et al.*, 2013; Lopes and Dias, 2014, 2015).

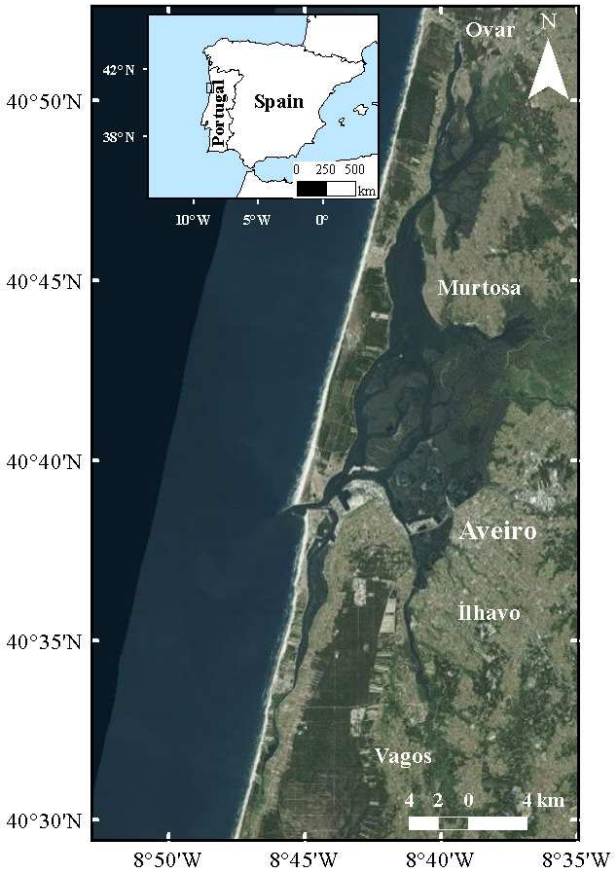

Figure 1.1: Ria de Aveiro location.

The substantial changes that have taken place in the Ria de Aveiro during its history, result of a combination of natural processes and human activities, has led to morphological and hydrodynamic changes. It is also expected that this ecosystem will be affect by climate change effects. Thus, is fundamental to investigate the suspended sediment transport evolution from the past to present and the influence of future anthropogenic actions and climate change effects in the lagoon suspended sediment dynamics, in order to contribute for the preparation of future scenarios. To achieve these goals, was defined a methodology based on the application of the suspended sediment transport numerical model MOHID to Ria de Aveiro. The modelling results will help in the understanding the main trends and to answer several questions: Is the present suspended sediment transport at main lagoon channels different from the observed in the past? How different would be if dredging operations at harbour area were not performed? Other questions can also be answered, such as: Dredging operations planned in the frame of Polis Litoral Ria de Aveiro/CIRA Actions and Ribeiradio-Ermida dam construction in Vouga river, will have a significant impact in

the main lagoon channels sediment fluxes? Do climate change effects influence the sediment fluxes and its direction at main lagoon channels? Climate change effects will have a greater influence in the sediment fluxes, due to changes in river discharges or do to MSLR at the inlet? To try answer these questions, specific goals were defined and a methodological approach based on numerical simulation of different scenarios was carried out.

1.2 Aims

As outlined in the previous section, the main aim of this work is to understand the Ria de Aveiro suspended sediment transport, its evolution from the past to present and how future changes, due to anthropogenic actions and climatic changes, may influence the lagoon suspended sediment dynamics and its potential to export sediments. In particular, the present work objectives are to:

- Characterize the past evolution of the Vouga drainage basin suspended sediment loads;
- Characterize the bottom sediment distribution and SSC evolution in the lower reach of the main lagoon channels;
- Understand the morphological trends of the inlet and the downstream areas of the main lagoon channels;
- Identify parameters that may influence the settling of fine sediments from the Ria de Aveiro, such as salinity and initial suspended sediment concentration;
- Implement and validate the numerical model MOHID, in order to simulate suspended sediment transport in the Ria de Aveiro;
- Investigate the changes on lagoon suspended sediment transport from the past (1987/88) to present (2012);
- Assess the influence of future changes, namely regarding the lagoon morphology and ocean and river forcing, on the suspended sediment dynamics and lagoon's potential to export sediments.

1.3 Literature review

1.3.1 Suspended sediment transport in estuaries and lagoons

Cohesive sediments, unlike non-cohesive sediments well characterized by their grain size distribution, are a complex mixture of clay and silt particles and organic matter (Shrestha, 1996; Cancino and Neves, 1999). Cohesive sediment transport is not predictable based on an easily measurable parameter (*e.g.* grain size) and can depend on the interactions between physical sediment properties and biological processes (Schaaff *et al.*, 2006; Ravens and Sindelar, 2008). In a suspension, the property that distinguishes both type of sediments is the cohesion, which leads to the approximation of the particles and the formation of flocs (flocculation). Other important property is the consolidation process of the layers of deposited particles (Parchure and Metha, 1985; Burban *et al.*, 1989; Metha *et al.*, 1989; Burban *et al.*, 1990).

The basic processes involved in suspended sediment transport are flocculation, deposition and erosion, which have been studied by many researches (*e.g.* Krone, 1962; Parteniades, 1965; Nicholson and O'Connor, 1986; Burban *et al.*, 1990; van Leussen, 1999; Winterwerp, 2002; You, 2004; Baugh and Manning, 2007).

Sedimentation processes in estuaries and lagoons are complex, since sediment particles from rivers are discharged in these coastal systems and then transported and dispersed offshore to deep waters (Jing and Ridd, 1997). In estuaries and lagoons, the suspended sediment transport depends primarily on the sediment availability, which includes river and sometimes marine sources, and the water movement induced by the tide, fluvial discharges and waves, generated by the wind (Abrantes, 2005). However, suspended sediment concentrations driven by river discharges and tides can be changed, sometimes drastically, by meteorological forcing such as storms and rainfall (Moskalski and Torres, 2012).

Hydrodynamic action is the most important mechanism involved in the fine sediment transport (Xie *et al.*, 2013). Fine sediments are eroded and transported upwards during flood, deposited during slack water, eroded again and transported downwards during ebb and re-deposited during next slack water, to restart their movement in the next tidal cycle (Cancino and Neves, 1999).

1.3.2 Suspended sediment dynamics numerical modelling

Understanding the suspended sediment transport processes has been a subject of interest to scientists and engineers for many years. Accurate predictions of suspended sediment transport in coastal areas and knowledge of reliable and space-distributed suspended sediment concentrations from observations, gives the necessary conditions for the definition and development of effective and quantitative monitoring schemes, which are of vital importance in environmental management (Liu *et al.*, 2002; Lin and Namin, 2005). Suspended sediment transport in coastal areas is of great interest, but difficult to forecast (Lumborg and Windelin, 2003). In recent years, major efforts have been made to implement the suspended sediment transport complex mechanisms into numerical models, due to its great potential, including its integration in biogeochemical process models and ultimately into coastal water quality and ecological models (Lopes *et al.*, 2006).

The implementation of suspended sediment transport in numerical models has started in the 1970's (Teisson, 1991). Models can range from zero dimensional to sophisticated 3D models. The simplest model, the zero dimensional, is based on the sediment conservation equation that represents the mass balance between sediment inflows, outflows and deposition. The spatial variability of the sediment properties is ignored. In more complex models, the governing equation is based on the mass conservation principle in 1D, 2D or 3D, with boundary conditions of no sediment flux at the free surface, and net erosional or depositional flux at the sediment–water interface (Shrestha and Blumberg, 2005).

Suspended sediment transport models use an advection-diffusion equation for the mass conservation of suspended sediments, taking into account the bottom exchanges by resuspension and deposition. In 3D models, the advection of the particles results of the addition of local velocity and fall velocity under the gravity (Douillet *et al.*, 2001). The suspended sediment transport predictions accuracy is dependent on flow field precision, since the advection-diffusion equation requires the flow velocity components and erosion and deposition formulations depend on the specification of bottom stress. Therefore, understanding the hydrodynamic circulation processes is essential, and consequently suspended sediment transport models are generally coupled to hydrodynamic models. In this case both models operate within the same computational framework in conjunction with each other, with outputs from one serving as inputs to another (Shrestha and Blumberg, 2005).

Sediment processes embedded in the numerical models generally include flocculation, deposition, consolidation and resuspension of sediments. Flocculation is generally embedded in the settling velocity formulation, and is usually described as a function of the sediment concentration. Consolidation is considered discretizing the bottom in layers, where for each layer is given a certain thickness, density and critical shear stress for erosion (Shrestha and Blumberg, 2005). Most of suspended sediment transport models describe the erosion and deposition processes by the classical approaches of Partheniades (1965) and Krone (1962), respectively. Although, some improvements and adaptations or even new formulations have been developed and applied.

Several studies worldwide have applied numerical models to simulate suspended sediment dynamics in coastal waters (estuaries, lagoons and bays) and lakes and estimate the effects of dredging operations in ports, building of dams, discharging environmental pollutants, MSLR, etc. (*e.g.* Portela and Neves, 1994; Cancino and Neves, 1994, 1999; Doulliet *et al.*, 2001; Liu *et al.*, 2002; Lumborg and Windelin, 2003; Temmerman *et al.*, 2003; Lopes *et al.*, 2006; Liu, 2007; Chao *et al.*, 2008; Etemad-Shahidi *et al.*, 2010; Hu *et al.*, 2011; Rao *et al.*, 2011; Benkhaldoun *et al.*, 2012; Xie *et al.*, 2013; Chen *et al.*, 2015; Mayerle *et al.*, 2015).

1.3.3 Ria de Aveiro suspended sediment dynamics

Suspended sediment dynamics in the Ria de Aveiro was previously studied based on observations (Silva, 1994; Lopes *et al.*, 2006; Martins *et al.*, 2009, 2011; Portela *et al.*, 2011), in the application of numerical models, previously validated and calibrated (Lopes *et al.*, 2001, 2006; Dias *et al.*, 2001, 2003, 2007; Lopes and Dias, 2007; Picado *et al.*, 2011a; Plecha *et al.*, 2014), and in combination of both methodologies, using *in situ* measurements and numerical results (Lopes *et al.*, 2001; Abrantes *et al.*, 2006).

Suspended sediment transport is governed essentially by the tide, with the suspended concentration following the tidal cycle and therefore presenting semi-diurnal variations and fortnightly patterns, related with spring and neap tide conditions (Dias *et al.*, 2003; Lopes *et al.*, 2006; Plecha *et al.*, 2014). Suspended sediment concentrations in Ria de Aveiro present also seasonal variability, with higher values in winter, possible related with higher fluvial discharges, wind climate, biological activity and coastal wave regime (Dias *et al.*, 2003, 2007; Abrantes *et al.*, 2006; Lopes and Dias, 2007).

Despite tidal currents are considered the main forcing in the suspended sediment transport, fluvial discharges have also an important influence on the suspended sediment transport. Residual currents induced by rivers are believe to contribute to the net exportation of sediments seaward, and can present a significant increase during the winter (Lopes and Dias, 2007). Moreover, at spring tide and during ebb, strong currents are able to mobilize a large volume of sediments at the river's mouth areas, which are transported towards the inlet (Dias *et al.*, 2003; Lopes *et al.*, 2006). Wind shear stress can also increase the suspended sediment advection, when is in phase with the tide currents (Lopes *et al.*, 2006).

Suspended sediment concentrations variations along the lagoon are believed to be mainly determined by tidal currents and characteristics of bottom sediments. Therefore, higher concentrations are observed at spring tide and during ebb period, due to the stronger currents (Abrantes *et al.*, 2006). In the areas near the river's mouth and along the main channels, higher suspended sediment concentrations are due to the river discharges and a combination of high current velocities and shallow areas (Lopes *et al.*, 2001). On the other hand, minimum concentrations are observed in the inlet and nearby areas, which are deeper areas with high velocities but with a sandy bed (Lopes *et al.*, 2001; Abrantes *et al.*, 2006; Plecha *et al.*, 2014). However, high coastal wave energetic conditions associated with north winds can induced high resuspension of the coastal particles, especially in neap tides and more sediments supply the lagoon during the flood period (Abrantes *et al.*, 2006).

Numerical particle tracking models were also used in the study of suspended sediment transport, which have indicated an increase of the residence time along the lagoon channels towards upstream areas. Suspended particles at the end of the channels experience a high residence time (predicted to be more than 2 weeks), and are more likely to remain there and deposit. In opposition, in the lagoon central area, particles have a low residence time (predicted to be 2-3 days) and tend to be rapidly exported to the ocean (Dias *et al.*, 2001, 2003, 2007; Lopes and Dias, 2007; Picado *et al.*, 2011a). These findings are in agreement with tidal asymmetry increase from the lagoon mouth to the upstream areas and the residual currents weaken towards upstream areas (Dias *et al.*, 2003; Lopes *et al.* 2006; Lopes and Dias, 2007).

Sediment fluxes between Ria de Aveiro main channels seem to be limited by the complex geometry of the lagoon, with small sediment exchanges between the various channels (Lopes *et al.*, 2001, 2006). Sediment fluxes between the lagoon and the ocean are believed to be

mainly in the seaward direction, being consistent with the lower lagoon's ebb dominance. However, for neap tide conditions, it has been suggested that upper lagoon can act as a trap for the fine sediments transported by the rivers and eroded from the lagoon system (Abrantes *et al.*, 2006; Dias *et al.*, 2007).

The previous performed works have addressed essentiality to studied the tide and rivers influence on the lagoon suspended sediment dynamics. Only recently, some studies have evaluated morphological and climate change effects in the lagoon suspended sediment dynamics. Picado *et al.* (2011a) have investigated the sediments pathways for the lagoon flooded area enlargement, result of salt pans walls degradation and Plecha *et al.* (2014) have evaluated the impact of a 0.42 m sea level rise at inlet on the lagoon suspended sediment distribution. Therefore, anthropogenic pressures and climate change effects influence on the lagoon suspended sediment transport have received limited attention and still need to be clarified.

1.4 Structure of the thesis

This work is divided in 8 chapters. After this Chapter 1, where is presented the motivation, general literature review and the structure of the work follows the Chapter 2, with a review of the origin, hydrodynamics and sediment characteristics of the Ria de Aveiro. In this chapter it is also presented a characterization of the bottom sediments distribution and suspended sediment concentrations at the inlet and the beginning of the main lagoon channels, based on samples collected at surveys. Additionally, an estimation of the suspended sediment loads past evolution for the lagoon main freshwater tributary, the Vouga river, by the application of sediment rating curves (SRC) is also presented.

In Chapter 3, a characterization of the morphological evolution of the Ria de Aveiro inlet and harbour area between 2001 and 2012 is performed, based on the analysis of bathymetric data collected by Aveiro Harbour Administration (APA), performed in a Geographic Information System (GIS) environment.

Chapter 4 presents the results of laboratory tests in a settling column carried out in the National Laboratory of Civil Engineering (LNEC) with fine sediments collected in the Ria de Aveiro, to evaluate the influence of salinity and initial suspended sediment concentration on the settling velocity. These experimental tests aim at contributing to the improvement of

the numerical modelling suspended sediment transport, through a better understanding of the deposition process.

Chapter 5 presents a general overview of the numerical model MOHID that was used to simulate the suspended sediment transport, as well as the setup and its validation for Ria de Aveiro. The model validation is also presented in this chapter, being the suspended sediment concentrations model predictions extensively compared with observations. In this chapter a sensitivity analysis of numerical model fine sediment's settling velocity is also presented.

In Chapter 6 and 7 the numerical model implemented is used to evaluate the changes verified at Ria de Aveiro suspended sediment transport from the past to present and assess the anthropogenic and climatic changes influence on future suspended sediment dynamics. Finally, in Chapter 8, the conclusions of the dissertation and suggestions for further work are drawn.

1.5 Prior dissemination

SCI Journal Papers

COSTA, S., COELHO, C. (2013). Northwest Coast of Portugal – Past behavior and future coastal defense options. Journal of Coastal Research, SI 65, pp. 921-926.

Conference proceedings

COSTA, S., COELHO, C., PORTELA, L. (2015). Morphodynamic evolution of the Aveiro lagoon harbor area (2001-2012), Portugal. In: Wang, P., Rosati, J.D., Cheng, J. (Eds.), The Proceedings of Coastal Sediments 2015, Singapore, World Scientific Co. Pte. Ltd, 14 p.

COELHO, C., COSTA, S., PORTELA, L., RIBEIRO, F., CUNHA, R. (2015). Aveiro lagoon fine sediment laboratory tests. In: Wang, P., Rosati, J.D., Cheng, J. (Eds.), The Proceedings of Coastal Sediments 2015, Singapore, World Scientific Co. Pte. Ltd, 14 p.

COSTA, S., PICADO, A., VAZ, N., COELHO, C., PORTELA, L., DIAS, J.M. (2015). Avaliação do transporte sedimentar coesivo na Ria de Aveiro. VIII Congresso sobre Planeamento e Gestão das Zonas Costeiras dos Países de Expressão Portuguesa, Aveiro, 14-16 Outubro 2015. ISBN 978-989-8509-12-3, 15 p.

Conference abstracts

CUNHA, R., COSTA, S., COELHO, C. (2013). Avaliação do transporte sedimentar coesivo. MEC2013 – 2ª Conferência sobre Morfodinâmica Estuarina e Costeira, Aveiro, 9-10 de Maio de 2013.

COSTA, S., PICADO, A., VAZ, N., COELHO, C., PORTELA, L., DIAS, J.M. (2015). Avaliação do transporte sedimentar coesivo na Ria de Aveiro. VIII Congresso sobre Planeamento e Gestão das Zonas Costeiras dos Países de Expressão Portuguesa, Aveiro, 14-16 Outubro 2015.

Conference communications

COSTA, S., COELHO, C. (2013). Northwest Coast of Portugal – Past behavior and future coastal defense options. ICS2013 – 12th International Coastal Symposium, Plymouth, United Kingdom, 8-12 de Abril de 2013.

COSTA, S., COELHO, C., PORTELA, L. (2015). Morphodynamic evolution of the Aveiro lagoon harbor area (2001-2012), Portugal. Coastal Sediments 2015, San Diego, 11-15 May 2015.

COELHO, C., COSTA, S., PORTELA, L., RIBEIRO, F., CUNHA, R. (2015). Aveiro lagoon fine sediment laboratory tests. Coastal Sediments 2015, San Diego, 11-15 May 2015.

COSTA, S., PICADO, A., VAZ, N., COELHO, C., PORTELA, L., DIAS, J.M. (2015). Avaliação do transporte sedimentar coesivo na Ria de Aveiro. VIII Congresso sobre Planeamento e Gestão das Zonas Costeiras dos Países de Expressão Portuguesa, Aveiro, 14-16 Outubro 2015.

2 Characterization of Ria de Aveiro and Vouga river drainage basin

2.1 Introduction

In this chapter, a characterization of the Ria de Aveiro is carried out, which includes a description of the lagoon origin, hydrodynamic regime, fluvial discharges and bottom sediments and suspended sediment concentrations based in previous studies. In addition to a literature review, a characterization of the bottom sediments distribution and suspended sediment concentrations at the inlet and main lagoon channels downstream areas is also performed. This characterization was made through the analysis of bottom sediment and water samples collected at surveys carried out in winter/spring and summer/autumn conditions in 2013/14.

Furthermore, Ria de Aveiro suspended sediment availability depends primarily on the rivers, making important characterize the suspended sediment loads from the lagoon tributaries. Vouga river is the lagoon main tributary, thus an evaluation of its suspended sediment loads was performed, by the application of suspended sediment rating curves (SRC). SRC were applied to data of paired discharges and SSC obtained at stations located in Vouga river from National Information System of Water Resources (SNIRH).

2.2 Ria de Aveiro

Ria de Aveiro is a coastal lagoon located on the northwest Portuguese coast, which is bordered by the municipalities of Albergaria-a-Velha, Aveiro, Estarreja, Ílhavo, Mira, Murtosa, Ovar and Vagos. It is the largest Portuguese coastal lagoon and classified as Special Protected Area under the Birds Directive and as a Site of Community Importance. The lagoon integrates the Vouga river catchment area, with a population of 353688 inhabitants (Census, 2011) in the watershed area, where the main activities are the industrial and service sector. However, for the local population, farming and fishing activities are socio-culturally and economically important (Lillebø *et al.*, 2013).

The lagoon covers a surface area of about 89.2 km^2 and 64.9 km^2 at high tide, during spring and neap tides (Lopes *et al.*, 2013a). It has an irregular and complex geometry characterized by large areas of intertidal flats and a web of narrow channels, communicating with the Atlantic Ocean by a single inlet. The inlet channel is about 1.3 km long, 350 m wide and 20 m deep (Dias and Picado, 2011; Silva and Leitão, 2011).

The development of the lagoon channels follows two main directions, the north-south direction, from Ovar to Mira, parallel to the coastline, and the east-west direction. There are four main channels (Figure 2.1):

- S. Jacinto channel, with a parallel orientation to the coastline, presents a first confluence with the Mira channel and then inflects to north, to the confluence of Ílhavo and Espinheiro channels. From this confluence, the channel continues to north until Ovar. The total channel length is about 29 km and is the most extensive and deep channel of the lagoon;
- Espinheiro channel is located at lagoon central area and extends northeast for approximately 17 km, with an average width of 200 m (Vaz *et al.*, 2009);
- Mira channel, located at southwest, with a length of 20 km and a maximum width of 1000 m, is the second longest channel of the lagoon. This channel coming from south converges with the S. Jacinto channel;
- Ílhavo channel extends in the southeast direction, limiting the Gafanhas at west, and the city of Ílhavo at east. This channel is shallow, with 15 km length and a maximum width of 200 m (Araújo *et al.*, 2008).

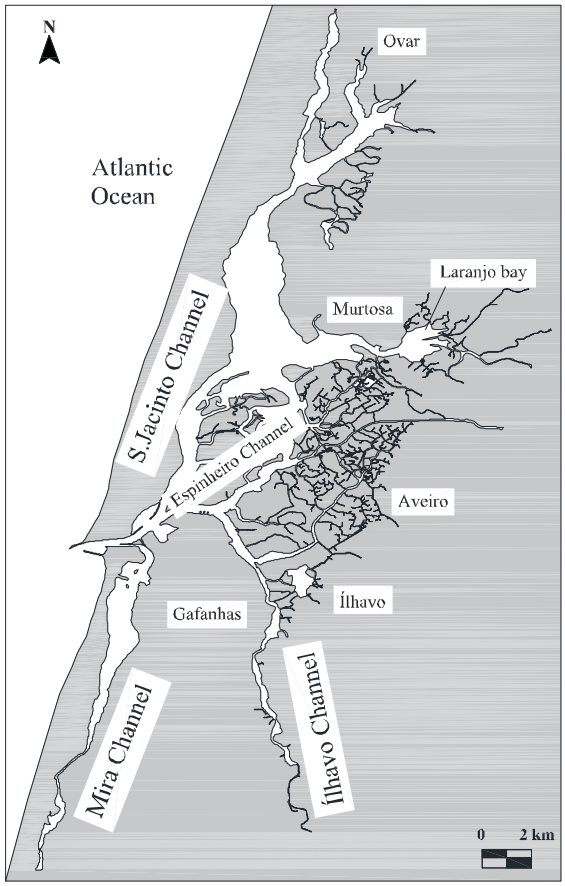

Figure 2.1: Ria de Aveiro main channels.

2.2.1 Origin and evolution

Ria de Aveiro is geologically recent, reflecting the coastal sediment transport along the coastline in the north-south direction (Figure 2.2). In the past, between Espinho and Cabo Mondego, the coastline had a totally different configuration, characterized by a bay near the mouth of the Vouga River. Over the years, due to a slow process of sand deposition and consequent formation of coastal dunes, the lagoon began to emerge (Abrantes *et al.*, 2006). These extensive coastal dunes made difficult the Vouga river discharge into the sea, resulting in the lagoon gradual filling up with sediments from fluvial discharges. The lagoon inlet had different locations along the time, oscillating between Ovar and Mira. During some years the lagoon was completely isolated from the sea. In wet periods, the entire area of the lagoon was constantly flooded by the rivers (Dias *et al.*, 1994).

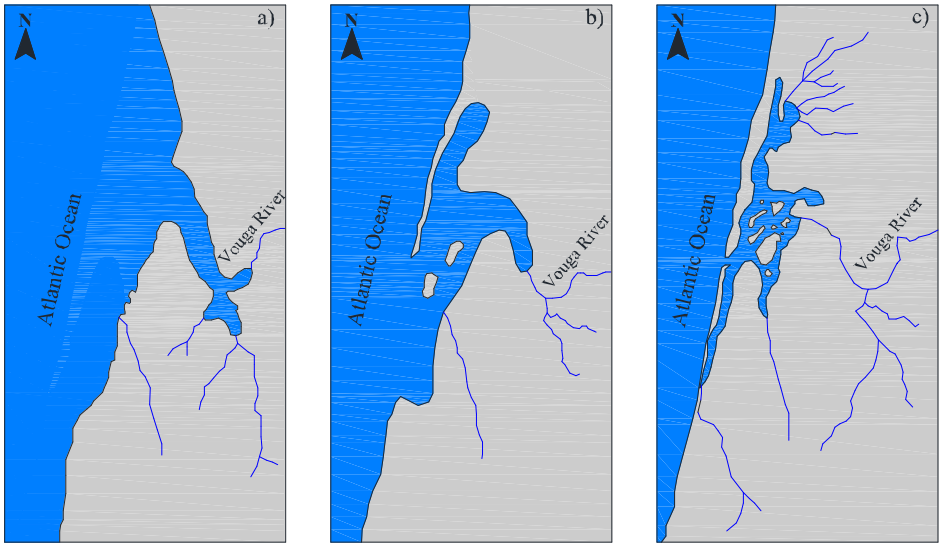

Figure 2.2: Ria de Aveiro evolution: a) A bay where the Vouga river discharge (10th century); b) Sediment deposition with sand spit growing southward (15th century); c) Lagoon configuration (19th century) (adapted from Dias *et al.*, 1994).

The decrease of the marine influence and the gradual silting up of the lagoon had a major effect on the ecological and socio-economic characteristics of the surrounding area. The years that the lagoon was closed to the sea usually corresponded to periods of poverty for the region's inhabitants. This led to human intervention, in order to keep always open the communication with the sea and locking the natural evolutionary process. Thus, in 1802, the works for the inlet establishment began, and on 3rd April of 1808 the Aveiro inlet was opened in the location where it stands today, and later fixed by two breakwaters.

After the inlet fixation, several interventions where carried out, with the breakwaters extension and navigation channels deepening, through dredging operations. Outside the harbour area, dredging operations were also made, being the more significant interventions performed in the beginning of the 1950's at S. Jacinto channel and in 1970's at Mira channel (EIA Vouga, 2001). After 1990, the major intervention was performed in 1997/98 at the S. Jacinto and Mira channels and Laranjo bay (Marinheiro, 2008).

Furthermore, in the last years the abandonment of the salt pans has led to the degradation of their walls, resulting in the lagoon flooded area increase (Picado *et al.*, 2009; 2010).

2.2.2 Tidal properties

Tide is the main forcing of the lagoon, being deformed in its propagation through the channels, due to its geometry and bathymetry (Lopes and Dias, 2007). The lagoon regime is characterized by several periodic time-scales, being the most important, the semi-diurnal (dominant tidal period) and the fortnightly (one-half the lunar month and associated to the spring–neap cycle) (Lopes and Dias, 2007).

Tides present an average range at the inlet of 2 m and maximum and minimum ranges of 3.2 m (spring tide) and 0.6 m (neap tide), respectively (Dias *et al.*, 1999; Sousa and Dias, 2007; Plecha, 2011). The lagoon is characterized as mesotidal, with tidal amplitudes decrease in the inner parts of the lagoon. Additionally, a phase delay is observed comparing to the oceanic tide (Dias *et al.*, 2000; Dias, 2001; Aráujo *et al.*, 2008; Plecha, 2011). Flood period is longer than ebb, inducing higher velocities in the ebb, characterizing the lagoon as ebb-dominant at central area and flood-dominant at upstream areas (Dias, 2001; Oliveira *et al.*, 2006; Lopes *et al.*, 2006; Lopes and Dias, 2015; Picado *et al.*, 2010).

Lopes *et al.* (2013b) determined the tidal prism for the most recent bathymetry, being obtained the values of 139.7×10^6 and 65.8×10^6 m^3, for spring and neap tides, respectively. The tidal prisms at S. Jacinto, Espinheiro, Mira and Ílhavo channels, relative to the tidal prism at the inlet are about 33%, 21%, 9% and 17%, respectively (Lopes *et al.*, 2013b).

Over time, the lagoon has presented significant changes in tidal dynamics, namely in its amplitude and propagation (Table 2.1), due to anthropogenic and natural morphologic changes in the channels depth and geometry (Araújo *et al.*, 2008). The channels deepening has led to the tidal amplitude and prim increase (Silva and Duck, 2001; Dias and Picado, 2011). Moreover, hydrodynamic model simulations showed a 5-14% amplitude increase in the lagoon central area, from 1987/88 to 2002/03 (Araújo *et al.*, 2008). Additionally, in the last years the abandonment of the salt pans has led to an increase of tidal currents, prism and asymmetry (Picado *et al.*, 2009; 2010).

Table 2.1: Tidal amplitude at inlet along the time (Silva and Duck, 2001).

Year	**1936**	**1963**	**1966**	**1987**
Tidal amplitude (m)	2.2	2.5	2.8	2.8

2.2.3 Fluvial discharges

Several rivers flow into Ria de Aveiro, being Vouga and Antuã rivers (flowing into Espinheiro channel and Laranjo bay) the major freshwater inputs, representing 75% of the drainage area. Generally, fluvial discharges are located at the head of the main lagoon channels (Figure 2.3):

- Vouga river flows into the Espinheiro channel, and its main tributaries are Caima and Águeda rivers (this with an important sub-tributary, the Cértima river);
- Antuã river flows into the Laranjo bay;
- Cáster river flows in the northern area of S. Jacinto channel, together with Gonde river, nearby Ovar;
- Boco river flows at south of the lagoon, into the Ílhavo channel;
- Valas de Mira flows into Mira channel, through a series of tributaries and drainage ditches.

Vouga river is the lagoon main fluvial discharge with a mean flow of 80 m^3/s. Boco, Valas de Mira, Cáster and Antuã rivers present significantly lower values, with mean values of 5, 10, 5 and 20 m^3/s, respectively (Génio *et al.*, 2008).

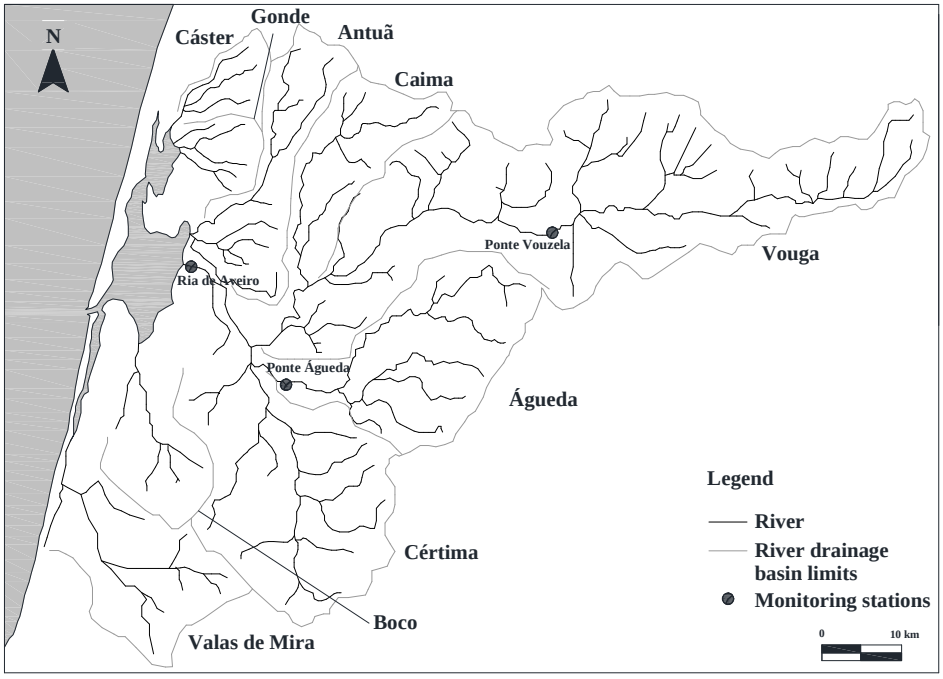

Figure 2.3: Drainage basin of the Ria de Aveiro, showing major fluvial tributaries and sub-basins.

The discharge values can be an order of magnitude higher during high rainfall periods (Lopes *et al.*, 2001), with Vouga river discharges presenting values higher than 1000 m^3/s (Silva and Duck, 2001). During summer, the base flow is reduced to 3-4 m^3/s (Figueiredo *et al.*, 2002). The mean total freshwater input during a tidal cycle is about 1.8×10^6 m^3 (Moreira *et al.*, 1993). The river discharge is negligible comparing to the flux related with tidal prism, but it can have long term influence in the residual transport (Vaz and Dias, 2008).

2.2.4 Bottom sediments distribution

The nature and granulometric distribution of the Ria de Aveiro channels bottom sediments is extremely variable, given the different sedimentary sources (Lopes *et al.*, 2006). The origin of finer sediments is mainly fluvial, being the Vouga and Antuã rivers responsible for the major contributions. Sediments from fluvial discharges present 20% of its content in sand and gravel, being the remaining silt and clay. The annual average sediment volume transported by the rivers into the lagoon it has been suggested that is 0.24×10^6 m^3 (Teixeira, 1994). However, since the lagoon origin is related with coastal processes, the sand percentage in the channels is high. Other sediment contributions are the erosion of the inner lagoon area (resuspension of the bottom sediments and intertidal areas), surface runoff of the margins and sediments from the shoreline, however with a low relevance (Abrantes, 2005).

Along the channels, a granulometric composition gradient of the bottom sediments, where the content of finer particles (silt and clay) increases with the inlet distance, is observed. Differences between the north and south channels, with the north channels presenting sediments composed by sand and coarser particles, in opposition to the south channels where the sediments are composed by sand and finer particles, are also observed. In the intertidal areas, the sediments are mainly composed by medium to fine sand, silty clay and sandy clay sediments (Abrantes *et al.*, 2006).

In order to complement the literature review, fieldwork has been conducted as part of the present research. A characterization of the bottom sediments granulometric distribution at the inlet and the main channels (Barra, S. Jacinto, Espinheiro and Ílhavo stations) was performed, through the analysis of data collected from surveys (Figure 2.4a).

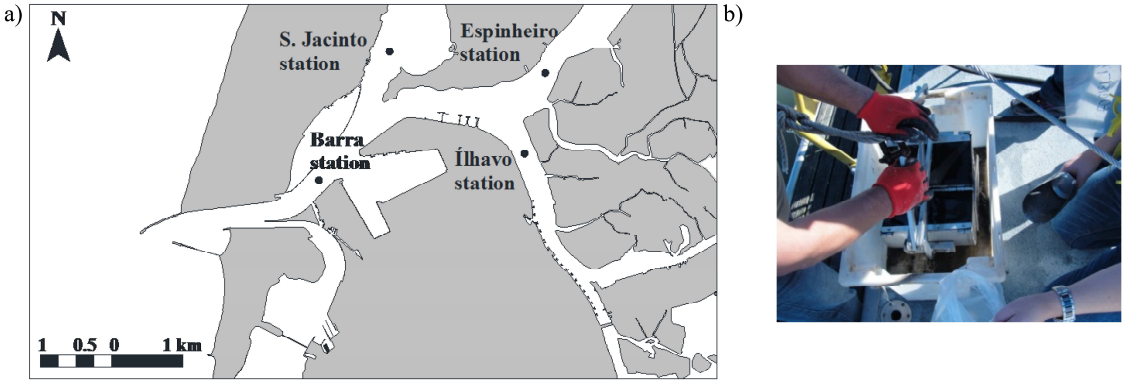

Figure 2.4: Bottom sediment samples: a) Sampling locations; b) Collection with the *Petit Ponar* dredge.

Twenty-four samples (three per channel and per campaign) were collected during low tide period at spring tide, with a *Petit Ponar* dredge (Figure 2.4b), in surveys performed on 7th October 2013 (summer/autumn survey) and 17th March 2014 (winter/spring survey). Sediments were wet-sieved passed through a 63 μm sieve, in order to separate the fine from the coarse fraction. The coarse fraction was taken to the laboratory oven, and after drying its size analysis was carried out by dry-sieving. Statistical analysis of granulometric distribution was performed to determine particle size parameters of sediment samples, namely d_{10}, d_{50} and d_{90}. The values of the granulometric fractions and particle size parameters for the samples at both surveys are presented in Tables 2.2 and 2.3.

The summer/autumn survey results indicate that samples are mainly composed of sand, with a percentage ranging between 71 and 97%. The sand fraction is higher at S. Jacinto station (>94%) followed by Espinheiro, with values around 80%. Barra and Espinheiro stations present the highest percentage of gravel, approximately 20%. The silt-clay fraction is present mainly in the Ílhavo station samples, with an average value approximately 15% (Table 2.2). Barra channel samples present coarse sand and S. Jacinto, Espinheiro and Ílhavo median sand, according to the Wentworth (1922) and Flemming (2000) terminologies.

In the winter/spring survey is verified a slight decrease in the samples sand percentage, ranging between 61 and 96%, with the S. Jacinto and Espinheiro stations presenting the highest values (around 90%). Additionally, there is an increase of the gravel fraction in the Barra and S. Jacinto stations, in opposition to the Espinheiro. The silt-clay fraction is still mainly observed in the Ílhavo station samples, but with higher values and in Espinheiro station is observed an increase, however is still a residual percentage (Table 2.2).

Table 2.2: Granulometric fractions of the sediment samples at Barra, S. Jacinto, Espinheiro and Ílhavo stations.

Station	Sample	7th October 2013			17th March 2014		
		Gravel (%)	Sand (%)	Silt-clay (%)	Gravel (%)	Sand (%)	Silt-clay (%)
Barra	1.1	21.2	78.8	0.0	30.5	69.5	0.0
	1.2	27.2	72.8	0.0	31.8	68.2	0.0
	1.3	23.7	76.3	0.0	38.7	61.3	0.0
S. Jacinto	2.1	5.5	94.5	0.0	11.9	88.1	0.0
	2.2	5.6	94.4	0.0	7.5	92.5	0.0
	2.3	3.3	96.7	0.0	6.5	93.5	0.0
Espinheiro	3.1	19.3	80.6	0.1	4.7	94.7	0.6
	3.2	18.5	81.4	0.1	3.3	95.9	0.8
	3.3	19.6	80.3	0.1	13.8	84.8	1.4
Ílhavo	4.1	9.5	75.7	14.8	0.0	93.2	6.8
	4.2	9.2	78.2	12.6	0.0	67.9	32.1
	4.3	11.1	70.9	17.9	0.0	73.5	26.5

Analysis of the particle size parameters (d_{10}, d_{50} and d_{90}) presented in Table 2.3 confirms the previous findings. There is an increase in the d_{50} from the summer/autumn to winter/spring survey, ranging from 0.82-0.87 mm to 1.07-1.32 mm at Barra station. In other hand, Espinheiro and Ílhavo stations sediment samples particle size decreases from summer/autumn to winter/spring survey, especially at Ílhavo.

Table 2.3: Particle size parameters of the sediment samples at Barra, S. Jacinto, Espinheiro and Ílhavo stations.

Station	Samples	7th October 2013			17th March 2014		
		d_{10} (mm)	d_{50} (mm)	d_{90} (mm)	d_{10} (mm)	d_{50} (mm)	d_{90} (mm)
Barra	1.1	0.45	0.87	4.22	0.38	1.07	6.48
	1.2	0.36	0.87	9.49	0.43	1.13	9.10
	1.3	0.36	0.82	8.30	0.41	1.32	17.65
S. Jacinto	2.1	0.28	0.49	1.08	0.30	0.60	2.85
	2.2	0.28	0.50	0.99	0.28	0.47	1.38
	2.3	0.28	0.46	1.78	0.28	0.46	1.16
Espinheiro	3.1	0.27	0.45	5.12	0.20	0.34	0.49
	3.2	0.27	0.45	4.79	0.23	0.35	0.49
	3.3	0.27	0.45	6.02	0.17	0.38	3.21
Ílhavo	4.1	0.13	0.30	3.13	0.11	0.17	0.23
	4.2	0.14	0.30	2.27	0.08	0.15	0.23
	4.3	0.15	0.34	4.08	0.08	0.16	0.24

2.2.5 Suspended sediment concentrations

In the performed fieldwork, in order to investigate the temporal variations of suspended sediment concentration (SSC) in the inlet and main lagoon channels (Figure 2.4a), it was

also collected water samples. Sampling was performed at approximately 2-hour intervals (timetable of samples collection at Appendix A1), during the flood period, at 1 m below the water surface, considering that SSC increase with depth is not significant (Martins *et al.*, 2011). Water samples were collected with a *Van Dorn*® horizontal bottle (4.5 l capacity) (Figure 2.5).

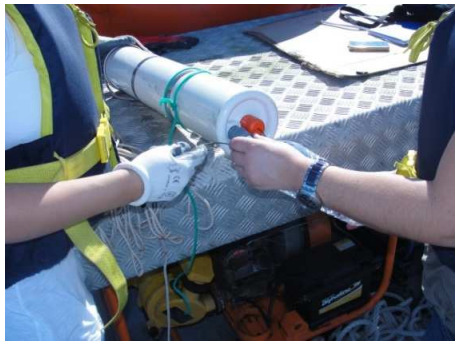

Figure 2.5: *Van Dorn* horizontal bottle.

SSC were determined by the gravimetric method in laboratory. Samples were filtered by the classic vacuum system and using 0.45 µm cellulose nitrate membrane *Whatman*® pre-weighted filters. The filters were dried at 40ºC during 24 h and re-weighted. Additionally, the water salinity was measured using a multiparameter probe.

SSC and salinities values of the water samples for both surveys are presented in Figure 2.6. Overall, the observed SSC are relatively low and decrease along the flood period. During the summer/autumn survey, high concentrations are observed for samples with low salinities at Ílhavo channel station (maximum value of 24.05 mg/l), which reveals that sediment sources are located within the channel, as observed by Silva (1994) (Figure 2.6a).

In general, at winter/spring survey, water samples present lower SSC (<15 mg/l). However, some samples with high concentrations and salinities are observed at the Barra and S. Jacinto stations (Figure 2.6b), which is in agreement with previous results of Martins *et al.* (2009, 2011) at inlet area. The only difference is that higher SSC are not observed in the winter/spring, which is maybe justified by the absence of rainfall in the days before the survey.

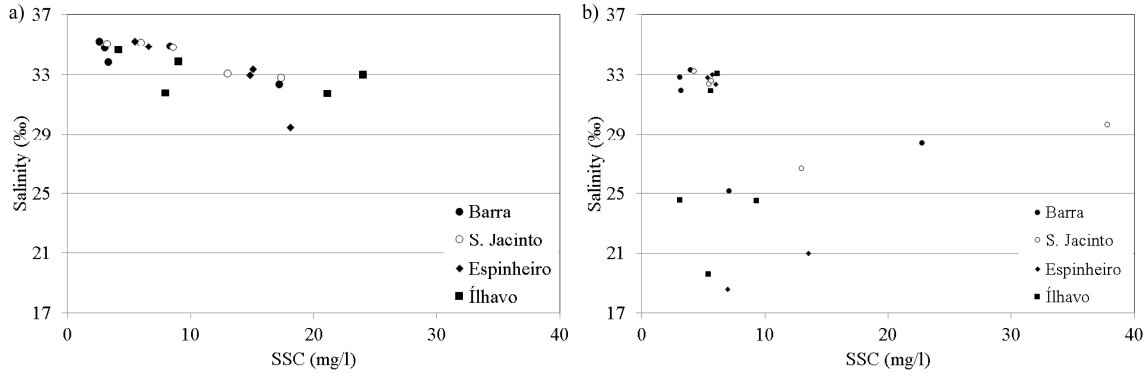

Figure 2.6: SSC and salinity at Barra, S. Jacinto, Espinheiro and Ílhavo stations in: a) 7th October 2013; b) 17th March 2014.

2.3 Vouga river drainage basin

The Vouga river basin has an area of approximately 3362 km^2 (Figure 2.3). The river origin is in the Lapa mountains at an altitude of about 930 m, traveling about 141 km before flowing into the Ria de Aveiro. The catchment area covers 31 municipalities, with a total population of 961316 inhabitants, being mostly occupied by forest and farmlands (Van der Weijden and Pacheco, 2006).

The main tributaries of the Vouga river are the Caima, Antuã and Águeda rivers (Figure 2.3). Águeda river is the larger tributary, that joins Vouga in the lower area near the lagoon. Thus, the catchment area of Vouga river, upstream Águeda river, is only 1500 km^2. This area is located in the mountains, characterize by rocks of low permeability. These characteristics, together with the regional weather pattern, cause a large seasonal difference between winter runoff events and summer base flow (Silva and Oliveira, 2005).

Currently, the Vouga river drainage basin has no sediment monitoring program. The only available data is river basin sediment production estimates, which were made by theoretical formulations (Table 2.4), for Ponte Vouzela, Ponte Águeda and Vouga river mouth at Ria de Aveiro stations (stations location presented in Figure 2.3). The sediment production values present an increase from Ponte Vouzela, at the upper Vouga river area to the mouth.

Table 2.4: Sediment production of the Vouga drainage basin (PBV, 2002; PBVML, 2012).

Station	Basin area (km^2)	Basin area not influenced by dams (km^2)	Sediment production coefficient (%)	Sediment production (ton/km^2/year)	Sediment production (ton/year)	Sediment production not influenced by dams (ton/year)
Ponte Vouzela	649	156	21	265	172115	41371
Ponte Águeda	427	-	8	329	140581	-
Ria de Aveiro	2418	-	8	172	415810	-

2.3.1 Evaluation of suspended sediment loads

Sediment transport in estuaries and coastal lagoons is directly connected to the rivers sediment input. Human activities in the rivers drainage basins such as land use and occupation, dams and reservoir's construction and implementation of structures (*e.g.* bridges) and catchment systems, influence the flux and composition of the rivers sediment loads delivered to the coastal areas, which can affect its morphology and productivity (Morehead *et al.*, 2003; Kitheka *et al.*, 2005; Wang *et al.*, 2010; Boateng *et al.*, 2012; Fan *et al.*, 2013; Worrall *et al.*, 2013; Wilkinson *et al.*, 2014).

In many areas, suspended sediment transport is predominantly the main river transport mechanism, while only a small component of the total transport corresponds to the bed-load (Wass *et al.*, 1997; Asselman, 2000; Fan *et al.*, 2013). In rivers of small to moderate drainage basin size (~10^1–10^4 km^2), as the Vouga river, active margins are recognized as transporting the majority of sediments, and sediment yields are often highly episodic, caused by high discharge floods (Gray *et al.*, 2014).

Estimations of river suspended sediment loads require the combination of SSC and water discharges records. In most cases, daily discharges are available from a discharge recorder, while SSC result from manually collected samples taken occasionally (Wass *et al.*, 1997; Iadanza and Napolitano, 2006). Therefore, it has been developed methodologies in order to determine the suspended sediment river loads, which not requires long data series. These methodologies, called sediment rating curves (SRC) are based in the application of a regression approach to the existing data, providing an extrapolation of the sediment yield (Asselman, 2000; Girolamo *et al.*, 2015).

In the present research, SRC were applied to a paired of daily discharges and SSC past data, for Vouga river and its larger tributary, the Águeda river, to obtain estimations of the Vouga and Águeda river's suspended sediment loads and its evolution along the time.

2.3.2 Methodology

Daily discharges (Q) and SSC in Ponte Vouzela and Ponte Águeda stations were obtained from the SNIRH (monitoring periods presented in Appendix A2). Ponte Vouzela station is placed in the Vouga main catchment (~60 km from the lagoon) and Ponte Águeda station at the lower reaches of the Águeda river (~20 km from the lagoon) (Figure 2.3). Daily discharges were automatically monitored. SSC were determined by laboratory analysis of water samples manually collected. In Table 2.5 are presented the discharges and SSC sample's number and the minimum and maximum values for each station used in this study. Firstly, an analysis of the discharges and SSC temporal evolution at Ponte Vouzela and Ponte Águeda stations was made. Therefore, discharges and SSC were grouped in classes and determine its frequency along the time. Additionally, it was evaluated the rainfall and dam's construction influence, through a comparative analysis of the discharges evolution along the time and the Vouga drainage basin rainfall and dam's date of implantation.

Table 2.5: Sample data at Ponte Vouzela and Ponte Águeda stations.

Station	**Discharges**			**SSC**		
	N. samples	**Min. (m^3/s)**	**Max. (m^3/s)**	**N. samples**	**Min. (mg/l)**	**Max. (mg/l)**
Ponte Vouzela	6492	0.0	224.8	256	0.0	110.0
Ponte Águeda	3072	0.0	126.9	249	0.1	10.5

Secondly, SRC methodology was applied to the Ponte Vouzela and Ponte Águeda stations existing data. Since the determination of suspended sediment loads is only possible when both discharges and SSC are available, it was only the samples that were paired water discharges and SSC data. SRC were determined by establishing a power function between the obtained suspended sediment loads (Q_s) and discharges (Q):

$$Q_s = a \cdot Q^b \tag{2.1}$$

where Q_s is the suspended sediment discharge (kg/day), Q is the discharge (m^3/s) and a and b are the rating curve parameters. Daily suspended sediment loads at both stations were determined by the multiplication of the SSC and daily discharges (Asselman, 2000):

$$Q_s = Q \cdot C \tag{2.2}$$

The obtained SRC were used to determine the monthly and annual suspended sediment loads at Ponte Vouzela and Ponte Águeda stations. Moreover, since these stations are ~30 km apart it was assumed as an approximation, that the suspended sediment flux at the Vouga river mouth (station E3) is the sum of the suspended sediment loads at the Ponte Vouzela (E1) and Ponte Águeda (E2) stations, and is also an approximation of the suspended sediment flux discharging into the Ria de Aveiro (Figure 2.7).

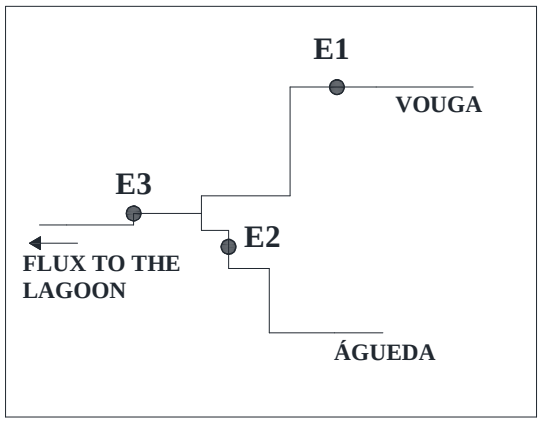

Figure 2.7: Schematic diagram of the Ponte Vouzela and Ponte Águeda stations location at Vouga and Águeda rivers.

2.3.3 Results and discussion

2.3.3.1 Discharges and SSC temporal evolution analysis

In Tables 2.6 and 2.7 are presented the Ponte Vouzela and Ponte Águeda stations daily discharges grouped in classes, for each decade and its frequency.

Discharge frequency at Ponte Vouzela station reveals that between 1920 and 2000 there are no significant variations in the discharge classes frequency, with most of data presenting values lower than 2.5 m^3/s and in the range 5-50 m^3/s (Table 2.6). Moreover, between 1970 and 2009 was not verified any occurrence for higher discharges (300-400 m^3/s).

In the Ponte Águeda station is observed a similar behaviour, with most of discharges in the lower discharge class (≤2.5 m^3/s). It is also observed that after 1990, no occurrence in the higher discharges classes (110-165 and 165-220 m^3/s) is verified (Table 2.7).

Table 2.6: Discharge (m^3/s) frequency (%) per decade, in the Ponte Vouzela station.

Decade	17/29	30/39	40/49	50/59	60/69	70/79	80/89	90/99	00/09
≤2.5	51.34	50.41	42.53	39.98	31.98	33.08	41.21	33.51	72.84
2.5-5	11.97	11.07	9.25	15.70	11.57	16.62	14.16	18.94	6.12
5-50	33.24	32.48	42.02	40.62	48.19	44.54	41.66	44.12	17.16
50-100	2.61	4.22	4.05	2.63	5.46	4.06	2.61	2.52	2.55
100-200	0.66	1.41	2.00	0.87	2.05	1.33	0.37	0.85	1.30
200-300	0.18	0.33	0.13	0.19	0.57	0.37	0.00	0.06	0.03
300-400	0.00	0.08	0.03	0.00	0.19	0.00	0.00	0.00	0.00

Table 2.7: Discharge (m^3/s) frequency (%) per decade, in the Ponte Águeda station.

Decade	30/39	40/49	50/59	60/69	70/79	80/89	90/99	00/13
≤2.5	39.39	41.10	43.53	38.69	39.66	54.61	78.39	4.12
2.5-5	27.08	31.48	25.78	15.76	20.57	17.15	8.06	28.06
5-55	28.87	25.44	28.87	41.94	36.60	25.36	12.09	67.83
55-110	3.89	1.78	1.65	2.98	2.48	2.41	1.47	0.00
110-165	0.66	0.19	0.17	0.47	0.60	0.47	0.00	0.00
165-220	0.12	0.00	0.00	0.16	0.09	0.00	0.00	0.00

The Vouga and Águeda rivers monthly average discharges, determined from the daily discharges, were compared with the monthly average rainfall between 1931 and 2013 at all rainfall stations located at the Vouga drainage basin (Figure 2.8).

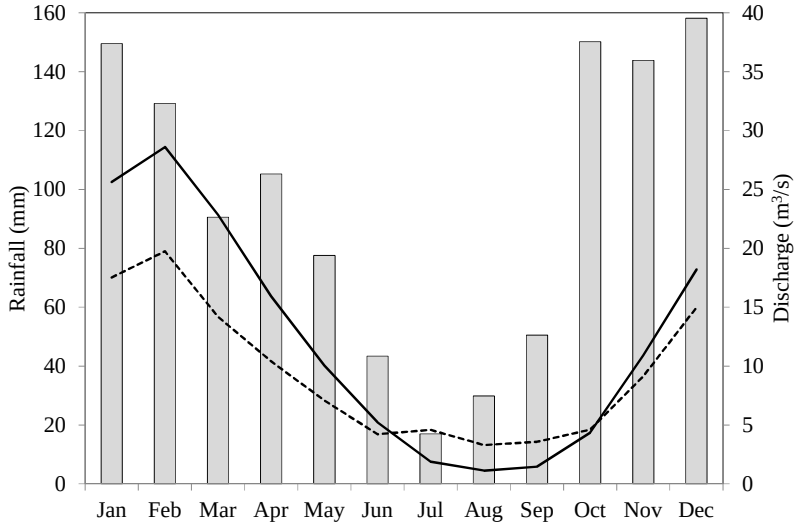

Figure 2.8: Comparison of Vouga and Águeda river's water discharge evolution along the year, with the Vouga drainage basin rainfall (continuous line - Ponte Vouzela station; dashed line - Ponte Águeda station; bars - rainfall).

The results show, as expected, that rivers discharges are directly related with the rainfall, following its variation, with low discharges recorded in the dry season months (between July and August) and high in the winter months (between October and February).

River water fluxes are sensitive to dams and reservoir's construction (Walling and Fang, 2003). Since there are some reservoirs implemented in the Vouga and Águeda rivers, it was compared the evolution of the annual maximum and average discharge values at the Ponte Vouzela and Ponte Águeda stations, with the dam's construction date (Figure 2.9).

Vouga maximum discharge evolution at Ponte Vouzela station shows there was a decrease since 1962 with values lower than 150 m^3/s after 2002, comparing to the values higher than 250 m^3/s observed in the 1930-1970 period (Figure 2.9a). However, a direct relation between the maximum discharges decrease observed between 1960 and 1990 and the dam's construction in 1955 cannot be established. Moreover, the lack of discharge data after 2009, does not allow to have a definitive conclusion relative to the dam's influence, since several dams were implemented in the 1994-2002 period.

In the case of the Ponte Águeda station, it is evident the reduction of the annual maximum discharge values between 1990 and 2004, which can be related with dams implantation between 1992 and 1997 (Figure 2.9b). However, the lack of discharge data in the 1990-2004 period does not allow drawing a definitive conclusion.

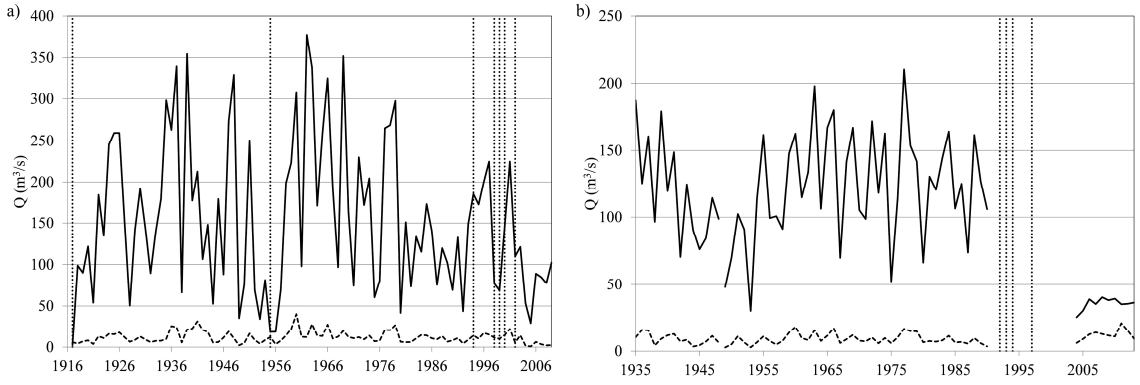

Figure 2.9: Annual water discharge evolution along the time (maximum - continuous line; average - dashed line; vertical dot line – dam's date of implantation) at: a) Ponte Vouzela station; b) Ponte Águeda station.

Similar to discharges, SSC data for Ponte Vouzela and Ponte Águeda stations was grouped in classes and determined its percentage of occurrence (Figure 2.10).

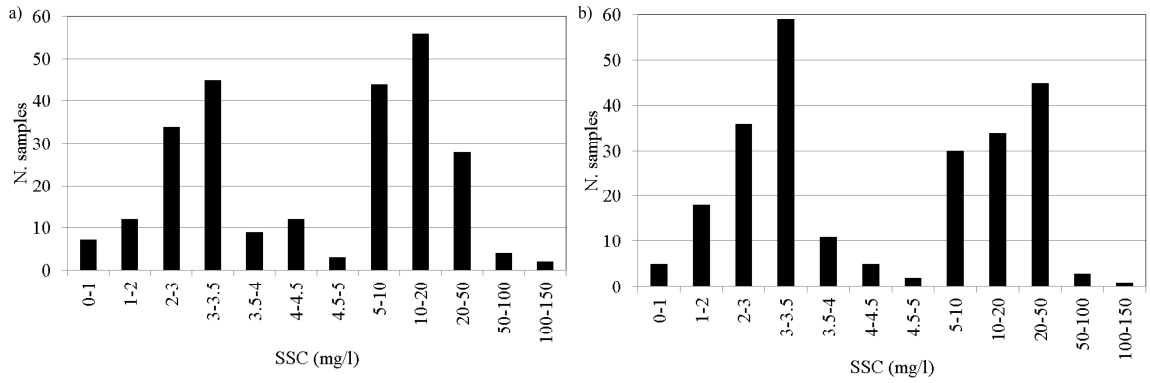

Figure 2.10: SSC histogram at: a) Ponte Vouzela station; b) Ponte Águeda station.

Results indicate that both stations present a similar distribution, with the low concentrations in the range of 2-3.5 mg/l, and high in the interval 5-50 mg/l. Ponte Vouzela presents higher values, with most of the samples presenting concentrations in the range 10-20 mg/l (Figure 2.10a). In opposition, in the Ponte Águeda most of the samples are in the range 3-3.5 mg/l (Figure 2.10b).

Additionally, was also analysed SSC temporal evolution at both stations (Figure 2.11).

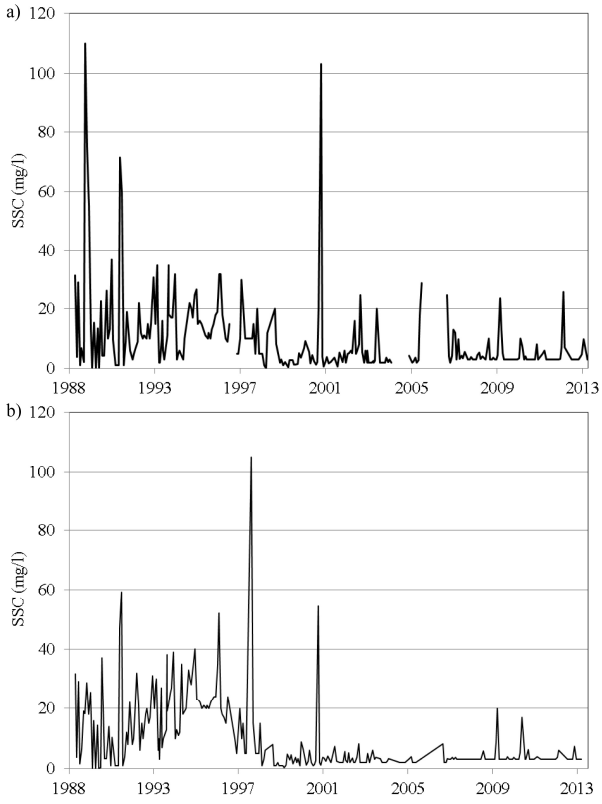

Figure 2.11: Temporal SSC evolution at: a) Ponte Vouzela station; b) Ponte Águeda station.

In the Ponte Vouzela station, the highest SSC registered was above 100 mg/l in the wet season. After 2001, there is an apparent decrease, with the maximum concentrations not exceeding 40 mg/l (Figure 2.11a). Ponte Águeda station presents a similar behaviour, with concentration peaks mainly in the range of 20-40 mg/l until 2001, but not exceeding 20 mg/l after this date (Figure 2.11b).

The river's discharge has an important role in the SSC. Therefore, it was compared discharges and SSC evolution along the time at Ponte Vouzela and Ponte Águeda stations (Figure 2.12). The obtained results show that similar discharges may have different SSC magnitudes. For example, in the Ponte Vouzela station, on 20th January 2003 (87.79 m^3/s; 5.4 mg/l) and 12th February 2007 (85.21 m^3/s; 25 mg/l). In the Ponte Águeda station, SSC data present some limitations, since the exact values for concentrations lower than 3 mg/l was not determined. However, the available data reveals that concentrations lower than 3 mg/l are usually observed for discharges lower than 8 m^3/s.

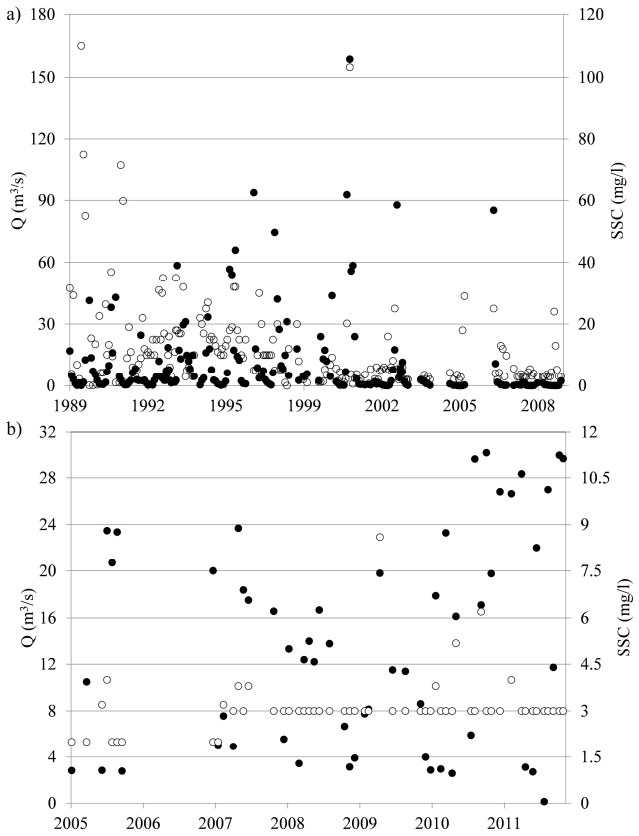

Figure 2.12: SSC (○) and discharges (●) temporal evolution at: a) Ponte Vouzela station; b) Ponte Águeda station.

2.3.3.2 Fitting SRC

Daily suspended sediment loads at Ponte Vouzela and Ponte Águeda stations were estimated from paired of daily discharges and SSC, by the application of Equation 2.1. Afterwards, SRC were created by the application of a power law function (Equation 2.2) to the obtained suspended sediment loads and discharges (Figure 2.13).

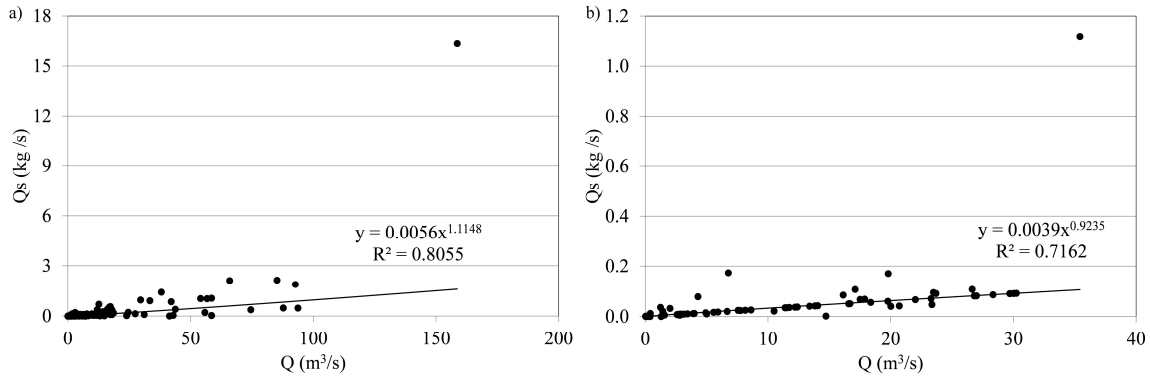

Figure 2.13: Sediment rating curves at: a) Ponte Vouzela station; b) Ponte Águeda station.

SRC performance evaluation was made by comparing estimated and predicted suspended sediment loads (Figure 2.14). Results reveal that SRC tend to underestimate the extreme peaks, which was already verified by Roy and Sinha (2014) for Ganga river. This can be related to the fact that the used methodology does not account for differences in SSC for similar discharges, in order to have a high correlation coefficient (Pont *et al.*, 2002), which is frequently observed, especially for high discharges events, as can be seen for both stations in Figure 2.13. Moreover, SSC data was sampled in one occasion and thus high discharge periods may are not included.

For low discharges the predicted suspended sediment loads are similar to estimations. SRC based in datasets divided into seasons were also created. Although, the results do not present major differences comparing to global analysis, as previous verified by Harrington and Harrington (2013) and Tóth and Bódis (2015). Additionally, in order to give a quantitative evaluation was determined the discrepancy ratio (R_i):

$$R_i = \frac{C_{pi}}{C_{ei}} \tag{2.3}$$

where C_{pi} and C_{ei} are the predicted and estimated suspended sediment loads and i the data set number. The overall performance was assessed by the mean discrepancy ratio ($\overline{R}$), that

presents a value of 1 to a perfect fit. The mean discrepancy ratios for the calibration period at Ponte Vouzela and Ponte Águeda stations were of 1.50 and 1.03, respectively. Moreover, the average differences between estimated and predicted suspended sediment loads are 7.60 and 2.20 ton/day at Ponte Vouzela and Ponte Águeda stations.

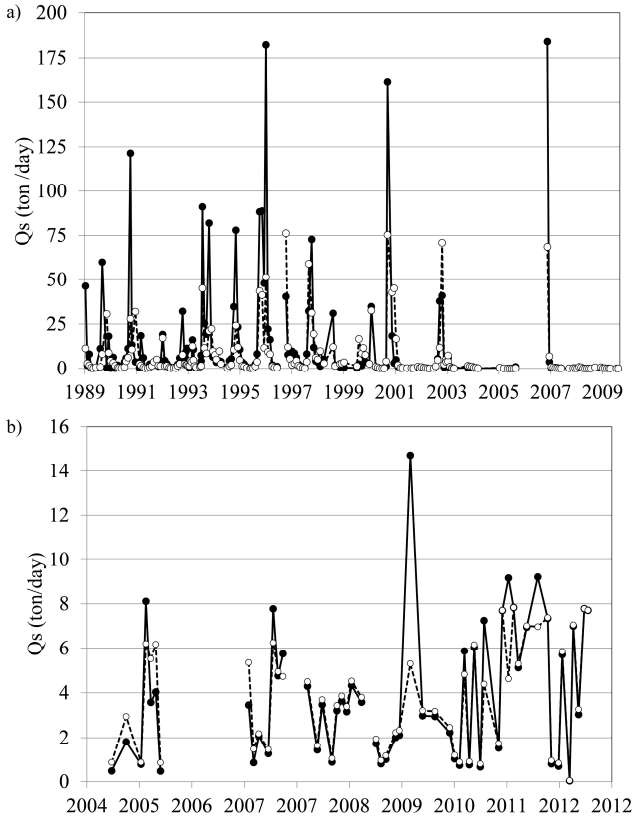

Figure 2.14: Estimated (●) and predicted (○) suspended sediment loads temporal evolution at: a) Ponte Vouzela station; b) Ponte Águeda station.

2.3.3.3 Annual suspended sediment loads

Monthly suspended sediment loads of Vouga and Águeda rivers were determined as the sum of the daily suspended sediment loads for each month, at Ponte Vouzela and Ponte Águeda stations, estimated from the daily discharges by the application of SRC, presented in Figure 2.13.

In Figure 2.15 are presented the average and maximum values along the year. The results indicate that major fluxes are expected in February at both stations, and lowest in August and September, at Ponte Vouzela and Ponte Águeda stations, respectively.

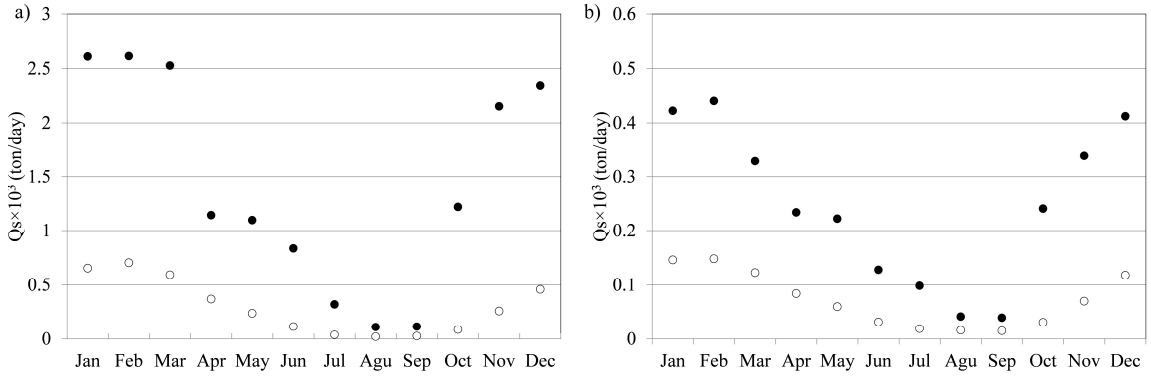

Figure 2.15: Monthly suspended sediment flux evolution along the year (○ - average; ● - maximum) at: a) Ponte Vouzela station; b) Ponte Águeda station.

Annual suspended sediment loads at Ponte Vouzela and Ponte Águeda stations were estimated adding the daily suspended sediment loads determined by SRC for each year, between 1918 and 2009 for Ponte Vouzela, and between 1936 and 1989 for Ponte de Águeda (Figure 2.16). Results show that Ponte Vouzela and Ponte Águeda stations present the values of 3500 and 850 tons, respectively, for the mean annual suspended sediment flux. Moreover, is verified that in Ponte Vouzela station there was an increase of the annual suspended sediment loads from 1920's to 1960's, mainly during the 1950's, and since then have decreased (Figure 2.16a). Ponte Águeda station present lower values, with a decrease trend in 1980's, with an average value of 700 ton comparing to 900 ton, estimated in the 1936-1980 period (Figure 2.16b).

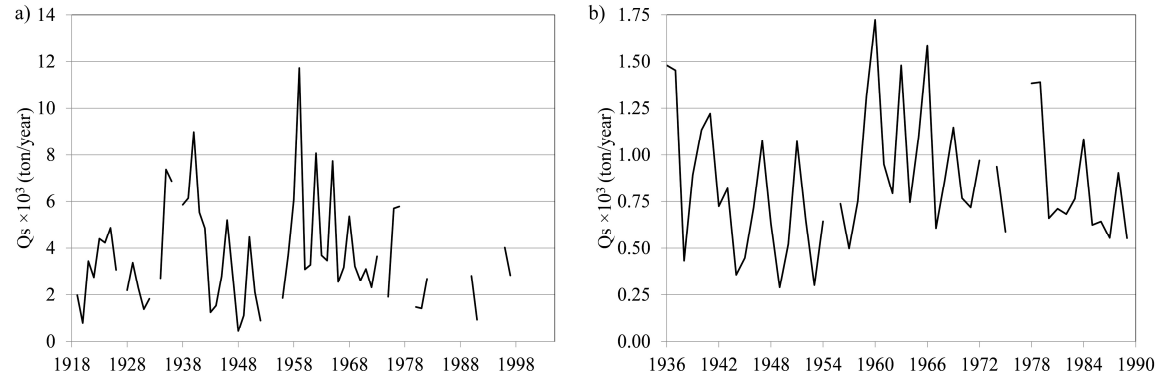

Figure 2.16: Annual suspended sediment fluxes temporal evolution at: a) Ponte Vouzela station; b) Ponte Águeda station.

Considering that suspended sediment flux at Vouga river mouth can be assumed as the sum of suspended sediment loads at the Ponte Vouzela and Ponte Águeda stations, and also an approximation of the suspended sediment flux discharging into Ria de Aveiro, the results show that there is a decrease between 1967 and 1988, with an average annual value of 4000 ton (Figure 2.17).

The obtained values for annual suspended sediment flux represent approximately only 1% of the Vouga drainage basin total sediment production at Ria de Aveiro lagoon mouth (Figure 2.17; Table 2.4). This is explained by the fact that the obtained values represent only a part of the sediment production, that corresponds to the total volume of eroded sediments. Moreover, the obtained results are significantly lower comparing to the estimations of Teixeira (1994) for the average sediment volume transported by the rivers into the lagoon, since is only an estimation for the Vouga river.

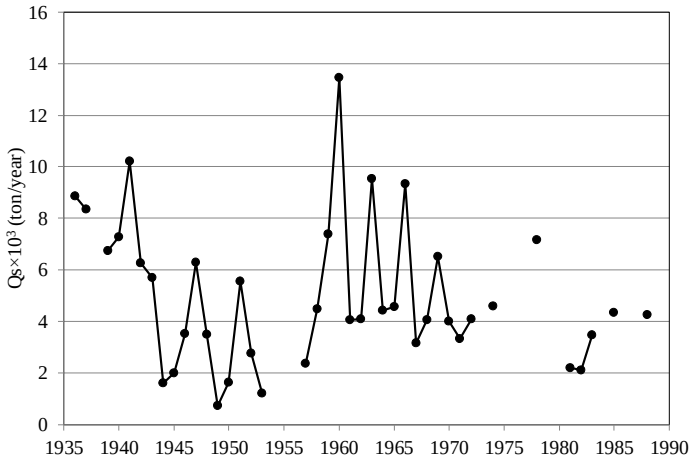

Figure 2.17: Vouga river suspended sediment flux evolution in the 1936-1988 period into the Ria de Aveiro.

Additionally, analysing the average monthly suspended sediment flux evolution along the year, it is expected to present maximum values at February (around 1000 ton) and minimum at August, of approximately 40 ton (Figure 2.18).

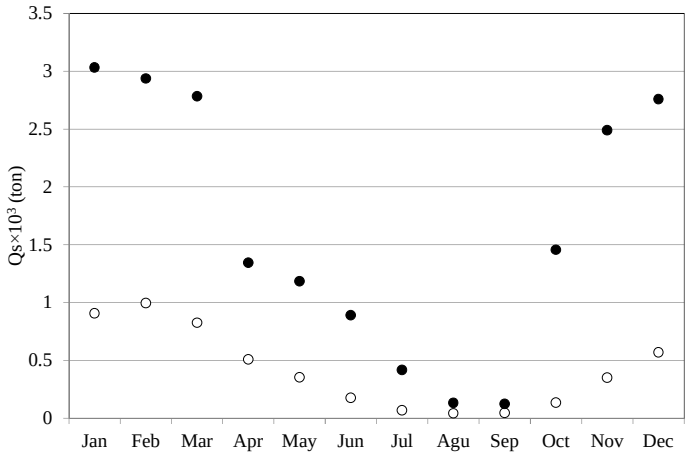

Figure 2.18: Monthly Vouga river suspended sediment flux into the Ria de Aveiro, along the year (○ – average and ● – maximum values).

2.4 Conclusions

Ria de Aveiro is a mesotidal lagoon, where the tide is the main forcing, which is characterized by semi-diurnal and fortnight periodic time-scales. Flood period is longer than the ebb, inducing higher velocities, characterizing the lagoon as ebb dominant at central area and flood dominant at upstream areas (Oliveira *et al.*, 2006; Lopes *et al.*, 2006; Picado *et al.*, 2010; Lopes and Dias, 2015). Over time, were observed significant changes in channels depths and geometry, due to anthropogenic and natural morphologic changes. These changes have an impact on tidal dynamics (Araujo *et al.*, 2008; Dias and Picado, 2011; Picado *et al.*, 2009; 2010).

Lagoon fine sediments derived mostly from the fluvial discharges, which present most of its content, silt and clay. However, since the lagoon origin is related with coastal sediment processes, the sand percentage is high. The granulometric distribution of the bottom sediments and SSC temporal evolution at the inlet and main lagoon channels, by the analysis of samples collected in surveys performed in the frame of this research, at winter/spring and summer/autumn conditions, showed that:

- There is an increase of silt-clay fraction on the bottom sediments for winter/spring conditions at Espinheiro and Ílhavo stations, highlighting the channel's upstream areas contribution;
- The bottom sediments present also an increase of gravel fraction in winter/spring conditions at Barra and S. Jacinto stations;

- SSC present higher values for samples with lower salinities, confirming that suspended sediments supply is done mainly by channels upstream areas.

Generally, lagoon fluvial tributaries are located at the head of the main channels, being the Vouga river the main tributary. Ria de Aveiro sediment transport is directly related with the river's sediment inputs, being the suspended sediment transport the main transport mechanism. However, there is currently no sediment data monitoring program in place, for the lagoon fluvial tributaries. Therefore, it was only possible to analysed the water discharges and SSC existing past data, for the Vouga river at Ponte Vouzela station and its main tributary, the Águeda river at Ponte Águeda station. The performed analysis indicated that:

- Vouga river discharges present most of its values lower than 100 m^3/s, but it can present higher discharges. The higher discharges are in the range of 200-400 m^3/s, being observed its frequency decrease in the 1980-2010 period;
- For Águeda river most of the discharges show values lower than 55 m^3/s, with the higher discharges in the range 110-165 m^3/s;
- Vouga and Águeda rivers discharges are directly related with the rainfall at the Vouga drainage basin, being observed that minimum and maximum values are recorded in August and February, respectively;
- SSC data reveal that most of the samples are in the interval 10-20 mg/l, at the Vouga river and in the interval 3-3.5 mg/l, at the Águeda river. However higher SSC in the 50-150 mg/l interval were observed at both station.

Considering the importance of the Vouga river suspended sediment fluxes into the Ria de Aveiro, it was applied the SRC methodology to the past existing paired of daily discharges and SSC data at Ponte Vouzela and Ponte Águeda stations, in order to obtain estimations of the Vouga and Águeda river's suspended sediment loads and evaluated its temporal evolution. The estimations results indicate that:

- There is a decrease of the suspended sediment loads along the time at both rivers;
- Major sediment fluxes are observed in February and the lowest in August/September.

Moreover, considering that the suspended sediment flux into the Ria de Aveiro corresponds approximately to the sum of the suspended sediment flux at the Ponte Vouzela and Ponte Águeda stations, it presents a decrease in the 1967-1988 period and the maximum and minimum fluxes are expected in February and August, respectively.

It must be highlighted that this evaluation of the Vouga river suspended sediment fluxes into the lagoon is not important by its quantitative information, since the used data and methodology have presented limitations, but it gives a qualitative indication of the suspended sediment flux evolution along the year.

3 Morphological evolution of the Ria de Aveiro harbour area

3.1 Introduction

Morphological changes in estuaries and coastal lagoons are very complex, and their study constitutes a challenging task in coastal research (Plecha *et al.*, 2007). However, knowledge of the spatial and temporal distribution of sediments, including the processes of transport, deposition and erosion, is fundamental for making comprehensive decisions on a wide variety of management issues (Molinaroli *et al.*, 2009). Long-term trends for proper management of coastal ecosystems are difficult to achieve from brief field experiments. Nevertheless, a long-term and large-scale perspective of the coastal system may be obtained by analysing a sequence of bathymetric surveys over a time period, despite the associated errors (Morton *et al.*, 2000; Sarreta *et al.*, 2010).

The substantial changes that have taken place in the Ria de Aveiro during its history result from a combination of natural processes and human activities, and the morphological responses to such activities. For several years the inlet and harbour area were subjected to major modifications (*e.g.* the artificial opening of the inlet in 1808 and the expansion of

harbour infrastructures between 2001 and 2006), which were decisive to the actual lagoon configuration.

In this chapter a morphodynamic characterization of the Aveiro harbour area and the main channels downstream areas between 2001 and 2012 is performed, based on the analyses of bathymetric data collected by APA. The morphological evolution was reconstructed through GIS analysis and was related with dredging operations and engineering works, arising from the harbour development. This analysis has provided insights in the morphodynamics of the inlet and main channel in the 2001-2012 period, as well as identifies the main morphological trends.

3.2 Aveiro harbour

The Aveiro harbour facilities occupies the inlet area and main lagoon channels downstream areas (red polygon in Figure 3.1). This area has a major role in the lagoon dynamics, since it is the transition zone between the ocean and the interior of the lagoon. The inlet dynamics affects the entire lagoon morphodynamics, influencing the tidal prism and the balance depths of the channels. Several engineering works were carried out to ensure harbour channels navigability, which have affected the natural morphological evolution of the lagoon.

The harbour area comprises the navigation channels that provide access and the operational areas. In the performed analysis, the harbour area was divided in different sub-areas (Figure 3.1), considering the harbour terminals (CFP, NT, LBT, HFP, ST) and navigation channels (MC, SJAB, SJC, EC).

Since the opening of the inlet in 1808, the harbour infrastructures has been vastly improved, with a major expansion in the period between 2001 and 2006, when new terminals were constructed (Table 3.1).

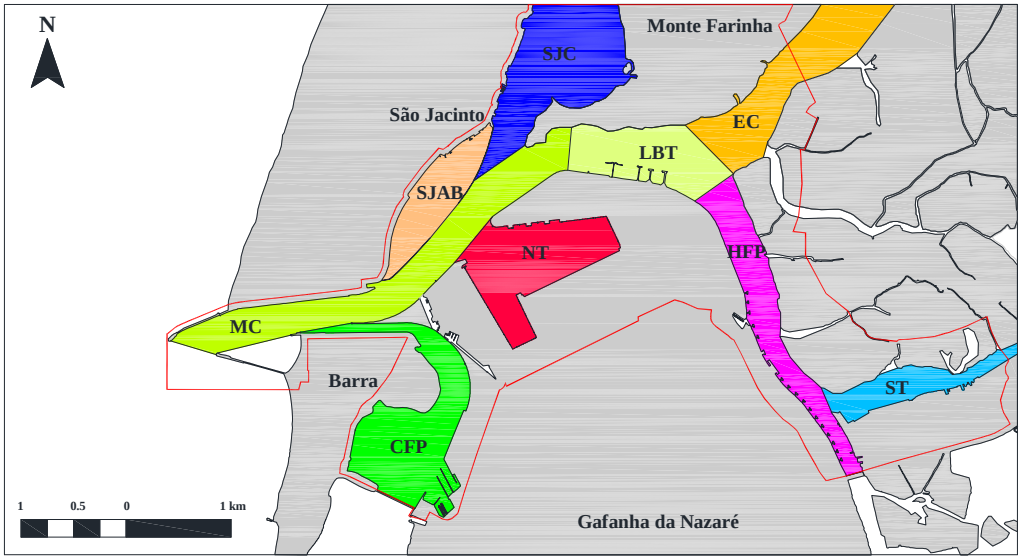

Figure 3.1: Harbour area division in sub-areas: MC – Main Channel; CFP – Coastal Fishing Port; SJAB – S. Jacinto Air Base; NT – North Terminal; SJC – S. Jacinto Channel; LBT – Liquid Bulk Terminal; EC – Espinheiro Channel; HFP – High-sea Fishing Port; ST – South Terminal.

Adding to the structural works, dredging operations were carried out regularly, in order to maintain the navigation depths necessary for harbour operation. In the Table 3.2 are presented the dredged volumes and its location, by year, for the period between 2001 and 2010. Dredging operations have taken place both at navigation channels ('Dredging operations in harbour channels') and harbour terminals ('Other dredging operations'). However, in the case of the dredging operations performed at navigation channels ('Dredging operations in harbour channels') its exact location was not available for this analysis.

The analysis of the dredged volumes in the navigation channels along the years show that after 2008, there is a decrease in comparison to the average annual volume of approximately 400000 m^3, registered until this date. The dredged volumes at harbour terminals present a high variability, with a maximum value registered in 2006, due to NT enlargement area by the excavation of dry areas.

Table 3.1: Chronology of major Aveiro harbour and inlet interventions (Teixeira, 1994; Plecha, 2011).

Period	Event	Description
1802-1808	Opening of the artificial inlet	
1818	Construction of the North breakwater	New breakwater built at 300 m North of the former
1858-1886	Several engineering works	Reinforcement of the South breakwater, construction of a new North breakwater (1859) and connection of the Mira channel to the lagoon
1932-1936	1st Phase of the inlet's improvements	New North breakwater with 470 m, a triangular 'dam' to regulate the tidal prism in the inlet and dredging operations in the inlet and navigation channel
1948-1958	Construction and extension of the breakwaters	Extension in 710 m of the North breakwater and constructing of a new South breakwater with 900 m
195?-1960	2nd Phase of the inlet's improvements	Extension of the North breakwater, construction of a new South breakwater and dredging operations at the inlet and surrounding areas
1968	Construction of ST	
1981-1986	Extension of the North breakwater	Extension in 520 m of the North breakwater
1998	Construction of CFP	
1999-2001	North breakwater reparation	
2000-2006	Expansion works	Expansion of the NT and construction of the LBT
2012-2013	Extension of the North breakwater	Extension in 200 m of the North breakwater

Table 3.2: Dredged volumes at Aveiro harbour area, between 2001 and 2010 (APA, 2012).

Year	Dredging operations in navigation channels (m^3)	Other dredging operations (m^3)		Total volume (m^3)
		Volume (m^3)	Location	
2001	333343			333343
2002	442024	753600	ST, NT, CFP	1195624
2003	435535			435535
2004	365364	1500000	NT	1865364
2005	397391			397391
2006	470090	5334362	NT	5804452
2007	448452	466760	NT	915212
2008	397247	412454	LBT, ST, Inlet	809701
2009	237572	1099223	Inlet	1336795
2010	97853	279000	CFP, HFP, LBT, ST	376853

3.3 Methodology

Bathymetric data can be embedded in surfaces through their interpolation, allowing an estimate of non-sampled locations depth from the points sampled in the same area. The accuracy of the generated surfaces depends on the ability of the interpolation methods in correctly predicting the depth at un-sampled locations (Merwade *et al.*, 2006). *ArcGis* software by *3D Spatial Analyst* extension allows creating a regular array based on scattered sample points (Merwade *et al.*, 2006; Gonçalves *et al.*, 2014).

The used bathymetric datasets were drawn from 9 monitoring campaigns, conducted by APA in June 2001, July 2003, November 2004, September 2005, October 2006, September 2007, December 2008, January 2010 and February 2012. The datasets were separately interpolated through the *Natural Neighbours* algorithm (cell size of 5 m) with the *ArcGis* software, to obtain the raster files representative of the channels bottom surfaces.

Bathymetric data analysis was performed through the determination of different indicators, namely the area distribution by depths intervals, the elevation differences and sediment budgets between surveys. These indicators were determined based on *ArcGis* tools, namely: a) area distribution using the '*Raster Calculator*' tool to determine the number of cells of the input raster in the defined depths interval; b) elevation differences with '*Minus*' tool, which subtracts the value of the second input raster from the value of the first input raster on a cell-by-cell basis, generating a raster map of depth differences, enabling a detailed assessment of the morphological changes location; and c) sediment budgets with '*Cut/Fill*' tool, which calculates the volume changes between two surfaces and generates a raster map with the volume differences and an attribute table, with the corresponding values.

The *ArcGis* tools previously described must be applied to an equal area of analysis. Since the bathymetric datasets cover different areas, two areas were defined that result of the intersection of the areas of the surveys between 2004 and 2008 (area A1) and the areas of all surveys (area A2). In Figure 3.2 the extension of both areas are presented. The main differences between the two areas is that area A1 includes the downstream area of S. Jacinto and Espinheiro channels.

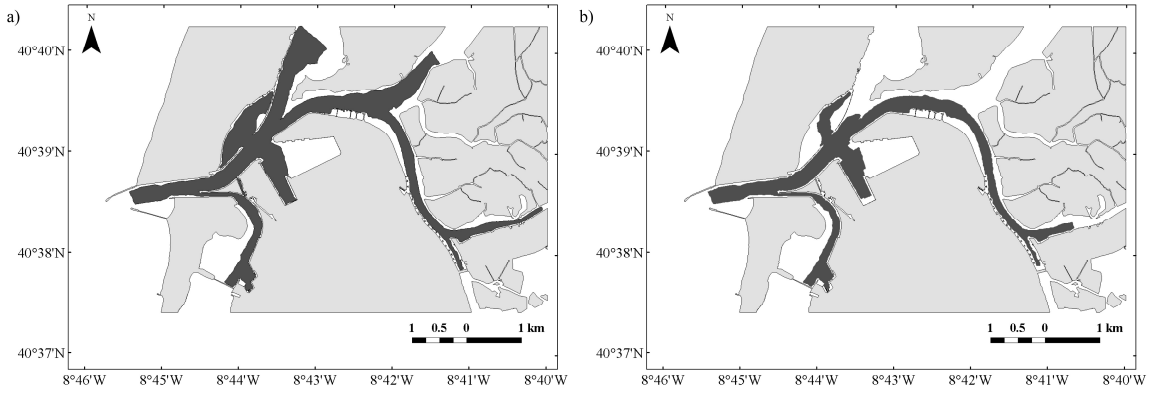

Figure 3.2: Areas of surveys intersection: a) A1; b) A2.

Moreover, the harbour area was subjected to annual dredging operations, although the month in which they were performed, was not available for this analysis. Therefore, in the sediment budgets estimates, the temporal location of the dredging operations (Table 3.2) relatively to surveys dates were considered according to Figure 3.3.

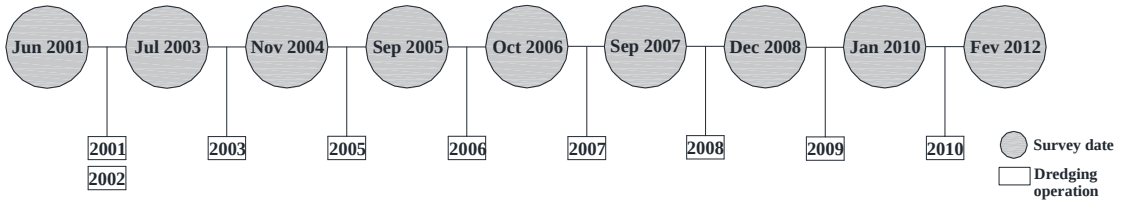

Figure 3.3: Timeline of the performed surveys and dredging operations.

3.4 Results and discussion

3.4.1 Area distribution by depth range

The analysis of the bathymetric datasets depth distribution reveals that the deepest areas are located in the main channel (MC), between the inlet and the NT terminal, with depths higher than -15 m (CD). Most of the study area shows depths between -10 and -5 m (CD). The S. Jacinto and Espinheiro channels present the minor depths, up to -5 m (CD) (results in Appendix B1).

In the Table 3.3 is presented the area percentage by depth interval, for the intersection area of all surveys (area A2; Figure 3.2). The results show that there is a deepening between 2001 and 2012. However, in the 2001-2006 period despite being observed an area increase in the

<-15 m and -15/-10 m depth intervals and a decrease in the -10/-5 m and -5/-1 m, the variations between consecutive surveys are minor. The main deepening is observed in 2006/2007, with an area increase of 0.23 km^2 in the -15/-10 m depth range (Figure 3.4), which is related to the NT enlargement area, due to harbour expansion works. After 2007, a similar behaviour to that observed in the 2001-2006 period is verified, with minor area differences between consecutive surveys, in the depths intervals.

Table 3.3: Aveiro harbour area distribution by depth range (CD), between 2001 and 2012.

Depth interval (m)	Area (km^2)								
	2001	**2003**	**2004**	**2005**	**2006**	**2007**	**2008**	**2010**	**2012**
<-15	0.44	0.47	0.50	0.48	0.54	0.55	0.62	0.61	0.62
-15/-10	0.59	0.58	0.56	0.59	0.62	0.85	0.81	0.80	0.76
-10/-5	1.25	1.29	1.25	1.22	1.15	0.89	0.90	0.87	0.90
-5/-1	0.53	0.48	0.50	0.51	0.49	0.51	0.49	0.52	0.52
>-1	0.05	0.05	0.05	0.05	0.06	0.06	0.05	0.06	0.07

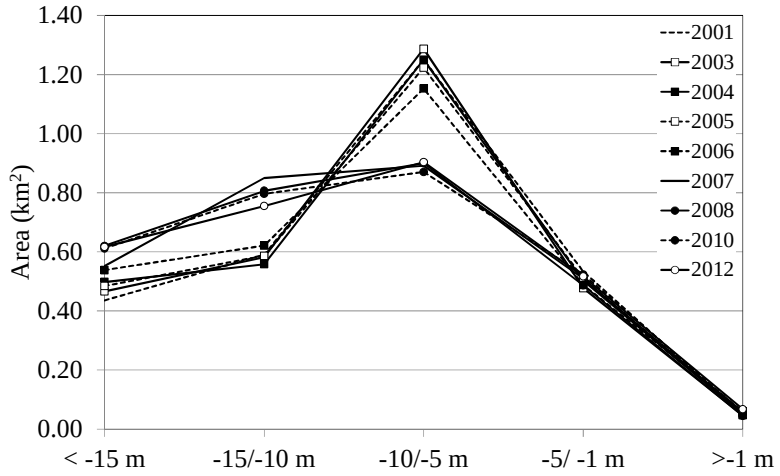

Figure 3.4: Area distribution by depth ranges, between 2001 and 2012.

Moreover, it was analysed the area percentage distribution by depth range for the different sub-areas of the harbour area, in order to assess where the major variations have occurred (Tables 3.4 and 3.5). In general, at the navigation channels is verified deepening, related mainly to the dredging operations. MC presents an area increase for depths higher than 15 m, from 40% in 2001 to 55% in 2012. The same is observed for SJC and EC channels, with area increase in the -15/-10 m and -10/-5 m depth intervals, respectively. However, at SJAB is observed an area decrease in the range -10/-5 m, which is expected, since is a shelter area.

Table 3.4: Area distribution (%) by depth range (CD), between 2001 and 2012, for navigation channels.

Depth interval (m)	2001	2003	2004	2005	2006	2007	2008	2010	2012
MC									
<-15	39.72	42.50	45.34	43.83	48.64	50.32	55.35	53.82	54.68
-15/-10	41.70	38.63	37.30	38.98	38.37	37.53	34.80	34.14	32.07
-10/-5	17.09	17.53	15.23	14.45	11.95	10.96	8.90	10.83	11.38
-5/-1	1.48	1.34	2.12	2.73	1.03	1.18	0.95	1.21	1.86
>-1	0.01	0.00	0.02	0.01	0.01	0.01	0.00	0.00	0.01
SJAB									
<-15	0.00	0.00	0.00	0.00	0.00	0.00	0.00	0.23	0.00
-15/-10	8.07	2.91	0.95	1.77	2.53	2.33	2.12	4.97	4.42
-10/-5	77.64	76.48	75.96	73.24	70.59	65.18	60.94	49.60	47.32
-5/-1	14.26	20.36	22.64	24.35	25.82	31.21	35.84	44.14	46.50
>-1	0.03	0.25	0.44	0.64	1.06	1.28	1.10	1.06	1.76
SJC									
<-15	0.12		0.61	1.04	0.92	0.86	0.79		0.92
-15/-10	6.84		9.29	13.60	10.20	11.08	11.08		14.77
-10/-5	48.25		37.09	38.64	36.00	36.51	35.83		33.26
-5/-1	42.71		38.82	42.13	37.01	34.20	38.37		40.91
>-1	2.07		14.20	4.60	15.87	17.34	13.92		10.15
EC									
<-15			0.00	0.00	0.00	0.00	0.00		0.00
-15/-10			0.00	0.00	0.73	1.65	2.21		7.74
-10/-5			27.66	30.94	34.30	31.54	33.54		32.41
-5/-1			71.57	68.64	64.66	66.64	64.00		59.68
>-1			0.77	0.41	0.30	0.16	0.24		0.17

Expansion works had an important role in the harbour terminals evolution, especially at NT, where new areas were created by excavation of dry areas. The area percentage by depth range shows that before 2005, NT had most of its area in the -10/-5 m interval, but as consequence of the enlargement of its area, an increase from 7 to 21% in 2005/06 and 21 to 97% in 2006/07 in the -15/-10 m interval is verified. The harbour expansion works have also influence the LBT terminal, with its deepening in the <-15 m and -15/-10 m ranges until 2008, mainly due to dredging operations. In the case of ST terminal, the expansion works have only an impact at 2002, where an area increase in the -10/-5 m range is verified, due to dredging operation. After this date is observed a depth decrease, only changed in 2008, when a dredging operation was performed. HFP and CFP terminals do not present major changes since no significant engineering works in the 2001-2012 period were carried out. The only exceptions are the 2001/03 at CFP and in 2010/12 at HFP, where a depth increase is

observed, which matches with the years when dredging operations were performed (2002 and 2010).

Table 3.5: Area distribution (%) by depth range (CD), between 2001 and 2012, for harbour terminals.

Depth interval (m)	2001	2003	2004	2005	2006	2007	2008	2010	2012
NT									
<-15	0.00	0.00	0.00	0.00	0.00	0.00	0.57	1.76	0.00
-15/-10	10.90	8.34	8.70	6.98	21.32	97.23	94.67	93.75	90.04
-10/-5	79.37	81.72	85.80	87.10	78.16	2.77	4.75	4.50	9.77
-5/-1	9.20	9.82	5.50	5.91	0.53	0.00	0.02	0.00	0.18
>-1	0.53	0.13	0.00	0.00	0.00	0.00	0.00	0.00	0.00
CFP									
<-15	0.00	0.00	0.02	0.03	0.11	0.09	0.16	0.15	0.34
-15/-10	3.44	5.26	3.54	5.35	5.75	6.37	4.68	5.48	5.51
-10/-5	37.20	34.16	33.81	30.81	30.92	30.42	30.97	30.32	27.38
-5/-1	49.16	50.22	52.26	52.17	50.41	51.70	54.45	51.40	51.12
>-1	10.19	10.36	10.37	11.63	12.81	11.43	9.75	12.65	15.65
LBT									
<-15	0.00	0.00	0.13	1.17	1.40	0.11	3.51	4.82	5.08
-15/-10	20.74	33.61	34.44	34.81	36.23	38.28	38.80	36.59	34.15
-10/-5	52.12	45.76	43.00	42.02	39.78	38.43	37.62	35.36	34.48
-5/-1	27.10	20.61	22.31	21.86	22.56	23.01	20.00	23.07	26.15
>-1	0.04	0.03	0.12	0.13	0.03	0.17	0.07	0.16	0.14
HFP									
<-15	0.00	0.00	0.00	0.00	0.00	0.00	0.00	0.00	0.00
-15/-10	1.96	1.51	1.06	2.28	0.00	0.04	0.00	0.00	0.00
-10/-5	74.89	74.90	74.10	73.72	75.58	75.69	74.78	74.23	80.15
-5/-1	23.02	23.49	24.68	23.66	24.34	24.22	25.21	25.71	19.82
>-1	0.13	0.11	0.16	0.35	0.07	0.05	0.02	0.06	0.03
ST									
<-15	0.00	0.00	0.00	0.00	0.00	0.00	0.00	0.00	0.00
-15/-10	0.00	0.00	0.00	0.00	0.00	0.00	0.00	0.00	0.00
-10/-5	31.79	74.77	67.26	66.29	57.17	51.69	80.23	65.49	69.87
-5/-1	65.36	24.69	31.79	32.78	41.32	46.31	19.75	34.44	29.89
>-1	2.85	0.54	0.95	0.93	1.51	2.00	0.02	0.07	0.24

3.4.2 Elevation differences

In order to have a better understanding of the depth differences between consecutive bathymetric data, a scale divided in six classes was created, function of the elevation variations: a) < -3 m; b) -3/-0.5 m; c) -0.5/0 m; d) 0/0.5 m; e) 0.5/3 m and f) > 3 m. Based on this scale it was determined the area percentage of each class for the different sub-areas (Figures 3.5 and 3.6) and created maps with the spatial classes' distribution (results in Appendix B2).

Navigation channels show mainly negative elevation differences between consecutive surveys, with exception of the SJAB. Elevation differences in SJC are mostly in the -0.5/0 m class in the period from 2006 to 2008 (approximately 40%), followed by the 0/0.5 m and -3/-0.5 m classes, with percentages of approximately 29 and 17% (on average), respectively. However, in the 2004/05 and 2005/06 periods, opposite patterns are observed, with an area percentage of around 80% in the -3/-0.5 m class, changing to the 0.5/3 m in the following period (Figure 3.5a), indicating that a dredging operation was probably performed. This way, only looking to the periods without dredging operations (2006/07 and 2007/08 periods), most of the area (around 60%) presents negative elevation differences, between consecutive surveys.

The EC channel presents a similar behaviour to SJC, with most of the area presenting elevation differences in the -0.5/0 m class, around 40% (on average), followed by the 0/0.5 m and -3/-0.5 m classes, with percentages of 34 and 19% (on average), respectively (Figure 3.5b). Additionally, the results show that there are no significant variations, being observed similar percentages for the different classes, except in the 2006/07 period, where an area increase in the 0/0.5 class is observed, which is probably related with the harbour area enlargement.

In MC is verified negative elevation differences in most of the period's between consecutive surveys, with a percentage of 34% (on average) in the -3/-0.5 m class, followed by 24% (on average) in the 0.5/3 m (Figure 3.5c). Noteworthy, is that in the 2001/03, 2005/06 and 2007/08 periods more than 40% of the area present elevation differences in the -3/-0.5 m class, which indicates that the verified deepening is probably associated with dredging operations.

In opposition to the other navigation channels, SJAB presents most of the elevation differences in the 0.5/3 m class, highlighting the deposition trend, as a shelter area (Figure 3.5d). However, in the 2001/03 period more than 60% of the area registered elevation differences in the 0.5/3 m class, which can indicate that a dredging operation was performed before 2001, since from 2003 until 2012 is observed stability with most of the elevation differences in the 0/0.5 m class, between consecutive surveys.

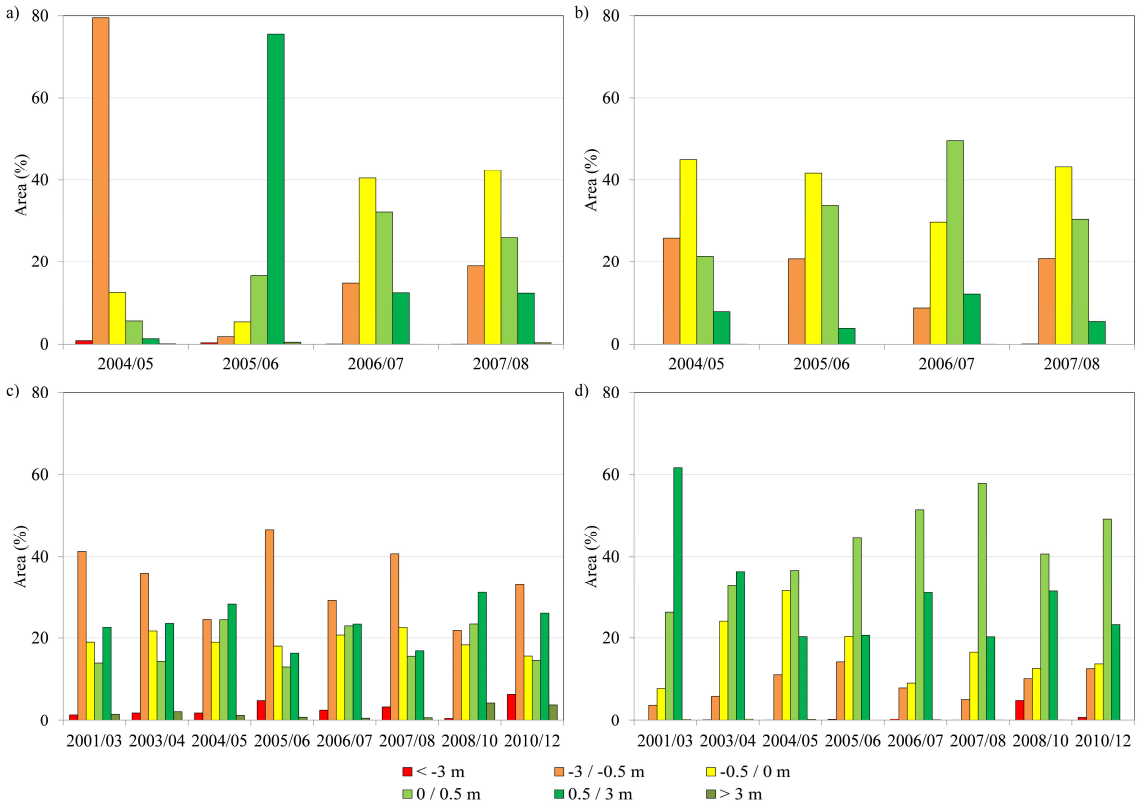

Figure 3.5: Area distribution as function of elevation differences, at the navigation channels: a) SJC; b) EC; c) MC; d) SJAB.

In the CFP and HFP terminals most of its area present elevation differences between consecutive surveys in the 0/0.5 m class, 40 and 45% (on average), respectively, followed by the -0.5/0 m, with percentages of 32 and 40% (Figure 3.6a,d). The results are consistent with the few performed dredging operations. ST terminal presents a similar behaviour, with most of its area presenting elevation differences in the 0/0.5 m class (50% on average), which is only changed in the 2001/03 and 2007/08 periods, where an area increase of 77 and 51%, respectively in the-3/-0.5m class is verified, due to dredging operations (Figure 3.6e). In opposition, LBT terminal presents mostly negative elevation differences between surveys, around 60% (on average), in the -3/-0.5 and -0.5/0 m classes (Figure 3.6c). Noteworthy, is the area percentage increase in the 0.5/3 m class after 2006, which can be related with the docks piers implantation, that acts as sediment traps.

NT terminal is the only harbour sub-area presenting the higher average area percentage with negative elevation differences lower than 3 m, being observed a maximum value of 64% in the 2006/07 period, when its area was enlarged by excavation of dry areas (Figure 3.6b).

After 2007, the elevation differences between surveys are in the 0/0.5 m class, highlighting the deposition trend of this area.

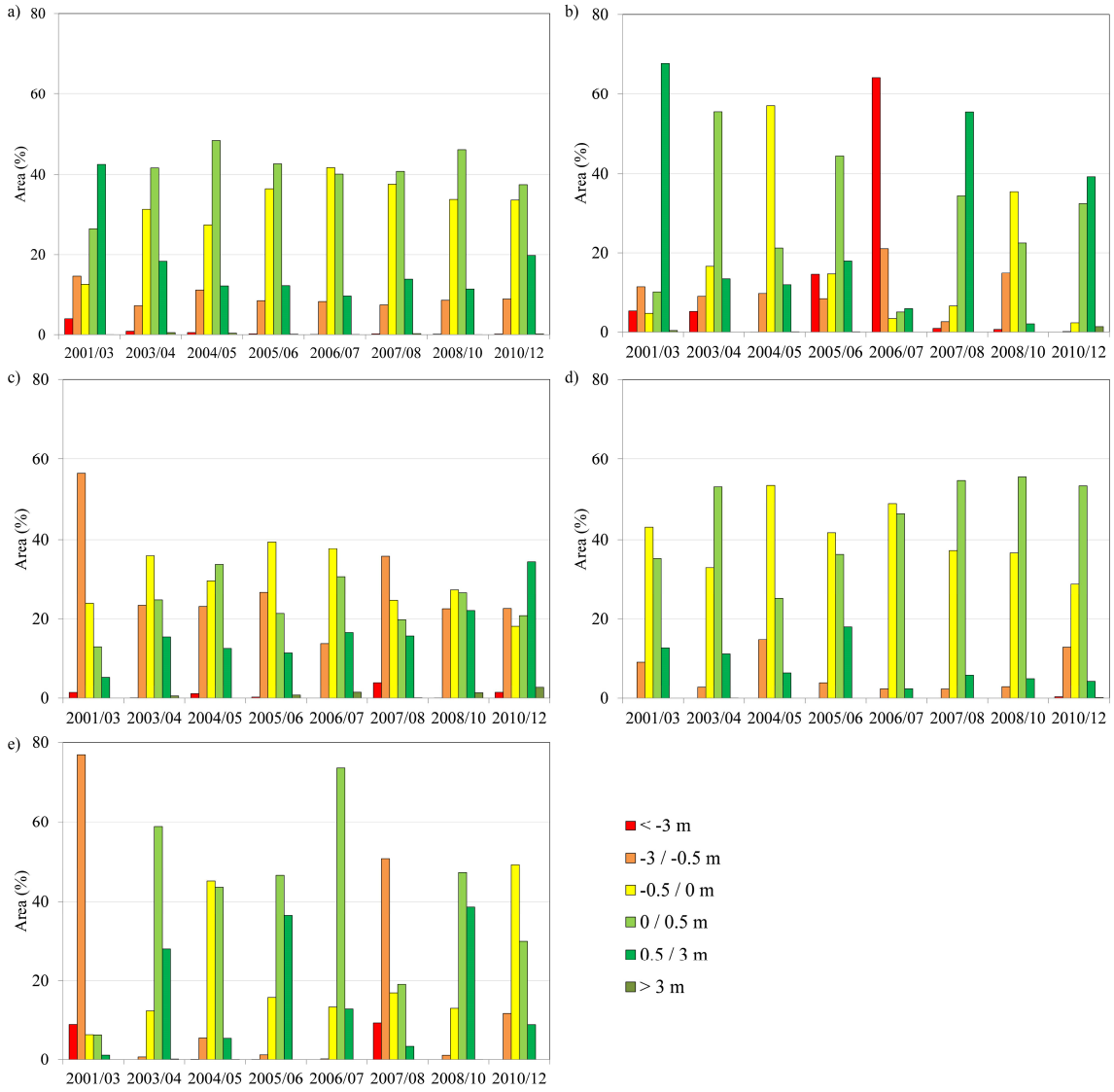

Figure 3.6: Area distribution as function of elevation differences, at the harbour terminals: a) CFP; b) NT; c) LBT; d) HFP; e) ST.

The quantification of the area percentage for the different classes was complemented with the representation of its spatial distribution (results in Appendix B2). This analysis allows to assess if previous results are dependent on natural evolution or dredging operations, since opposite patterns in consecutive years, is an indication of possible dredging operations.

The spatial distribution of the elevation differences in SJC shows that in fact a dredging operation was performed in 2004/05, leading to deposition in the following period 2005/06.

The same is observed in the MC channel and NT, LBT and ST terminals, especially in areas with negative elevation differences higher than 3 m (*e.g.* 2005/06 in MC, 2006/07 in NT, 2007/08 in LBT and ST). This indicates that negative elevation differences lower than 3 m are associated with dredging operations. Moreover, after dredging operations, positive elevation differences in the 0.5/3 m class are observed. In the case of the LBT, is observed that the deposition areas are restricted to the docking piers area, which indicate that the docking piers act as sediment traps.

3.4.3 Sediment budgets

The previous analysis has given a qualitative indication of the different harbour sub-areas morphological trends. In this section, a quantitative analysis by the estimation of net balance volumes and deposition/erosion rates for the different harbour sub-areas considering the dredged volumes, is made.

In the case of the harbour terminals, the date and dredging operations volumes are well known (Table 3.2). However, its exact location was not available for this analysis, so it was assumed that the dredged volume was removed uniformly in all area. Additionally, due to NT area enlargement by excavation from dry areas, there are no bathymetric data of these new areas in the 2001-2005 period. Therefore, it was not considered the dredged volumes of 2004 and 2006 in the sediment budgets estimates.

For the navigation channels, the sediment budgets estimates were more difficult to determine, due to the lack of detailed information on the dredging operation's location ('Dredging operations in harbour channels'; Table 3.2). Thus, for the MC, SJC and EC channels it was assumed, as an approximation, that the dredged volumes in each year were proportional to its area and uniformly removed in all area. In the case of SJAB, it was considered that no dredging operations were performed.

In the case of the navigation channels, despite the previous referred difficulties due to lack of information, the obtained balance volumes are coherent with the previous analysis (Table 3.6). SJAB sediment budgets results indicate deposition, which is expectable since it is a shelter area. The same trend is observed for the MC channel, despite considering annual dredging operations, which is expect since it is the main harbour access and is necessary to ensure its navigability, leading to frequent dredging operations. In opposition, the EC channel has experienced an erosive balance, even without considering dredging operations.

This behaviour can be explained by the fact that areas nearby EC channel have been dredged and due to stronger currents observed at this channel (Dias *et al.*, 2003), the sediments may have been transported to the dredged areas.

In the SJC channel, only in the 2006/07 and 2007/08 periods no dredging operations were performed, according to the previous findings. Moreover, since this channel is not access of harbour terminals, probably less dredging operations were performed and the assumption of annual dredging operations in the 2006-2008 period is not totally correct. Therefore, only looking to the bathymetric differences volume, the SJC has experienced erosion, which is in agreement with the previous elevation differences results in the 2006/07 and 2007/08 periods, presenting mainly negative differences. This behaviour is similar to observed at EC channel and is probably related to the sediment transport to dredged areas in the MC channel, since high velocities are expected at this channel.

Table 3.6: Sediment budget at navigation channels. between 2001 and 2012.

	Period	**01/03**	**03/04**	**04/05**	**05/06**	**06/07**	**07/08**	**08/10**	**10/12**
MC	**DV (×10³ m³)**	740	223	243	287	274	243	145	60
	BD (×10³ m³)	-207	-144	-13	-652	-207	-461	335	-193
	NB (×10³ m³)	533	79	230	-365	67	-219	481	-133
	Rate (cm/year)	49	7	21	-33	6	-20	44	12
SJAB	**DV (×10³ m³)**								
	BD (×10³ m³)	148	67	22	10	46	42	-8	22
	NB (×10³ m³)	148	67	22	10	46	42	-8	22
	Rate (cm/year)	80	36	12	5	25	23	-4	12
SJC	**DV (×10³ m³)**			101	119	114	101		
	BD (×10³ m³)			-595	502	-24	-42		
	NB (×10³ m³)			-494	621	90	59		
	Rate (cm/year)			-78	98	14	9		
EC	**DV (×10³ m³)**			54	63	60	53		
	BD (×10³ m³)			-73	-65	24	-60		
	NB (×10³ m³)			-19	-2	84	-7		
	Rate (cm/year)			-6	-0.4	25	-2		

DV – Dredged volume; BD – Bathymetric differences volume; NB – Net balance volume (Minus sign indicates erosion).

Generally, the sediment volume balance indicate deposition in the harbour terminals (Table 3.7). The periods in which is verified erosion, present low rates (*e.g.* HFP in the 2004/05 and 2006/07 periods). The deposition rates show different orders of magnitude, with CFP and HFP terminals presenting values lower than 10 cm/year. On the other hand, in ST the deposition rates are approximately 20 cm/year (on average), and can reach 40 cm/year in the periods following dredging operations. This can be explained by the fact that CFP and HFP

are located at Mira and Ílhavo channels downstream areas, where stronger currents are expected.

NT and LBT terminals were subjected to significant changes as a result of the harbour expansion works, with the area enlargement and the docking piers construction, respectively. NT sediment budgets results indicate high erosion rates in most of the analysed periods, until 2007. These results are in disagreement with previous findings, since until 2007 important dredging operations where performed, being expected a deposition balance. However, these results can be related to the fact that in the sediment budgets not all dredged volumes were taken into account, as previously referred. In the case of LBT erosion was observed before 2007, changing to deposition after this date, when docking piers were implemented. This opposite pattern can be related with the piers effect, that act as sediment traps.

Table 3.7: Sediment budgets at harbour terminals, between 2001 and 2012.

	Period	01/03	03/04	04/05	05/06	06/07	07/08	08/10	10/12
CFP	DV (×10³ m³)	34							45
	BD (×10³ m³)	-5	48	8	44	10	38	9	-31
	NB (×10³ m³)	29	48	8	44	10	38	9	14
	Rate (cm/year)	6	8	2	9	3	7	2	3
NT	DV (×10³ m³)	520				467			
	BD (×10³ m³)	24	-248	-12	-354	-966	133	-74	208
	NB (×10³ m³)	544	-248	-12	-354	-499	133	-74	208
	Rate (cm/year)	149	-55	-4	-97	-162	32	-20	57
LBT	DV (×10³ m³)						138		50
	BD (×10³ m³)	-207	-17	-71	-66	33	-145	24	76
	NB (×10³ m³)	-207	-17	-71	-66	33	-7	24	126
	Rate (cm/year)	-52	-3	-18	-14	9	-1	7	38
HFP	DV (×10³ m³)								104
	BD (×10³ m³)	6	51	-6	44	-3	26	22	-31
	NB (×10³ m³)	6	51	-6	44	-3	26	22	73
	Rate (cm/year)	1	9	-2	9	-1	5	5	16
ST	DV (×10³ m³)	199					121		70
	BD (×10³ m³)	-202	45	-1	46	22	-144	72	-8
	NB (×10³ m³)	-3	45	-1	46	22	-23	71	62
	Rate (cm/year)	-2	23	0	20	12	-9	49	42

DV – Dredged volume; BD – Bathymetric differences volume; NB – Net balance volume (Minus sign indicates erosion).

3.5 Conclusions

In this chapter, an analysis of the morphological evolution between 2001 and 2012 of the Aveiro harbour area, which includes the inlet area and main lagoon channels downstream areas, was performed. The adopted methodology, with analysis of different indicators,

allowed to overcome some of the data limitations, namely the dredging operations location and volumes at navigation channels and identified morphological trends for the different sub-areas that integrate the harbour area.

The harbour area was subject to major changes in 2006, due to expansion works, with the NT area enlargement from dry areas and docking piers construction at LBT. Between 2001 and 2012 there was a deepening, equally distributed in the -10/-15 m and lower than -15 m ranges, which have resulted mainly from dredging operations. In general, negative elevation differences between consecutive surveys higher than 3 m are associated with dredging operations, being observed pronounced deposition in the following period, with positive elevation differences in the 0.5/3 m interval.

From the analysis of the different indicators for the harbour terminals areas, the following conclusions can be drawn:

- Main morphological trend is deposition, with NT and ST terminals presenting higher deposition rates, in comparison with CFP and HFP;
- NT terminal is the sub-area where major dredging operations were performed, due to expansion works, presenting between 2003 and 2006 a significant percentage area with negative elevation differences lower than 3 m;
- LBT presents a change in its morphological behaviour in 2006, which is related with docking piers construction, that acts as sediment traps.

Regarding the navigation channels, it was more difficult to identify morphological trends, since the exact location and volumes of the dredging operations was not available. Moreover, the data short time period for SJC and EC channels have also difficult the analysis. Nevertheless, using approximations in the sediment budgets and the different determined indicators, it was possible to identified morphological trends, that look admissible. Overall, for each of the navigation channels area was concluded that:

- MC morphological trend is deposition, which is in agreement with the frequent dredging operations;
- SJAB has been subject to few dredging operations, presenting mainly deposition;
- For SJC there is a short time analysis period, making difficult the identification of a morphological trend. However, the results indicate erosion, which is maybe due to dredging operations in areas nearby and the high velocities, leading to sediment transport to the dredge areas;

- The EC channel present a similar behaviour than SJC, with an erosive balance, which is probably due to the same reasons.

Despite the short period examined and the several human actions performed in the study area, the analysis of different indicators determined from bathymetric data and its relation with performed dredging operations, gives new insights about the morphological trends. Results indicate that in the recent past (2001-2012), the Ria de Aveiro inlet and the main channels downstream areas have shown significant morphological changes, mainly deepening, due to Aveiro harbour development works and dredging operations.

4 Fine sediment laboratory tests

4.1 Introduction

The state of the art in numerical simulation of cohesive sediment transport has advanced considerably in the past years. For engineering applications, reliable predictive results are necessary. Thus, to improve the reliability and predictive capacity of numerical models and obtain better quantitative results, it is necessary to have a complete knowledge of the basic processes of cohesive sediment (Teisson, 1991). Erosion and deposition properties of cohesive sediments are usually described by cohesive transport parameters, *e.g.* critical bed shear stresses, erosion rate coefficient and settling velocity, and their determination can be based on observations and experiments, either *in situ* or in the laboratory (You, 2004; Andersen *et al.*, 2007; Costa and Coelho, 2011; Coelho *et al.*, 2015).

A critical parameter in the fine sediment behaviour and dynamics is the settling velocity, since it is used to calculate the deposition rate and therefore has a significant impact on the temporal and spatial patterns of sediment deposition, because it influences how far a suspended particle may travel before settling (You, 2004; Manning and Dyer, 2007; Markusen and Andersen, 2013). Settling velocity also determines both the vertical distribution of SSC and near-bed deposition flux (Wan *et al.*, 2015). Therefore, its accurate

determination has been a priority in characterizing fine sediment transport, since it increases the reliability and estimation ability of the numerical models.

This chapter presents the results of laboratory tests performed in a settling column at LNEC, with fine sediments collected in the Ria de Aveiro. The main objective of the study was to identify which factors may influence the settling velocity of fine sediments. In particular, tests were performed to evaluate the influence of salinity and initial suspended concentration in the settling velocity. The study also aimed to contribute to the identification of a reference range of settling velocity values and provide insights into deposition processes, and this way, improve the accuracy of the Ria de Aveiro suspended sediment transport numerical modelling.

4.2 Settling velocity of fine sediments

Settling velocity corresponds to the constant velocity at which a particle settles through a static fluid, when the resistance of the fluid exactly equals the downward force of gravity acting on the particle (Mantovanelli and Ridd, 2006). For non-cohesive sediments, the settling velocity is dependent on sediment size, specific gravity and shape, which can be determined with accuracy by Stokes' law (Kumar *et al.*, 2010). However, for cohesive sediment this is not the case, as the sediment is clustered in porous flocs of various sizes and varied composition of clay and silt particles and sometimes organic material (Winterwerp *et al.*, 2006).

Settling properties of cohesive sediments are influenced by flocculation, which is the result of simultaneous processes of aggregation and breakage of particles into aggregates or flocs (Markussen and Andersen, 2013; Shen and Maa, 2015). The flocculation process is complex, due to its dependence on the sediment properties (surface texture, density, shape, size, roundness, structure, degree of aggregation and organic content), inter-particle interactions, ambient fluid properties (density, viscosity, turbulence and salinity) and suspended concentration (You, 2004; Mantovanelli and Ridd, 2008; Cuthbertson *et al.*, 2008, Soulsby *et al.*, 2013). Flocs are less dense, but faster settling than their constituent particles. As flocs grow their effective density generally decreases, but their settling rates rise (Manning and Bass, 2006). Floc settling velocities can be up to four orders of magnitude larger than those of the primary particles (van Leussen, 1999).

Aggregation of the particles depends upon inter-particle collision and cohesion resulting from collision (Liu, 2005; Manning and Bass, 2006; Manning and Dyer, 2007). The collisions lead to the particles aggregation with the formation of flocs. Turbulence can increase particle collisions. However, turbulence may tear large floc apart, thereby limiting the floc size and settling velocity (Hunt, 1986; Johansen and Larsen, 1998).

Due to the fragility of the flocs and its disruption for laboratory analysis, it has been recommended that the settling velocity study should be whenever possible based on *in situ* experiments (Berlamont *et al.*, 1993; Dyer and Manning, 1999; Mantovanelli and Ridd, 2008). Field experiments have the advantage of minimizing the impact on the size distribution of the flocculated sediments. However, the variability of the conditions that occurs in the field, does not allow a study of the settling velocity and its regulating factors in a systematic manner, which can be achieved in controlled laboratory tests (Manning *et al.*, 2007; Portela *et al.*, 2013). Therefore, for many decades the study of the settling velocity was made through laboratory experiments using settling columns (*e.g.* Al Ani *et al.*, 1991; Dankers and Winterwerp, 2007; Kumar *et al.*, 2010; Wan *et al.*, 2015). The results of these experiments have been useful in understanding the physical process of fine sediment settling and to propose empirical and semi-empirical formulas for settling velocity.

4.2.1 Influence of salinity

The role of salinity in the flocculation of fine sediments and the resulting settling velocities have been studied for many decades (*e.g.* Krone, 1962; Jiufa and Zhang, 1998; van Leussen, 1999; Portela *et al.*, 2013; Wan *et al.*, 2015). Salinity was proposed as an important factor in the flocculation of fine sediments, with the ability to modify the settling velocity in brackish and saline waters.

In water with a very low salinity, particles are usually found in a dispersed state. A slight increase in salinity may be sufficient to enable the particles to aggregate and form flocs and induce greater settling velocity (Burt, 1986; Liu, 2005). The fine sediments flocculate because of electrostatic forces created by the surface ionic charges. Salinity modifies the charges by adsorption of cations and the formation of an electrical double layer (Al Ani *et al.*, 1991; Winterwerp and van Kesteren, 2004). This led to the classical theory in estuarine fine sediment transport, where dispersed fine sediment particles in the fresh river water were

expected to flocculate when they meet the more saline water in the estuary (van Leussen, 1999).

However, the role of salinity has come into question more and more, since higher salinities not always seem to increase the settling velocity (Al Ani *et al.*, 1991; van Leussen, 1999; Jiang *et al.*, 2002; Wang *et al.*, 2015). This has led to question the role of salt in the flocculation and even some researchers argued that salinity has no significant effect on the settling velocity (*e.g.* Chen *et al.*, 1994; Berhane *et al.*, 1997).

4.2.2 Influence of sediment concentration

Settling velocity of suspended sediment in estuaries is generally found to increase with SSC, as a consequence of inter-particle collisions and flocculation processes increase (Temmerman *et al.*, 2003). Kranck and Milligan (1992) verified that floc size increases with increasing SSC. However, the floc size is not always positively correlated with SSC. Hill *et al.* (2000) found that the floc size was uniform despite a wide variability in SSC, suggesting that high turbidity might limit floc growth. Therefore, SSC is only important at low levels of turbulence. At high levels of turbulence, the limiting properties of turbulence dominate (van Leussen, 2011). Moreover, above a limit of SSC, the settling flux starts to decrease, because of inter-particle hindrance (Gratiot *et al.*, 2005).

Many studies were carried out to investigate the variation of settling velocity with SSC and have proven the influence of SSC (Krone, 1962; Nicholson and O'Connor (1986); Winterwerp, 2002; You, 2004; Sanchez, 2005; Mantovanelli and Ridd, 2008). However, the degree of its influence varies greatly and settling velocity can vary over orders of magnitude. The dependence of the settling velocity on SSC has been divided into three regimes: free, enhanced and hindered settling. Free settling occurs at low concentrations, the enhanced settling at moderate concentrations and hindered settling at high concentrations (You, 2004). In the free settling regime, the particles settle at a settling velocity that can be determined by application of the Stokes' law (Cuthbertson *et al.*, 2008). At the enhanced settling regime, the settling velocity increases with the SSC, being usually described by the formula:

$$w_s = K \cdot C^m \tag{4.1}$$

where K and m are constants dependent of the type of sediment, turbulence and salinity (Krone, 1962; You, 2004). When the concentration becomes high enough, the settling flocs start to hinder each other in their movements, often resulting in settling rates that are lower

than that for individual, isolate particles, a process generally known as hindered settling (Winterwerp, 2002; Cuthbertson *et al.*, 2008).

4.3 Methodology

4.3.1 Sediment samples

The sediments used in the settling column experiments were collected in the bottom of a tidal channel in the inner part of the Ria de Aveiro on 31th March 2015 (Figure 4.1a). The sediment sample (Figure 4.1b) was passed through a 63 μm sieve, in order to separate the fine and the coarse fraction, being only used the fine fraction.

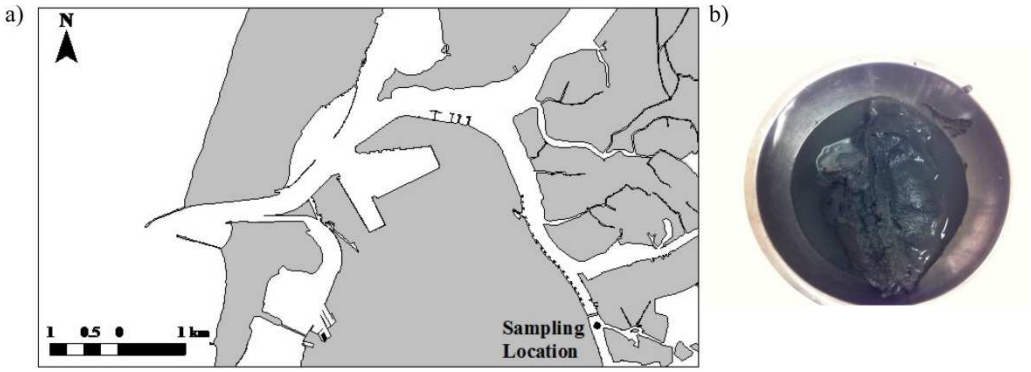

Figure 4.1: Sediment sampling: a) Location; b) Complete sample.

The sediment fine fraction consists mainly of silt sized particles, as indicated by the laser diffraction analysis (*Malvern Mastersized Micro*), with d_{10}, d_{50} and d_{90} of 5, 34 and 84 μm, respectively. Additionally, a mineralogical analysis was carried out using X-ray diffraction techniques, according to the procedures described by Martins *et al.* (2007). The results indicated that quartz is the main constituent (≈60%) followed by feldspars and plagioclases, with approximately 10% and in lower percentages opal, mica and kaolinite (Table 4.1).

Table 4.1: Mineralogical composition of the sediment sample.

Mineral	**(%)**
Quartz	57
Feldspar	13
Plagioclase	12
Opal	5
Mica	8
Kaolinite	5

4.3.2 Experimental set-up

The settling column consists of an acrylic glass tube equipped with electro-valves placed at 10 different levels (0.05, 0.15, 0.30, 0.55, 0.80, 1.05, 1.30, 1.55, 1.80 and 2.05 m), with a height of 2.60 m and an internal diameter of 0.11 m (Portela and Brito, 2009). The column is supported by a rotating sample-container structure, and the opening of the electro-valves and rotation of the sample container structure are operated by a programmable controller (Figure 4.2).

Figure 4.2: General view of the settling column and sample-container structure.

The column presents free rotation around a fixed axis allowing the homogenization of the suspension at the beginning of each experiment (Portela *et al.*, 2013) (Figure 4.3).
The experiments were conducted for the initial sediment concentration of 1.5 g/l and six different water salinities (0, 3.3, 6.7, 10, 15 and 30‰), and for four different initial concentrations (0.15, 0.30, 0.60 and 0.90 g/l) and a salinity of 30‰ (Table 4.2). The option for initial sediment concentration values higher than the values observed in the Ria de Aveiro was to minimize errors due to the small water volumes collected (c. 0.05 l) during the experiments. The initial height of the water column was 2.25 m (volume of c. 21.4 l) and the salinity was achieved by adding sea salt to the water volume.

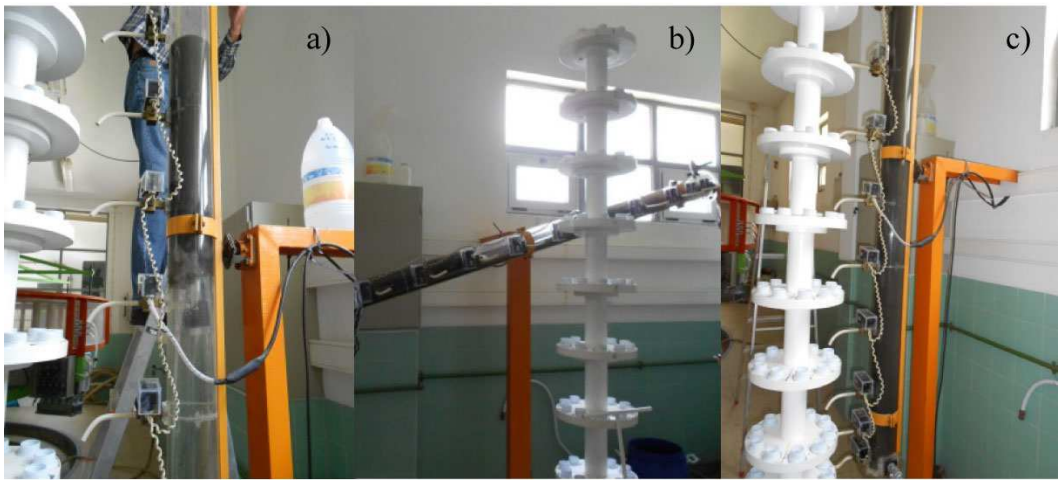

Figure 4.3: Suspension homogenization: a) Placement of the sediment sample in the settling column; b) Mixing of the sample; c) Start-up of the test.

Table 4.2: Initial conditions of the settling column tests.

Test	Salinity (‰)	Initial concentration (g/l)
1	0	1.50
2	3.3	1.50
3	6.7	1.50
4	10	1.50
5	15	1.50
6	30	1.50
7	30	0.15
8	30	0.30
9	30	0.60
10	30	0.90

During each experiment, water samples were collected at all vertical levels simultaneously at 10 different time instants (0, 1, 6, 16, 36, 66, 106, 156, 216 and 306 min). The water samples collected at four levels (0.30, 0.80, 1.30 and 1.80 m) were used to determine sediment concentrations by the gravimetric method. The samples were filtered through pre-weighed cellulose nitrate membrane filters with 0.45 μm pore size, dried at 40ºC and weighed after 24 h in an analytical balance and the weight of the dried residue divided by the original sample volume (Figure 4.4) (Portela *et al.*, 2013).

Figure 4.4: Determination of the samples concentration by gravimetric method: a) Filtration of the water samples; b) Drying of the filters at 40ºC for 12 h in the oven; c) Filters weighing in the analytical balance.

Samples collected from the remaining levels of the settling column were examined for grain size by laser diffraction, using a *Malvern Mastersizer Micro* particle size analyser. This analyser consists of an optical unit and a computer where the *Mastersizer Micro v2.19 software* is installed for the acquisition of data (Figure 4.5).

The solution used in the analysis is constituted by the sample and distilled water, which is the dispersant. The optical unit consists of a sampling unit, a control panel and a measuring cell. It is in the sampling unit that the process of dispersion and homogenization of the suspension is performed, promoting the movement of the sample in the measuring cell. In order to have a detectable signal, the obscuration should have a value between 10 and 15%, for tests with silt-clay sediments and different concentrations (Freire, 2003).

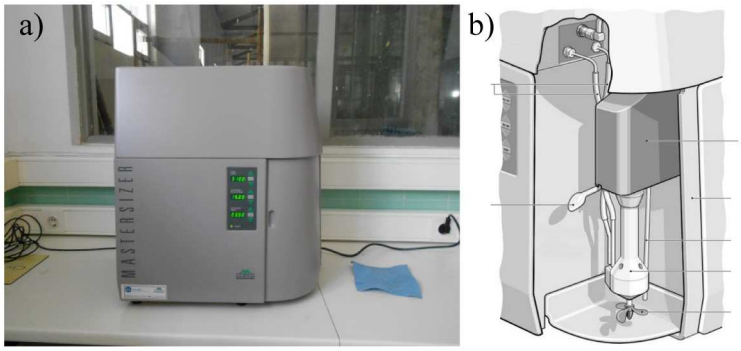

Figure 4.5: *Malvern Mastersizer Micro* particle size analyser: a) Overview of the instrument; b) Sampling unit.

Settling velocities were determined on the basis of the time-evolution of SSC, according to the equation for mass conservation:

$$\frac{dC}{dt} + \frac{d\,(w_s \cdot C)}{dz} = 0 \tag{4.2}$$

where C is the concentration, t is the time, w_s is the settling velocity and z is the vertical coordinate. An approximate solution by finite differences is:

$$w_s^t = -\left(\frac{C^{t+1} - C^t}{\Delta t^t}\right)\frac{H^t}{C^t} \tag{4.3}$$

where w_s^t is the vertically averaged settling velocity at time t, C^{t+1} and C^t are the vertically averaged SSC at times t+1 and t, H^t is the height of the water column after sample collection at time t and Δt^t is the time interval between t+1 and t (Portela *et al*., 2013).

4.4 Results and discussion

Figures 4.6 and 4.7 show the SSC evolution along the time in each of the experiments. In all the experiments, during the first 6 minutes, no substantial decrease in suspended concentration is observed. This is most likely caused by residual turbulence generated by the homogenization of the suspension which prevents settling, as previously verified by Portela *et al.* (2013). The sharpest decrease is observed between the 6 and 36 minutes, independently of the salinity and initial suspended concentration value. After this initial quick sediment concentration reduction, the decrease is slower. This initial decrease is more marked for higher salinities (15 and 30‰) and initial concentrations (0.6, 0.9 and 1.5 g/l) (Figures 4.6e,f and 4.7c,d).

The previous results are presented in Figure 4.8 in vertical averaged and normalized form. The concentrations were normalized by dividing the experiment concentrations by the reference concentrations (average concentration of minutes 0 and 1) (results in Appendix C1 and C2).

In the case of experiments with different salinities, it is clear the importance of salinity on settling velocity. A significant increase occurs even for low salinities of 3.3‰, in agreement with previous studies (Whitehouse *et al.*, 2000). Noteworthy is the similarity of the SSC evolution for salinities of 3.3, 6.7 and 10‰ and of 15 and 30‰, between minutes 66 and 306. After the 5 hours' test, the proportion of the initial sediment remaining in suspension is 20% for fresh water conditions (S=0‰), about 10% for salinity of 10‰, and approximately 5% for salinities of 15 and 30‰.

In the experiments with different initial concentrations, it is also clear the importance of the initial concentration on the settling velocity. Noteworthy is the similarity of the SSC evolution for the C=0.15 and 0.30 g/l experiments between minutes 156 and 306. The proportion of the initial sediment remaining in suspension after 5 hours is 12-13% for C=0.15 and 0.30 g/l, about 9% for C=0.6 g/l and about 6-4% for C=0.9 and 1.5 g/l.

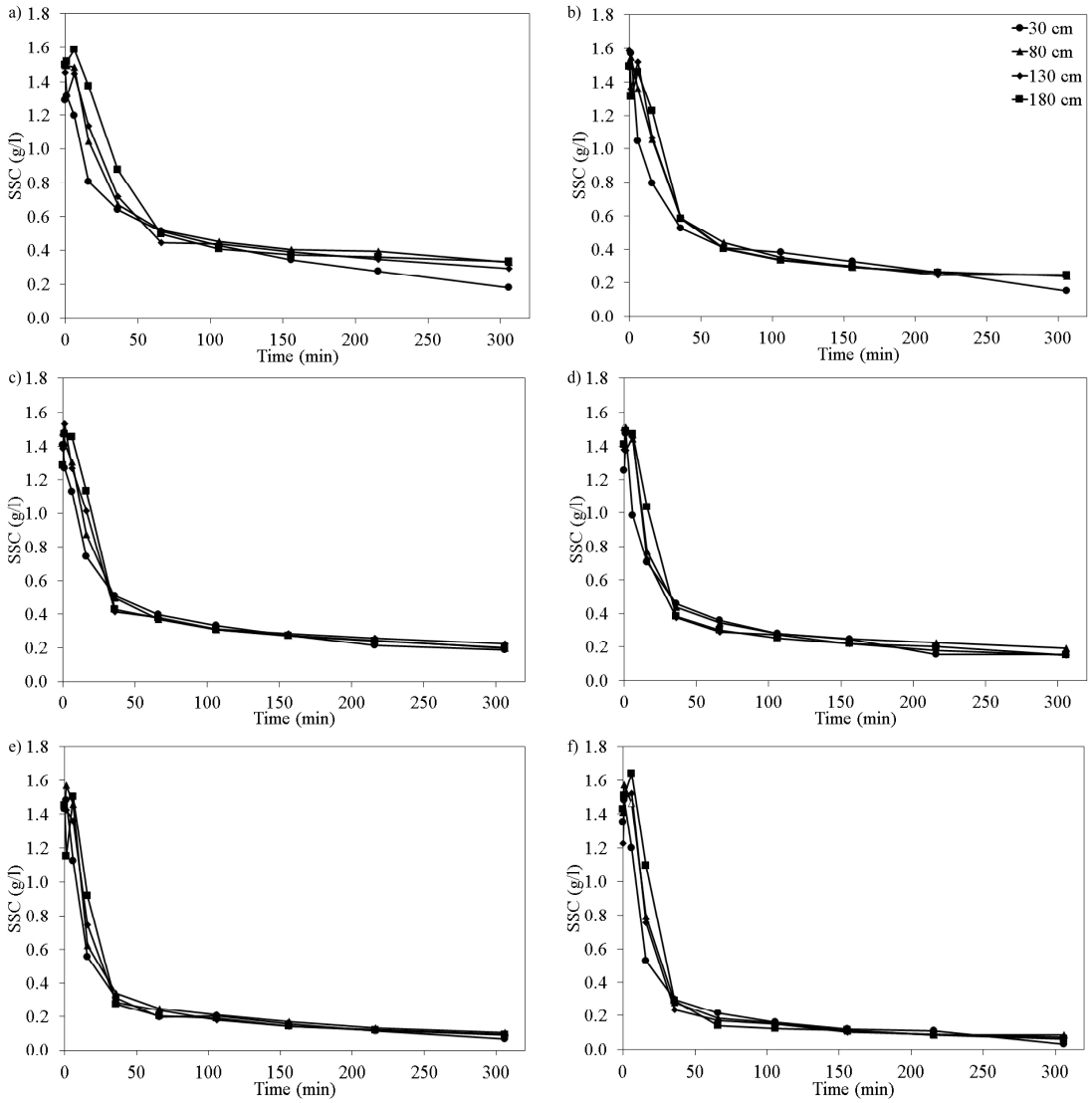

Figure 4.6: SSC temporal evolution at four levels in each experiment, with salinity of: a) S=0‰; b) S=3.3‰; c) S=6.7‰; d) S=10‰; e) S=15‰; f) S=30‰.

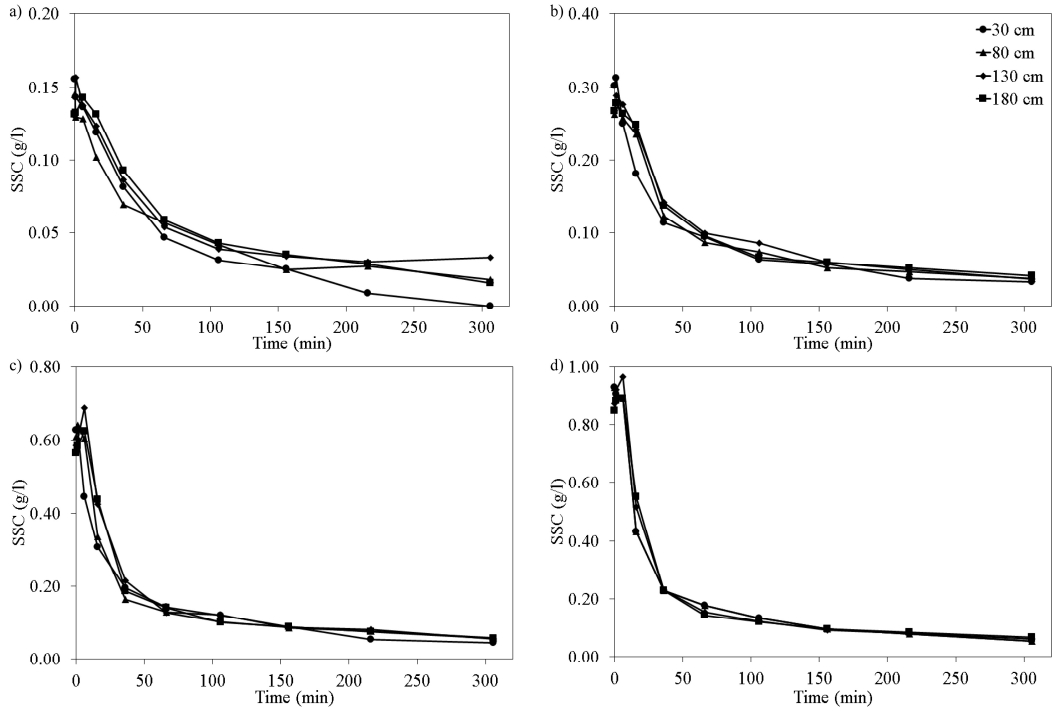

Figure 4.7: SSC temporal evolution at four levels in each experiment, with initial concentration: a) C=0.15 g/l; b) C=0.30 g/l; c) C=0.60 g/l; d) C=0.90 g/l.

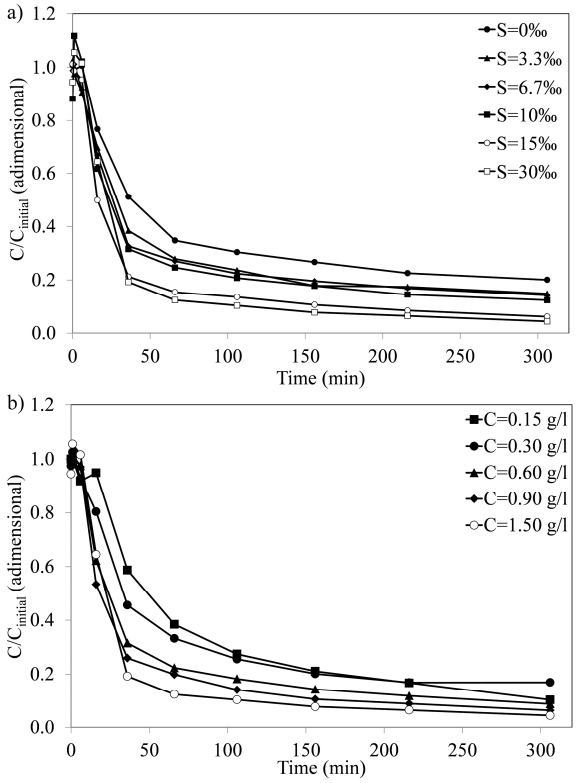

Figure 4.8: Vertically averaged normalized SSC temporal evolution for the experiments, with different: a) Salinities; b) Initial concentrations.

Figure 4.9 shows the settling velocities (w_s^n) in each experiment and at each time interval, considering the results obtained between minutes 16 and 306. Settling velocities are presented in function of sediment concentration, although no cause-effect relationship is implied.

Settling velocities present maximum values at the first minutes (16-36 minutes), ranging between 0.8 mm/s for fresh water conditions and 1.4 mm/s for a salinity of 30‰. In the experiments with different initial concentrations the settling velocities range from 0.5 to 1.5 mm/s for an initial concentration of 0.15 and 0.9 g/l, respectively. In each experiment, a relationship can be established between the settling velocity and the SSC, apparently to some extent as a consequence of sediment sorting.

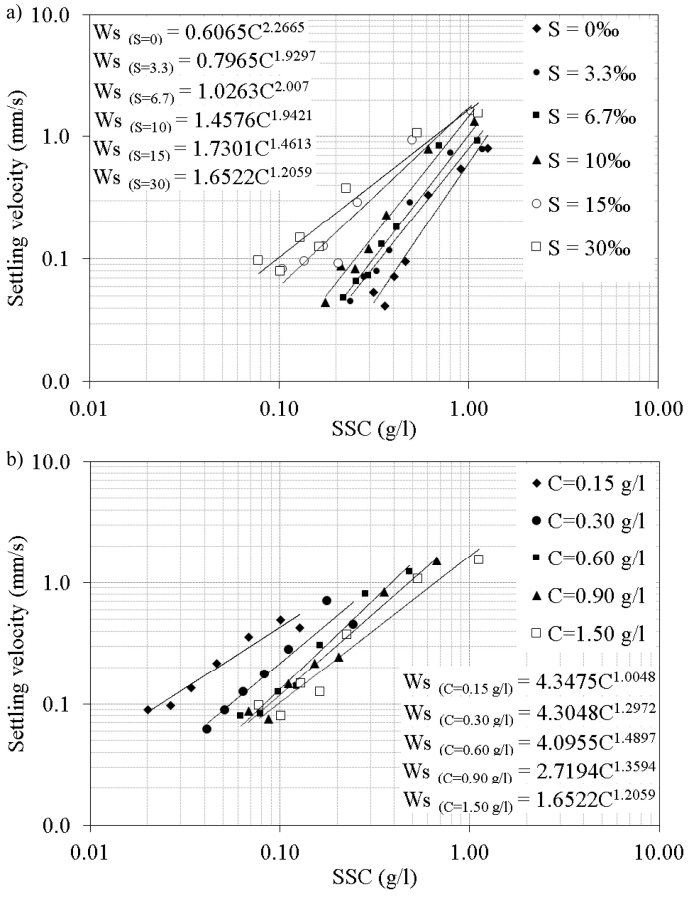

Figure 4.9: Settling velocities as function of SSC, for different: a) Salinities; b) Initial concentrations.

Figure 4.10 presents the percentage of the initial sediment remaining in suspension as a function of the settling velocity previously determined. The median settling velocity (w_{s50}) is defined as the value of settling velocity when the sediment concentration has decreased to half the initial value.

Results indicate that the median settling velocity increases with the increase in salinity and initial concentration. The experiment for fresh water conditions presents a settling velocity of 0.40 mm/s, while for the salinity 30‰ experiment is 1.21 mm/s. Regarding the experiments with different initial concentrations, the results show that for initial concentrations of 0.15 and 0.3 g/l the settling velocity is 0.37 and 0.47 mm/s, for C=0.6 g/l a median settling velocity of 0.84 mm/s was found, while for C=0.9 g/l the median settling velocity was 1.03 mm/s.

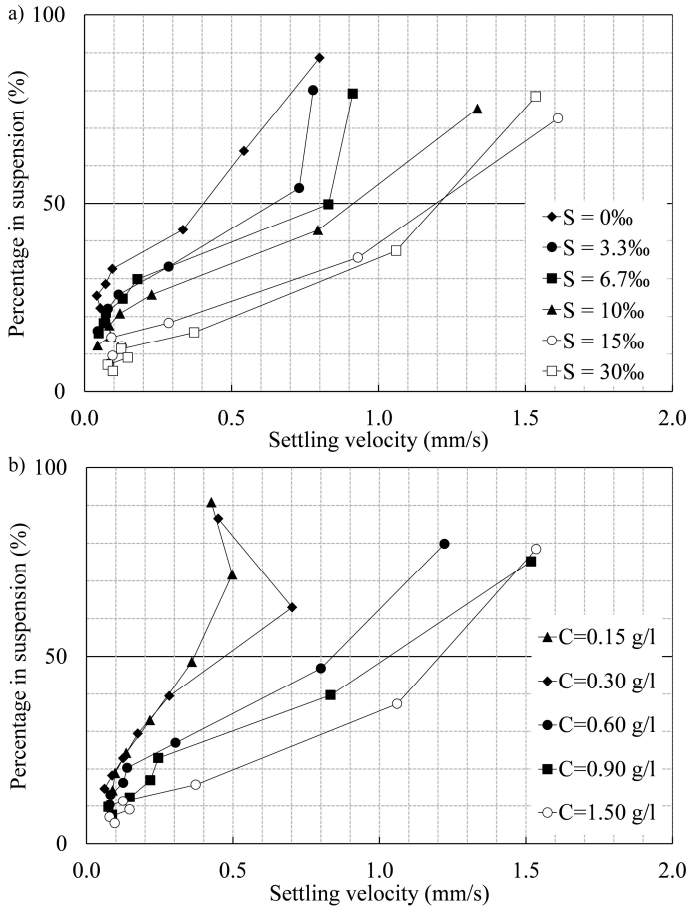

Figure 4.10: Median settling velocity for different: a) Salinities; b) Initial concentrations.

Figure 4.11 presents the comparison between the median and mass-weighted mean settling velocities, for different salinity and initial suspended concentration. The mass-weighted mean settling velocities were determined considering that experiments start at 16 minutes, after the end of turbulence, and the initial sediment concentration is the concentration at this time instant. Since at the end of the experiment (306 minutes) material is still observed in suspension, the mass-weighted mean settling velocities were determined assuming that the remaining particles in suspension present a settling velocity equal to the previous interval (206 and 306 minutes) (Portela *et al.*, 2013).

Mass-weighted settling velocity increases from 0.40 mm/s for fresh water to 1.10 mm/s for S=30‰, displaying a similar value for 15 and 30‰ salinities (Figure 4.11a). This indicates that 15‰ may be a salinity limit, above which the settling velocity remains approximately constant. The existence of a salinity limit was already previously observed by Krone (1962), Al Ani *et al.*, (1991), van Leussen (1999) and Wang *et al.* (2015). Furthermore, for salinity values lower than 10‰, the mass-weighted and median settling velocities show significant differences.

In the case of the experiments with different initial SSC, the mass-weighted settling velocity increases from 0.31 mm/s for an initial C=0.15 g/l to 0.97 mm/s for C=0.9 g/l (Figure 4.11b). The minimum and maximum mass-weighted settling velocities present lower values in comparison with the median settling velocities, but with low differences. Noteworthy, is the minimum and maximum mass-weighted means are almost coincident for both experiment sets.

Despite the fact that an increase is observed in the settling velocity with the SSC, which is consistent with the enhanced settling regime, for the experiments with initial SSC of 0.15 and 0.30 g/l the variation is less pronounced, which may indicate an approximation to the free settling regime, where the settling velocity is not influenced by SSC. For initial SSC between 0.3 and 0.9 g/l a more pronounced variation is observed, consistent with enhanced settling regime. On other hand, for initial SSC higher than 0.9 g/l, the variation is again less pronounced, which may indicate an approximation to a hindered settling regime, possibly still distant. The obtained range of SSC that would characterize the limits of the three regimes appears to be relatively close to the values presented by Costa (1995).

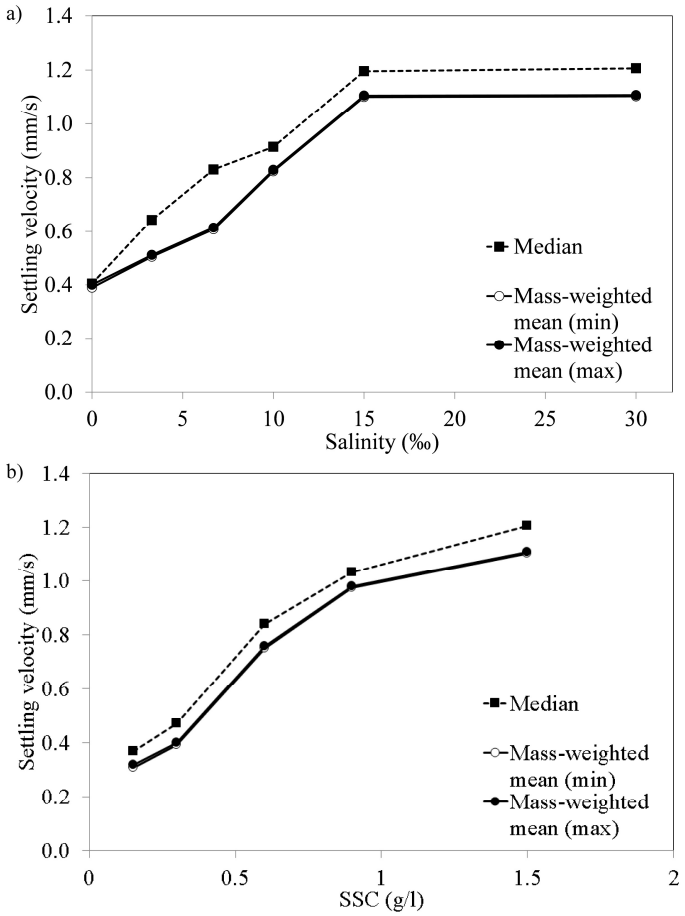

Figure 4.11: Comparison of the median settling velocity with mass-weighted mean settling velocities, for different: a) Salinities; b) Initial concentrations (Note: results for min and max mass-weighted means are almost coincident).

The temporal evolution of the d_{10}, d_{50}, and d_{90} obtained by laser diffraction in each experiment is shown in Figure 4.12. The results show that higher values of d_{10}, d_{50}, and d_{90} at the end of the experiments are obtained for lower values of salinity and initial concentration.

In the experiments where salinity was varied between 3.3 to 30‰, the ratio between the final and initial d_{50} showed similar values (approximately 15%). Additionally, the highest ratio between the final and initial d_{50} of 21.5% was obtained for fresh water conditions (Figure 4.12a). For experiments with different initial concentrations the ratios are approximately 37, 19 and 16% for the initial concentrations of 0.15, 0.60 and 1.50 g/l, respectively, with the lowest ratio being observed in the experiment with the highest initial concentration (Figure 4.12b).

The initial d_{50} is rather coarse (26-30 µm), when compared with other fine sediment samples previously tested (*e.g.* Portela *et al.*, 2013). This may explain why the effect of salinity on the setting velocity, although clearly present, appears to be less marked than in those previous works.

The obscuration values obtained in the laser diffraction analysis are lower than 10% in most of the salinity experiments (results in Appendix C3 and C4). The same was verified for the initial concentrations experiments, due to the low sediment concentrations. Nevertheless, the obtained results for the two experimental sets seem admissible.

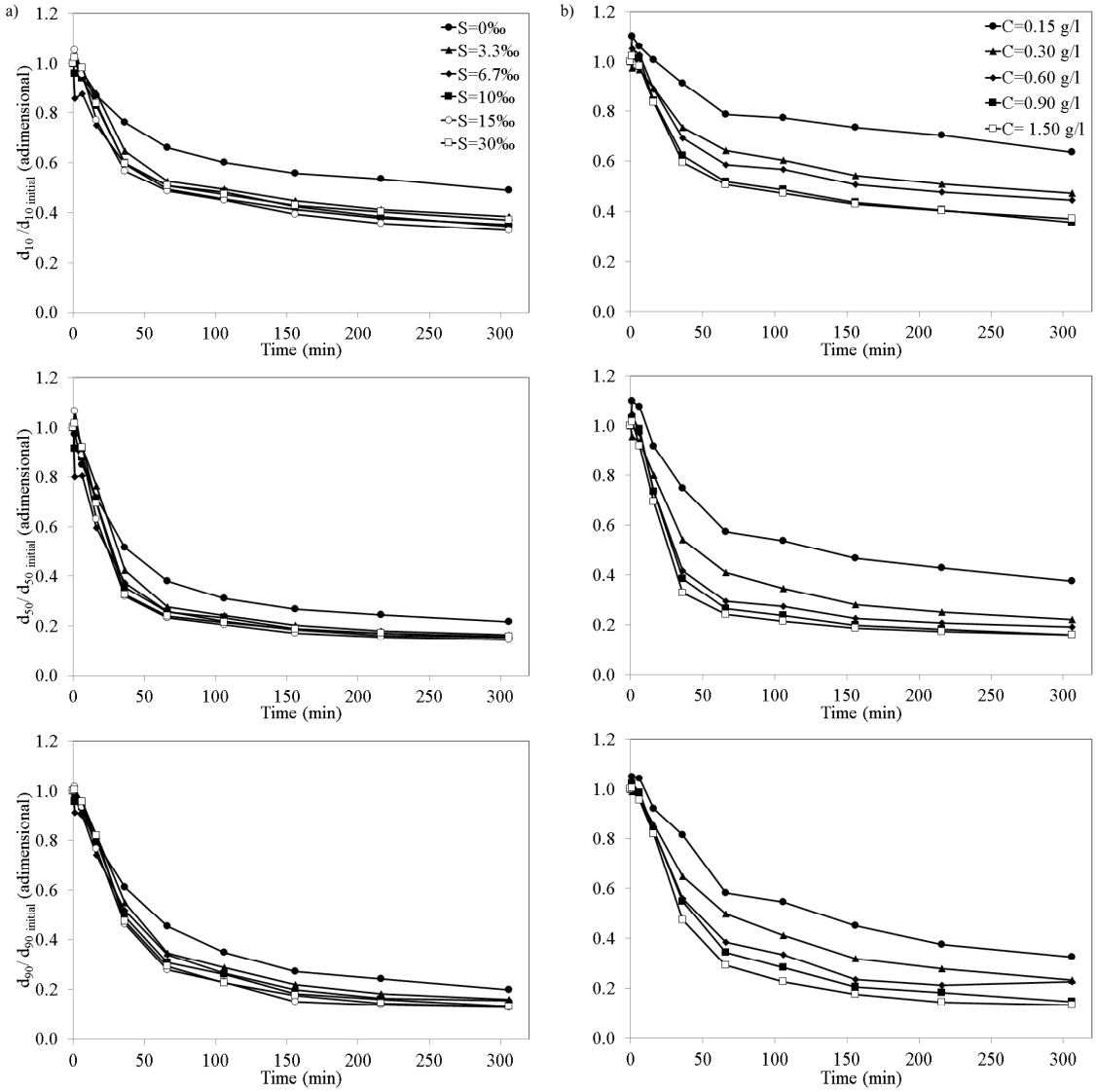

Figure 4.12: Normalized d_{10}, d_{50} and d_{90} temporal evolution along the experiments: a) Salinities; b) Initial concentrations.

4.5 Conclusions

The effect of salinity and initial sediment concentration on the fine sediments collected in the Ria de Aveiro was studied in settling column experiments. The following main conclusions where reached:

- In all the experiments, no substantial decrease in SSC was observed during the first 6 minutes, being the sharpest decrease observed between minutes 6 and 36;
- The influence of salinity on settling velocity is important even for low salinity values, with a significant increase from fresh water conditions to salinity of 3.3‰ until 15‰;
- The influence of the initial SSC on settling velocity was consistent with the enhanced settling regime, being more significant for values between 0.3 and 0.9 g/l, with lower initial SSC suggesting an approximation to the free settling regime and higher initial SSC to the hindered settling regime;
- Median settling velocity increases with salinity, from 0.4 mm/s for fresh conditions to 1.21 mm/s for S=30‰ and with initial concentration, from 0.37 mm/s to 1.03 mm/s for 0.15 to 0.9 g/l;
- Median settling velocity presents similar values for salinity values of 15 and 30‰, which can indicate a salinity limit as previously observed by other authors.
- Temporal variation of the parameters d_{10}, d_{50} and d_{90} is slower for the experiments with fresh water conditions and an initial concentration of 0.15 g/l;
- The decrease of settling velocity over time appears to be mainly a consequence of sorting;
- Salinity effect on settling velocity is less marked than in previous experiments, which may be explained by the fact that the sediments are rather coarse.

Summarizing, the results indicate that the settling velocity of Ria de Aveiro fine sediments is influenced by salinity, initial sediment concentration and particle size. These results are in agreement with previous fine sediment laboratory studies, showing that salinity and sediment concentration, in addition to particle size, are important factors in fine sediment settling velocity and must be taken into account when evaluating fine sediment deposition.

The settling column experiments present some limitations. The initial concentrations are higher than the ones observed in the Ria de Aveiro, and moreover, only a single sample collected at one of the lagoon channels was used. However, the performed laboratory tests

have provided insights into deposition processes, which can be used to improve suspended sediment transport numerical models of Ria de Aveiro.

5 Numerical modelling of suspended sediment transport

5.1 Introduction

The suspended sediment dynamics in Ria de Aveiro was evaluated using the numerical model MOHID (www.mohid.pt). MOHID is under permanent development by MARETEC (Marine and Environmental Technology Research Center) at Instituto Superior Técnico (IST). MOHID is a three-dimensional free surface water modelling system that uses a finite volume approach to perform the spatial discretization and is fully described in Martins *et al.* (2001) and Leitão (2003). This model has the ability to simulate flows and sediment transport in shallow systems, such as Ria de Aveiro, and has been previously applied to simulate its hydrodynamic (Vaz, 2007; Vaz *et al.*, 2007, 2009; Picado *et al.*, 2013) and suspended sediment dynamics (Plecha *et al.*, 2014).

In this chapter, a general overview of the MOHID is performed, presenting the main formulations solved by the model. It is also presented a sensitivity analysis of the numerical model to some of the cohesive sediment transport parameters, namely the settling velocity. To complete the chapter, the model implementation to Ria de Aveiro and respective validation are presented.

5.2 Numerical model equations

MOHID solves the 3D incompressible primitive equations, adopting hydrostatic equilibrium as well as Boussinesq and Reynolds approximations. A more detailed description of the numerical algorithms can be found in Martins *et al.* (2001), Leitão (2003) and Vaz (2007). The mass momentum equation is given by:

$$\frac{\partial u_i}{\partial t} + \frac{\partial (u_i u_j)}{\partial x_j} = -\frac{1}{\rho_0} \cdot \frac{\partial p_{atm}}{\partial x_i} - g \cdot \frac{\rho(\eta)}{\rho_0} \cdot \frac{\partial \eta}{\partial x_i} - \frac{g}{\rho_0} \cdot \int_{x_3}^{\eta} \frac{\partial \rho'}{\partial x_i} \cdot dx_3 + \frac{\partial}{\partial x_j}\left(\upsilon \frac{\partial u_i}{\partial x_j}\right) - 2 \cdot \varepsilon_{ijk} \Omega_j u_k \qquad (5.1)$$

where u_i are the velocity vector components in the horizontal Cartesian directions (i=1; 2) and u_j are the velocity vector components in the three Cartesian directions (j=1; 2; 3), ν is the turbulent viscosity, η is the free surface level, g is the acceleration of gravity, p_{atm} is the atmospheric pressure, ρ is the specific mass, ρ' is its anomaly, ρ_0 is the reference specific mass and $\rho(\eta)$ represents the specific mass at the free surface, t is the time, Ω is the Earth´s velocity of rotation and ε is the alternate tensor.

MOHID system assumes that the transport of cohesive sediment occurs only in suspension. Therefore, the transport depends only on the advection-diffusion equation, with a settling velocity included in the vertical advection. This equation requires diffusion coefficients in the three directions. The transport equation for suspended sediments is given by:

$$\frac{\partial C}{\partial t} + \frac{\partial u_1 C}{\partial x_1} + \frac{\partial u_2 C}{\partial x_2} + \frac{\partial (u_3 + w_s) C}{\partial x_3} = \frac{\partial}{\partial x_1}\left(\varepsilon_1 \frac{\partial C}{\partial x_1}\right) + \frac{\partial}{\partial x_2}\left(\varepsilon_2 \frac{\partial C}{\partial x_2}\right) + \frac{\partial}{\partial z}\left(\varepsilon_3 \frac{\partial C}{\partial x_3}\right) + E - D \qquad (5.2)$$

where C is the depth average SSC, ε_1, ε_2 and ε_3 the diffusion coefficients in the Cartesian coordinates, E the erosion rate and D the deposition rate. SSC is considered a conservative property and consequently, the total mass in the model domain can change only due to river inputs, fluxes between the bottom and water column and fluxes to or from the ocean.

The settling velocity w_s (m/s) can be computed by different ways in the numerical model, being constant or determined considering the effect of sediment concentration on flocculation and the hindered settling effect above a concentration (C_{HS}), based on the formulation proposed by Nicholson and O'Connor (1986), described in Equations 5.3 and 5.4:

$$w_s = K_1 C^{m_1} \qquad \text{for } C < C_{HS} \qquad (5.3)$$

$$w_s = K_1 C_{HS}^{m_1} [1-K_2(C-C_{HS})]^{m_2} \qquad \text{for } C > C_{HS} \tag{5.4}$$

where K_1 and K_2 parameters depend on sediment mineralogy and the exponents m_1 and m_2 depend on particle size and shape.

The exchange between the water column and the bottom is calculated with the Partheniades' erosion formula (Partheniades, 1965) described in Equations 5.5 and 5.6, and Krone's deposition formula (Krone, 1962) described in Equations 5.7 and 5.8:

$$\frac{\partial M_E}{\partial t} = E\left(\frac{\tau}{\tau_E} - 1\right) \qquad \text{for } \tau > \tau_E \tag{5.5}$$

$$\frac{\partial M_E}{\partial t} = 0 \qquad \text{for } \tau < \tau_E \tag{5.6}$$

$$\frac{\partial M_D}{\partial t} = C\, w_s \left(1 - \frac{\tau}{\tau_D}\right) \qquad \text{for } \tau < \tau_D \tag{5.7}$$

$$\frac{\partial M_D}{\partial t} = 0 \qquad \text{for } \tau > \tau_D \tag{5.8}$$

where M_E is the mass eroded, M_D is the mass deposited, τ is the bed shear stress, τ_E is a critical shear stress for erosion and τ_D is the critical stress for deposition. Sediments are eroded when the bottom shear stress exceeds the critical value for erosion, but are deposited when the bottom shear stress is lower than the critical shear stress for deposition.

In this work, MOHID was used in 2D mode, since the Ria de Aveiro is a shallow usually vertically homogenous lagoon (Dias *et al.*, 1999, 2000; Vaz *et al.*, 2009). Suspended sediment transport module was coupled to the hydrodynamic model that was previously calibrated and validated to the Ria de Aveiro. Hydrodynamic model was calibrated based on water level observations recorded at 24 stations and velocity measurements at 10 stations, being obtained RMSE values lower than 5% for local tide range (Vaz *et al.*, 2007). More details about the model accuracy to reproduce the lagoon hydrodynamics after calibration and validation are described in Vaz (2007), Vaz *et al.* (2007, 2009) and Vaz and Dias (2011).

5.3 Initial conditions

In the present study, an initial elevation equal to the MSL of the study area was prescribed for the entire domain, as well as null velocity. Water temperature and salinity for all the cells of numerical domain were set constant with the 19ºC and 36 values, respectively, as used in previous numerical modelling implementations for Ria de Aveiro (Vaz, 2007). The suspended sediment transport model was initialized with a sediment concentration of

0.1 mg/l inside the lagoon. The variation of SSC was simulated by imposing different SSC values at each river mouth.

5.4 Boundary conditions

In this study five different types of boundaries were used:

- Surface boundary, where the advective fluxes of mass and momentum across the surface are assumed null and the diffusive flux of momentum is imposed explicitly by means of a wind surface stress. At the surface, heat fluxes were imposed, using latent and sensible heat fluxes parametrization based on Dalton and Bowen laws, respectively (Chapra, 1997). Surface boundary conditions are computed by the model from meteorological data provided by the user. In this case, relative humidity, atmospheric pressure, air temperature, wind intensity and solar radiation from University of Aveiro meteorological station were provided;
- Bottom boundary, where the bottom stress is calculated using a non-slip method with a quadratic law that depends on the near bottom velocity and bottom drag coefficient, expressed by the equation:

$$C_D = g \cdot n^2 \cdot h^{-\frac{1}{3}} \tag{5.9}$$

  where n is the Manning coefficient. In the present study the manning coefficients were imposed ranging from 0.022 to 0.045, as described in Vaz (2007). No salinity and water temperature fluxes were considered at the bottom;
- Closed boundaries of the domain that corresponds to land, where is imposed a zero normal component of mass and momentum diffusive fluxes, at the cell faces in contact with land;
- Open boundaries, at the ocean and river boundaries. At the ocean boundary, amplitude and phase of 36 tidal constituents determined for Barra tidal gauge station were imposed. The values were corrected in order to account for the tidal distortion between the open boundary and Barra station. For water temperature and salinity were specified the values of 14ºC and 36.5, respectively. At the landward boundaries, fluvial discharges and associated SSC, water temperature and salinity were specified (19ºC and 0, respectively). For the water temperature and salinity were adopted values used in previous numerical modelling implementations for Ria de Aveiro (Vaz, 2007). Fluvial discharges and SSC details are defined in the next sub-section;

- Moving boundaries are closed boundaries whose position varies in time and corresponds to the intertidal zones, which are frequent in Ria de Aveiro and were considered in the model implementation. To track the uncovered cells a criterion is used (Figure 5.1), that establishes a depth below which cells are considered uncovered and is described in Martins *et al.* (2001) and Leitão (2003).

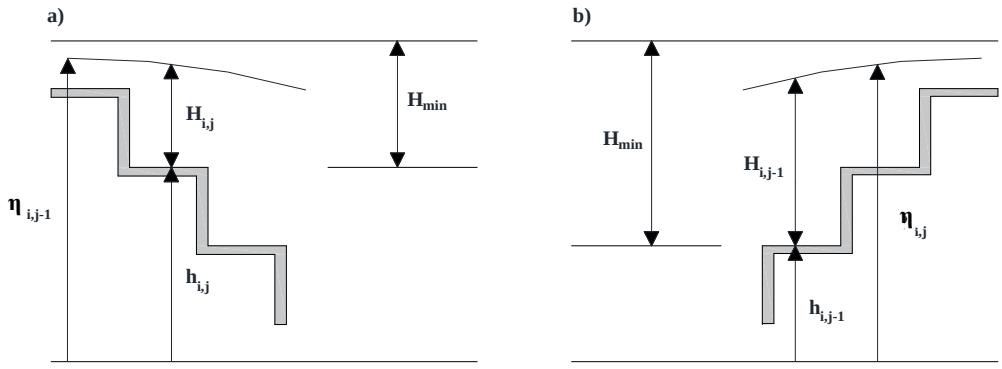

Figure 5.1: Conditions for a cell to be considered uncovered (Leitão, 2003).

H_{min} is the depth bellow which cell is considered uncovered. In this case a thin water volume above the cell is conserved. The cell of position *i, j* is considered uncovered when one of the two following situations is verified (Leitão, 2003; Vaz, 2007).

$$H_{i,j} < H_{min} \cap \eta_{i,j-1} < -h_{i,j} + H_{min} \tag{5.10}$$

$$H_{i,j-1} < H_{min} \cap \eta_{i,j} < -h_{i,j-1} + H_{min} \tag{5.11}$$

The second condition of Equation 5.10 assures that the cell is not being covered by the tidal wave propagating from left to right and the second condition of Equation 5.11 assures that the cell is not being covered by the tidal wave propagating from right to left. The noise formed by the abrupt change in velocity at the dry cells is controlled with a careful choice of H_{min} (in this work was considered equal to 0.10 m) (Vaz, 2007).

5.5 Model set-up

Numerical simulations were performed with a time step of 5 seconds, using a grid with variable dimensions, being 40×40 m^2 in the central area of the lagoon and 40×100 m^2 in the north and south areas. Bathymetric data was collected in a general survey carried out in 1987/1988, by the Hydrographic Institute of Portuguese Navy (IH), but was updated for the

majority of the lagoon with recent data provided by different sources (Figure 5.2), namely, Polis Litoral Ria de Aveiro, which provided bathymetric data collected during 2011 for the principal channels of the lagoon (Mira, Ílhavo, S. Jacinto and the second half of Espinheiro channel) and the Aveiro Harbour Administration that provided inlet bathymetric data collected during 2012 (Picado *et al.*, 2013).

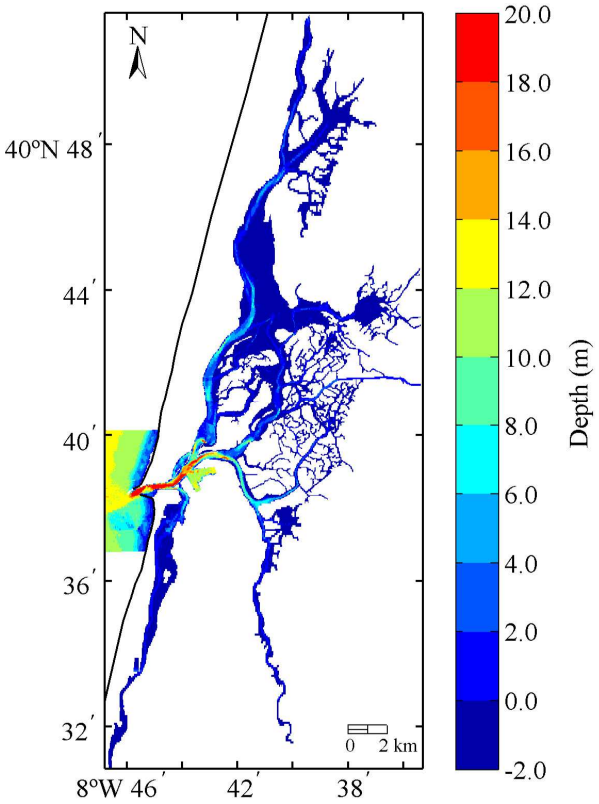

Figure 5.2: Ria de Aveiro bathymetry considered in the numerical model.

Regarding the critical shear stresses for erosion and deposition, it was considered that for values above 0.4 N/m^2 the sediments are eroded and that deposition occurs for values below 0.2 N/m^2. These limits were obtained from tidal experiments with fine sediments of Ria de Aveiro in annular flume (Coelho *et al.*, 2015). The erosion rate was considered equal to 5×10^{-5} kg/m^2/s, based on values used for other coastal systems such as Tagus estuary (Franz *et al.*, 2014). In the case of the settling velocity it was adopted a constant value of 1×10^{-5} m/s to the entire lagoon. This option will be validated through sensitivity analysis to be performed in Section 5.6. The model parameters used are described in Table 5.1.

Table 5.1: Parameters considered in the suspended sediment transport model.

Name	Value	Units
Settling velocity	1×10^{-5}	m/s
Erosion rate	5×10^{-5}	$kg/m^2/s$
Critical shear stress for erosion	0.4	N/m^2
Critical shear stress for deposition	0.2	N/m^2
Horizontal diffusion coefficient	5	m^2/s

The erosion of consolidated sediments and the consolidation process were neglected. Therefore, it was assumed that the bottom layer of unconsolidated sediments is the only source of sediments to the water column by erosion and the only sink due to sedimentation. The performed simulations integrate a spin-up period of 60 days, in order to compass four times, the Ria de Aveiro maximum residence time.

5.5.1 Seaward boundary conditions: tides and SSC

At ocean boundary, located about 5 km far from the Ria de Aveiro inlet were imposed the harmonic constituents determined through harmonic analysis (Pawlowicz *et al.*, 2002) of the sea surface elevation measured at Barra tidal gauge (as referred in Section 5.4).

SSC seaward boundary conditions are more difficult to access, as SSC responds to several factors. In the case of Ria de Aveiro the interface between the inlet and the ocean occurs a few hundred meters away from the shore, so a reduced amount of sediment re-suspended by wave breaking in the surf zone is available to reach the inlet during the flood phase. This is supported by the SSC observations at inlet area performed by Abrantes *et al.* (2006) and Martins *et al.* (2009, 2011). Therefore, the SSC at the seaward boundary was considered very low, with a value of 0.1 mg/l.

5.5.2 Landward boundary conditions: discharges and suspended sediment of the rivers

Net freshwater flow into Ria de Aveiro is provided through the Vouga, Antuã, Cáster and Boco rivers and Valas de Mira discharges. Actually, is not implemented a monitoring program for Ria de Aveiro fluvial discharges as previous referred, so were used the daily series predicted by the *SWIM - Soil and Water Integrated Model*.

SWIM model was developed at PIK - Potsdam Institute for Climate Impact Research and is an eco-hydrological numerical model based in the SWAT and MATSALU models, coupled to geographic information tools (Krysanova *et al.*, 2000). For Ria de Aveiro it was used the

topography, soil use, lithology and river network, to model the lagoon drainage basin. The model was calibrated and validated by Stefanova *et al.* (2015), based on the river discharges data for gauges placed on the different rivers.

As previous referred there is no monitoring program, so there are no recent SSC observations for lagoon fluvial tributaries. Therefore, for Vouga river were adopted slightly higher values than SSC observations at upper reaches in the Ponte Vouzela station (Section 2.3.3.1). This option was related to the fact that Ponte Vouzela station is located at the Vouga river drainage basin upstream area located at the mountains, characterized mainly by rock soil. In opposition, at downstream areas, more intensive land use is verified, which implies the increase of soil erosion. For the remain lagoon tributaries, were adopted lower values comparing to Vouga river, since their drainage basins have lower areas. Moreover, SSC were varied according to the season and considered constant along each month. In Table 5.2 are presented the values used in different months along almost a year, between July and June.

Table 5.2: SSC (mg/l) associated to the fluvial discharges.

River	Jul/Aug	Sep/Oct	Nov	Dec-May
Vouga	30	200	250	150
Antuã	8	100	100	50
Boco	8	20	25	10
Valas de Mira	28	38	50	30
Cáster	8	20	20	10

5.6 Sensitivity analysis

Settling velocity is a critical parameter, since it influences the vertical distribution of SSC. Settling column experiments have demonstrated that Ria de Aveiro fine sediments settling is affected by salinity (Chapter 4). Additionally, previous works of suspended sediment numerical modelling in the Ria de Aveiro have used constant settling velocity of 1×10^{-5} m/s (Lopes *et al.*, 2006; Sener, 2012; Plecha *et al.*, 2014). This way, in order to evaluate which settling velocity leads to SSC in the range of observed values, tests with different formulations were performed. It was considered two constant values of $w_{s1}=1\times10^{-5}$ and $w_{s2}=1\times10^{-3}$ m/s and a salinity-dependent formulation, which resulted from the performed laboratory experiments (Section 4.4):

$$w_s = 0.0475 \cdot S + 0.3597 \quad \text{(mm/s), for } S < 15‰ \tag{5.12}$$

$$w_s = 1.0722 \quad \text{(mm/s), for } S \geq 15‰ \tag{5.13}$$

The formulations used by MOHID to compute settling velocity are those presented in Equations 5.3 and 5.4. Therefore, to implement salinity-dependent settling velocity were performed changes in the model source code in the *Free Vertical Movement* module, in the frame of this work.

Simulations were performed for a month period, considering a spin-up period of 60 days and the model set-up conditions previous described. Results were analysed for neap (17th July) and spring tide (24th July) conditions.

Table 5.3 presents the average predicted SSC at stations located at the beginning of the main channels (stations S1, S6, S9 and S11 presented in Figure 5.3) for neap and spring tide conditions, considering constant values for settling velocity and salinity dependent formulation. It is also presented the minimum and maximum values of SSC observations obtained from bibliography.

The results show that a salinity-dependent settling velocity leads to higher SSC values, especially at stations close to the fluvial discharges, namely S6 and S11 stations. Moreover, for spring tide conditions, is verified an increase of SSC predictions at S1 and S9 stations in the Mira and S. Jacinto channels, despite high salinities in these areas. This indicates that sediment transport from river's mouth areas towards the inlet overlaps sediment deposition. Regarding the simulations with constant settling velocity, the value of 1×10^{-3} m/s leads to lower SSC comparing to 1×10^{-5} m/s, being approximately null for neap tide conditions. The settling velocity of 1×10^{-5} m/s is the value which leads to SSC values closer to observations for both tide conditions at all analysed stations. Therefore, the value of 1×10^{-5} m/s was adopted in the performed simulations.

Table 5.3: Comparison between average SSC (mg/l) at a tidal cycle for different settling velocity formulations and observations, at stations located at Mira (S1), Espinheiro (S6), S. Jacinto (S9) and Ílhavo (S11) channels. Observed data from Abrantes (2005) and ARH Centro (2009).

Station	**Observations**	**Neap tide**			**Spring tide**		
		w_{s1}	w_{s2}	**Salinity-dependent formulation**	w_{s1}	w_{s2}	**Salinity-dependent formulation**
S1	6.8-47.0	8.84	0.03	10.66	38.64	14.70	104.04
S6	6.2-18.0	9.80	0.52	146.95	18.57	4.10	174.33
S9	9.7-13.3	7.53	0.14	25.44	15.93	8.20	78.57
S11	11.3-32.3	11.53	0.57	73.16	25.60	7.60	178.75

5.7 Model validation

In order to validate the daily and seasonal variability of SSC, the model predictions obtained between July 2013 and June 2014 were compared with *in situ* SSC data measure in the frame of BioChangeR project at three stations, located in the Mira (S1 - Costa Nova), Ílhavo (S2 - Vista Alegre) and S. Jacinto channels (S3 - Ponte da Varela) (Figure 5.3). SSC field data was stored every minute during a tidal cycle, at several days including spring and neap tide conditions for all seasons (Table 5.4). Simulations were performed considering the model set-up conditions previous described.

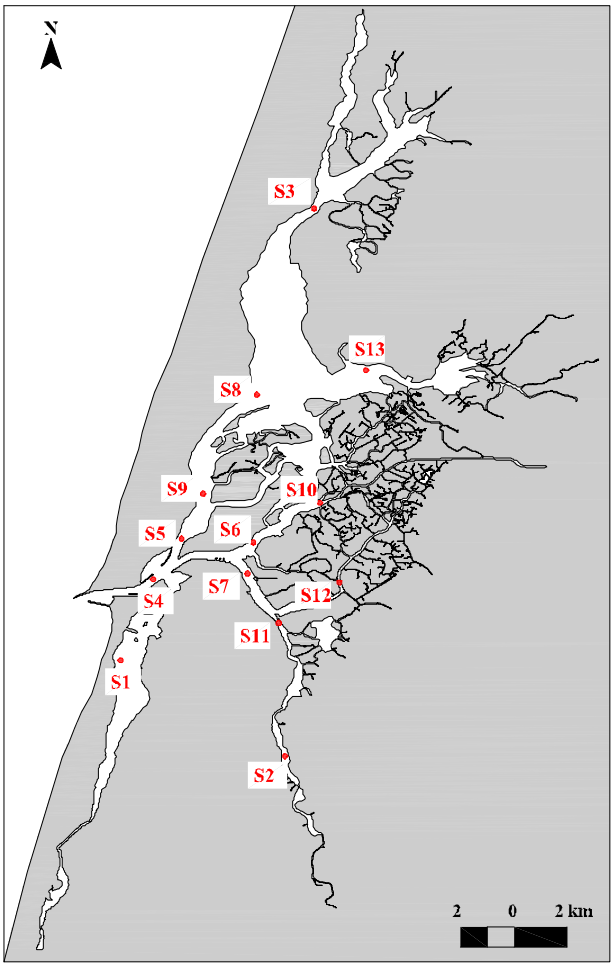

Stations	
S1	Costa Nova
S2	Vista Alegre
S3	Ponte da Varela
S4	Barra
S5	S. Jacinto
S6	Espinheiro
S7	Ílhavo
S8	Muranzel
S9	Bico do Pragal
S10	Parrachil
S11	Friopesca
S12	Vera Cruz
S13	Bico

Figure 5.3: Location of the stations with SSC observations.

Table 5.4: Monitoring days at S1, S2 and S3 stations.

Station	Summer	Autumn	Winter	Spring
Costa Nova (S1)	17th July 2013 24th July 2013	30th October 2013 4th November 2013	12th February 2014 19th February 2014	28th May 2014 4th June 2014
Vista Alegre (S2)	18th July 2013 25th July 2013	31th October 2013 6th November 2013	13th February 2014 20th February 2014	
Ponte da Varela (S3)	16th July 2013 23th July 2013	29th October 2013 5th November 2013	18th February 2014	3th June 2014

Due to the lagoon complex geometry, numerical SSC predictions were also compared with data presented in bibliography (stations S4 to S13, presented in Figure 5.3). These values correspond to instantaneous measurements, with the collection of water samples and further laboratory analysis carried by Abrantes (2005), the Portuguese Environmental Agency (ARH Centro, 2009) and Portela *et al.* (2011). Moreover, the SSC obtained from the surveys carried out in the frame of this study in October 2013 and March 2014 (Section 2.2.5) were also considered. Figure 5.4 presents a qualitative comparison of model predictions and field data for Costa Nova, Vista Alegre and Ponte da Varela stations. Two days were chosen as representative of summer and autumn seasons.

In order to give a less subjective evaluation of the model accuracy, the root mean squared error (RMSE), relative error (RE) and differences between predictions and observations were also determined and are presented in Table 5.5:

$$RMSE=\left\{\frac{1}{N}\sum_{i=1}^{N}\left[\xi_p(t_i)-\xi_o(t_i)\right]^2\right\}^{\frac{1}{2}} \tag{5.14}$$

$$RE=\left|\sum_{i=1}^{N}\left[\frac{\xi_p(t_i)-\xi_o(t_i)}{\xi_o(t_i)}\right]\right| \tag{5.15}$$

where $\xi_p(t)$ and $\xi_o(t)$ are the predicted and observed SSC, respectively.

Generally, the model reproduces satisfactory the SSC evolution along the tidal cycle, in most of the monitored days, for the three stations. The daily variation observed in the turbidity data is clearly seen in the predicted SSC, with higher values at ebb comparing to the flood period (Figure 5.4).

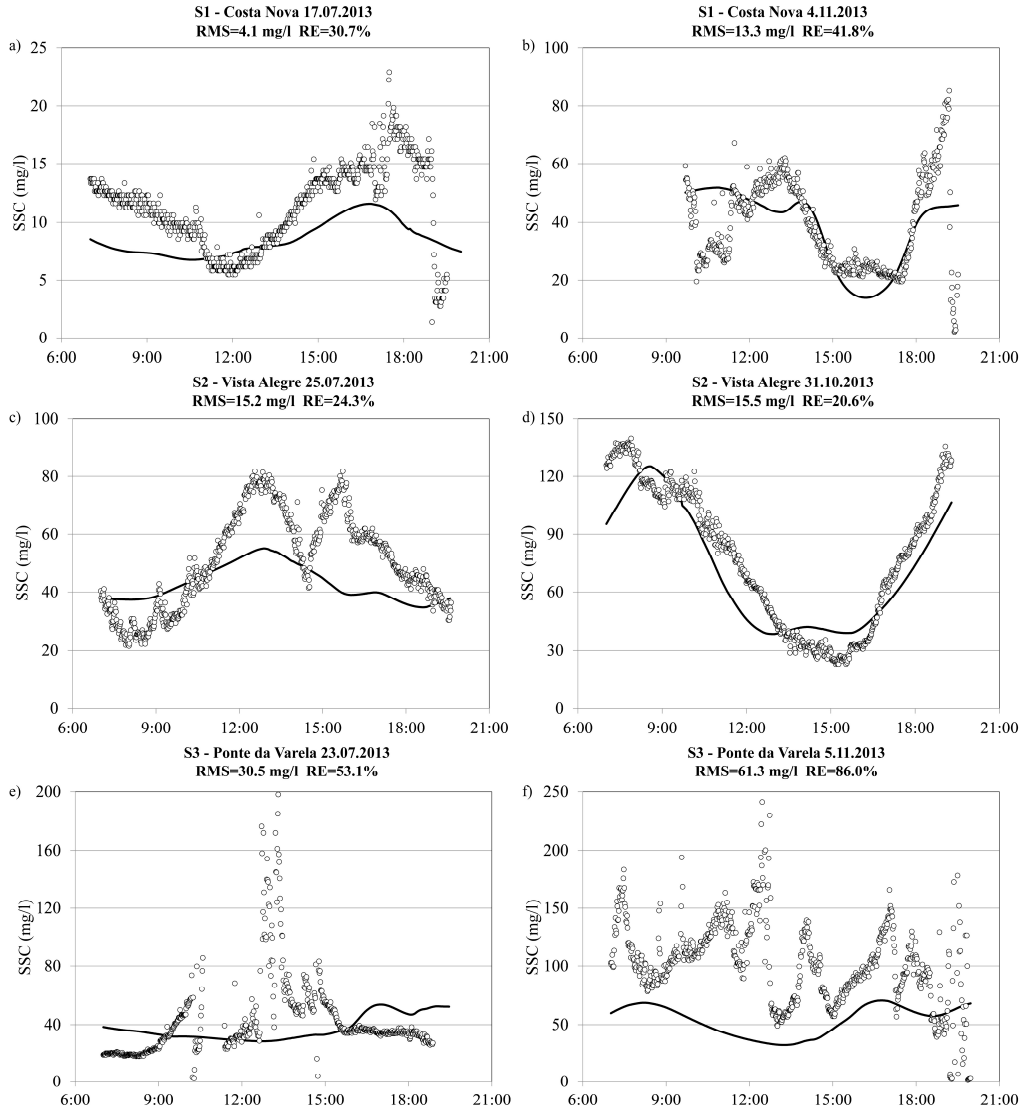

Figure 5.4: Comparison between observed (○) and predicted (─) SSC along a tidal cycle, at stations S1 (a, b), S2 (c, d) and S3 (e, f).

Regarding the average SSC values, the differences between predicted and observed SSC are minor in July for all stations (Table 5.5). In opposition, highest differences are observed at Vista Alegre and Ponte da Varela stations in November, with the model generally underestimating the observed values. This can be explained by the fact that Vista Alegre and Ponte da Varela stations are more close to the river's mouth, presenting higher uncertainty for SSC associated to fluvial discharges.

RMSE and RE values obtained for stations S1, S2 and S3 are acceptable, given the data limitations, namely the absence of SSC series for the different rivers discharging into the lagoon, which were considered constant along a month in the simulations (Table 5.5).

Table 5.5: Comparison between observed and predicted average SSC and associated differences, RE and RMSE values, at S1, S2 and S3 stations.

Season	Stations	Date	Observed SSC (mg/l)	Predicted SSC (mg/l)	Differences (mg/l)	RE (%)	RMSE (mg/l)
Summer	S1	17.07.2013	11.3	8.4	2.9	30.7	4.1
		24.07.2013	48.9	37.7	11.2	56.3	32.4
	S2	18.07.2013	29.9	13.7	16.2	52.3	18.5
		25.07.2013	50.8	42.8	8.0	24.3	15.2
	S3	16.07.2013	51.1	13.8	37.3	67.8	58.3
		23.07.2013	41.6	37.8	3.8	53.1	30.5
Autumn	S1	30.10.2013	19.5	24.2	4.7	62.0	10.7
		4.11.2013	38.8	38.0	0.8	41.8	13.3
	S2	31.10.2013	77.8	70.9	6.9	20.6	15.5
		6.11.2013	45.7	116.8	71.1	259.7	71.5
	S3	29.10.2013	60.9	20.5	40.4	86.6	57.5
		5.11.2013	101.4	53.6	47.8	860	61.3
Winter	S1	12.02.2014	85.6	86.1	0.5	109.8	89.7
		19.02.2014	53.2	45.0	8.2	57.3	35.0
	S2	13.02.2014	135.1	52.3	82.8	71.2	106.1
		20.02.2014	72.5	80.6	8.1	206.4	70.3
	S3	18.02.2014	96.9	104.6	7.7	109.0	29.6
Spring	S1	28.05.2014	33.8	15.8	18.0	82.6	41.3
		4.06.2014	10.1	14.5	4.4	100.4	8.2
	S3	3.06.2014	60.4	12.6	47.8	80.7	32.4

Moreover, the results obtained reveal that the best fit is obtained in July for all stations, when lower fluvial inflows occurred, with a RE of approximately 44, 38 and 60% (on average), for Costa Nova, Vista Alegre and Ponte da Varela stations, respectively. Errors increase in February, when higher river discharges are expected, due to the uncertainty associated.

Figure 5.5 presents the model predictions and observations for some of the stations from S4 to S13. Since the observations referred in the bibliography are from different dates (generally before the simulation period) and there is no information regarding the sampling hour for most of the data, it was only performed a qualitative comparison between the predicted and observed SSC. The observed data was compared with the average values of model predictions over the tidal cycle.

Despite the limitations of the observed data, results show reasonable agreement between the model predictions and field observations. Generally, the model overestimates the SSC, maybe due to the fact that observations are a punctual measure, while the model results correspond to the SSC daily average. The major deviations are observed in the winter/spring months (February and March), which is mainly related to the values uncertainty for high

fluvial discharges. This is the case of stations S6 and S10, located nearby Vouga river mouth and station S13, nearby Antuã river mouth.

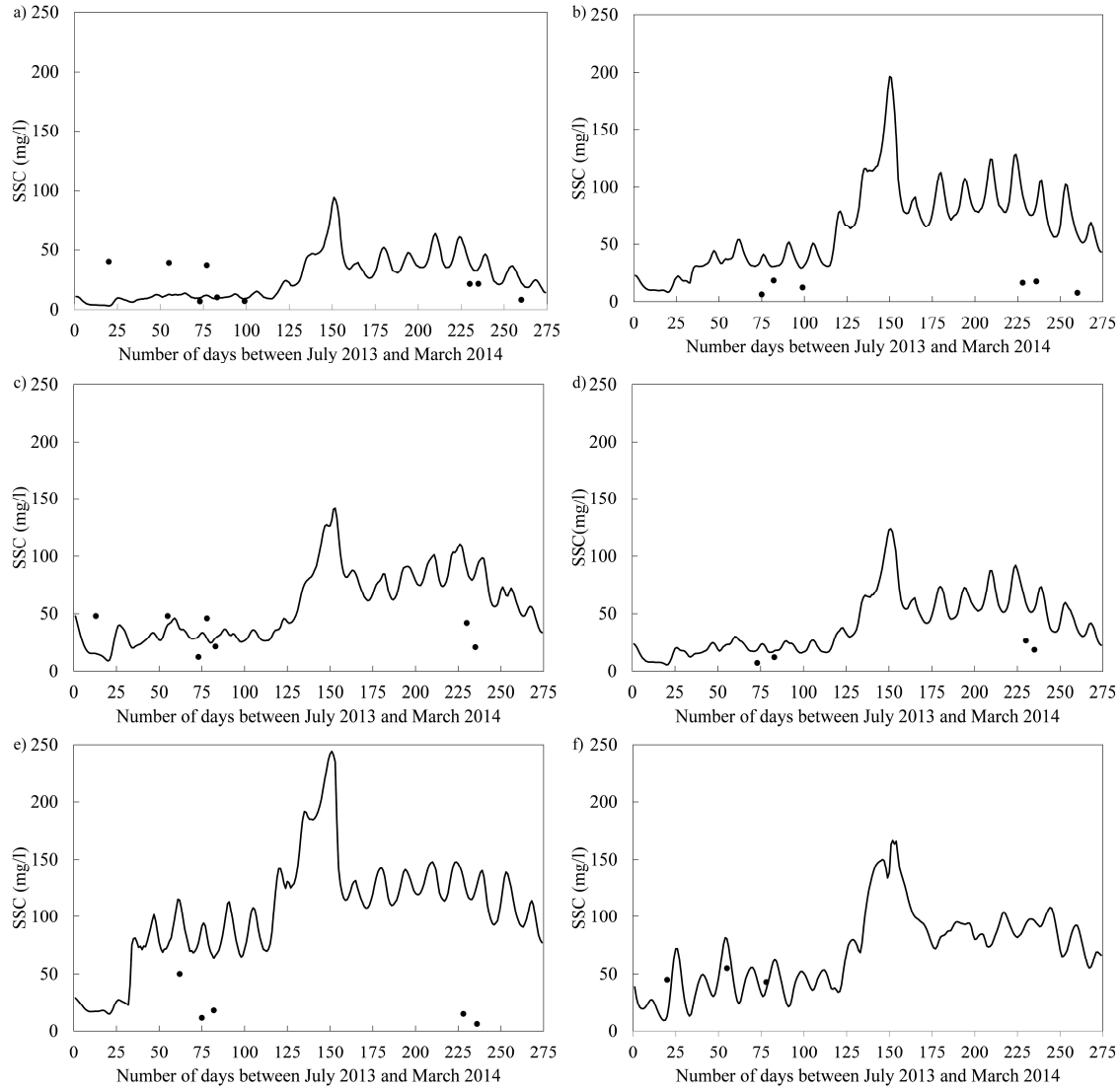

Figure 5.5: Comparison between observed (●) and predicted (─) SSC at stations: a) S4; b) S6; c) S8; d) S9; e) S10; f) S13. Observed data from Abrantes (2005), ARH Centro (2009), Portela *et al.* (2011) and surveys performed in 2013/14 (Section 2.2.5).

5.8 Conclusions

The numerical model MOHID was implemented for Ria de Aveiro to study the suspended sediment transport. Previous to model validation, a sensitivity analysis was undertaken, to determine the influence of fine sediments settling velocity in the lagoon SSC predictions. Analysis of obtained results for different settling velocity formulations showed that:

- For a settling velocity salinity-dependent formulation, SSC predictions present higher values than observations range. This was observed especially for spring tide conditions, showing that despite high salinity values at areas nearby the inlet, the suspended sediments are transported towards the inlet;
- For a constant settling velocity of 1×10^{-3} m/s very low SSC predictions were obtained, being observed deposition of the sediments;
- For a lower constant settling velocity of 1×10^{-5} m/s, the SSC predictions values are closer to the range of observations, for both tide conditions at all analysed stations, showing to be the most appropriate value and therefore used in the performed simulations.

Results from the model validation show that SSC evolution at lagoon is successfully reproduced along the tidal cycle in the Costa Nova, Vista Alegre and Ponte da Varela stations. Daily variations of SSC data are clearly observed in the predicted SSC, with higher values in ebb than in flood periods.

The best fit between model predictions and observations was obtained in July and the higher disagreement in February, at Ponte da Vista Alegre and Ponte da Varela stations, due to uncertainty of SSC associated to high fluvial discharges. RMSE and RE obtained values are acceptable, considering the fact that were imposed constant monthly SSC and daily fluvial discharges at rivers boundaries.

Due to the limited SSC *in situ* data for Ria de Aveiro for only three stations, a comparison with bibliographic data at more stations was also performed. The obtained results indicate reasonable agreement between model predictions and observations although the model generally overestimates the observed SSC, especially during winter months (February and March).

6 Ria de Aveiro suspended sediment transport evolution

6.1 Introduction

Over time, Ria de Aveiro has experience geomorphological changes, result of natural and anthropogenic pressures. Harbour facilities development at the inlet area was decisive to the actual lagoon configuration. Moreover, several dredging operations were performed at lagoon channels. In Chapter 3 was verified that inlet and main lagoon channels downstream areas have experienced significant deepening, between 2001 and 2012, mainly as result of dredging operations.

Tidal propagation at Ria de Aveiro depends strongly on the lagoon geomorphologic configuration. Changes in the channels depth and geometry have a significant impact in lagoon tidal dynamics (Araújo *et al.*, 2008; Dias and Picado, 2010; Lopes *et al.*, 2013b). Moreover, changes in tidal propagation influence the sediment balance, modifying the lagoon potential to export sediments. Therefore, it is important to understand the evolution of the Ria de Aveiro suspended sediment transport over time, considering the morphological changes that have occurred. In this chapter, numerical model simulations were performed to

assess Ria de Aveiro suspended sediment dynamics changes occurred from the past to present lagoon conditions.

6.2 Methodology

Evaluation of the Ria de Aveiro suspended sediment dynamics changes occurred from the past to present was performed simulating the present and past lagoon conditions with the numerical model MOHID, previously validated (Chapter 5). Present conditions were simulated using the most recent bathymetry (Figure 5.2; Chapter 5) and for past conditions, a bathymetry from 1987/88 based on data provided by IH.

A comparative analysis of past and present bathymetry show that channels geometry was almost unchanged, being only verified the enlargement of the Aveiro harbour. Major variations were observed in the inlet and harbour region depths, where between 1987/1988 and 2001 the deepening of the inlet achieved 10 m in some areas. Relatively to the main channels, Mira channel deepening was up to 3 m, while at the S. Jacinto and Espinheiro channels downstream areas achieved 8 m (Figure 6.1). In the Ílhavo channel downstream area slight deposition was observed. These results are in agreement with those presented by Dias *et al.* (2011) and Lopes *et al.* (2013b).

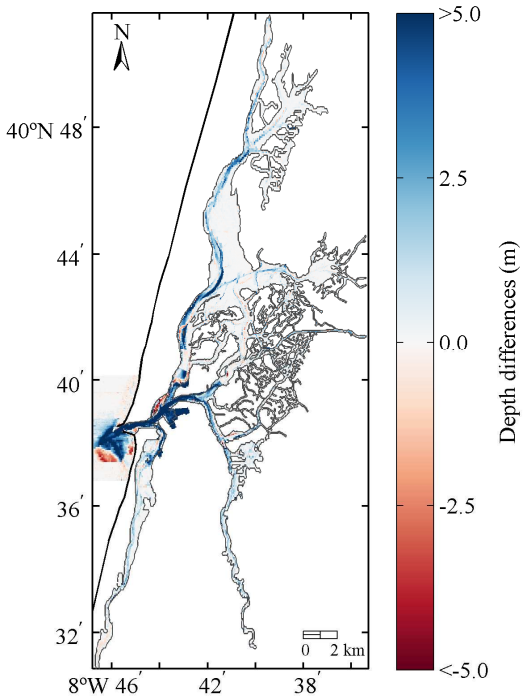

Figure 6.1: Ria de Aveiro bathymetric differences between actual and 1987/88 bathymetry.

Simulation results were analysed for both spring and neap tide conditions. A spin-up period of 60 days was set in order to ensure the results independence from the initial conditions. The present mean sea level was imposed at the open ocean boundary through tidal harmonic constituents, as described in Chapter 5.

Predicted daily discharges from watershed model SWIM for present climate were imposed at Cáster, Antuã, Vouga, Boco and Valas de Mira. Time series of February, May and August months were chosen to force the model, as representative of wet and dry seasons and mean fluvial conditions, referred as high, mean and low fluvial discharge conditions.

Monthly average discharges for the lagoon fluvial tributaries determined from daily discharges predictions of SWIM model for present climate are presented in Figure 6.2. Vouga monthly average discharges ranges from 39 m^3/s at August and 147 m^3/s at February, with an annual average discharge of 87 m^3/s. Comparatively to Vouga, Antuã and Valas de Mira have a low flow, with monthly average discharges ranging from 2 and 0.02 m^3/s at August and 12 and 14 m^3/s at February, respectively. Its annual average discharges are 7 and 6 m^3/s for the 1981-2010 period. Finally, the Cáster and Boco rivers, its annual average discharges are around 2 m^3/s, ranging from 0.06 and 0 m^3/s at August, respectively and 4 m^3/s at February.

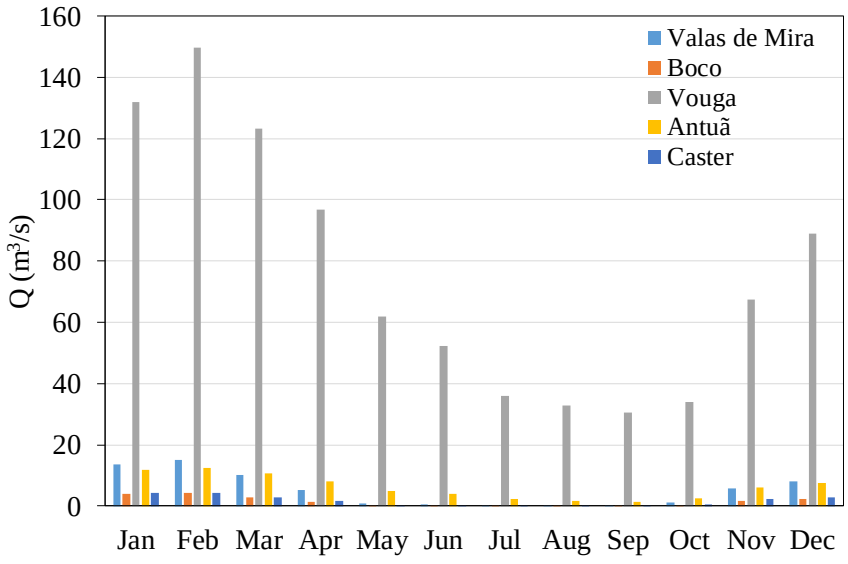

Figure 6.2: Monthly mean discharges for present climate.

In order to determine the year that better represents the present climate discharges, a statistical analysis was performed. This analysis was performed only for the Vouga river, since it is the lagoon main fluvial tributary, as referred in Section 2.2.3. In this frame, the Vouga discharges were grouped in classes and the percentage of occurrence was determined for the 30 year's data and for each year. Afterwards, the correlation coefficient between each year and the 30 years' data of present climate was computed (Figure 6.3). The year of 1985 was chosen has representative of present climate, since it presented the highest correlation coefficient (0.98).

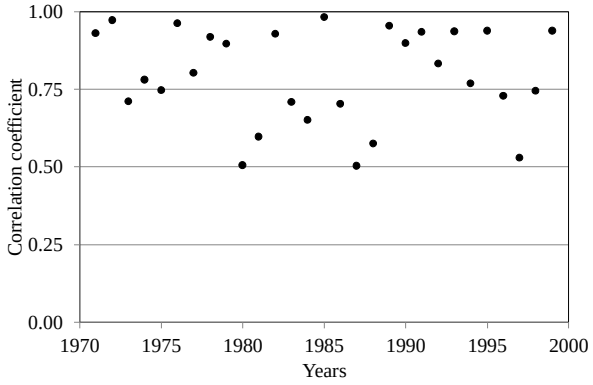

Figure 6.3: Correlation coefficient of Vouga discharge between each year and the 30 years data, for present climate.

Since there is no river's SSC data available for present climate, was considered a constant value along the analysed periods for each lagoon fluvial tributaries, but varying according to high, mean and low fluvial discharges (Table 6.1). The considered values were chosen taking into account the values used in the model validation (Section 5.5.2).

Table 6.1: SSC (mg/l) associated to the high, mean and low fluvial discharge conditions.

River	High	Mean	Low
Vouga	150	100	30
Antuã	50	40	10
Boco	20	15	8
Valas de Mira	30	20	5
Cáster	10	5	5

Evaluation of the lagoon suspended sediment transport evolution from past to present was made through a comparative analysis between the two scenarios in terms of velocity, SSC, water and sediment fluxes values at five cross sections located at lagoon central area (Figure

6.4). These cross sections were selected in order to evaluate the main channels, Barra, S. Jacinto, Espinheiro, Ílhavo and Mira.

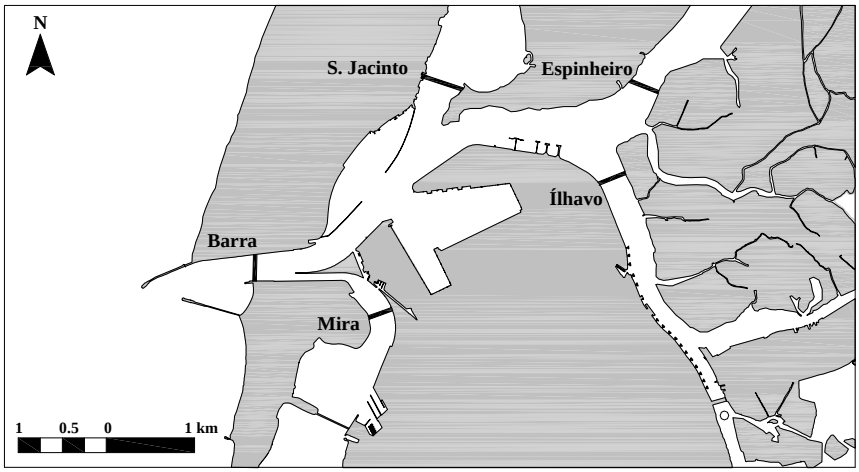

Figure 6.4: Main lagoon channels cross sections location.

Water fluxes (q) at each cross section for the ebb and flood periods were determined as the sum of the product of the cross sectional area and the velocity at each vertical profile:

$$q_{ebb/flood} = \sum_{j=1}^{n} A_j \cdot v_j \tag{6.1}$$

where n is the total number of sampling points at each cross section, v_j is the velocity projected in the channel direction (m/s) at each vertical profile in the section and A_j (m^2) the cross sectional area contributing for location j.

Suspended sediment fluxes at each vertical profile were determined by multiplying SSC and the velocity projected in the channel direction:

$$q_{sj} = C_j \cdot v_j \tag{6.2}$$

Suspended sediment fluxes across the cross section for ebb and flood periods were determined as:

$$q_{s,ebb/flood} = \sum_{j=1}^{n} q_{sj} \cdot A_j \tag{6.3}$$

where q_{sj} ($mg/m^2/s$) is the suspended sediment flux at each vertical profile. Total suspended sediment volume transported in the tidal cycle across the cross section was determined as the sum of suspended sediment fluxes at ebb and flood periods.

6.3 Results and discussion

6.3.1 Present conditions

The temporal evolution of velocity and water fluxes along two tidal cycles at the middle of the five cross sections of main lagoon channels, during spring and neap tide conditions for high, mean and low fluvial discharge conditions are presented in Figure 6.5. Positive values of velocity and water fluxes indicate flood and negative represent ebb. Time-averaged values during flood and ebb periods are given in Table 6.2.

In general, ebb currents are higher than flood currents (Figure 6.5; Table 6.2), evidencing the ebb-dominance of the lagoon central area, as stated by Oliveira *et al.* (2006), Lopes *et al.* (2006) and Lopes and Dias (2015). Additionally, spring tide conditions present higher velocities for all analysed situations, in accordance with Dias *et al.* (2003). During high fluvial discharge conditions, velocities are slightly higher than for low discharges, approximately 5% (on average). Although, for neap tide conditions is verified the opposite, with 4% lower velocities comparing to low discharge conditions (Table 6.2).

Velocities are stronger at the lagoon deeper channels, Barra and S. Jacinto channels, with mean values at spring tide of 0.66 and 0.64 m/s for high fluvial discharges, 0.64 and 0.62 m/s, for mean and 0.63 and 0.61 m/s for low fluvial discharges. In these channels are also predicted higher differences between ebb and flood currents. In opposition, at Ílhavo and Mira channels in neap tide conditions the differences between flood and ebb velocities are almost zero (Table 6.2).

Regarding the water fluxes, similar trends to those found for velocities are expected, with higher values for high fluvial discharge conditions at spring tide, presenting Barra and S. Jacinto channels the highest values (4.76×10^3 and 2.34×10^3 m^3/s, respectively) (Figure 6.5; Table 6.2). In general, water fluxes are higher at ebb period. However, the opposite is expected at Ílhavo channel, where fluxes are 20% higher in the flood than in the ebb. This pattern is also found at Espinheiro and Mira channels for spring tide conditions, but with lower differences (3 and 2% on average, respectively) (Table 6.2).

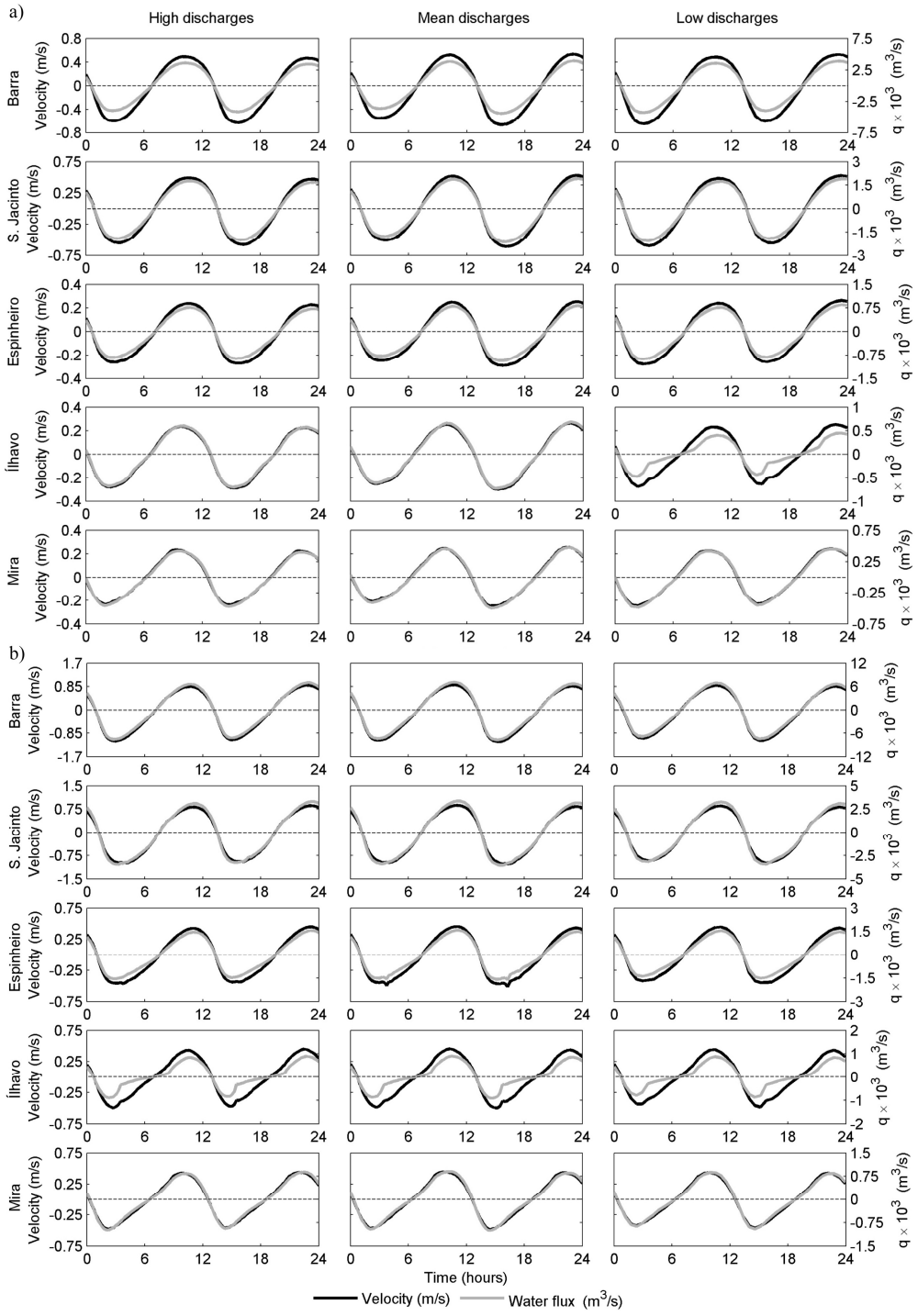

Figure 6.5: Velocity and water fluxes for present conditions, at Barra, S. Jacinto, Espinheiro, Ílhavo and Mira channels cross sections: a) Neap tide; b) Spring tide.

Table 6.2: Time-averaged velocities and water fluxes for present conditions, at Barra, S. Jacinto, Espinheiro, Ílhavo and Mira channels cross sections.

	Transect	Spring tide				Neap tide			
		Flood		Ebb		Flood		Ebb	
		v (m/s)	$q \times 10^3$ (m^3/s)	v (m/s)	$q \times 10^3$ (m^3/s)	v (m/s)	$q \times 10^3$ (m^3/s)	v (m/s)	$q \times 10^3$ (m^3/s)
High discharges	**Barra**	0.60	4.55	0.73	4.76	0.33	2.36	0.39	2.56
	S. Jacinto	0.58	2.18	0.69	2.34	0.33	1.16	0.37	1.27
	Espinheiro	0.30	1.00	0.31	0.97	0.16	0.49	0.18	0.54
	Ílhavo	0.27	0.74	0.32	0.79	0.15	0.23	0.15	0.20
	Mira	0.27	0.54	0.28	0.54	0.15	0.26	0.14	0.27
Mean discharges	**Barra**	0.59	4.44	0.70	4.59	0.36	2.61	0.43	2.82
	S. Jacinto	0.57	2.12	0.67	2.26	0.36	1.28	0.40	1.41
	Espinheiro	0.29	0.97	0.30	0.94	0.17	0.53	0.19	0.61
	Ílhavo	0.26	0.47	0.27	0.36	0.16	0.26	0.17	0.23
	Mira	0.27	0.53	0.27	0.52	0.16	0.30	0.16	0.31
Low discharges	**Barra**	0.57	4.34	0.68	4.46	0.34	2.46	0.40	2.58
	S. Jacinto	0.56	2.06	0.65	2.20	0.34	1.19	0.37	1.29
	Espinheiro	0.29	0.95	0.29	0.91	0.17	0.52	0.17	0.54
	Ílhavo	0.26	0.46	0.26	0.35	0.15	0.24	0.15	0.20
	Mira	0.26	0.52	0.26	0.50	0.16	0.30	0.16	0.31

The temporal evolution along two tidal cycles of the SSC and sediment fluxes at the middle of the main lagoon channels cross sections for high, mean and low fluvial discharge conditions is present in Figure 6.6. Positive values occur during flood and negative during ebb. Time-averaged values for flood and ebb periods are given in Table 6.3.

SSC and suspended sediment fluxes evolution follows the tidal cycle, as previously referred by Lopes *et al.* (2001) and Dias *et al.* (2003), with extreme values at low and high tide, suggesting that sediments are transported from the upstream areas towards the inlet during the ebb. In the flood period, currents transport sediments to the upstream areas, which allied to the sea water entry leads to SSC reduction (Figure 6.6). SSC and suspended sediment fluxes present the highest values for high fluvial discharge conditions, decreasing to low fluvial discharges, highlighting the river's importance as lagoon sediment sources.

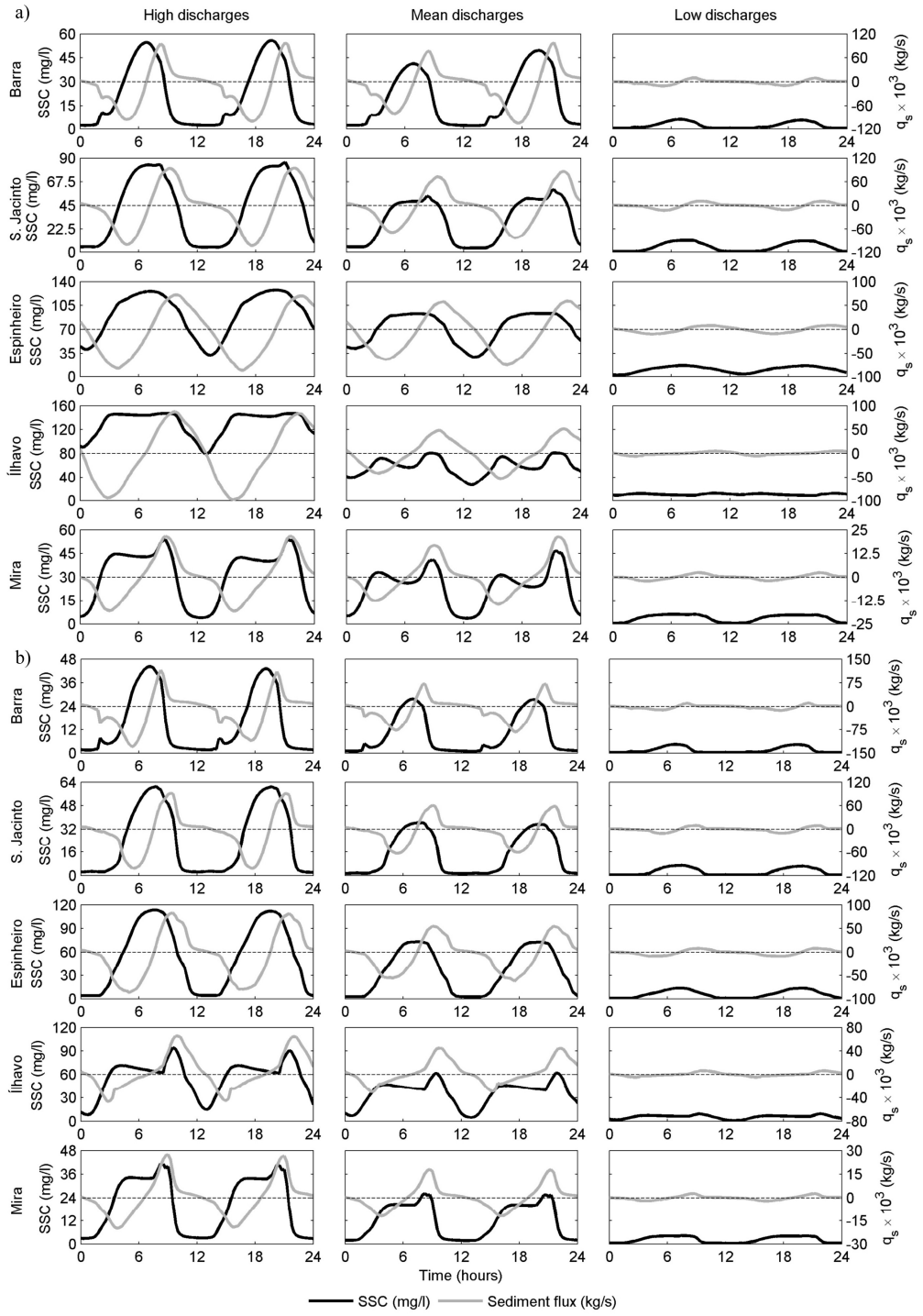

Figure 6.6: SSC and sediment fluxes for present conditions, at Barra, S. Jacinto, Espinheiro, Ílhavo and Mira channels cross sections: a) Neap tide; b) Spring tide.

Generally, higher SSC are expected during ebb period. However, there are some exceptions with higher values at flood period, but with small differences around 3%, namely at Ílhavo

for high (both tidal conditions) and mean (spring tide) and low fluvial discharge conditions (neap tide), and at Mira channel for high (neap tide) and mean fluvial discharge conditions (both tidal conditions). Additionally, spring tide presents lower values comparing to neap tide (Table 6.3). Espinheiro and Ílhavo cross sections presents the highest SSC values of 43 mg/l (on average). In opposition, lower values (9.50 mg/l on average) are predicted for Barra channel, where larger SSC differences between ebb and flood (approximately 35%) are also found (Table 6.3).

Table 6.3: Time-averaged SSC and sediment fluxes, for reference scenario, at Barra, S. Jacinto, Espinheiro, Ílhavo and Mira channels cross sections.

		Spring tide				**Neap tide**			
	Transect	**Flood**		**Ebb**		**Flood**		**Ebb**	
		SSC (mg/l)	**q_s (ton/s)**	**SSC (mg/l)**	**q_s (ton/s)**	**SSC (mg/l)**	**q_s (ton/s)**	**SSC (mg/l)**	**q_s (ton/s)**
High discharges	**Barra**	11.2	28.0	16.9	56.5	18.3	30.8	24.1	50.0
	S. Jacinto	21.0	30.1	24.5	43.4	41.1	42.1	43.5	49.8
	Espinheiro	47.9	36.0	55.3	45.3	91.8	43.5	97.0	51.4
	Ílhavo	54.5	27.8	50.9	17.2	87.6	22.1	86.7	18.4
	Mira	18.8	8.6	19.8	9.1	30.8	9.0	30.6	8.7
Mean discharges	**Barra**	7.6	19.2	11.1	35.9	16.8	30.4	20.6	47.2
	S. Jacinto	13.2	19.5	16.0	27.9	29.9	35.3	31.2	40.2
	Espinheiro	32.7	24.6	38.5	31.5	68.7	35.6	73.3	44.3
	Ílhavo	37.5	18.9	35.7	12.1	61.3	18.2	62.3	15.8
	Mira	12.3	5.8	12.2	5.5	24.0	8.1	23.6	7.5
Low discharges	**Barra**	1.2	3.3	1.7	5.4	1.8	3.2	2.3	4.8
	S. Jacinto	2.3	3.2	2.7	4.5	4.8	4.7	5.0	5.4
	Espinheiro	5.6	4.0	6.1	4.5	10.3	5.2	10.6	5.5
	Ílhavo	5.7	2.8	5.3	1.7	10.4	2.7	10.3	2.2
	Mira	2.2	0.9	2.2	1.0	3.2	0.9	3.3	1.0

Sediment fluxes present the same evolution as SSC along the tidal cycle (Figure 6.6). Results point out higher values during ebb period at neap tide conditions. Higher differences between flood and ebb are found at Barra and S. Jacinto channels (70 and 29%, on average, respectively). However, at Ílhavo channel is predicted a 27% decrease of sediment fluxes from flood to ebb (Table 6.3). Noteworthy, is the small differences between flood and ebb sediment fluxes expected at Mira channel, which is in agreement with Dias *et al.* (2001) results, that indicate high residence time at downstream area of this channel.

In Figure 6.7 are presented the suspended sediment volumes predicted to be transported during ebb and flood periods, at the five cross sections located at the main channels, for high, mean and low fluvial discharge conditions in spring and neap tide conditions.

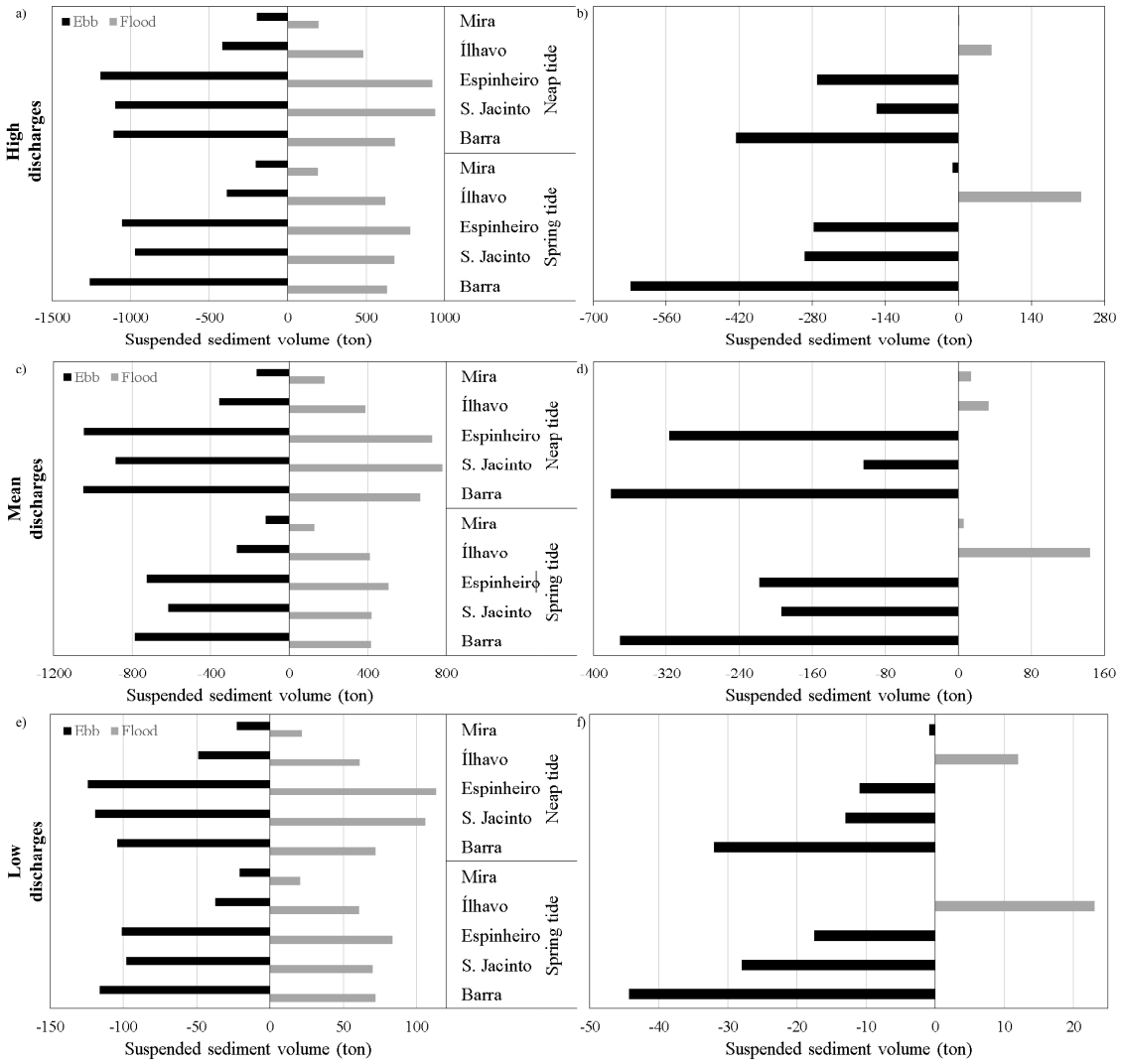

Figure 6.7: Total suspended sediment transported volumes for present lagoon conditions at Barra, S. Jacinto, Espinheiro, Ílhavo and Mira channels cross sections, for high (a, b), mean (c, d) and low fluvial discharge conditions (e, f), in the flood and ebb periods (a, c, e) and tidal cycle balance (b, d, f).

Higher suspended sediment volumes are found for high fluvial discharge conditions, as expected. The sediment fluxes direction is predicted to be mainly directed towards the ocean, except at Ílhavo channel and at Mira channel in neap tide for mean fluvial discharge conditions (Figure 6.7b,d,f). These results are in agreement with previous works which have indicated that Ria de Aveiro can act as a trap of fine sediments, especially at neap tide conditions (Abrantes *et al.*, 2006; Dias *et al.*, 2007).

Suspended sediment balance for a tidal cycle at Barra channel ranges between 426 and 627 tons and 32 and 44 tons for high and low fluvial discharge conditions, at spring and neap

tide, respectively. The obtained values are lower than those referred in previous works, of 500 and 11000 tons at winter and 250 and 600 tons at summer, for neap and spring tide conditions, respectively (Abrantes et *al.* 2006). These differences can be related to the fact that the periods dates are different. Moreover, the sediment fluxes estimated at this study were based on computed SSC at each minute along the tidal cycle, while in Abrantes *et al.* (2006) were estimated based on SSC field observations at 2-hour intervals.

Spatial SSC distribution along the lagoon at different tidal stages (low and high tide periods at inlet) is presented in Figures 6.8, 6.9 and 6.10, for high, mean and low fluvial discharge conditions, respectively, at spring and neap tide. SSC maps show a longitudinal gradient, with higher concentrations at upstream areas due to river's discharges, in agreement with previous results from Lopes *et al.* (2001). In opposition, lower SSC are found nearby the lagoon inlet, due to tidal influence. Moreover, higher SSC are predicted for high fluvial discharges, reflecting the river's sediment loads importance on the SSC distribution along the lagoon.

The lagoon central area presents the higher SSC, ranging between 30 and 150 mg/l, highlighting the Vouga river importance as sedimentary source. The extension of the high SSC area increases from low to high fluvial discharge conditions and from high to low tide, being detected the influence of different fluvial lagoon tributaries at low tide (Figures 6.8a,c, 6.9a,c and 6.10a,c).

At channels downstream areas are predicted higher SSC variations due to tidal action, with highest SSC found at the ebb period, explained by the strong currents that produces a downstream advection of water with high SSC, in agreement with Lopes *et al.* (2006) results. In S. Jacinto channel upstream area, nearby the entry of the Laranjo bay, are expected higher SSC, especially at spring tide (Figures 6.8a,b, 6.9a,b and 6.10a,b). This pattern was previous verified by Lopes *et al.*, (2001, 2006) and Lopes and Dias (2007), which can be explained by the strong currents generated by the narrow entrance connecting S. Jacinto channel and Laranjo bay.

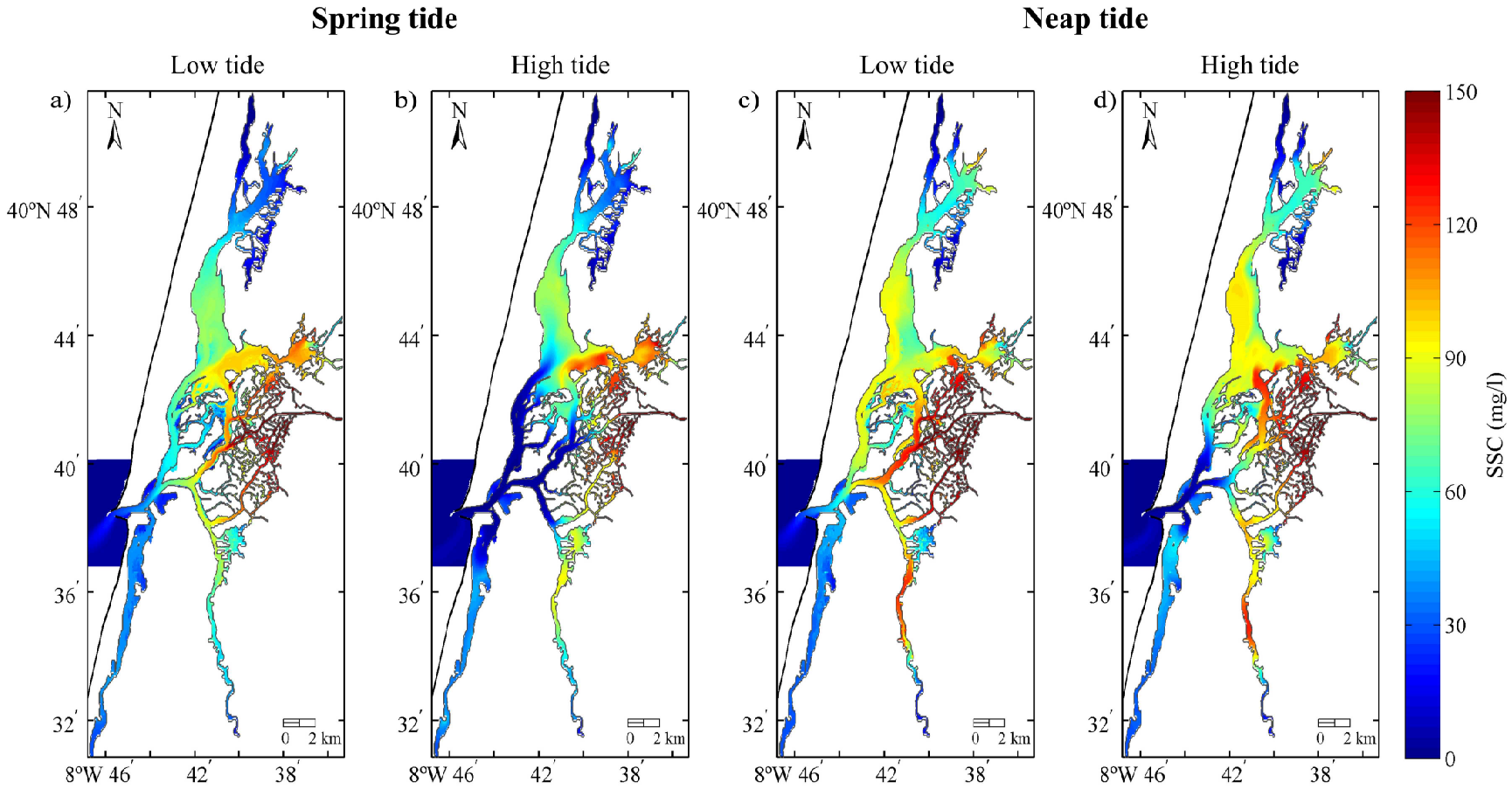

Figure 6.8: Spatial SSC for high fluvial discharge conditions, in spring (a, b) and neap (c, d) tide, at low (a, c) and high (b, d) tide at the inlet.

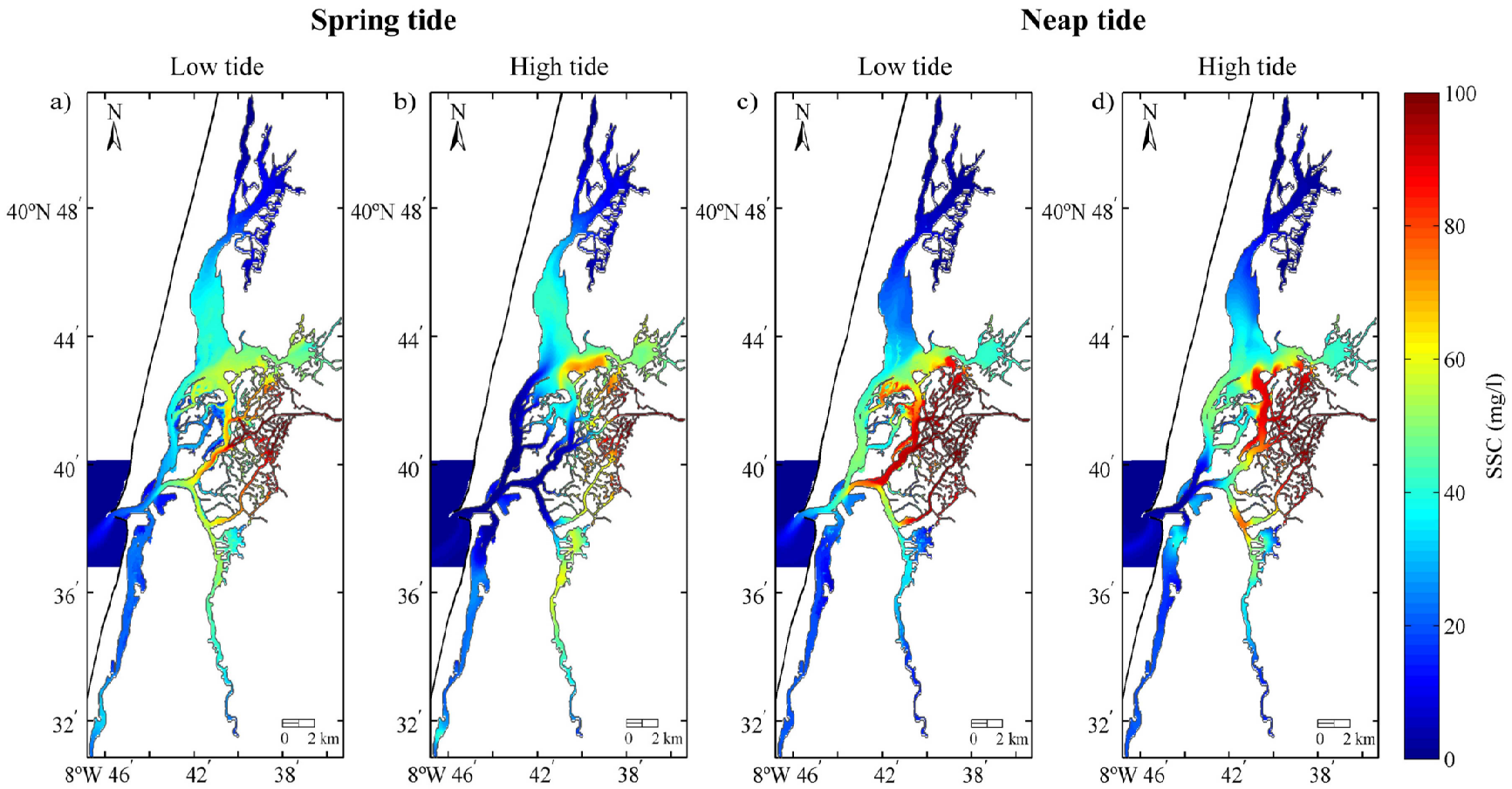

Figure 6.9: Spatial SSC for mean fluvial discharge conditions, in spring (a, b) and neap (c, d) tide, at low (a, c) and high (b, d) tide at the inlet.

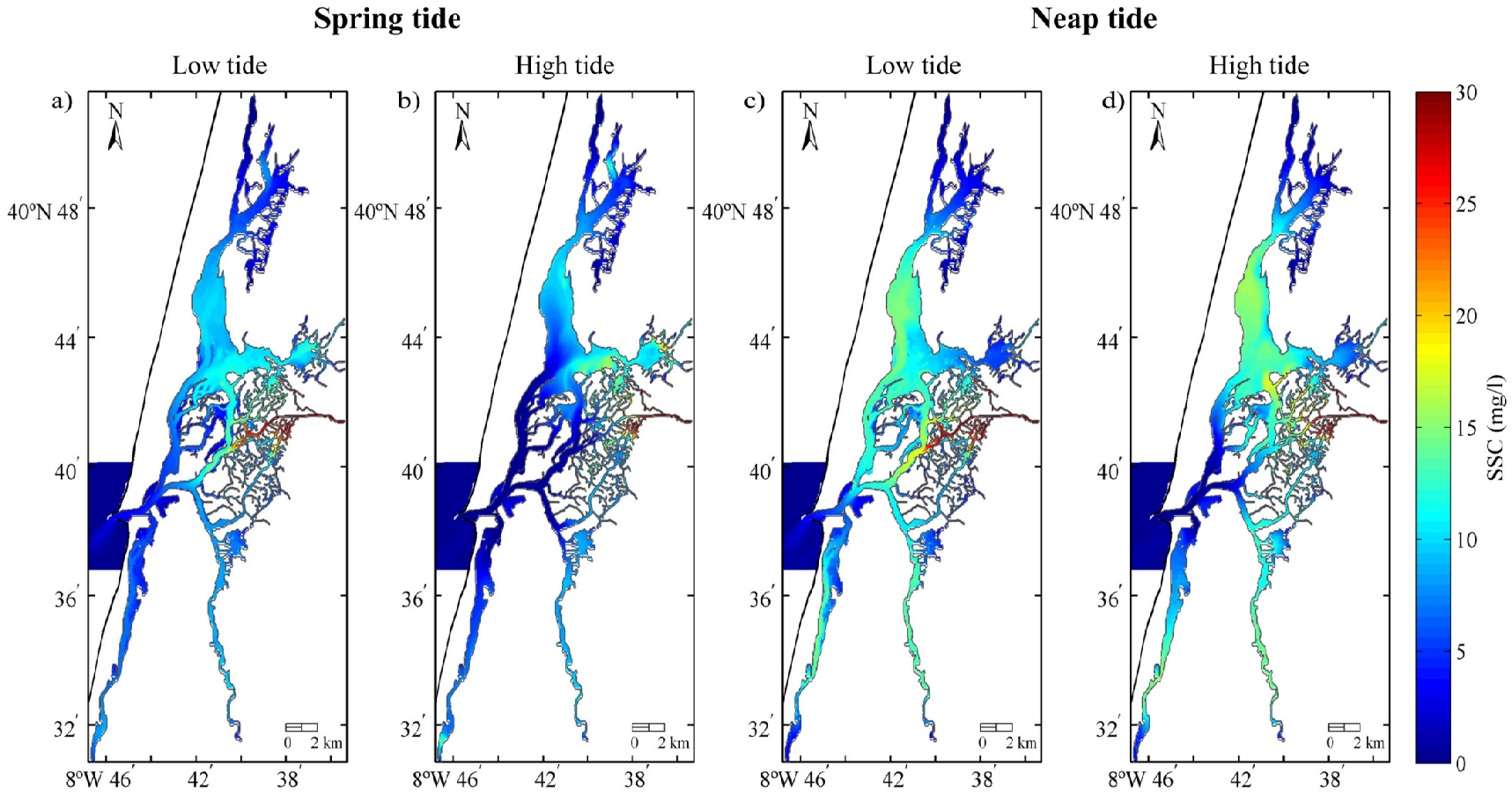

Figure 6.10: Spatial SSC for low fluvial discharge conditions, in spring (a, b) and neap (c, d) tide, at low (a, c) and high (b, d) tide at the inlet.

In the S. Jacinto, Espinheiro and Ílhavo channels are expected high concentrations, with sediments being propagated along the channels following the tidal cycle. In Mira channel, high SSC are restricted to downstream area, with most part of the channel presenting low values, which is due to weak tidal influence and low depths, as previous verified by Lopes *et al.* (2006). In the inlet area, high SSC occurred during ebb period, which is explained by strong ebb currents that produces a downstream advection of water with high SSC, in agreement with results of Lopes *et al.* (2006).

Furthermore, at spring tide due to high tidal prism is expected lower SSC, especially at the northern areas, upstream area of the S. Jacinto channel and central area (Figures 6.8b, 6.9b and 6.10b).

6.3.2 Past conditions

Over time, Ria de Aveiro has experienced deepening of its main channels, due to harbour development and dredging operations. Therefore, the changes in the suspended sediment transport from the past (1987/88) to present (2012) were evaluated.

Generally, was found that velocity differences between lagoon past and present conditions at main channels are low, not exceeding 0.1 m/s, except at Mira channel (Table 6.4).

Table 6.4: Time-averaged velocities and water fluxes differences between past and present conditions, at Barra, S. Jacinto, Espinheiro, Ílhavo and Mira channels cross sections.

	Transect	Spring tide				Neap tide			
		Flood		Ebb		Flood		Ebb	
		v (m/s)	q×10^3 (m^3/s)	v (m/s)	q×10^3 (m^3/s)	v (m/s)	q×10^3 (m^3/s)	v (m/s)	q×10^3 (m^3/s)
High discharges	**Barra**	-0.02	1.41	-0.09	1.03	-0.01	0.78	-0.05	0.77
	S. Jacinto	0.00	0.84	0.09	0.80	0.00	0.47	0.03	0.52
	Espinheiro	-0.08	0.16	-0.12	0.13	-0.04	0.08	-0.07	0.06
	Ílhavo	0.00	0.17	-0.04	0.06	0.01	0.08	-0.02	0.02
	Mira	-0.07	0.24	-0.18	0.25	-0.04	0.08	-0.09	0.07
Mean discharges	**Barra**	-0.01	1.69	-0.09	1.38	-0.01	0.86	-0.06	0.83
	S. Jacinto	0.01	0.83	0.07	0.91	0.00	0.51	0.03	0.57
	Espinheiro	-0.07	0.16	-0.12	0.12	-0.04	0.09	-0.08	0.07
	Ílhavo	0.00	0.16	-0.04	0.05	0.01	0.09	-0.03	0.03
	Mira	-0.07	0.24	-0.17	0.24	-0.05	0.09	-0.10	0.08
Low discharges	**Barra**	-0.02	1.65	-0.08	1.37	-0.01	0.93	-0.05	0.81
	S. Jacinto	0.01	0.81	0.08	0.90	0.00	0.48	0.03	0.53
	Espinheiro	-0.08	0.15	-0.11	0.12	-0.05	0.07	-0.07	0.06
	Ílhavo	0.00	0.16	-0.04	0.05	0.01	0.08	-0.03	0.02
	Mira	-0.07	0.24	-0.17	0.24	-0.03	0.16	-0.07	0.15

However, model results predict the velocities differences decrease between the flood and ebb periods, except at S. Jacinto channel, for present lagoon conditions. Moreover, at Ílhavo and Mira channels these differences became approximately null.

Regarding water fluxes was found an increase from lagoon past to present conditions, with average differences of 40% at S. Jacinto and Mira channels, followed by Barra, Ílhavo and Espinheiro channels with 32, 24 and 14%, respectively. These results are in agreement with the numerical modelling results performed by Dias and Picado (2011) and Lopes *et al.* (2013b), which show tidal prism increase, due to channels deepening at inlet (Table 6.4).

Overall, for lagoon past conditions, higher SSC are expected, due to the entrance of a lower sea water volume (Table 6.5). However, this pattern was not found for some conditions at Espinheiro and Ílhavo channels and for low fluvial discharge conditions.

The sediment fluxes for lagoon present conditions are expected to be higher (Table 6.5). These results are in agreement with Dias and Picado (2011) and Lopes and Dias (2015) numerical analysis, showing that tidal prism increase, leads to residence time decrease and tidal currents increase at lagoon central area, resulting in higher sediment exchange. Noteworthy, is the sediment fluxes differences between ebb and flood from the past to present at Ílhavo channel, where an increase from 9 to 27% was found.

Table 6.5: Time-averaged SSC and sediment fluxes differences between past and present conditions, at Barra, S. Jacinto, Espinheiro, Ílhavo and Mira channels cross sections.

	Transect	Spring tide				Neap tide			
		Flood		Ebb		Flood		Ebb	
		SSC (mg/l)	q_s (ton/s)	SSC (mg/l)	q_s (ton/s)	SSC (mg/l)	q_s (ton/s)	SSC (mg/l)	q_s (ton/s)
High discharges	**Barra**	2.47	-0.64	1.85	-0.90	6.44	-0.58	10.06	-0.15
	S. Jacinto	2.56	-0.95	-2.22	-1.61	5.75	-1.24	5.55	-1.32
	Espinheiro	-1.25	-0.74	1.54	-0.40	0.07	-0.58	3.01	-0.31
	Ílhavo	-2.71	-1.48	-4.31	-0.69	6.40	-0.75	2.16	-0.34
	Mira	2.70	-0.42	1.11	-0.50	8.28	-0.38	5.59	-0.34
Mean discharges	**Barra**	1.81	-0.51	2.19	-0.20	4.47	-0.66	7.79	-0.15
	S. Jacinto	1.97	-0.59	0.08	-0.84	3.48	-1.10	3.36	-1.17
	Espinheiro	-0.86	-0.49	1.49	-0.18	-4.31	-0.70	-1.08	-0.45
	Ílhavo	-1.98	-0.98	-3.09	-0.45	5.29	-0.63	1.18	-0.31
	Mira	2.01	-0.28	0.78	-0.30	5.98	-0.33	3.97	-0.29
Low discharges	**Barra**	0.00	-0.14	-0.08	-0.15	0.30	-0.10	0.40	-0.10
	S. Jacinto	-0.14	-0.14	-0.55	-0.21	-0.02	-0.18	-0.05	-0.20
	Espinheiro	-0.65	-0.11	-0.20	-0.07	-0.80	-0.10	-0.16	-0.07
	Ílhavo	-0.54	-0.16	-0.89	-0.08	-0.57	-0.12	-1.32	-0.07
	Mira	-0.15	-0.06	-0.34	-0.06	0.85	-0.04	0.35	-0.05

The total suspended sediment transport across the sections at main channels is predicted to increase from lagoon past conditions to present, with higher differences found at S. Jacinto and Mira channels of approximately 54% and 78% (on average), respectively (Figure 6.11). Regarding the sediment balance, its direction is predicted to be mainly towards the ocean, except at Ílhavo and Mira channels, as found for lagoon present conditions (Figure 6.11b,d,f).

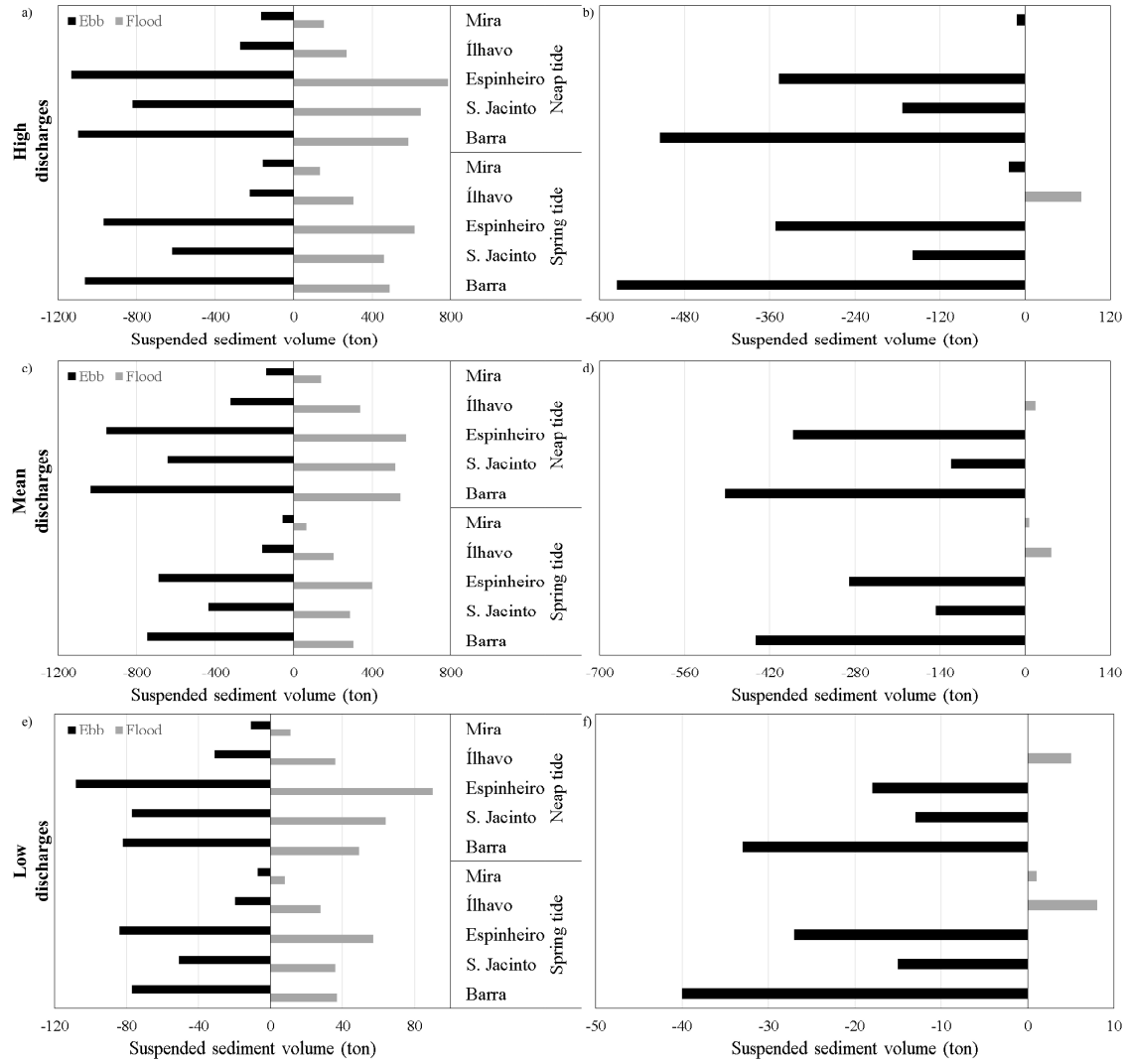

Figure 6.11: Total suspended sediment transported volumes for past lagoon conditions at Barra, S. Jacinto, Espinheiro, Ílhavo and Mira channels cross sections, for high (a, b), mean (c, d) and low fluvial discharge conditions (e, f), in the flood and ebb periods (a, c, e) and tidal cycle balance (b, d, f).

Spatial SSC differences along the lagoon between the lagoon present and past conditions during different tidal instants are presented in Figures 6.12, 6.13 and 6.14, for high, mean and low fluvial discharge conditions, in spring and neap tides.

The results show that for lagoon past conditions, higher SSC were found at central area, which is in agreement with the higher water volume entering in the lagoon at the present. However, for low fluvial discharge conditions, the differences at the central area are expected to be approximately zero.

Otherwise at river's mouth areas, lower concentrations are expected for lagoon past conditions, especially nearby Cáster, Gonde and Antuã rivers, which is maybe related with the combination of stronger tidal currents and shallow areas for present conditions, that are able to re-suspended sediments (Figure 6.14).

Moreover, for high and mean fluvial discharge conditions are expected high SSC at S. Jacinto channel upstream area, nearby the Laranjo bay. This situation can be explained by the strong currents which area enhanced for present conditions, since at S. Jacinto channel higher deepening was observed from 1987/88 to 2012, as previously referred.

6.4 Conclusions

Lagoon suspended sediment dynamics evolution from the past to present was studied through numerical modelling, using the past (1987/88) and actual (2012) bathymetries and imposing at lagoon fluvial tributaries, the discharges predictions for present climate. From the analysis of the obtained results the follow conclusions can be draw:

- The velocities differences between lagoon past and present conditions at the main lagoon channels are expected to be low, except at Mira channel. Moreover, a decrease in the velocities differences of the ebb and flood periods was found for present conditions, being approximately negligible at Ílhavo and Mira channels;
- An increase of the water fluxes was found from past to present conditions, with major average differences of 40% at S. Jacinto and Mira channels. Additionally, an opposite pattern is expected at Ílhavo channel, with higher water fluxes during flood than ebb;
- Generally, lower SSC are expected for present lagoon conditions at main channels. However, for sediment fluxes are predicted an increase with major differences found at Mira and Ílhavo channels, where is also predicted lower differences between the ebb and flood sediment fluxes;

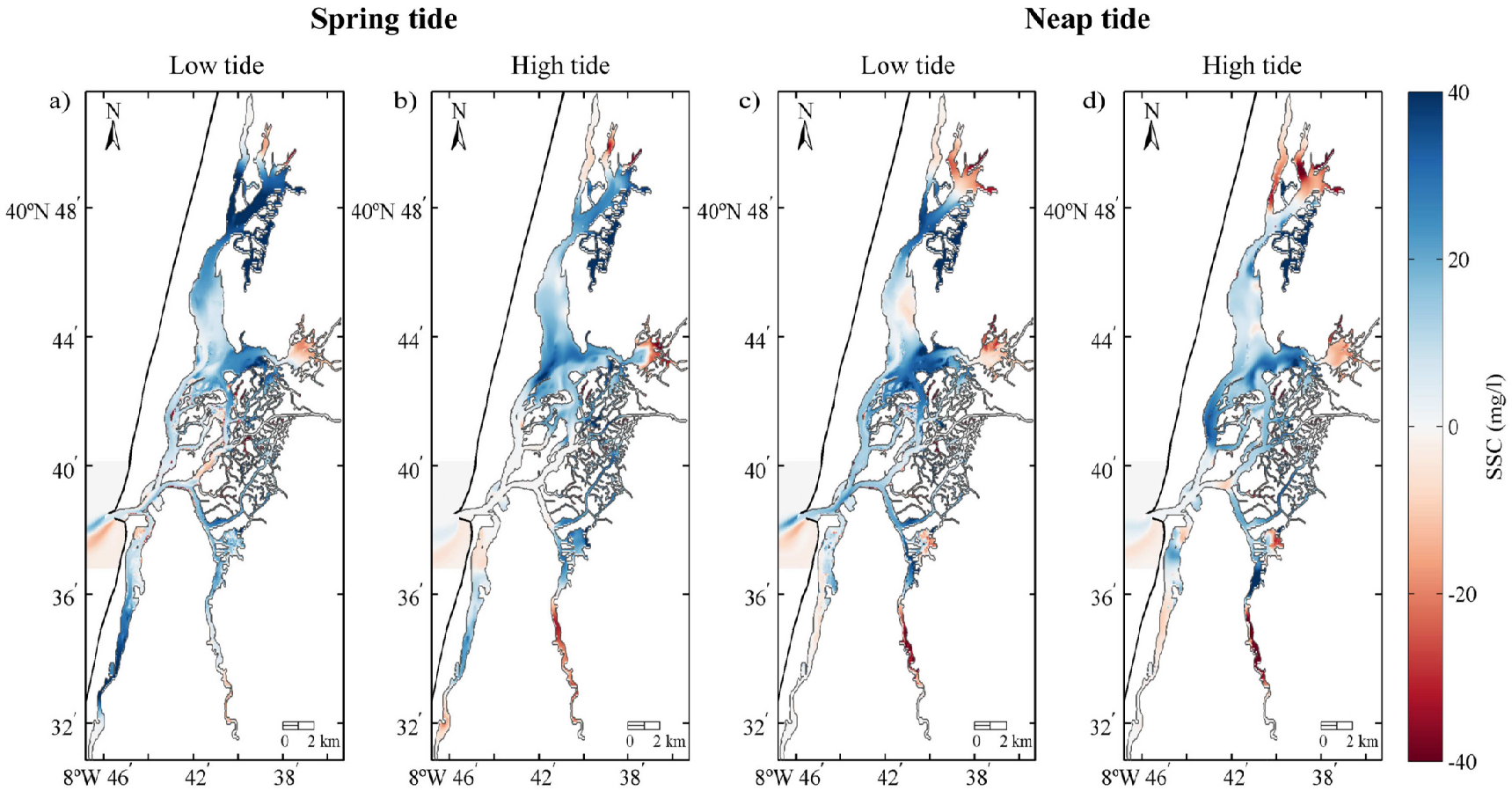

Figure 6.12: Spatial SSC differences between past and present conditions for high fluvial discharge conditions, in spring (a, b) and neap (c, d) tide, at low (a, c) and high (b, d) tide at the inlet.

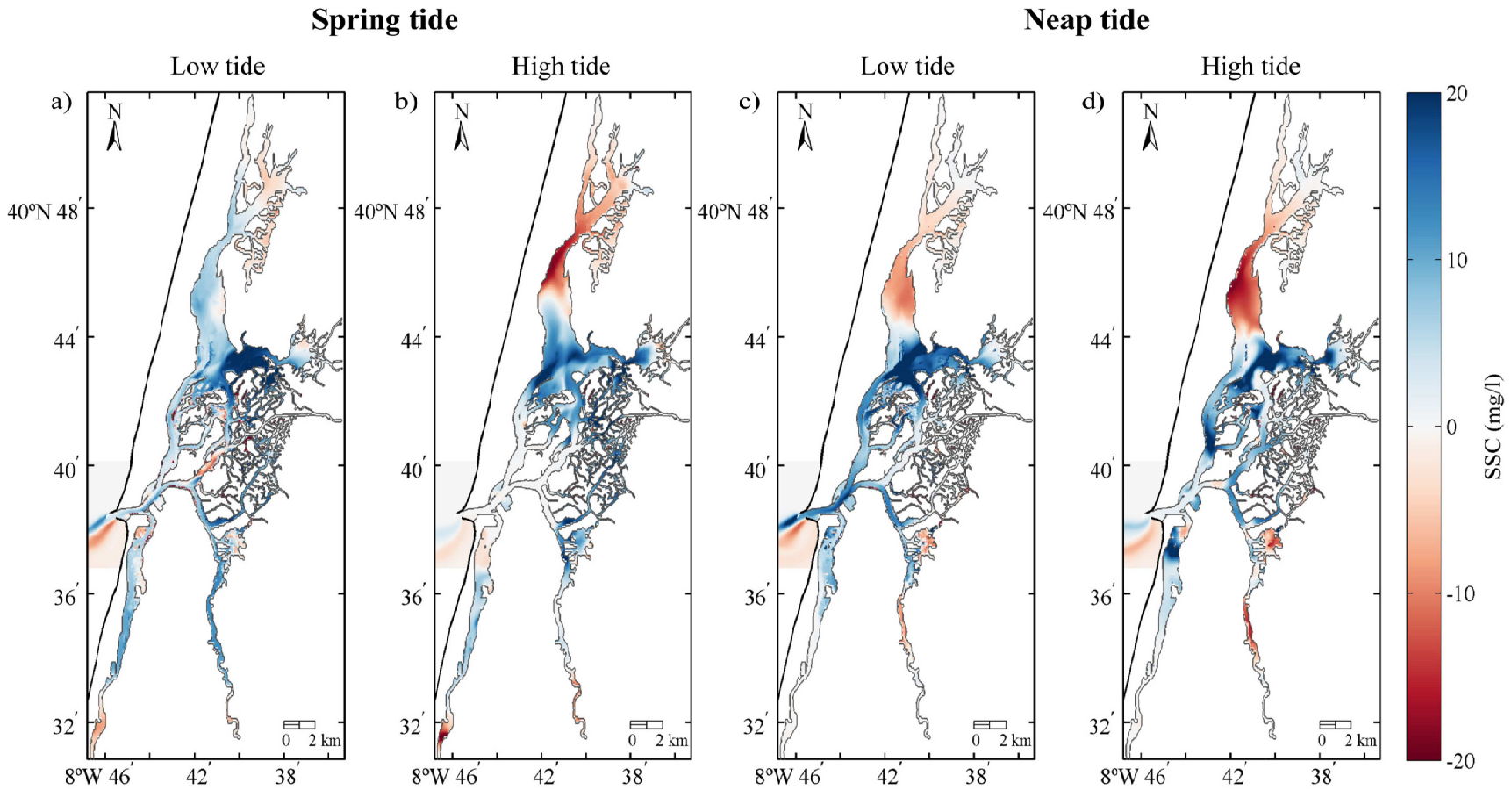

Figure 6.13: Spatial SSC differences between past and present conditions for mean fluvial discharge conditions, in spring (a, b) and neap (c, d) tide, at low (a, c) and high (b, d) tide at the inlet

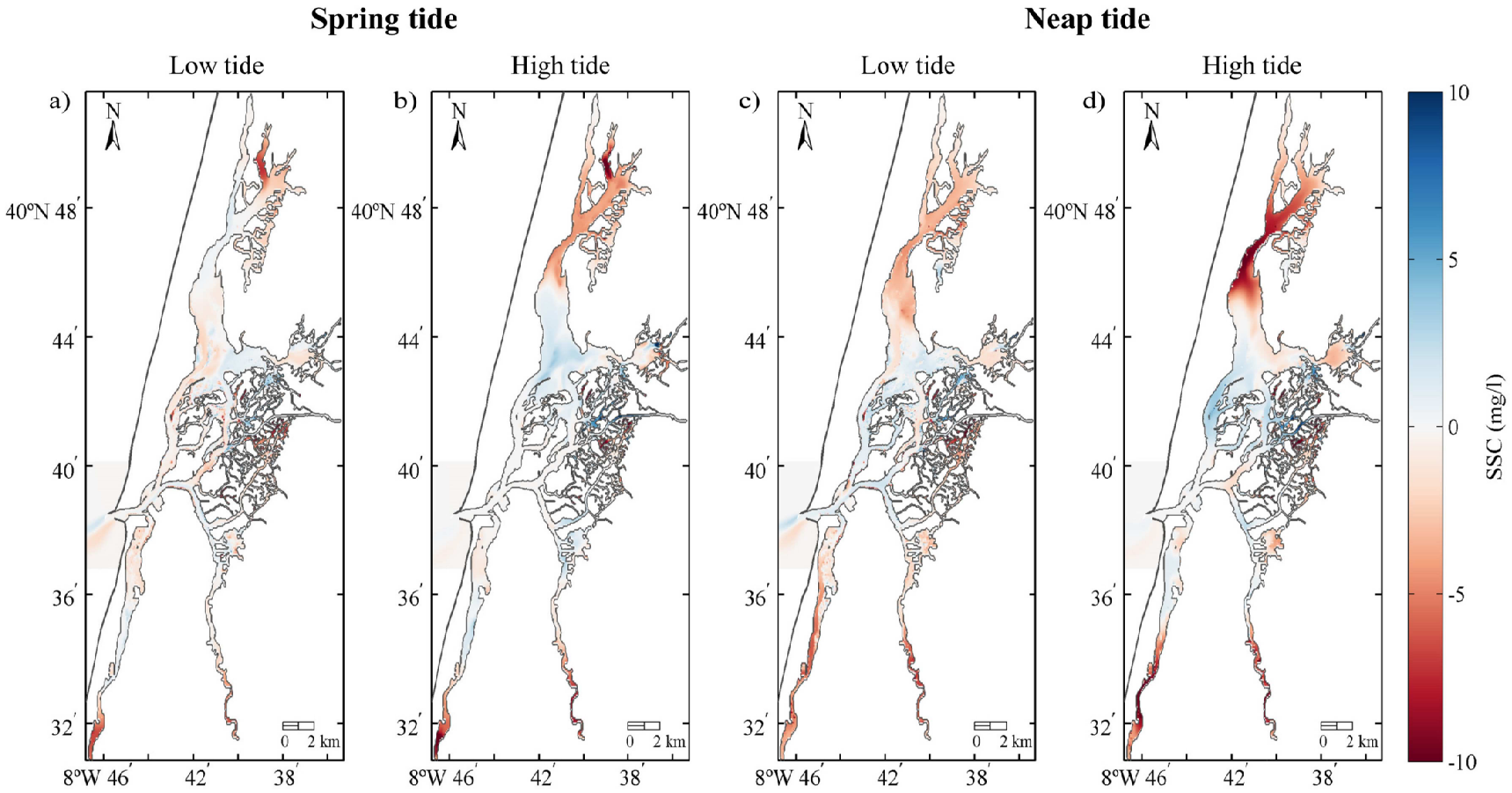

Figure 6.14: Spatial SSC differences between past and present conditions for low fluvial discharge conditions, in spring (a, b) and neap (c, d) tide, at low (a, c) and high (b, d) tide at the inlet.

- Total suspended sediment volumes transported in the tidal cycle is expected to present an increase for the lagoon present conditions at all channels, with larger differences of 50 and 40% found at S. Jacinto and Ílhavo channels, respectively. Regarding sediment fluxes direction there are not predicted any changes, being expected mostly exportation;
- SSC spatial differences distribution between the past and present conditions reflects the tidal prism increase, being expected lower concentrations at lagoon central area.

The results obtained in this chapter are in agreement with the morphological trends found for the downstream areas of main lagoon channels in Chapter 3. Indeed, Mira and Ílhavo channels downstream areas have showed a deposition trend, since at these channels are predicted high SSC at low tide instants for present conditions, comparing to S. Jacinto channel. However, the deposition rates present low values at these channels since is expected low sediment fluxes, comparing to the other channels. Moreover, the deposition with high rates at South Terminal is also consistent with high SSC values found at all analysed tidal instants at this area.

7 Assessment of future suspended sediment transport in Ria de Aveiro

7.1 Introduction

Coastal systems are very important areas, as interface zones between ocean and land, especially estuaries and lagoons, which are constantly changed and threatened by natural and anthropogenic pressures (Lopes *et al.*, 2011; Dias and Picado, 2011; Beer and Joyce, 2013).

Over time, there has been an increase of anthropogenic pressures at Ria de Aveiro adjacent area, related to the population growth. The same has been verified on the fluvial tributaries drainage basins, with the decline in forest cover and increase in agricultural and urban land uses, influencing the river discharges. Moreover, since the open of Ria de Aveiro inlet in 1808, the harbour infrastructures have been subjected to several works. Besides the structural works, dredging operations were performed to guarantee the navigability, being also planned a future intervention in the frame of Polis Litoral Ria de Aveiro/CIRA Actions.

Simultaneously, natural pressures are being intensified as result of climate change. An important consequence of climate change is the MSLR. Analysis of tidal-gauge data indicated global MSLR during the 20th century and several studies predict that will continue

to rise during the 21st century (Church and White, 2006; Meehl *et al.*, 2007). In Portugal, Ria de Aveiro is expected to be one of the regions most affected by sea level change (Andrade *et al.*, 2006; Lopes *et al.*, 2011). Changes in air temperature and precipitation will also modulate river discharges and sediment loads (Ganju and Schoellhamer, 2009). Therefore, understanding the impact of future anthropogenic pressures and climate change effects on the Ria de Aveiro suspended sediment transport is fundamental, in order to protect the ecosystem and prevent its degradation.

In this chapter, numerical model simulations of future scenarios were performed, to assess the influence of future anthropogenic actions and climate change effects in the Ria de Aveiro suspended sediment dynamics and on its potential to export sediments.

7.2 Methodology

In order to evaluate future morphologic and climatic changes in Ria de Aveiro suspended sediment dynamics, consequence of anthropogenic and natural pressures, a set of simulations was performed with the numerical model MOHID, previously validated (Chapter 5). Seven scenarios were designed (Table 7.1), with scenarios #1 and #2 corresponding to anthropogenic actions and scenarios #3, #4A, #4B, #5A and #5B to natural pressures, resulting from climate change effects that will induce modifications on fluvial discharges and MSLR. The details for each scenario are described in next sections.

Predicted daily discharges time series of February, May and August months from the SWIM model were selected as representative of wet season, mean fluvial discharge conditions and dry season, respectively, and used to force the model. Results were analysed for both spring and neap tide conditions. A spin-up period of 60 days was set in order to ensure the results independence from the initial conditions. The initial and boundary conditions for all seven scenarios are described in the next sections.

Table 7.1: Scenarios conditions of the numerical simulations.

Scenario	Bathymetry	Fluvial Discharges	MSL (m)
#1	Dredging plan	Present climate	0.00
#2	2012	Present climate, except for Vouga river	0.00
#3	2012	Future climate	0.00
#4A	2012	Present climate	0.42
#4B	2012	Present climate	0.64
#5A	2012	Future climate	0.42
#5B	2012	Future climate	0.64

The scenarios were compared with the lagoon present conditions results, referred as reference scenario (Section 6.3.1), in terms of values of velocity, water and sediment fluxes and SSC distribution along the lagoon. The water and sediment fluxes were determined at five cross sections located at lagoon central area (Figure 6.4; Chapter 6), considering the methodology presented in Section 6.2.

7.2.1 Influence of anthropogenic actions

7.2.1.1 Morphological changes

In the future, dredging operations are planned in the frame of Polis Litoral Ria de Aveiro/CIRA Actions, in order to guarantee channels navigability beyond harbour area. Since were proposed two solutions in a previous study performed by Sener (2012) for these institutions, it was considered the one that represents high dredging volumes and a larger intervention area. In the Figure 7.1 are presented the intervention areas at the lagoon channels and the depths to achieve. Major changes will be verified in Mira (with 2 to 3 m deepening), Ílhavo and Espinheiro channels, and at lagoon northern area.

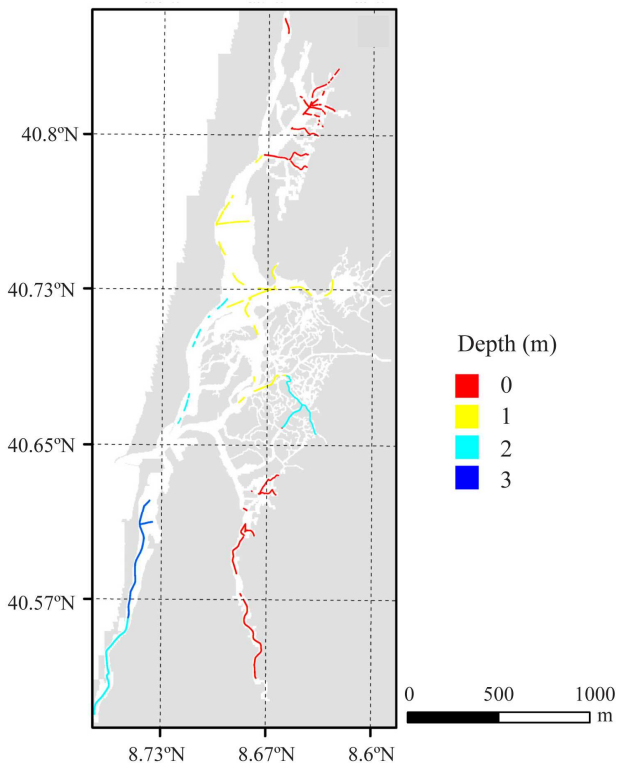

Figure 7.1: Dredging areas and deepening depths of the dredging plan (Source: Sener, 2012).

Therefore, future morphologic changes influence in the lagoon suspended sediment transport were evaluated by defining one scenario that considers a bathymetry with the deepening of particular regions, according to the dredging plan (scenario #1). All the other conditions of the reference scenario were kept (Section 6.2).

7.2.1.2 Ribeiradio-Ermida dam construction at Vouga river

It was constructed at Vouga river the Ribeiradio-Ermida dam, which is in operation since the 2015 autumn and will change Vouga river flow regime and sediment transfer. Therefore, its influence on Ria de Aveiro suspended sediment dynamics was simulated by imposing for the high, mean and low Vouga river discharge conditions, the ecological values (Table 7.2). Additionally, was imposed a zero SSC value for Vouga river to represent the extreme conditions, with no suspended sediment transport due to dam implantation.

For the Cáster, Antuã, Boco and Valas de Mira fluvial discharges were imposed the predictions of watershed model SWIM for present climate (Section 6.2). All the other conditions defined for reference scenario (Section 6.2) were kept.

Table 7.2: Ecological discharges of Vouga river (m^3/s) (COBA, 2008).

Fluvial discharges conditions	Ecological discharges (m^3/s)
High	11.60
Mean	3.04
Low	0.19

7.2.2 Influence of natural actions

7.2.2.1 Climate change effects on fluvial discharges

Changes in the lagoon fluvial discharges are expected due to climate change effects. Therefore, future suspended sediment dynamics due to changes in lagoon fluvial discharges were analysed considering modifications for all lagoon tributaries (scenario #3).

For future lagoon fluvial discharges were also used predictions from the watershed model SWIM (Section 5.6.2) for future climate (2071-2100). Firstly, an analysis identical to the that one made to Vouga river discharge values for present climate (Section 6.2) was performed, in order to determine the year that better represents the typical fluvial discharge for future climate. The year of 2073 presents the higher correlation (0.97), being considered representative of future climate.

The Vouga discharge distribution was analysed and compared the values for 2073 and 1985 (the year representative of present climate; Section 6.2). Future climate will present an increase of lower (30-35 m^3/s) and higher discharges (200-300 m^3/s), with a percentage of occurrence of 21 and 4%, respectively, comparing to 7 and 1% for present climate. Moreover, was determined the Vouga river base flow value for present and future climate, being obtained the values of 83 and 67 m^3/s, respectively (Figure 7.2). These results are in agreement with previous works, indicating that climate change effects will accent the seasonal asymmetry, with an increase on the frequency and values for extreme events (Cunha *et al.*, 2006).

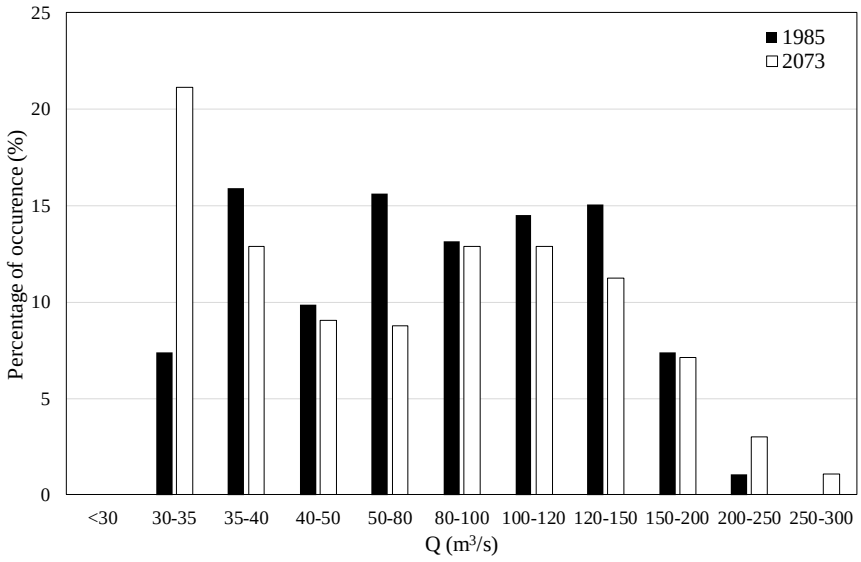

Figure 7.2: Percentage of occurrence of Vouga discharge, for present and future climate.

Since there is no river´s SSC data available for future climate, were considered the same values adopted for the present climate for each lagoon fluvial tributaries (Table 6.1; Section 6.2). All the other conditions defined for reference scenario (Section 6.2) were kept.

7.2.2.2 MSL changes

In order to understand the MSLR implications on the suspended sediment dynamics, two simulations were performed, considering a MSLR of 0.42 m (scenario #4A) and 0.64 m (scenario #4B), both considering present conditions configuration (Section 6.2). The referred values were predicted for the Portuguese coast by Lopes *et al.* (2011). All the other conditions defined for reference scenario (Section 6.2) were kept.

7.2.2.3 Combined effects of fluvial discharges and MSL

Once in future both MSL and fluvial discharges are expected to be modified due to climate change effects, two scenarios combining the predicted changes were set with the 2012 model configuration (Section 6.2). For both scenarios future climate fluvial discharges predictions from SWIM model were imposed along with a MSLR of 0.42 m (scenario #5A) and of 0.64 m (scenario #5B).

7.3 Results and discussion

7.3.1 Influence of anthropogenic actions

7.3.1.1 Morphological changes

Dredging operations are planned to Ria de Aveiro in the frame of Polis Litoral Ria de Aveiro/CIRA Actions, which will lead to channels deepening at some locations. Thus, the influence of this operation on suspended sediment dynamics was evaluated.

For scenario #1 were found higher velocities than for reference scenario, but not exceeding 7%, except at Mira channel cross section where is expected an velocity amplification of approximately 14% (Table 7.3). These results are in agreement with Picado *et al.* (2010) forecasts, which have concluded through numerical modelling that a depth increase from 1 to 3 m has little influence on the lagoon velocities magnitude.

Regarding water fluxes, is predicted an increase that not exceed 3%, except at Ílhavo and Mira channels, where was verified an increase of 50 and 14%, respectively, comparing to reference scenario (Table 7.3). Moreover, at Ílhavo and Mira channels in spring tide conditions is predicted an opposite pattern, being expected higher fluxes during the ebb than during the flood.

For scenario #1, time-averaged SSC and sediment fluxes are expected to be 9 and 12% lower than for reference scenario (Table 7.4). However, Ílhavo and Mira channels are exceptions being found higher sediment fluxes (around 50 and 15%, respectively). Noteworthy, is the opposite pattern from the predicted for reference scenario at Ílhavo channel, with higher sediment fluxes during the ebb period, for high and mean fluvial discharge conditions.

Table 7.3: Time-averaged velocities and water fluxes differences between #1 and reference scenarios, at Barra, S. Jacinto, Espinheiro, Ílhavo and Mira channels cross sections.

	Transect	Spring tide				Neap tide			
		Flood		Ebb		Flood		Ebb	
		v (m/s)	q×10³ (m³/s)	v (m/s)	q×10³ (m³/s)	v (m/s)	q×10³ (m³/s)	v (m/s)	q×10³ (m³/s)
High discharges	Barra	0.01	0.09	0.02	0.15	0.01	0.07	0.01	0.07
	S. Jacinto	0.03	0.00	0.01	-0.03	0.02	0.02	0.01	0.01
	Espinheiro	0.00	0.00	0.00	0.00	0.00	0.01	0.00	-0.01
	Ílhavo	0.01	0.33	0.02	0.47	0.00	0.20	0.01	0.26
	Mira	0.06	0.10	0.05	0.11	0.02	0.04	0.03	0.05
Mean discharges	Barra	0.01	0.07	0.02	0.18	0.01	0.06	0.01	0.08
	S. Jacinto	0.03	0.00	0.01	-0.02	0.02	0.02	0.01	0.00
	Espinheiro	0.00	0.00	0.00	0.00	0.00	0.01	0.00	-0.01
	Ílhavo	0.01	0.33	0.02	0.46	0.00	0.20	0.01	0.27
	Mira	0.06	0.10	0.06	0.12	0.02	0.04	0.03	0.06
Low discharges	Barra	0.01	0.09	0.02	0.16	0.01	0.07	0.01	0.08
	S. Jacinto	0.03	0.00	0.01	-0.02	0.02	0.02	0.01	0.00
	Espinheiro	0.00	0.00	0.00	0.00	0.00	0.00	0.00	-0.01
	Ílhavo	0.01	0.34	0.02	0.45	0.00	0.21	0.01	0.26
	Mira	0.06	0.11	0.06	0.12	0.01	0.01	0.01	0.02

Table 7.4: Time-averaged SSC and sediment fluxes differences between #1 and reference scenarios, at Barra, S. Jacinto, Espinheiro, Ílhavo and Mira channels cross sections.

	Transect	Spring tide				Neap tide			
		Flood		Ebb		Flood		Ebb	
		SSC (mg/l)	q_s (ton/s)	SSC (mg/l)	q_s (ton/s)	SSC (mg/l)	q_s (ton/s)	SSC (mg/l)	q_s (ton/s)
High discharges	Barra	-1.12	-0.22	-1.57	-0.21	-2.46	-0.36	-3.17	-0.48
	S. Jacinto	-3.38	-0.53	-3.23	-0.62	-6.38	-0.61	-5.54	-0.66
	Espinheiro	-4.83	-0.35	-6.36	-0.44	-8.74	-0.29	-9.25	-0.55
	Ílhavo	-3.88	1.85	-2.59	3.10	-2.17	1.75	-0.86	2.34
	Mira	-0.63	0.19	-1.63	0.19	-0.95	0.06	-1.06	0.19
Mean discharges	Barra	-0.73	-0.18	-1.21	-0.18	-1.30	-0.22	-1.90	-0.26
	S. Jacinto	-2.20	-0.35	-2.28	-0.43	-3.29	-0.35	-2.82	-0.39
	Espinheiro	-3.18	-0.23	-4.03	-0.30	-2.66	-0.03	-3.01	-0.22
	Ílhavo	-2.43	1.27	-1.71	2.07	10.04	1.59	9.89	2.09
	Mira	-0.34	0.12	-0.71	0.13	0.33	0.11	-0.57	0.13
Low discharges	Barra	-0.12	-0.03	-0.16	-0.02	-0.26	-0.04	-0.32	-0.05
	S. Jacinto	-0.37	-0.06	-0.37	-0.07	-0.76	-0.07	-0.63	-0.07
	Espinheiro	-0.72	-0.05	-0.79	-0.05	-1.19	-0.05	-1.22	-0.07
	Ílhavo	-0.78	0.16	-0.68	0.26	-1.01	0.19	-0.96	0.24
	Mira	-0.19	0.02	-0.23	0.02	0.16	0.01	-0.04	0.01

In scenario #1, total suspended sediment transport volumes across the lagoon main channel sections along tidal cycle are expected to present lower values than for reference scenario,

except at Mira and Ílhavo channels (Figure 7.3). Moreover, at Ílhavo channel were found less situations of suspended sediment retention comparing to reference scenario, for high and mean fluvial discharge conditions (Figure 7.3b,d,f).

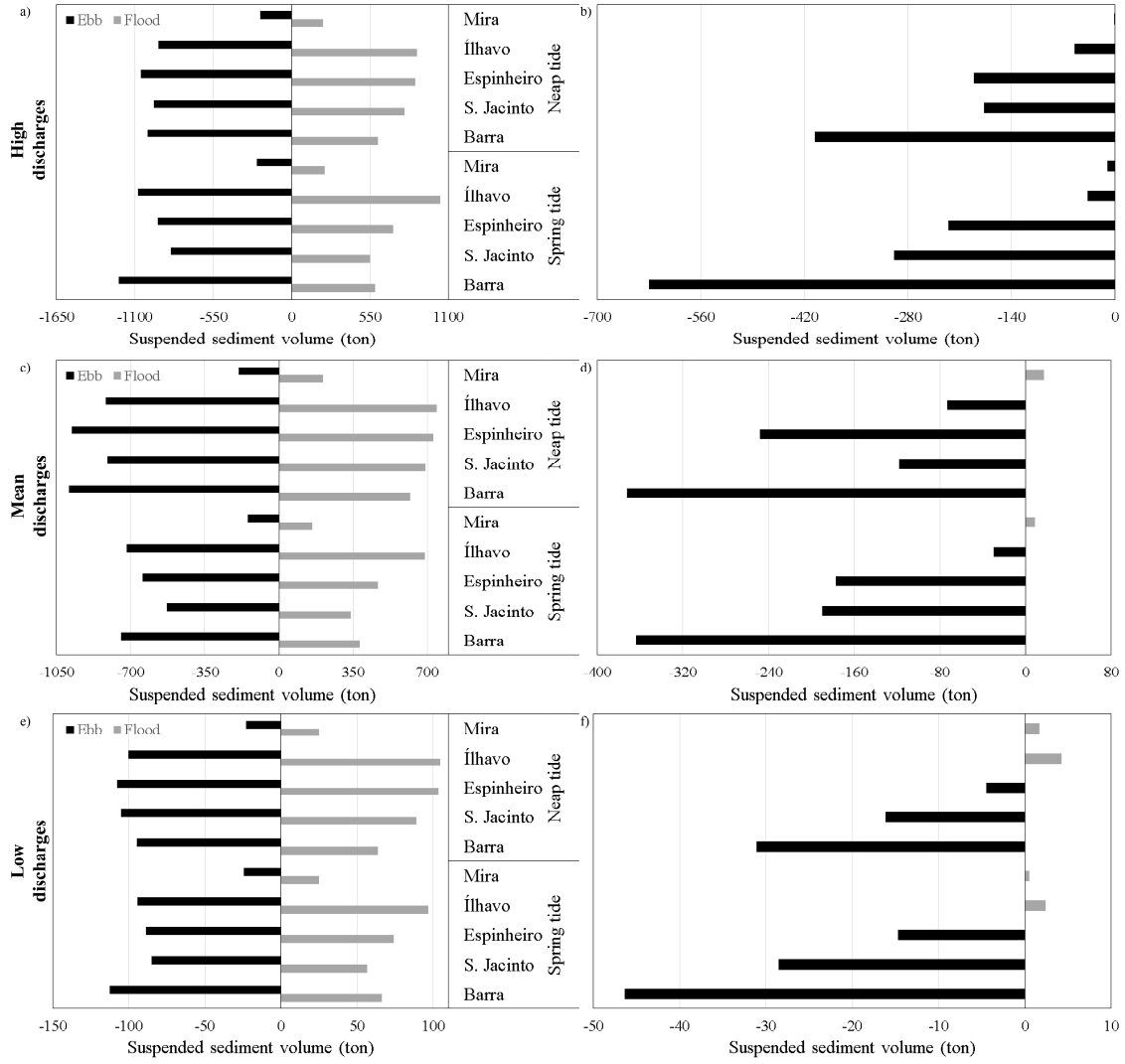

Figure 7.3: Total suspended sediment transport for scenario #1 at Barra, S. Jacinto, Espinheiro, Ílhavo and Mira channels cross sections, for high (a, b), mean (c, d) and low fluvial discharge conditions (e, f), in the flood and ebb periods (a, c, e) periods and tidal cycle balance (b, d, f).

Spatial SSC differences between the scenarios on different tidal stages are presented in Figures 7.4, 7.5 and 7.6. Generally, in scenario #1, the SSC are expected to be lower than in reference scenario at central and northern lagoon areas, as well as at Mira and Ílhavo downstream areas, with differences not exceeding 15 mg/l. This can be explained by the tidal prism increase, due to channels deepening.

However, at Ílhavo upstream area are expected higher concentrations, especially at neap tide for high and mean fluvial discharge conditions, due to channels deepening leading to higher sediment fluxes (Figure 7.4c,d).

7.3.1.2 Ribeiradio-Ermida dam construction at Vouga river

Due to Ribeiradio-Ermida dam, which came operational in 2015, changes in the Vouga discharges are expected. Therefore, scenario #2 was set to research these changes.

A comparative analysis shows that in scenario #2 is expected the velocities and water fluxes increase during flood and its decrease during ebb comparing to reference scenario. However, the differences between scenarios are low, not exceeding 2%. The highest differences are predicted at Espinheiro channel, where Vouga flows, as expected, with a 3% increase in velocities and water fluxes for the flood period and a 2% decrease in the ebb period (Table 7.5).

Table 7.5: Time-averaged velocities and water fluxes differences between #2 and reference scenarios, at Barra, S. Jacinto, Espinheiro, Ílhavo and Mira channels cross sections.

	Transect	Spring tide				Neap tide			
		Flood		Ebb		Flood		Ebb	
		v (m/s)	$q \times 10^3$ (m^3/s)	v (m/s)	$q \times 10^3$ (m^3/s)	v (m/s)	$q \times 10^3$ (m^3/s)	v (m/s)	$q \times 10^3$ (m^3/s)
High discharges	**Barra**	0.00	0.00	0.00	0.01	0.01	0.03	0.00	-0.03
	S. Jacinto	0.00	0.01	0.00	-0.02	0.00	0.01	0.00	-0.01
	Espinheiro	0.00	0.01	0.00	-0.01	0.01	0.03	0.00	-0.02
	Ílhavo	0.00	0.00	0.00	0.00	0.00	0.00	0.00	0.00
	Mira	0.00	0.00	0.00	0.00	0.00	0.00	0.00	0.00
Mean discharges	**Barra**	0.00	0.03	0.00	-0.03	0.01	0.06	-0.01	-0.03
	S. Jacinto	0.00	0.01	0.00	-0.01	0.00	0.01	0.00	-0.02
	Espinheiro	0.01	0.03	-0.01	-0.02	0.02	0.05	-0.01	-0.03
	Ílhavo	0.00	0.00	0.00	0.00	0.00	0.00	0.00	-0.01
	Mira	0.00	0.00	0.00	0.00	0.00	0.00	0.00	0.00
Low discharges	**Barra**	0.00	0.01	0.00	-0.01	0.00	0.02	0.00	0.00
	S. Jacinto	0.00	0.01	0.00	-0.02	0.00	0.01	0.00	0.00
	Espinheiro	0.00	0.01	0.00	0.00	0.00	0.01	0.00	-0.01
	Ílhavo	0.00	0.00	0.00	0.00	0.00	0.00	0.00	0.00
	Mira	0.00	0.00	0.00	0.00	-0.01	-0.03	-0.02	-0.04

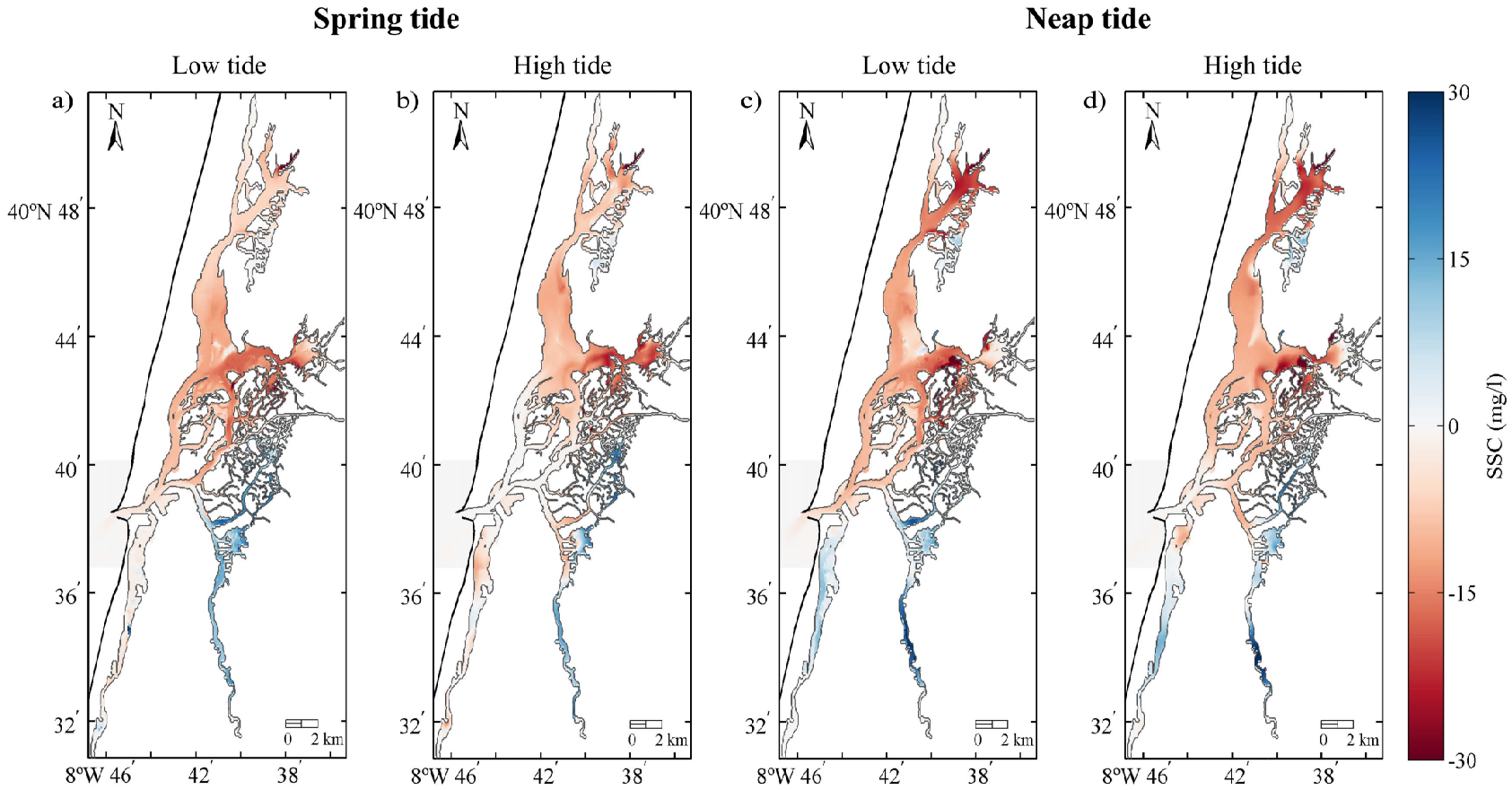

Figure 7.4: Spatial SSC differences between reference scenario and scenario #1 for high fluvial discharge conditions, in spring (a, b) and neap (c, d) tide, at low (a, c) and high (b, d) tide at inlet.

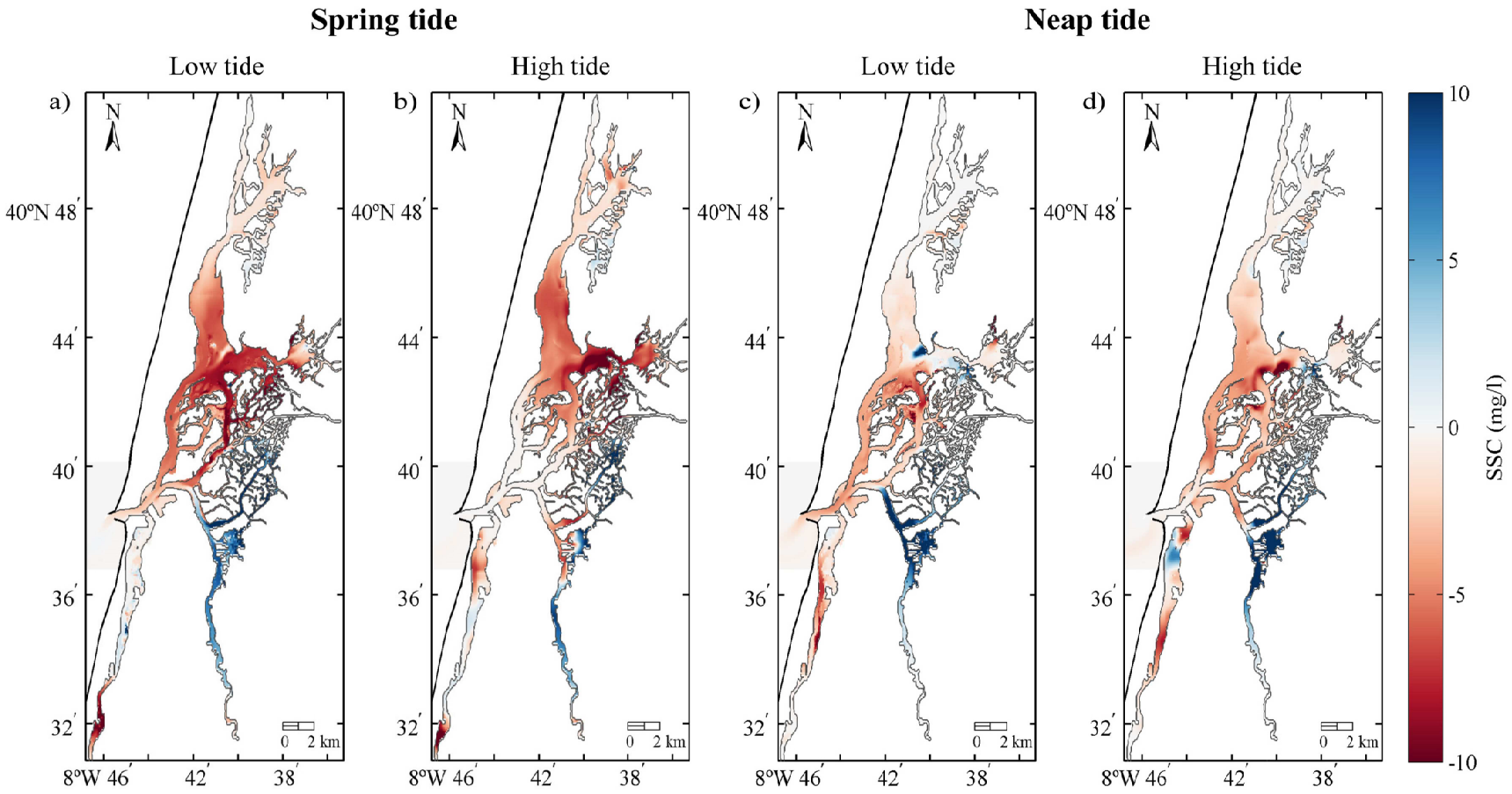

Figure 7.5: Spatial SSC differences between reference scenario and scenario #1 for mean fluvial discharge conditions, in spring (a, b) and neap (c, d) tide, at low (a, c) and high (b, d) tide at the inlet.

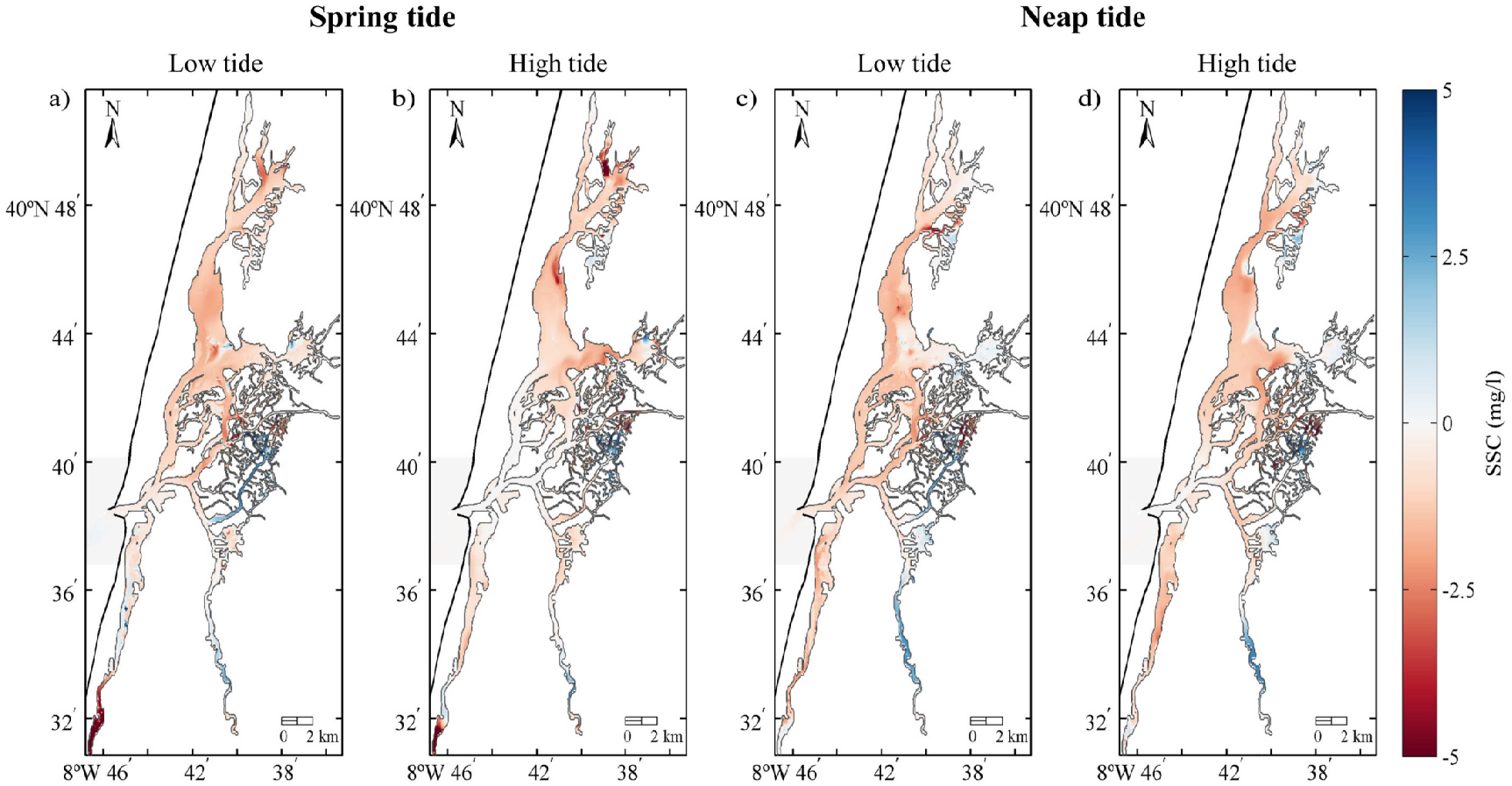

Figure 7.6: Spatial SSC differences between reference scenario and scenario #1 for low fluvial discharge conditions, in spring (a, b) and neap (c, d) tide, at low (a, c) and high (b, d) tide at the inlet.

In opposition to hydrodynamic parameters, for time-averaged SSC and sediment fluxes values are expected significant changes in scenario #2, with differences of approximately 230, 720 and 115%, for high, mean and low fluvial discharge conditions, respectively (Table 7.6). Major differences are found at Espinheiro and Ílhavo channels and in spring tide conditions, showing that Vouga river effect on SSC is enhanced during spring tide, as previously verified by Dias *et al.* (2003). Noteworthy, is SSC and sediment fluxes expected decrease from the flood to ebb at Espinheiro channel under neap tide conditions (Table 7.6).

Table 7.6: Time-averaged SSC and sediment fluxes differences between #2 and reference scenarios, at Barra, S. Jacinto, Espinheiro, Ílhavo and Mira channels cross sections.

	Transect	Spring tide				Neap tide			
		Flood		Ebb		Flood		Ebb	
		SSC (mg/l)	q_s (ton/s)	SSC (mg/l)	q_s (ton/s)	SSC (mg/l)	q_s (ton/s)	SSC (mg/l)	q_s (ton/s)
High discharges	**Barra**	-8.56	-2.10	-12.75	-4.24	-11.34	-1.91	-15.32	-3.22
	S. Jacinto	-15.87	-2.29	-17.95	-3.20	-23.08	-2.49	-24.36	-2.94
	Espinheiro	-38.35	-2.85	-44.89	-3.69	-60.52	-2.70	-67.54	-3.55
	Ílhavo	-42.84	-2.20	-39.67	-1.36	-48.58	-1.25	-48.55	-1.07
	Mira	-12.77	-0.62	-12.14	-0.58	-16.89	-0.51	-15.91	-0.46
Mean discharges	**Barra**	-6.88	-1.73	-10.13	-3.27	-13.91	-2.52	-17.38	-4.00
	S. Jacinto	-12.01	-1.77	-14.45	-2.52	-23.36	-2.84	-24.64	-3.26
	Espinheiro	-30.10	-2.26	-35.59	-2.94	-57.31	-2.88	-62.46	-3.80
	Ílhavo	-34.72	-1.75	-32.95	-1.12	-46.53	-1.40	-47.94	-1.25
	Mira	-10.71	-0.52	-10.38	-0.48	-18.45	-0.65	-17.84	-0.58
Low discharges	**Barra**	-0.72	-0.18	-1.00	-0.31	-0.81	-0.14	-1.06	-0.21
	S. Jacinto	-1.34	-0.19	-1.62	-0.27	-1.93	-0.20	-2.04	-0.23
	Espinheiro	-3.87	-0.26	-4.30	-0.32	-5.22	-0.24	-5.73	-0.29
	Ílhavo	-3.66	-0.18	-3.38	-0.11	-4.22	-0.11	-4.21	-0.09
	Mira	-1.15	-0.05	-1.11	-0.05	-0.93	-0.03	-1.02	-0.04

In the scenario #2 is expected lower suspended sediment volumes transported along the tidal cycle comparing to the reference scenario and the sediment balance direction mainly towards the ocean (Figure 7.7). The only exception is Espinheiro channel, where is predicted suspended sediment retention for neap tide conditions (Figure 7.7b,d). These results are in agreement with Dias *et al.* (2003) conclusions, which have verified that Vouga river contributes to the sediments exportation towards the ocean. Additionally, at Mira channel are expected less situations of suspended sediment retention than in reference scenario (Figure 7.7b,d,f).

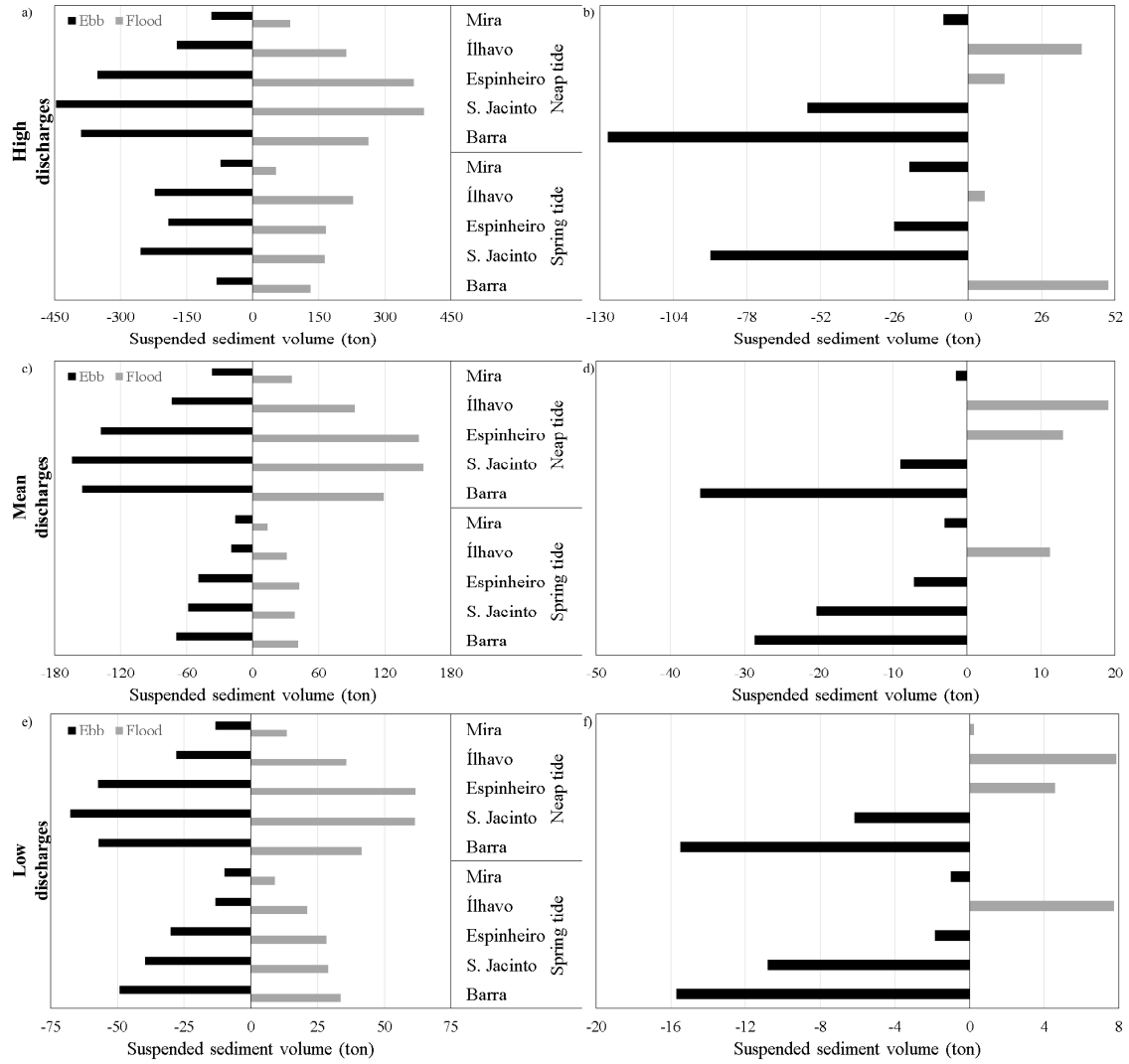

Figure 7.7: Total suspended sediment transport for scenario #2 at Barra, S. Jacinto, Espinheiro, Ílhavo and Mira channels cross sections for high (a, b), mean (c, d) and low fluvial discharge conditions (e, f), in the flood and ebb periods (a, c, e) and tidal cycle balance (b, d, f).

SSC differences distribution along the lagoon between scenario #2 and reference scenario are presented in Figures 7.8, 7.9 and 7.10. The results, as expected, reflect the Vouga river importance as the lagoon major suspended sediment source, with higher negative differences found for high fluvial discharges (<100 mg/l) and decreasing for mean (<80 mg/l) and low fluvial discharge conditions (<20 mg/l) at the central area. Therefore, the sediment supply reduction due to Ribeiradio-Ermida dam at Vouga river, may lead to intertidal areas erosion at lagoon central area.

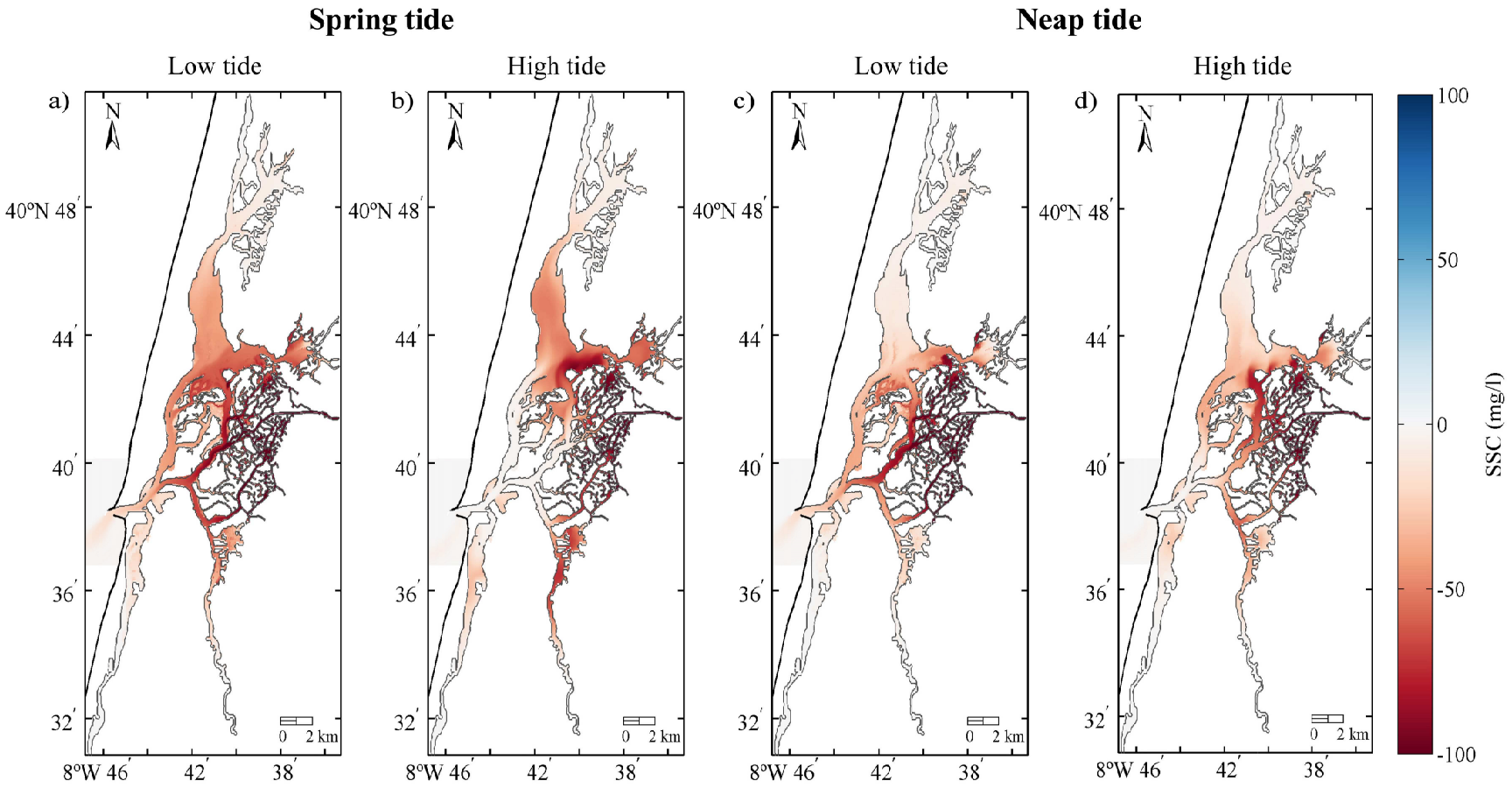

Figure 7.8: Spatial SSC differences between reference scenario and scenario #2 for high fluvial discharge conditions, in spring (a, b) and neap (c, d) tide, at low (a, c) and high (b, d) tide at the inlet.

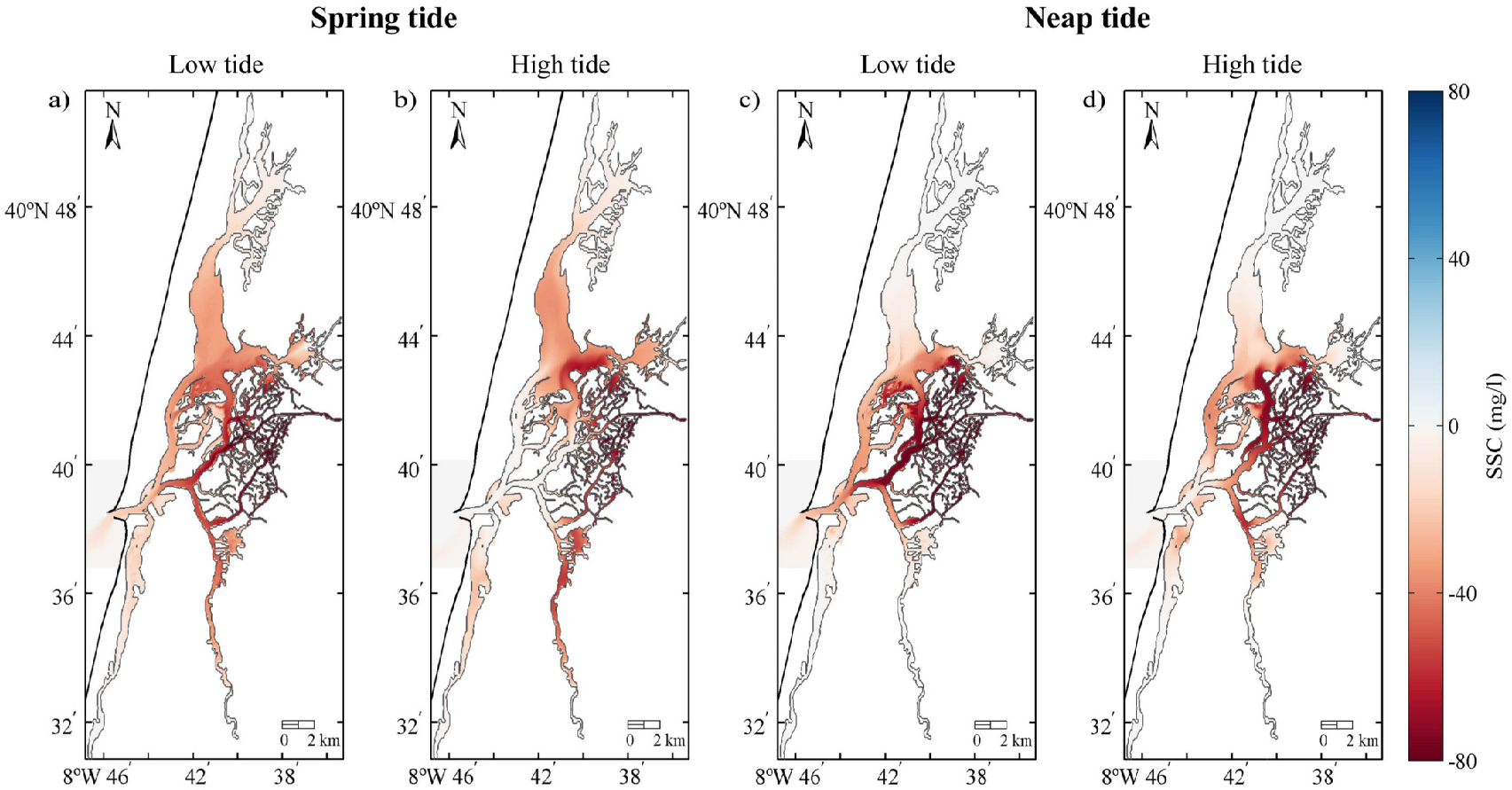

Figure 7.9: Spatial SSC differences between reference scenario and scenario #2 for mean fluvial discharge conditions, in spring (a, b) and neap (c, d) tide, at low (a, c) and high (b, d) tide at the inlet.

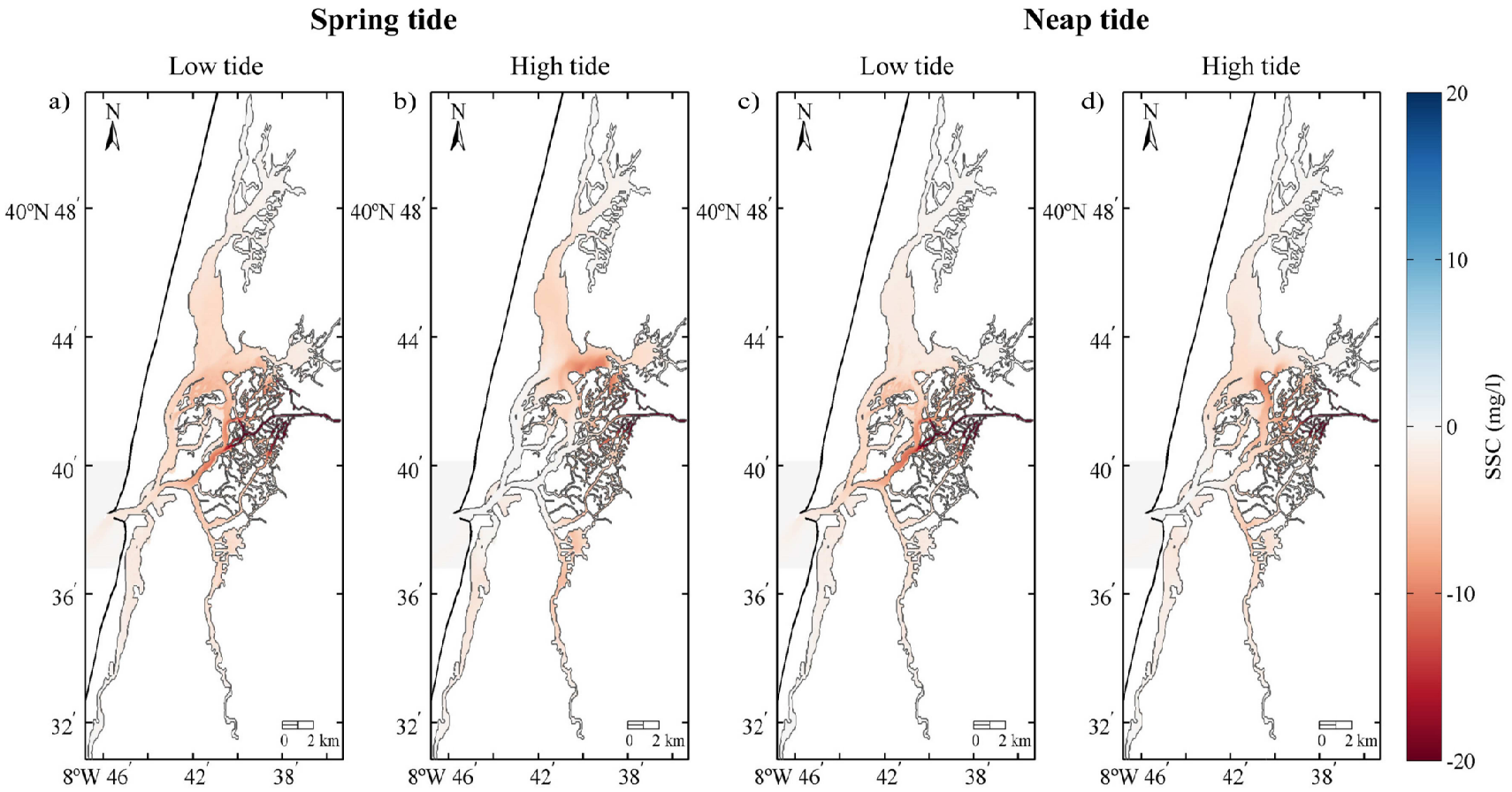

Figure 7.10: Spatial SSC differences between reference scenario and scenario #2 for low fluvial discharge conditions, in spring (a, b) and neap (c, d) tide, at low (a, c) and high (b, d) tide at the inlet.

The SSC negative differences are not restricted to lagoon central area where Vouga river flows, but also to S. Jacinto and Ílhavo downstream areas. This can be explained by the suspended sediment transport from Vouga river's mouth area to the inlet during ebb, as previously verified by Lopes *et al.* (2006).

Noteworthy, for low fluvial discharges, the Vouga sediment supply reduction has a minor influence in the SSC along the lagoon, being expected SSC differences between scenarios lower than 5 mg/l, with the major differences of 20 mg/l restricted to the Espinheiro channel upstream area (Figure 7.10).

7.3.2 Influence of natural actions

7.3.2.1 Climate change effects on fluvial discharges

Climate change effects influence on the Ria de Aveiro suspended sediment transport due to modifications on lagoon fluvial discharges is analysed in scenario #3. The velocities and water fluxes in scenario #3 are expected to present no significant differences comparing to reference scenario, for high and mean fluvial discharge conditions (not exceeding 1%) and are approximately null for low fluvial discharges (Table 7.7). However, the obtained results reflect the fluvial discharges variations, with velocities and water fluxes decrease/increase during flood/ebb for high fluvial discharges and the opposite for mean discharge conditions.

Table 7.7: Time-averaged velocities and water fluxes differences between #3 and reference scenarios, at Barra, S. Jacinto, Espinheiro, Ílhavo and Mira channels cross sections.

	Transect	Spring tide				Neap tide			
		Flood		Ebb		Flood		Ebb	
		v (m/s)	q×10³ (m³/s)	v (m/s)	q×10³ (m³/s)	v (m/s)	q×10³ (m³/s)	v (m/s)	q×10³ (m³/s)
High discharges	**Barra**	0.00	-0.02	0.00	0.03	-0.01	-0.04	0.00	0.03
	S. Jacinto	0.00	0.00	0.00	0.00	0.00	-0.01	0.00	0.01
	Espinheiro	0.00	-0.01	0.00	0.01	-0.01	-0.03	0.00	0.01
	Ílhavo	0.00	0.00	0.00	0.00	0.00	0.00	0.00	0.00
	Mira	0.00	0.00	0.00	0.01	0.00	0.00	0.00	0.00
Mean discharges	**Barra**	0.00	0.01	0.00	-0.03	0.00	0.03	-0.01	-0.04
	S. Jacinto	0.00	0.01	0.00	-0.01	0.00	0.01	0.00	-0.02
	Espinheiro	0.00	0.01	0.00	-0.01	0.01	0.02	0.00	-0.01
	Ílhavo	0.00	0.00	0.00	0.00	0.00	0.00	0.00	-0.01
	Mira	0.00	0.00	0.00	0.00	0.00	0.00	0.00	-0.01
Low discharges	**Barra**	0.00	-0.01	0.00	0.00	0.00	0.00	0.00	0.00
	S. Jacinto	0.00	0.00	0.00	0.00	0.00	0.00	0.00	0.00
	Espinheiro	0.00	0.00	0.00	0.00	0.00	0.00	0.00	0.00
	Ílhavo	0.00	0.00	0.00	0.00	0.00	0.00	0.00	0.00
	Mira	0.00	0.00	0.00	0.00	0.00	0.00	0.00	0.00

Regarding SSC and sediment fluxes, are expected significant differences comparing to the reference scenario, with 33 and 35% higher SSC and sediment fluxes for high fluvial discharges, 44 and 48% lower values for mean fluvial discharges and 5 and 8% lower for low fluvial discharge conditions (Table 7.8).

Table 7.8: Time-averaged SSC and sediment fluxes differences between #3 and reference scenarios, at Barra, S. Jacinto, Espinheiro, Ílhavo and Mira channels cross sections.

	Transect	Spring tide				Neap tide			
		Flood		Ebb		Flood		Ebb	
		SSC (mg/l)	q_s (ton/s)	SSC (mg/l)	q_s (ton/s)	SSC (mg/l)	q_s (ton/s)	SSC (mg/l)	q_s (ton/s)
High discharges	**Barra**	6.51	1.66	9.79	3.48	14.95	2.62	20.13	4.59
	S. Jacinto	10.61	1.64	12.23	2.27	22.72	2.69	23.91	3.25
	Espinheiro	15.92	1.42	18.82	1.96	34.22	1.44	33.54	2.14
	Ílhavo	25.64	1.27	26.84	0.97	51.18	0.98	51.34	0.91
	Mira	8.57	0.45	8.48	0.47	14.61	0.60	12.30	0.53
Mean discharges	**Barra**	-2.85	-0.73	-4.41	-1.44	-5.47	-1.02	-7.44	-1.82
	S. Jacinto	-4.80	-0.73	-5.92	-1.06	-7.21	-0.97	-8.10	-1.22
	Espinheiro	-9.59	-0.79	-11.93	-1.10	-12.37	-0.59	-14.37	-1.00
	Ílhavo	-13.34	-0.67	-13.21	-0.46	-10.28	-0.28	-10.61	-0.30
	Mira	-4.43	-0.22	-4.41	-0.21	-6.44	-0.23	-6.50	-0.23
Low discharges	**Barra**	-0.04	-0.01	-0.06	-0.02	-0.09	-0.02	-0.12	-0.02
	S. Jacinto	-0.10	-0.01	-0.11	-0.02	-0.20	-0.02	-0.21	-0.03
	Espinheiro	-0.22	-0.02	-0.24	-0.02	-0.48	-0.22	-0.53	-0.03
	Ílhavo	-0.28	-0.01	-0.25	-0.01	-0.45	-0.01	-0.45	-0.01
	Mira	-0.09	0.00	-0.09	0.00	-0.14	0.00	-0.14	0.00

In general, for total suspended sediment transported volumes during tidal cycle are expected lower values comparing to reference scenario, except for high fluvial discharge conditions (Figure 7.11). These findings are in agreement with predictions from Dias *et al.* (2003), which indicate that residual currents induced by rivers are important. Regarding the fluxes direction, are predicted less situations of sediment retention than in reference scenario at Mira channel (Figure 7.11b,d,f).

Figures 7.12, 7.13 and 7.14 present the spatial SSC distribution differences along the lagoon between scenario #3 and reference scenario. The obtained results highlight the climate change effects on fluvial discharges, being predicted higher SSC in scenario #3 for high fluvial discharge conditions, with positive differences (<50 mg/l), and the opposite for mean and low fluvial discharge conditions, with negative differences (<20 mg/l). The major differences are found at lagoon central area and S. Jacinto, Espinheiro and Ílhavo channels.

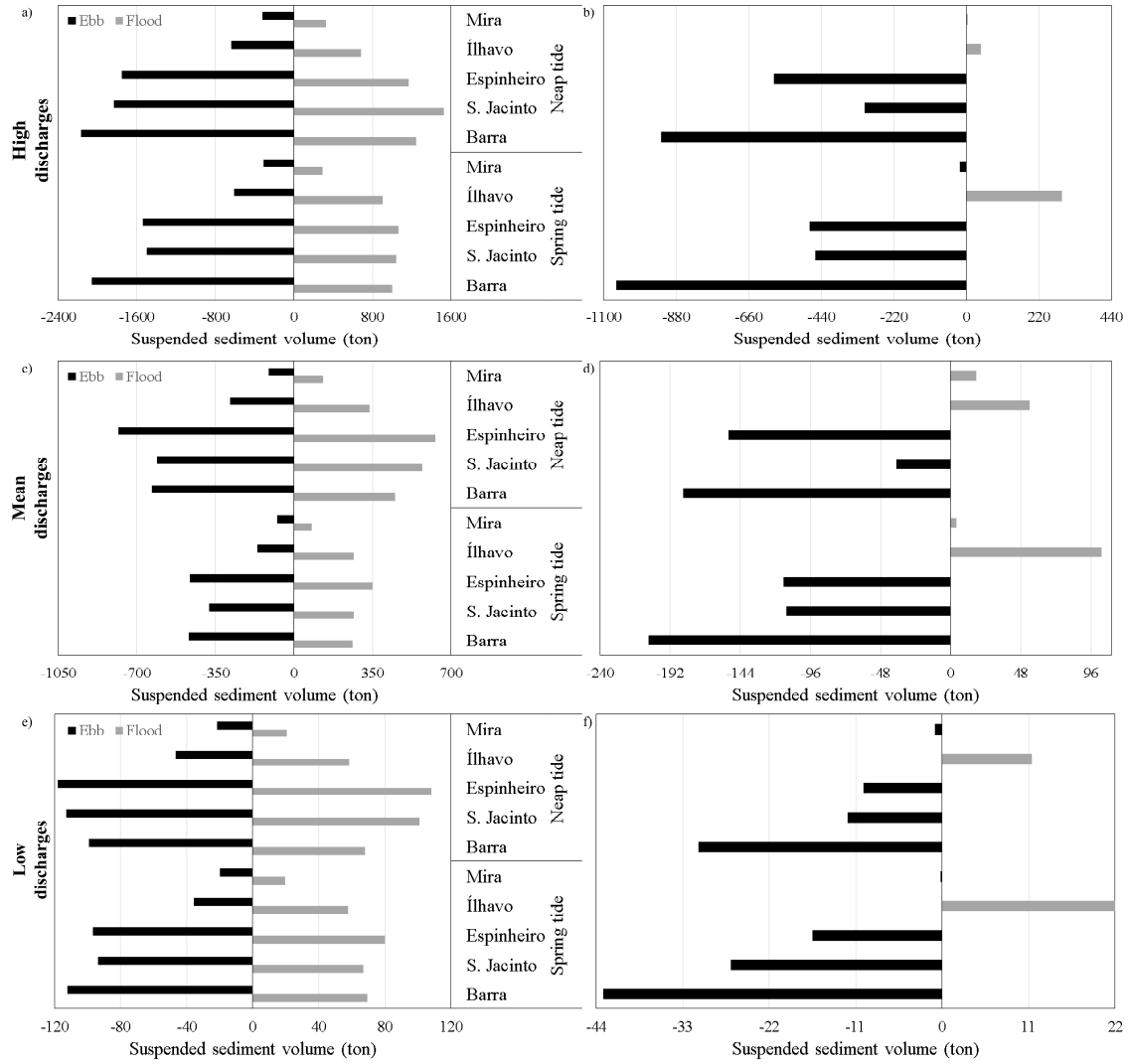

Figure 7.11: Total suspended sediment transport for scenario #3 at Barra, S. Jacinto, Espinheiro, Ílhavo and Mira channels cross sections, for high (a, b), mean (c, d) and low fluvial discharge conditions (e, f), in the flood and ebb periods (a, c, e) and tidal cycle balance (b, d, f).

For high fluvial discharge conditions is clear the influence of the freshwater inflow, especially from Vouga, Antuã and Boco rivers, being expected higher concentrations at central area and lower at river's mouths areas (Figure 7.12). In other hand, for mean and low fluvial discharges an opposite pattern is predicted, with higher SSC at the river's mouths and lower at central area, due sediment transport decrease towards the inlet.

Noteworthy, is the higher influence of fluvial discharges variations for high and mean fluvial discharge conditions, comparing to low discharges, where the SSC differences between scenarios are expected to not exceed 2 mg/l, being negligible at central area at high tide in spring tide conditions.

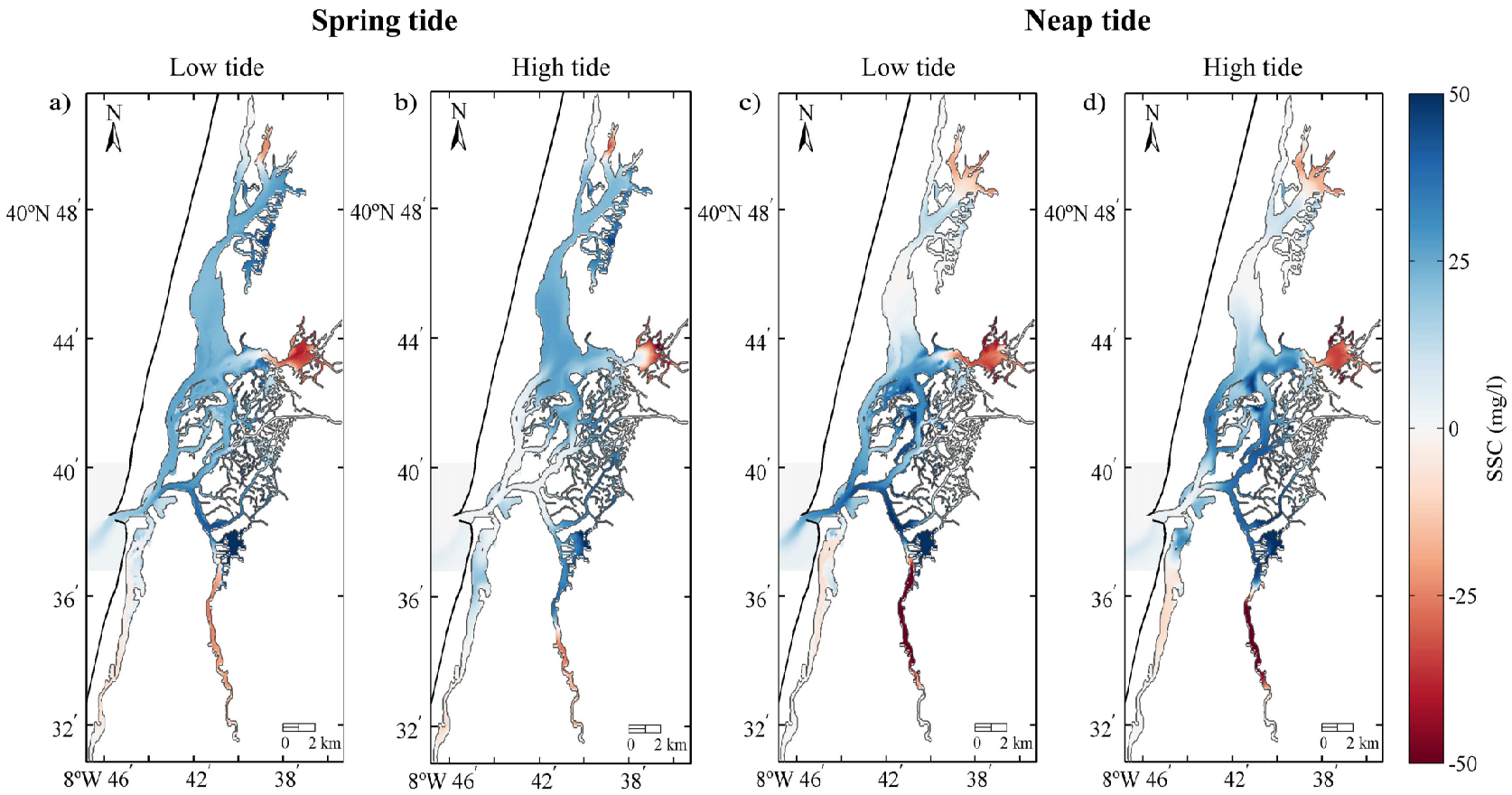

Figure 7.12: Spatial SSC differences between reference scenario and scenario #3 for high fluvial discharge conditions, in spring (a, b) and neap (c, d) tide, at low (a, c) and high (b, d) tide at the inlet.

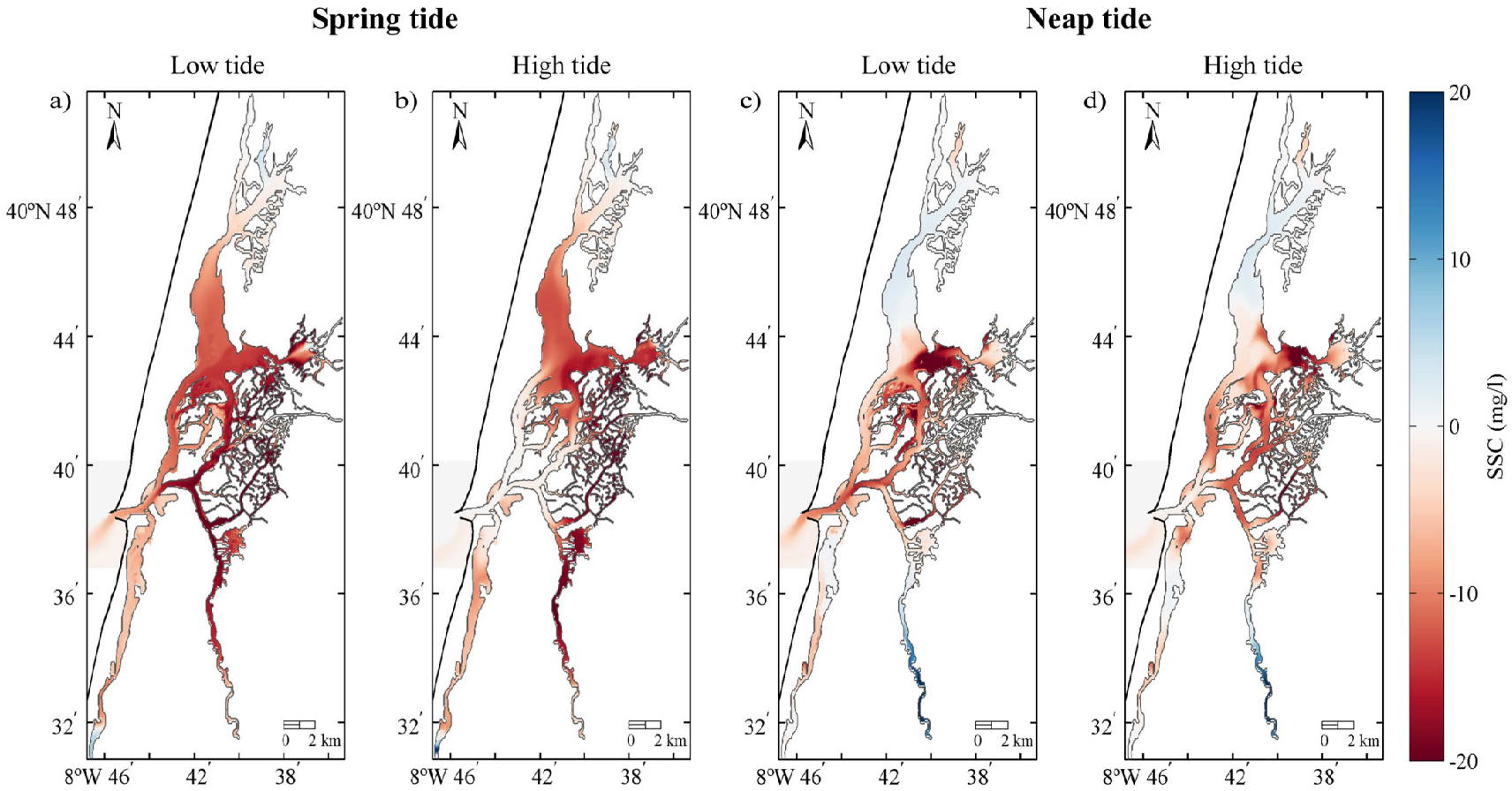

Figure 7.13: Spatial SSC differences between reference scenario and scenario #3 for mean fluvial discharge conditions, in spring (a, b) and neap (c, d) tide, at low (a, c) and high (b, d) tide at the inlet.

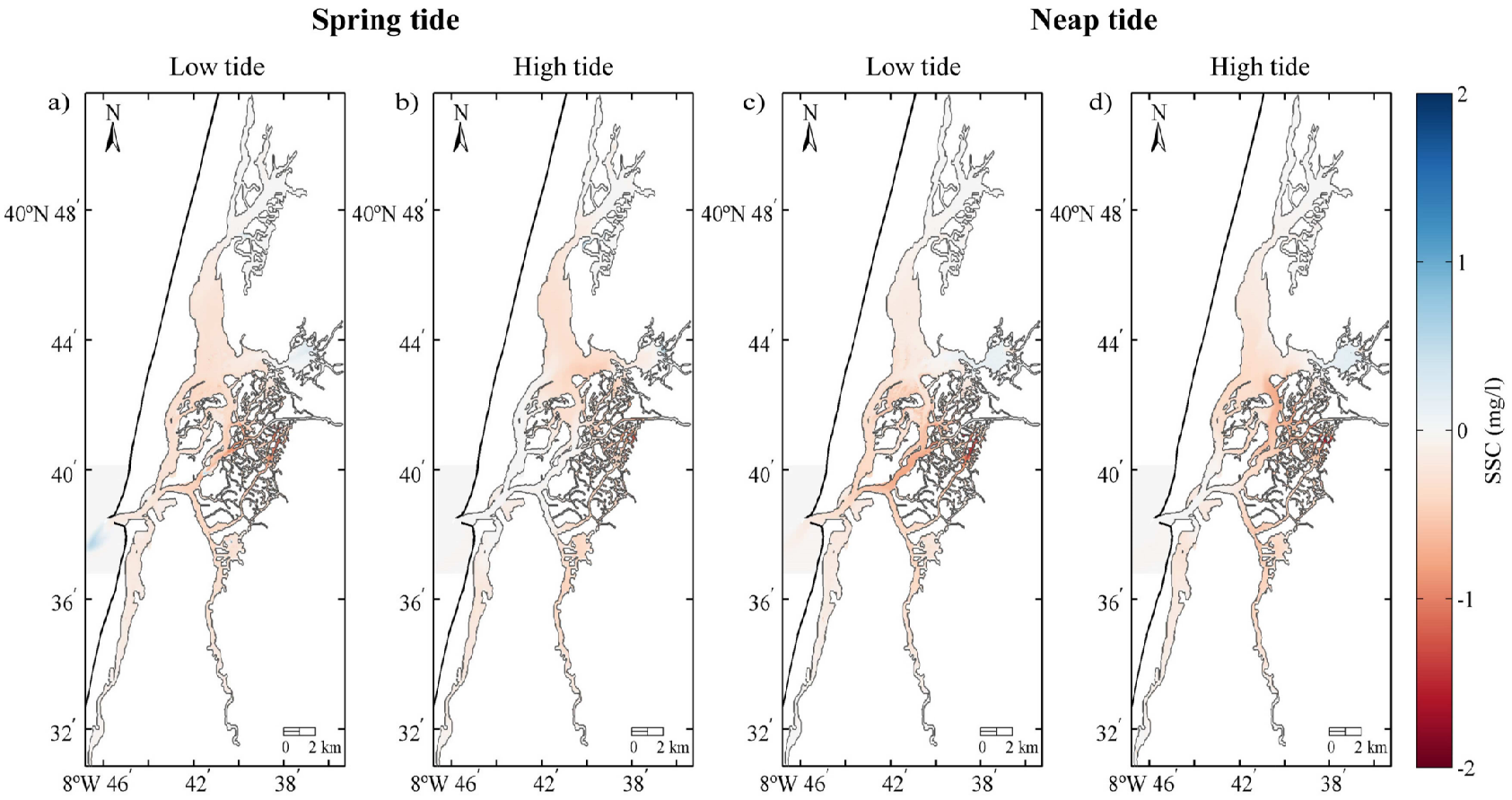

Figure 7.14: Spatial SSC differences between reference scenario and scenario #3 for low fluvial discharge conditions, in spring (a, b) and neap (c, d) tide, at low (a, c) and high (b, d) tide at the inlet.

7.3.2.2 MSL changes

As previous referred, two scenarios regarding MSLR (0.42 and 0.64 m) were set and their influence on the lagoon suspended sediment dynamics was evaluated. For both MSLR scenarios was found an increase on time-averaged velocities and water fluxes comparing to the reference scenario. Indeed, for scenario #4A a 15 and 20% increase of the velocity and water fluxes, respectively, was found, while for scenario #4B was approximately 20 and 26%. Previous studies regarding the effects of MSLR (0.42 m) corroborate these results (Lopes and Dias, 2014, 2015).

Moreover, at S. Jacinto and Espinheiro channels a decrease of the velocities differences between ebb and flood is predicted. In opposition, at Ílhavo and Mira channels a slightly increase is expected (Tables 7.9 and 7.10). These results are in agreement with Lopes *et al.* (2011), which have predicted tidal asymmetry decrease at lagoon downstream areas for MSLR scenarios.

Table 7.9: Time-averaged velocities and water fluxes differences between #4A and reference scenarios, at Barra, S. Jacinto, Espinheiro, Ílhavo and Mira channels cross sections.

	Transect	Spring tide				Neap tide			
		Flood		Ebb		Flood		Ebb	
		v (m/s)	q×10³ (m³/s)	v (m/s)	q×10³ (m³/s)	v (m/s)	q×10³ (m³/s)	v (m/s)	q×10³ (m³/s)
High discharges	**Barra**	0.10	0.88	0.09	0.72	0.08	0.64	0.07	0.53
	S. Jacinto	0.10	0.47	0.07	0.36	0.08	0.34	0.06	0.28
	Espinheiro	0.05	0.23	0.04	0.20	0.05	0.17	0.03	0.14
	Ílhavo	0.04	0.13	0.04	0.14	0.04	0.11	0.04	0.12
	Mira	0.07	0.10	0.09	0.11	0.03	0.07	0.03	0.07
Mean discharges	**Barra**	0.10	0.86	0.09	0.73	0.08	0.65	0.07	0.54
	S. Jacinto	0.10	0.47	0.07	0.36	0.08	0.35	0.06	0.29
	Espinheiro	0.06	0.23	0.04	0.20	0.05	0.18	0.03	0.14
	Ílhavo	0.04	0.13	0.04	0.14	0.03	0.11	0.04	0.13
	Mira	0.04	0.11	0.04	0.11	0.05	0.07	0.06	0.07
Low discharges	**Barra**	0.10	0.86	0.09	0.72	0.08	0.64	0.07	0.55
	S. Jacinto	0.10	0.48	0.07	0.35	0.08	0.35	0.06	0.28
	Espinheiro	0.05	0.22	0.04	0.20	0.04	0.17	0.03	0.14
	Ílhavo	0.04	0.13	0.04	0.14	0.04	0.11	0.04	0.12
	Mira	0.04	0.10	0.04	0.11	0.02	0.05	0.01	0.04

Table 7.10: Time-averaged velocities and water fluxes differences between reference and #4B scenarios, at Barra, S. Jacinto, Espinheiro, Ílhavo and Mira channels cross sections.

	Transect	Spring tide				Neap tide			
		Flood		Ebb		Flood		Ebb	
		v (m/s)	q×10³ (m³/s)	v (m/s)	q×10³ (m³/s)	v (m/s)	q×10³ (m³/s)	v (m/s)	q×10³ (m³/s)
High discharges	Barra	0.14	1.29	0.14	1.13	0.11	0.93	0.10	0.77
	S. Jacinto	0.14	0.69	0.10	0.55	0.11	0.50	0.09	0.42
	Espinheiro	0.08	0.33	0.07	0.32	0.06	0.25	0.05	0.21
	Ílhavo	0.06	0.20	0.06	0.22	0.05	0.15	0.06	0.19
	Mira	0.06	0.16	0.05	0.16	0.04	0.11	0.04	0.10
Mean discharges	Barra	0.14	1.28	0.14	1.11	0.11	0.95	0.10	0.78
	S. Jacinto	0.14	0.69	0.10	0.55	0.11	0.51	0.08	0.42
	Espinheiro	0.08	0.34	0.06	0.31	0.06	0.26	0.05	0.21
	Ílhavo	0.06	0.20	0.07	0.22	0.04	0.15	0.06	0.20
	Mira	0.06	0.16	0.06	0.16	0.04	0.11	0.04	0.10
Low discharges	Barra	0.14	1.26	0.14	1.12	0.11	0.94	0.10	0.78
	S. Jacinto	0.14	0.70	0.10	0.54	0.12	0.52	0.09	0.41
	Espinheiro	0.08	0.34	0.06	0.31	0.06	0.24	0.05	0.21
	Ílhavo	0.06	0.20	0.07	0.21	0.05	0.16	0.06	0.19
	Mira	0.06	0.16	0.06	0.16	0.03	0.08	0.02	0.07

Regarding SSC, is predicted its decrease for high and mean fluvial discharge conditions, due to lagoon tidal prism increase for MSLR scenarios (Lopes *et al.*, 2013a). This increase is expected to be higher for scenario #4B of 26 and 35%, comparing to 19 and 20% (on average) found for scenario #4A, for high and mean fluvial discharge conditions, respectively.

For the sediment fluxes was found its increase, except at S. Jacinto and Espinheiro channels and also Barra, but only for neap tide conditions at scenario #4A (Tables 7.11 and 7.12). This increase is related with residual currents magnitude increase at lagoon central area, previously predicted by Dias and Picado (2011) and Lopes and Dias (2014) under MSLR conditions. As found for SSC, the higher increase of 18 and 13% at high and mean fluvial discharge conditions, respectively, is expected for scenario #4B, comparing to 13 and 9% (on average) predicted for scenario #4A.

Results also show that larger SSC differences, comparing to reference scenario are expected at S. Jacinto and Espinheiro channels, while for sediment fluxes at Mira and Ílhavo channels. For low discharge conditions, is predicted both SSC and sediment fluxes increase, with higher differences for scenario #4B of 26 and 46% and 17 and 37% (on average) for scenario #4A, respectively.

Table 7.11: Time-averaged SSC and sediment fluxes differences between #4A and reference scenarios, at Barra, S. Jacinto, Espinheiro, Ílhavo and Mira channels cross sections.

	Transect	Spring tide				Neap tide			
		Flood		Ebb		Flood		Ebb	
		SSC (mg/l)	q_s (ton/s)	SSC (mg/l)	q_s (ton/s)	SSC (mg/l)	q_s (ton/s)	SSC (mg/l)	q_s (ton/s)
High discharges	**Barra**	-1.39	0.28	-1.25	0.60	-4.06	-0.12	-5.07	-0.29
	S. Jacinto	-5.05	-0.18	-3.41	-0.08	-11.69	-0.45	-9.79	-0.50
	Espinheiro	-10.65	-0.11	-9.28	0.18	-25.20	-0.02	-25.53	-0.33
	Ílhavo	-7.91	0.11	-6.80	0.18	-10.17	0.55	-12.08	0.59
	Mira	0.39	0.13	2.53	0.21	-2.04	0.06	-0.72	0.11
Mean discharges	**Barra**	-1.29	-0.99	-0.67	0.35	-3.85	-0.18	-4.85	-0.49
	S. Jacinto	-2.80	-0.11	-2.76	-0.16	-8.10	-0.40	-7.22	-0.51
	Espinheiro	-7.18	-0.05	-6.84	0.06	-18.53	-0.02	-17.23	-0.22
	Ílhavo	-5.21	0.11	-4.53	0.14	-7.27	0.31	-8.20	0.47
	Mira	-0.63	0.06	-0.02	0.09	-3.41	0.01	-3.07	0.01
Low discharges	**Barra**	0.51	0.27	0.95	0.46	0.51	0.21	0.61	0.27
	S. Jacinto	0.60	0.19	0.92	0.26	0.34	0.17	0.71	0.20
	Espinheiro	0.12	0.14	0.45	0.18	-0.06	0.18	-0.17	0.15
	Ílhavo	0.98	0.13	1.18	0.11	3.03	0.21	2.60	0.20
	Mira	1.02	0.07	1.31	0.08	1.91	0.07	1.86	0.07

Table 7.12: Time-averaged SSC and sediment fluxes differences between #4B and reference scenarios, at Barra, S. Jacinto, Espinheiro, Ílhavo and Mira channels cross sections.

	Transect	Spring tide				Neap tide			
		Flood		Ebb		Flood		Ebb	
		SSC (mg/l)	q_s (ton/s)	SSC (mg/l)	q_s (ton/s)	SSC (mg/l)	q_s (ton/s)	SSC (mg/l)	q_s (ton/s)
High discharges	**Barra**	-2.15	0.36	-1.91	0.90	-4.20	0.24	-5.39	0.03
	S. Jacinto	-6.61	-0.24	-4.46	-0.03	-13.66	-0.36	-11.61	-0.45
	Espinheiro	-14.00	-0.17	-12.11	0.36	-31.39	0.05	-31.66	-0.30
	Ílhavo	-10.33	0.23	-8.77	0.34	-13.69	0.73	-14.93	1.03
	Mira	-0.89	0.18	0.68	0.27	-1.87	0.13	-0.45	0.18
Mean discharges	**Barra**	-4.64	0.00	-1.73	0.34	-4.37	0.02	-5.73	-0.40
	S. Jacinto	-3.61	-0.15	-3.53	-0.16	-9.68	-0.36	-8.94	-0.55
	Espinheiro	-9.45	-0.09	-9.03	0.17	-23.78	-0.06	-22.81	-0.29
	Ílhavo	-6.92	0.20	-6.12	0.25	-10.29	0.40	-11.27	0.67
	Mira	-0.72	0.10	-0.17	0.13	-3.82	0.05	-3.62	0.04
Low discharges	**Barra**	0.46	0.25	0.94	0.55	0.95	0.37	1.08	0.46
	S. Jacinto	0.69	0.21	1.32	0.37	0.83	0.31	1.35	0.34
	Espinheiro	0.21	0.20	0.81	0.29	0.64	0.31	0.46	0.27
	Ílhavo	1.49	0.21	1.75	0.18	4.91	0.35	4.44	0.36
	Mira	1.21	0.10	1.62	0.11	2.72	0.12	2.76	0.11

Generally, the suspended sediment volumes transported at main channels along a tidal cycle in scenarios #4A and #4B are expected to be higher than in the reference scenario, especially

for scenario #4B (Figures 7.15 and 7.16). Moreover, for MSLR scenarios is expected less situations of suspended sediment retention at Mira channel in neap tide conditions (Figures 7.15b,d,f and 7.16b,d,f). Noteworthy, is that for scenario #4B are predicted less situations of suspended sediment retention at Ílhavo and Mira channels than for scenario #4A. These results are in agreement with Picado *et al.* (2011b) and Lopes and Dias (2014, 2015) findings, which have predicted the enhancement of the ebb dominance for MSLR conditions.

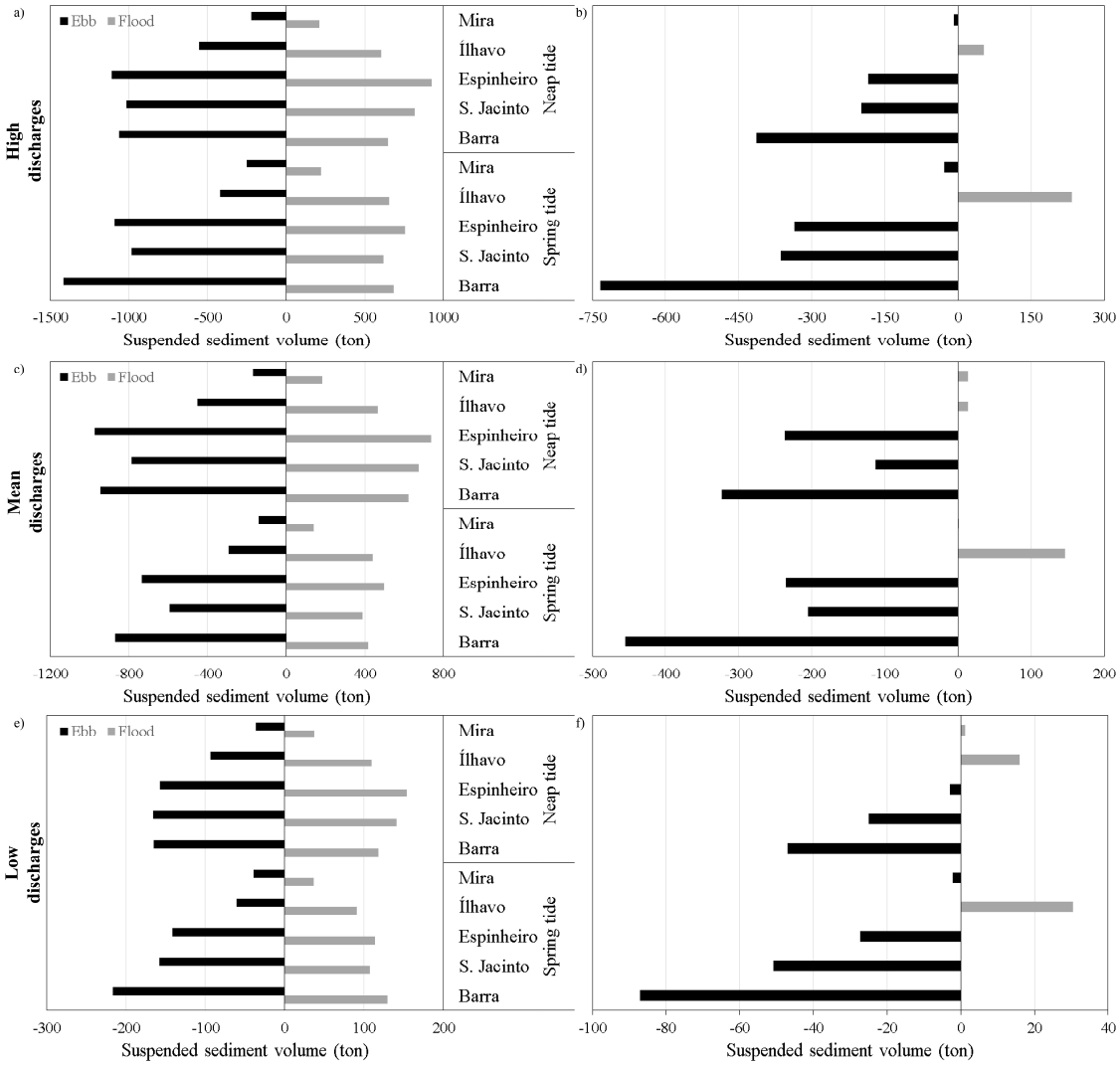

Figure 7.15: Total suspended sediment transport for scenario #4A at Barra, S. Jacinto, Espinheiro, Ílhavo and Mira channels cross sections, for high (a, b), mean (c, d) and low fluvial discharge conditions (e, f), in the flood and ebb periods (a, c, e) and tidal cycle balance (b, d, f).

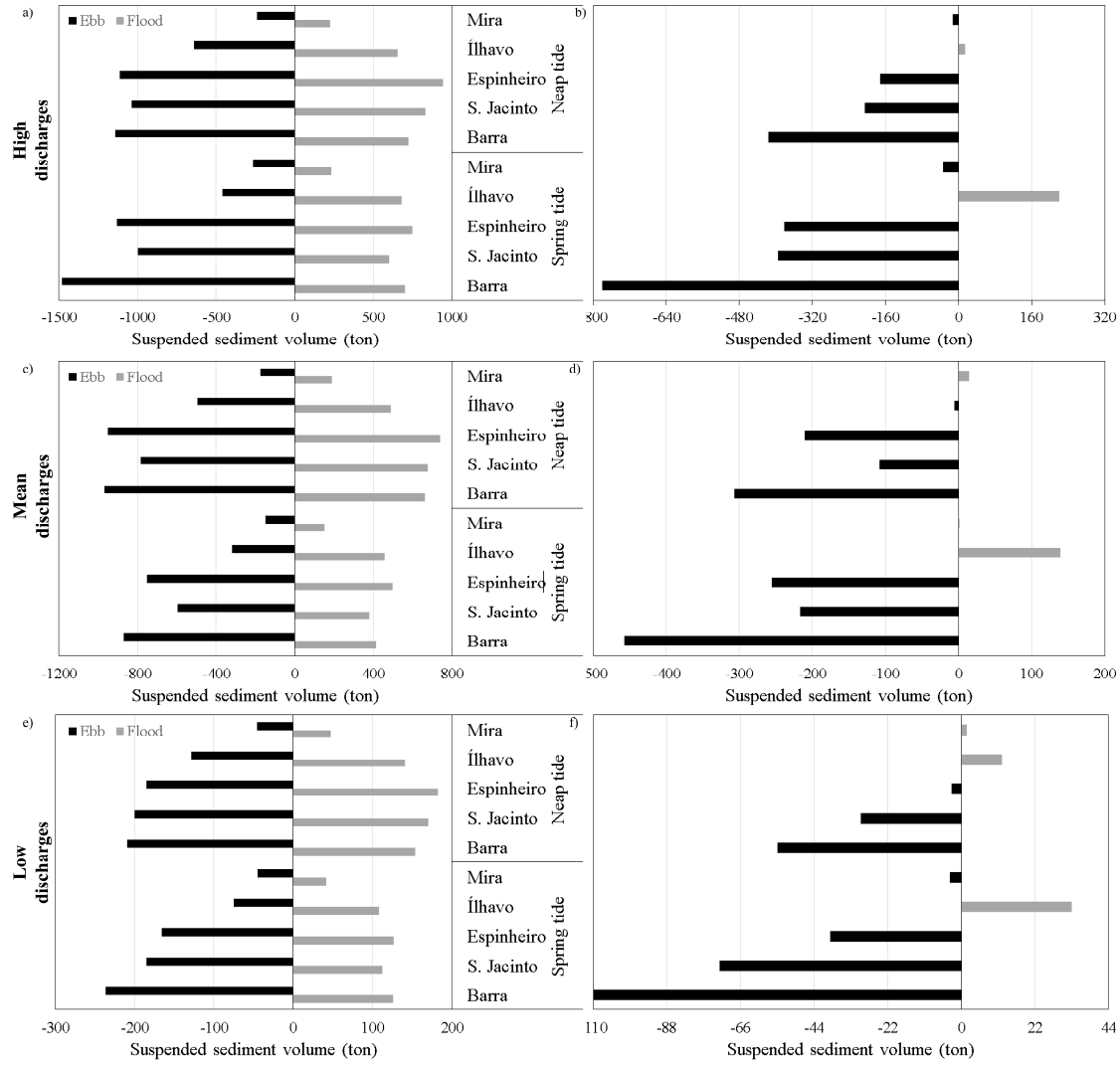

Figure 7.16: Total suspended sediment transport for scenario #4B at Barra, S. Jacinto, Espinheiro, Ílhavo and Mira channels cross sections, for high (a, b), mean (c, d) and low fluvial discharge conditions (e, f), in the flood and ebb periods (a, c, e) and tidal cycle balance (b, d, f).

Spatial distribution of SSC differences between MSLR and reference scenarios along the lagoon are presented from Figure 7.17 to Figure 7.22. Overall, scenarios #4A and #4B present the same patterns, with highest differences comparing found for scenario #4B. MSLR scenarios are expected to induce SSC decrease at lagoon central area, due to tidal prism and currents increase (Dias and Picado, 2011; Lopes *et al.*, 2011, 2013a; Lopes and Dias, 2014, 2015). Otherwise, at upstream areas higher SSC are predicted, which are related with the flood dominance found by Picado *et al.* (2011b) forecasts at channels upstream areas for MSLR scenarios (Figures 7.17, 7.18, 7.20 and 7.21).

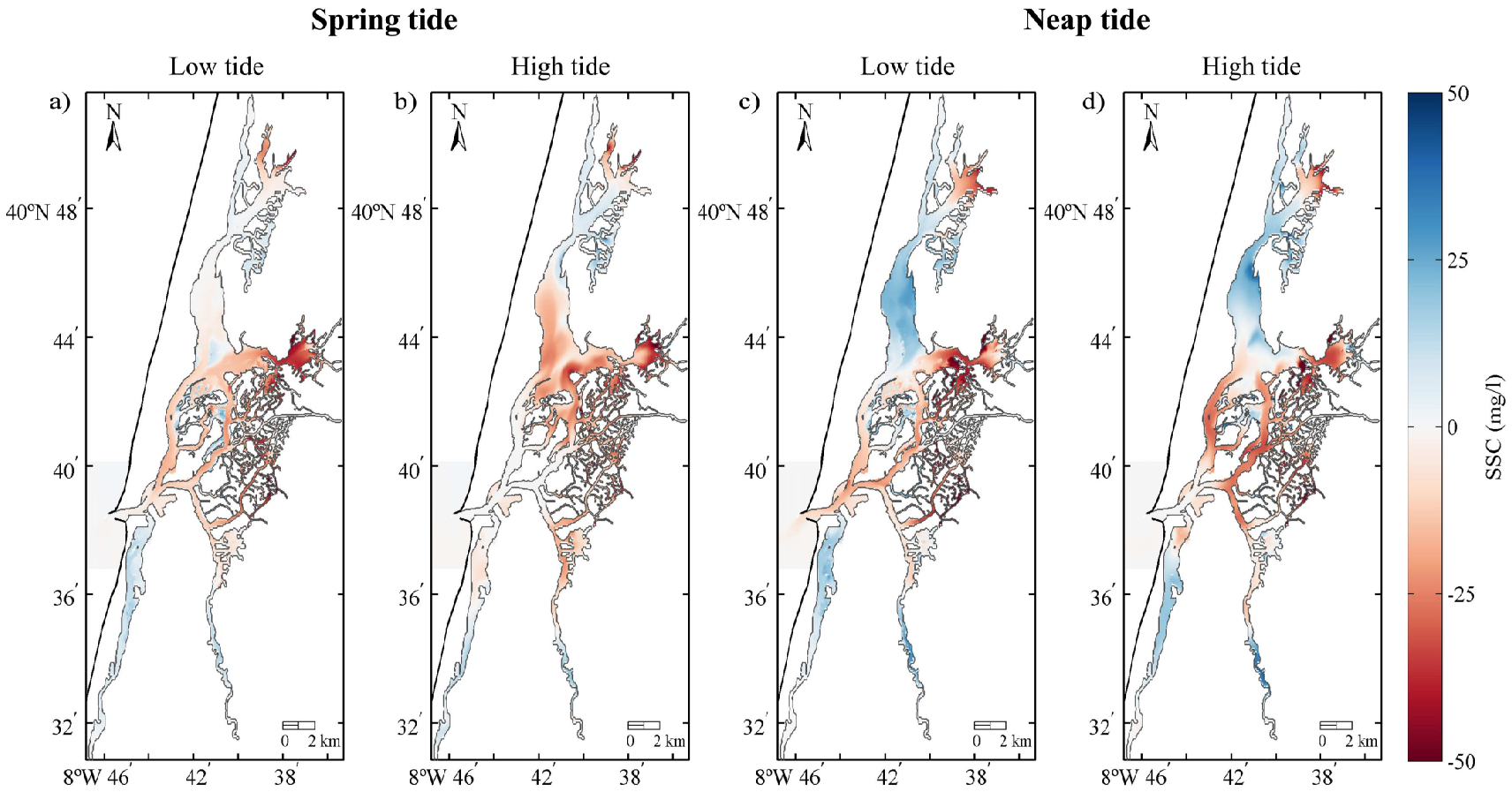

Figure 7.17: Spatial SSC differences between reference scenario and scenario #4A for high fluvial discharge conditions, in spring (a, b) and neap (c, d) tide, at low (a, c) and high (b, d) tide at the inlet.

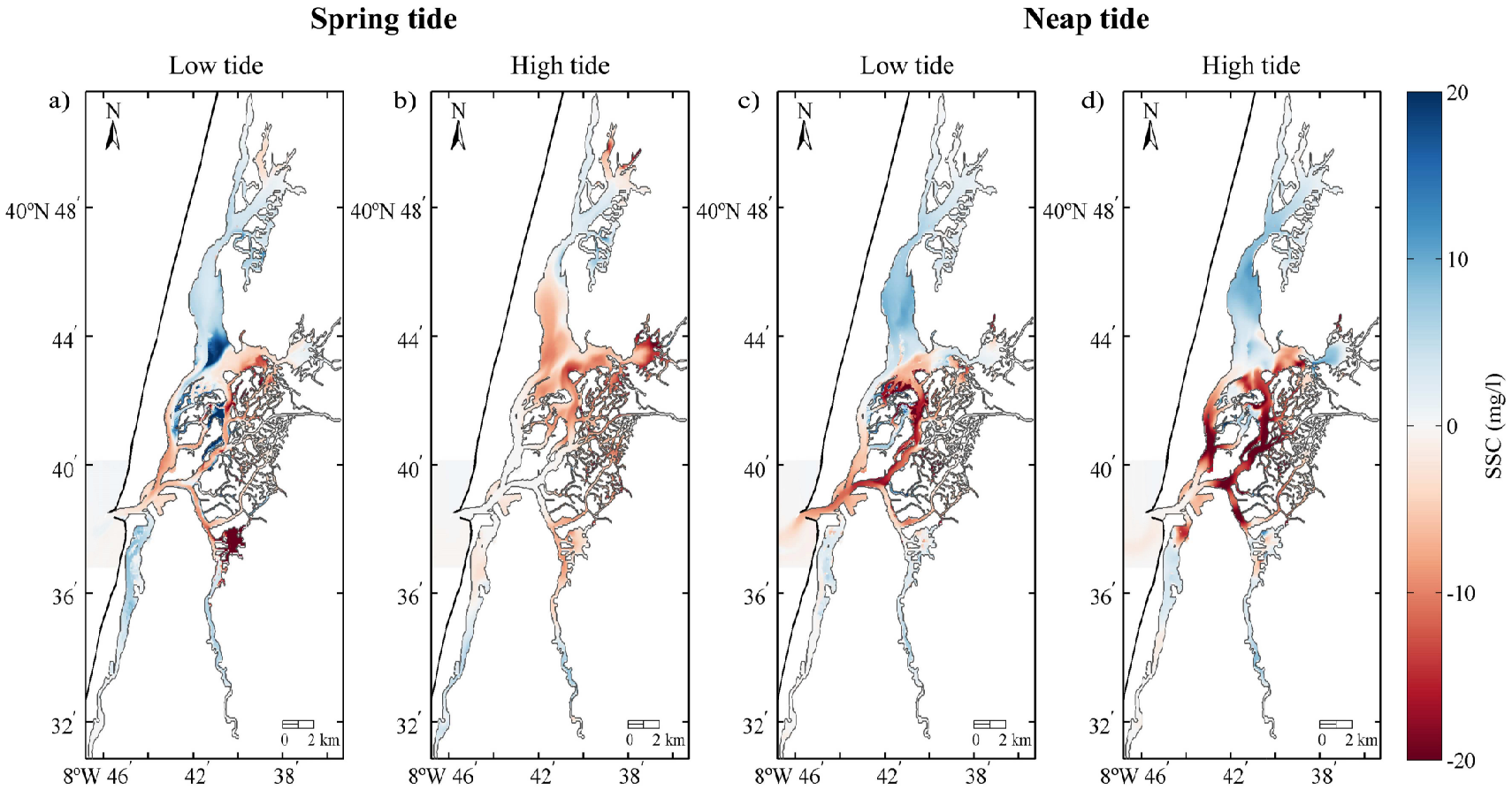

Figure 7.18: Spatial SSC differences between reference scenario and scenario #4A for mean fluvial discharge conditions, in spring (a, b) and neap (c, d) tide, at low (a, c) and high (b, d) tide at the inlet.

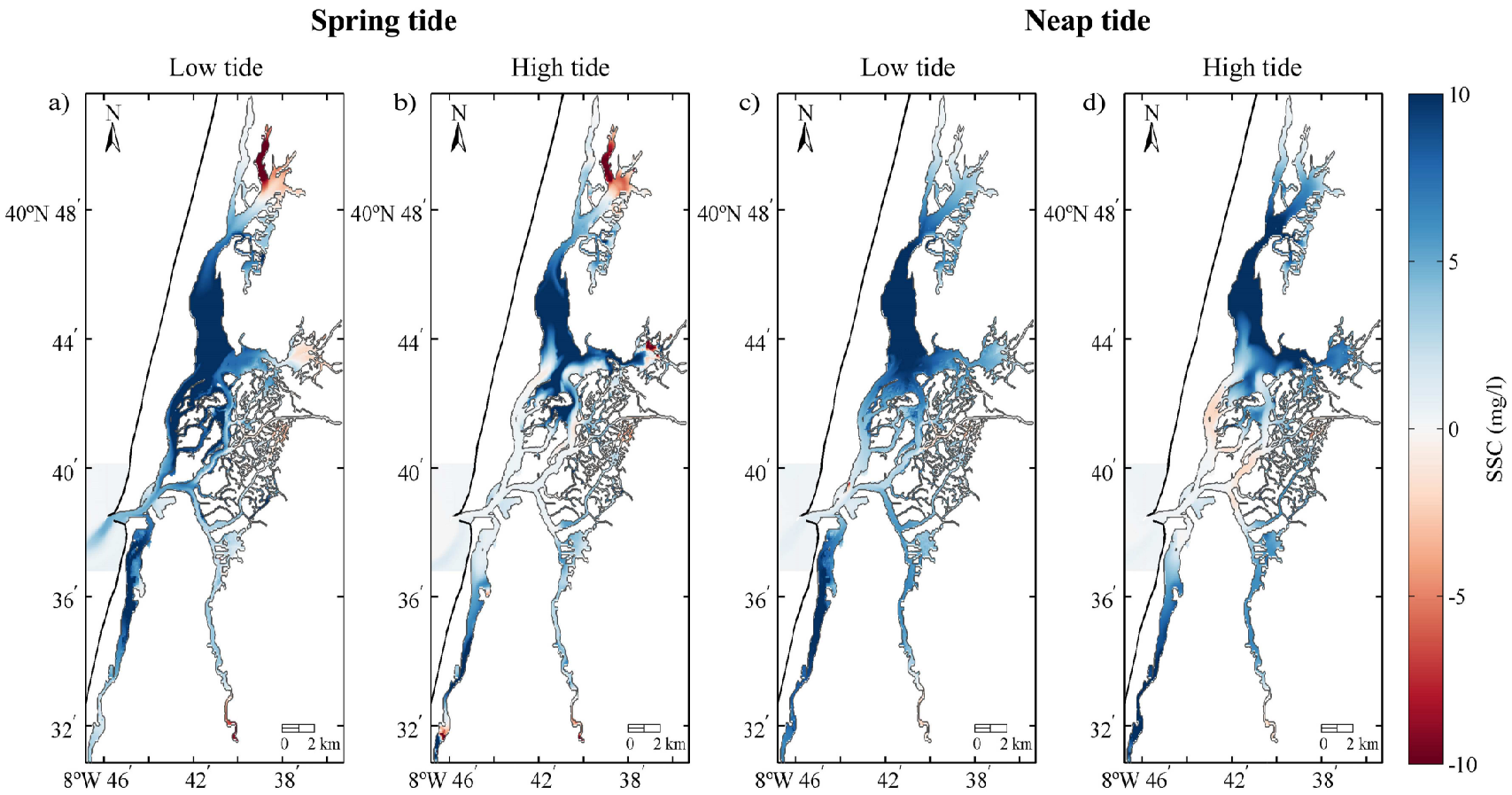

Figure 7.19: Spatial SSC differences between reference scenario and scenario #4A for low fluvial discharge conditions, in spring (a, b) and neap (c, d) tide, at low (a, c) and high (b, d) tide at the inlet.

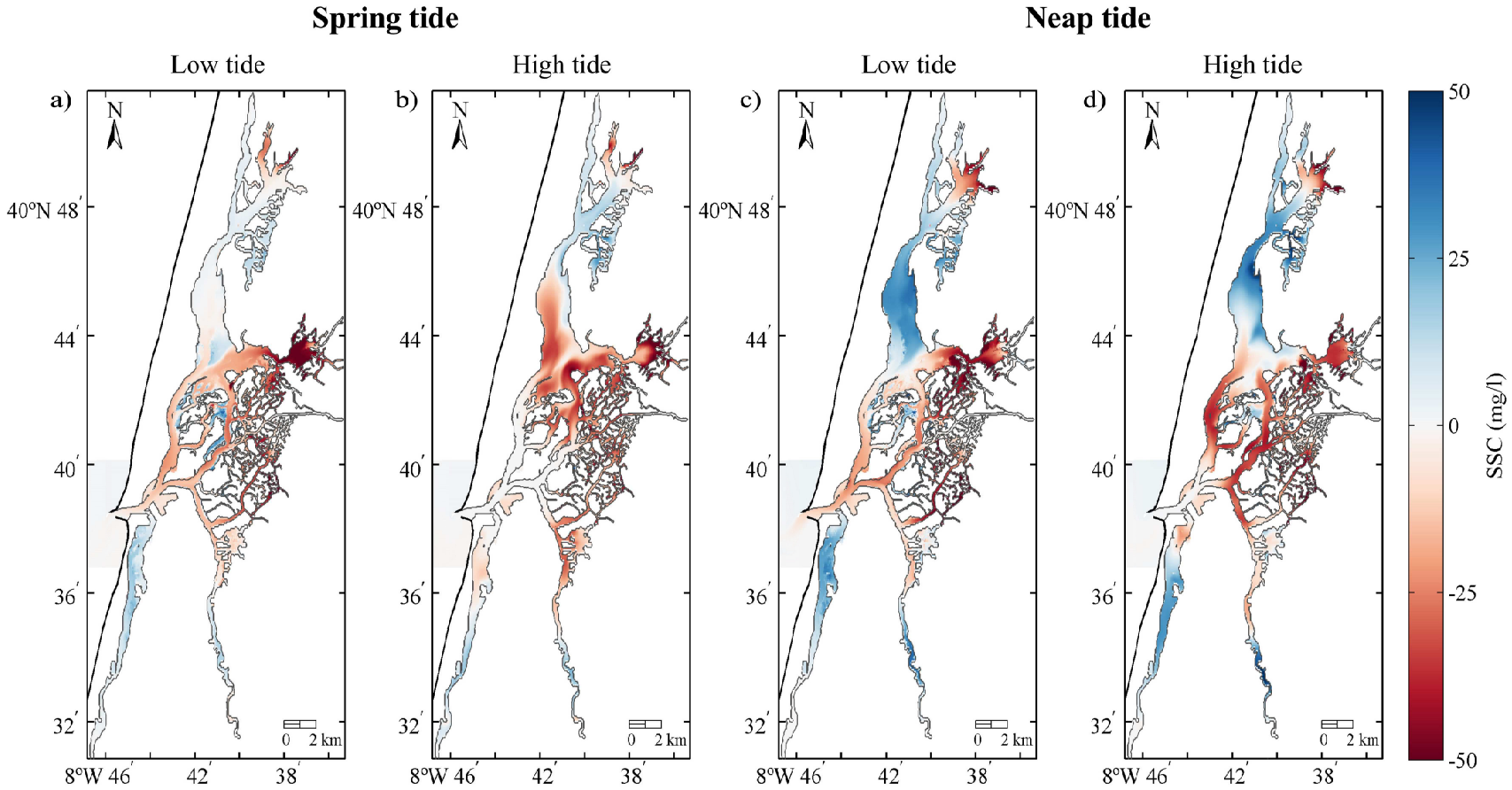

Figure 7.20: Spatial SSC differences between reference scenario and scenario #4B for high fluvial discharges, in spring (a, b) and neap (c, d) tide, at low (a, c) and high (b, d) tide at the inlet.

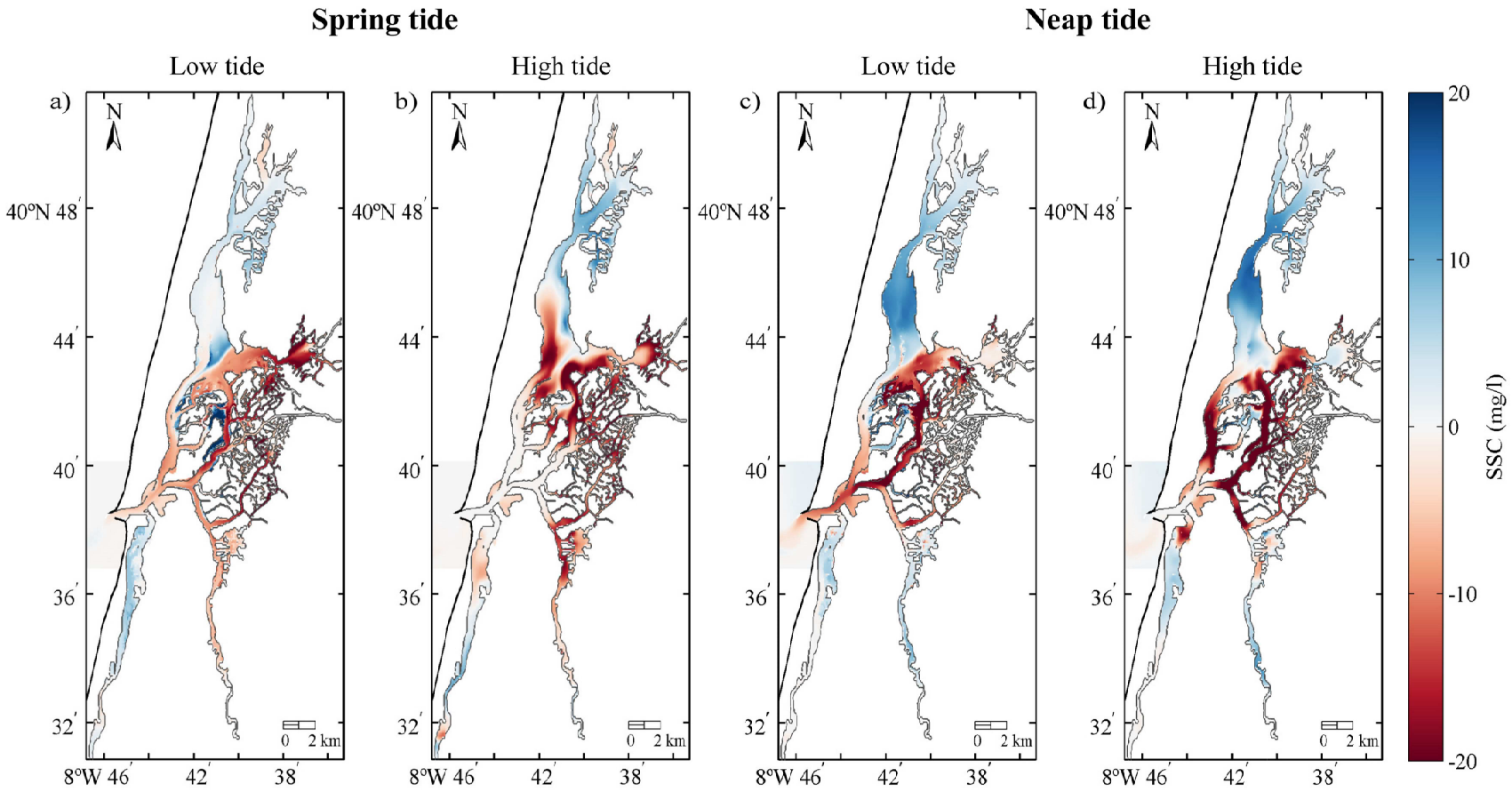

Figure 7.21: Spatial SSC differences between reference scenario and scenario #4B for mean fluvial discharge conditions, in spring (a, b) and neap (c, d) tide, at low (a, c) and high (b, d) tide at the inlet.

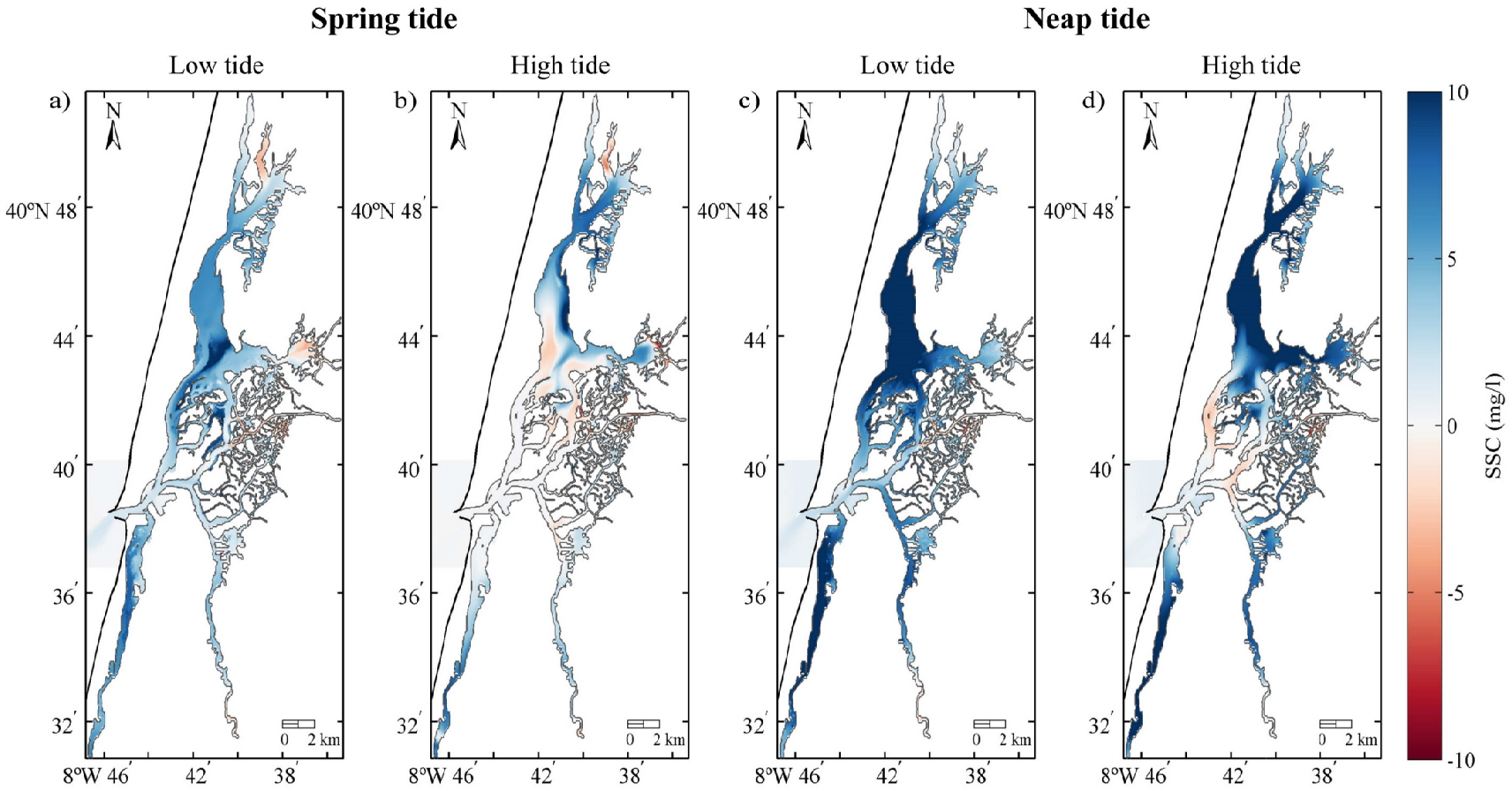

Figure 7.22: Spatial SSC differences between reference scenario and scenario #4B for low fluvial discharge conditions, in spring (a, b) and neap (c, d) tide, at low (a, c) and high (b, d) tide at the inlet

However, for low fluvial discharge conditions the differences at lagoon central area comparing to reference scenario are almost null. The high differences comparing are expected at S. Jacinto upstream areas (Figures 7.19 and 7.22), which is explained by the ebb-dominance extension in the upstream direction at this channel, as forecasted by Lopes and Dias (2014) for MSLR conditions.

Moreover, higher sea water intrusion in spring tide at S. Jacinto and Espinheiro channels is expected, comparing to Mira and Ílhavo. This behaviour is explained by the higher rates of tidal prism increase at these channels, verified by Lopes *et al.* (2013a) for MSLR scenarios.

7.3.2.3 Combined effects of fluvial discharges and MSL

In future, MSL and fluvial discharges are expected to change simultaneously due to climate change effects. Therefore, in scenarios #5A and #5B were evaluated the combined influence of these changes in Ria de Aveiro suspended sediment dynamics. The results of scenarios #5A and #5B show that are expected similar patterns to those found for MSLR scenarios (scenarios #4A and #4B), with higher velocities (18 and 26%, respectively) and water fluxes (30 and 42%, respectively) comparing to reference scenario (Tables 7.13 and 7.14).

Table 7.13: Time-averaged velocities and water fluxes differences between #5A and reference scenarios, at Barra, S. Jacinto, Espinheiro, Ílhavo and Mira channels cross sections.

	Transect	Spring tide				Neap tide			
		Flood		Ebb		Flood		Ebb	
		v (m/s)	q×10³ (m³/s)	v (m/s)	q×10³ (m³/s)	v (m/s)	q×10³ (m³/s)	v (m/s)	q×10³ (m³/s)
High discharges	Barra	0.09	0.84	0.10	0.76	0.07	0.59	0.08	0.56
	S. Jacinto	0.09	0.46	0.07	0.36	0.07	0.33	0.06	0.30
	Espinheiro	0.05	0.21	0.04	0.21	0.04	0.15	0.04	0.15
	Ílhavo	0.03	0.36	0.09	0.55	0.03	0.11	0.04	0.12
	Mira	0.04	0.11	0.04	0.11	0.03	0.07	0.03	0.07
Mean discharges	Barra	0.10	0.88	0.09	0.70	0.08	0.69	0.07	0.51
	S. Jacinto	0.10	0.48	0.06	0.34	0.08	0.36	0.06	0.27
	Espinheiro	0.06	0.24	0.04	0.19	0.05	0.20	0.03	0.13
	Ílhavo	0.04	0.13	0.04	0.14	0.04	0.11	0.04	0.13
	Mira	0.04	0.10	0.04	0.11	0.03	0.08	0.03	0.07
Low discharges	Barra	0.12	1.04	0.12	0.93	0.08	0.65	0.07	0.55
	S. Jacinto	0.12	0.57	0.10	0.45	0.08	0.35	0.06	0.29
	Espinheiro	0.06	0.27	0.06	0.25	0.04	0.17	0.03	0.14
	Ílhavo	0.05	0.15	0.05	0.16	0.04	0.11	0.04	0.12
	Mira	0.04	0.10	0.04	0.11	0.02	0.05	0.01	0.04

Table 7.14: Time-averaged velocities and water fluxes differences between #5B and reference scenarios, at Barra, S. Jacinto, Espinheiro, Ílhavo and Mira channels cross sections.

	Transect	Spring tide				Neap tide			
		Flood		Ebb		Flood		Ebb	
		v (m/s)	q×10³ (m³/s)	v (m/s)	q×10³ (m³/s)	v (m/s)	q×10³ (m³/s)	v (m/s)	q×10³ (m³/s)
High discharges	Barra	0.14	1.26	0.15	1.16	0.10	0.88	0.11	0.81
	S. Jacinto	0.14	0.68	0.10	0.57	0.11	0.48	0.09	0.43
	Espinheiro	0.07	0.32	0.07	0.32	0.06	0.23	0.05	0.22
	Ílhavo	0.05	0.43	0.11	0.61	0.04	0.15	0.06	0.20
	Mira	0.06	0.16	0.05	0.16	0.04	0.10	0.04	0.10
Mean discharges	Barra	0.15	1.30	0.14	1.08	0.12	0.99	0.10	0.75
	S. Jacinto	0.14	0.70	0.10	0.53	0.11	0.52	0.08	0.40
	Espinheiro	0.08	0.35	0.06	0.30	0.07	0.27	0.05	0.20
	Ílhavo	0.06	0.20	0.06	0.21	0.05	0.16	0.05	0.19
	Mira	0.06	0.16	0.06	0.16	0.04	0.11	0.04	0.10
Low discharges	Barra	0.16	1.45	0.17	1.33	0.11	0.94	0.10	0.78
	S. Jacinto	0.14	0.69	0.10	0.54	0.12	0.52	0.09	0.41
	Espinheiro	0.09	0.38	0.08	0.35	0.06	0.24	0.05	0.21
	Ílhavo	0.07	0.22	0.08	0.24	0.05	0.16	0.06	0.19
	Mira	0.06	0.16	0.06	0.16	0.03	0.08	0.02	0.07

On the other hand, for the SSC and sediment fluxes are expected the same trends found for scenarios considering only climate change effects on fluvial discharges (scenario #3), for high and mean fluvial discharge conditions (Tables 7.15 and 7.16).

Table 7.15: Time-averaged SSC and sediment fluxes differences between #5A and reference scenarios, at Barra, S. Jacinto, Espinheiro, Ílhavo and Mira channels cross sections.

	Transect	Spring tide				Neap tide			
		Flood		Ebb		Flood		Ebb	
		SSC (mg/l)	q_s (ton/s)	SSC (mg/l)	q_s (ton/s)	SSC (mg/l)	q_s (ton/s)	SSC (mg/l)	q_s (ton/s)
High discharges	Barra	4.03	1.91	7.36	4.23	6.45	2.13	9.79	3.66
	S. Jacinto	3.28	1.35	6.96	2.07	5.00	1.89	9.17	2.40
	Espinheiro	5.47	1.44	9.45	2.40	5.42	1.91	7.75	2.23
	Ílhavo	2.90	1.48	8.10	3.07	26.82	1.71	27.46	1.82
	Mira	8.04	0.65	9.40	0.72	11.51	0.62	11.07	0.58
Mean discharges	Barra	-3.11	-0.53	-3.89	-0.89	-7.88	-1.09	-10.40	-2.04
	S. Jacinto	-5.67	-0.63	-6.48	-0.92	-13.40	-1.25	-13.62	-1.57
	Espinheiro	-13.40	-0.69	-15.20	-0.88	-28.95	-0.76	-30.51	-1.36
	Ílhavo	-14.61	-0.47	-13.92	-0.27	-18.29	-0.07	-19.48	0.03
	Mira	-3.79	-0.12	-3.26	-0.09	-8.71	-0.22	-8.40	-0.21
Low discharges	Barra	0.46	0.23	0.94	0.51	0.47	0.21	0.55	0.25
	S. Jacinto	0.32	0.15	0.95	0.27	0.24	0.16	0.62	0.18
	Espinheiro	-0.43	0.10	0.26	0.18	-0.31	0.17	-0.44	0.13
	Ílhavo	0.45	0.11	0.61	0.09	2.81	0.20	2.40	0.19
	Mira	0.79	0.06	1.26	0.09	1.73	0.07	1.78	0.06

For low fluvial discharge conditions is expected SSC and sediment fluxes increase, as predicted considering only the MSLR effect. The major SSC and sediment fluxes differences comparing to reference scenario are found for mean fluvial discharge conditions (39 and 67% for scenario #5A and 41 and 70% for scenario #5B, respectively).

Table 7.16: Time-averaged SSC and sediment fluxes differences between #5B and reference scenarios, at Barra, S. Jacinto, Espinheiro, Ílhavo and Mira channels cross sections.

	Transect	Spring tide				Neap tide			
		Flood		Ebb		Flood		Ebb	
		SSC (mg/l)	q_s (ton/s)	SSC (mg/l)	q_s (ton/s)	SSC (mg/l)	q_s (ton/s)	SSC (mg/l)	q_s (ton/s)
High discharges	**Barra**	2.59	1.88	5.75	4.38	4.91	2.32	7.43	3.68
	S. Jacinto	0.55	1.15	4.55	1.98	0.52	1.83	5.13	2.25
	Espinheiro	-0.40	1.36	5.16	2.63	-5.00	1.95	-2.03	2.23
	Ílhavo	-2.65	1.46	3.77	2.95	17.58	1.87	17.22	2.29
	Mira	7.04	0.69	8.43	0.79	9.68	0.66	9.35	0.62
Mean discharges	**Barra**	-3.20	-0.50	-4.33	-0.78	-7.88	-0.85	-10.58	-1.85
	S. Jacinto	-5.94	-0.61	-6.58	-0.83	-14.33	-1.17	-14.49	-1.53
	Espinheiro	-14.73	-0.66	-16.46	-0.75	-32.76	-0.77	-34.68	-1.38
	Ílhavo	-15.09	-0.37	-14.30	-0.17	-20.33	0.01	-21.66	0.21
	Mira	-3.61	-0.08	-3.08	-0.04	-8.80	-0.18	-8.58	-0.18
Low discharges	**Barra**	0.23	0.20	0.88	0.56	0.90	0.37	1.03	0.44
	S. Jacinto	0.63	0.20	1.26	0.36	0.74	0.30	1.25	0.32
	Espinheiro	-0.45	0.13	0.63	0.29	0.42	0.30	0.24	0.25
	Ílhavo	0.80	0.17	0.97	0.14	4.74	0.34	4.26	0.36
	Mira	1.15	0.09	1.55	0.11	2.62	0.11	2.64	0.11

Generally, for scenarios #5A and #5B higher suspended sediment volumes are expected to be transported during the tidal cycle, comparing to reference scenario, except for mean fluvial discharge conditions (Figures 7.23 and 7.24). Sediment balance direction is predicted to be mostly towards the ocean, with less situations of suspended sediment retention at Ílhavo and Mira channels, for high fluvial discharge conditions (Figures 7.23d and 7.24d). This behaviour is related with the fluvial discharges increase, which contributes to the sediment exportation, as previous verified by Dias *et al.* (2003).

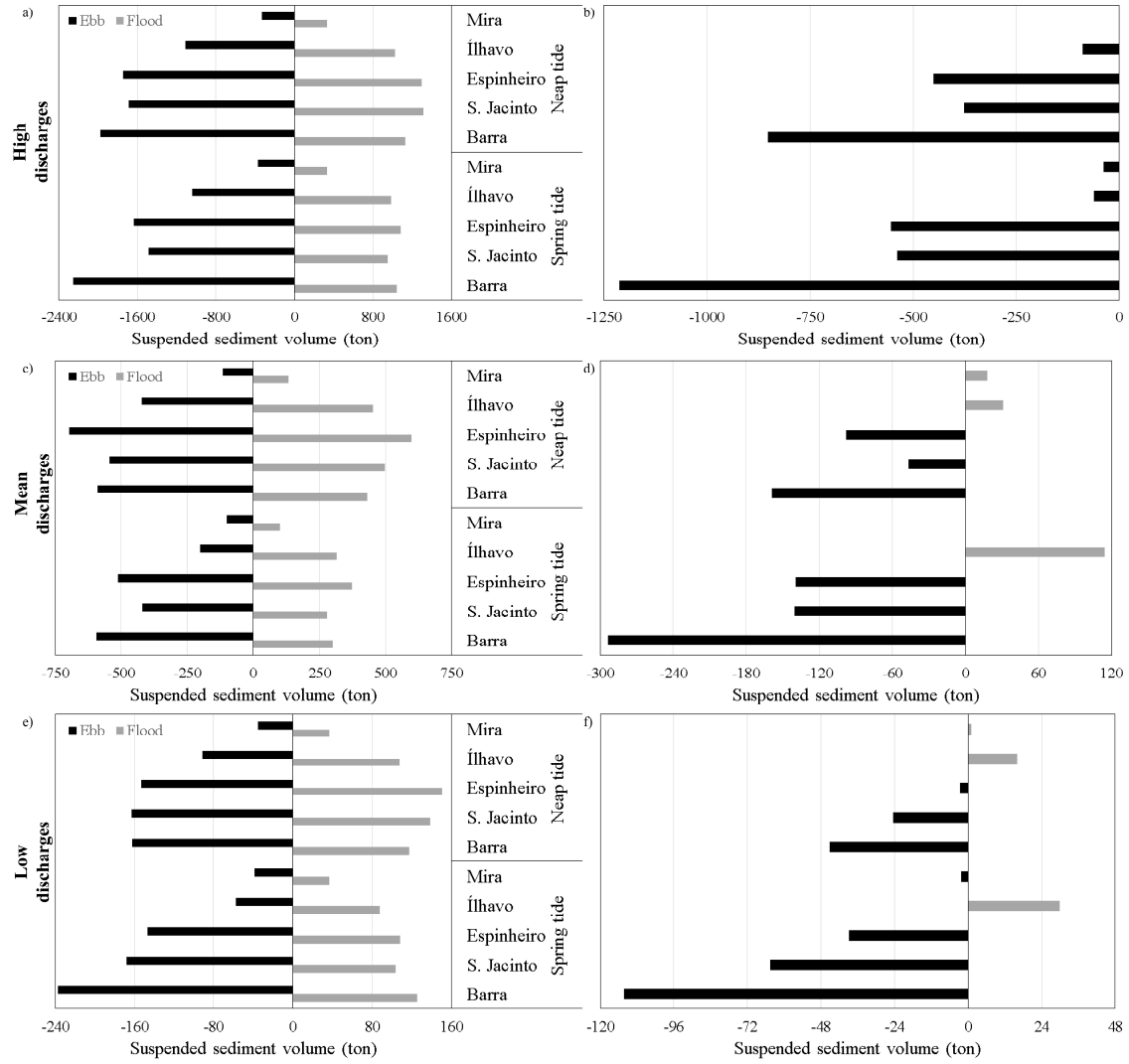

Figure 7.23: Total suspended sediment transport for scenario #5A at Barra, S. Jacinto, Espinheiro, Ílhavo and Mira channels cross sections, for high (a, b), mean (c, d) and low fluvial discharge conditions (e, f), in the flood and ebb periods (a, c, e) and tidal cycle balance (b, d, f).

Spatial SSC differences along the lagoon between scenarios #5A and #5B and the reference are presented from Figure 7.25 to Figure 7.30. Comparing with reference scenario, for high fluvial discharge conditions is expected higher SSC at lagoon central area and along S. Jacinto and Espinheiro channels. However, at Mira and Ílhavo channels, only at downstream areas were found higher SSC (Figures 7.25 and 7.28).

For mean fluvial discharge conditions, the combination of fluvial discharges reduction and higher sea water intrusion induced by MSLR, lower SSC at lagoon central area are expected, comparing to reference scenario (Figures 7.26 and 7.29).

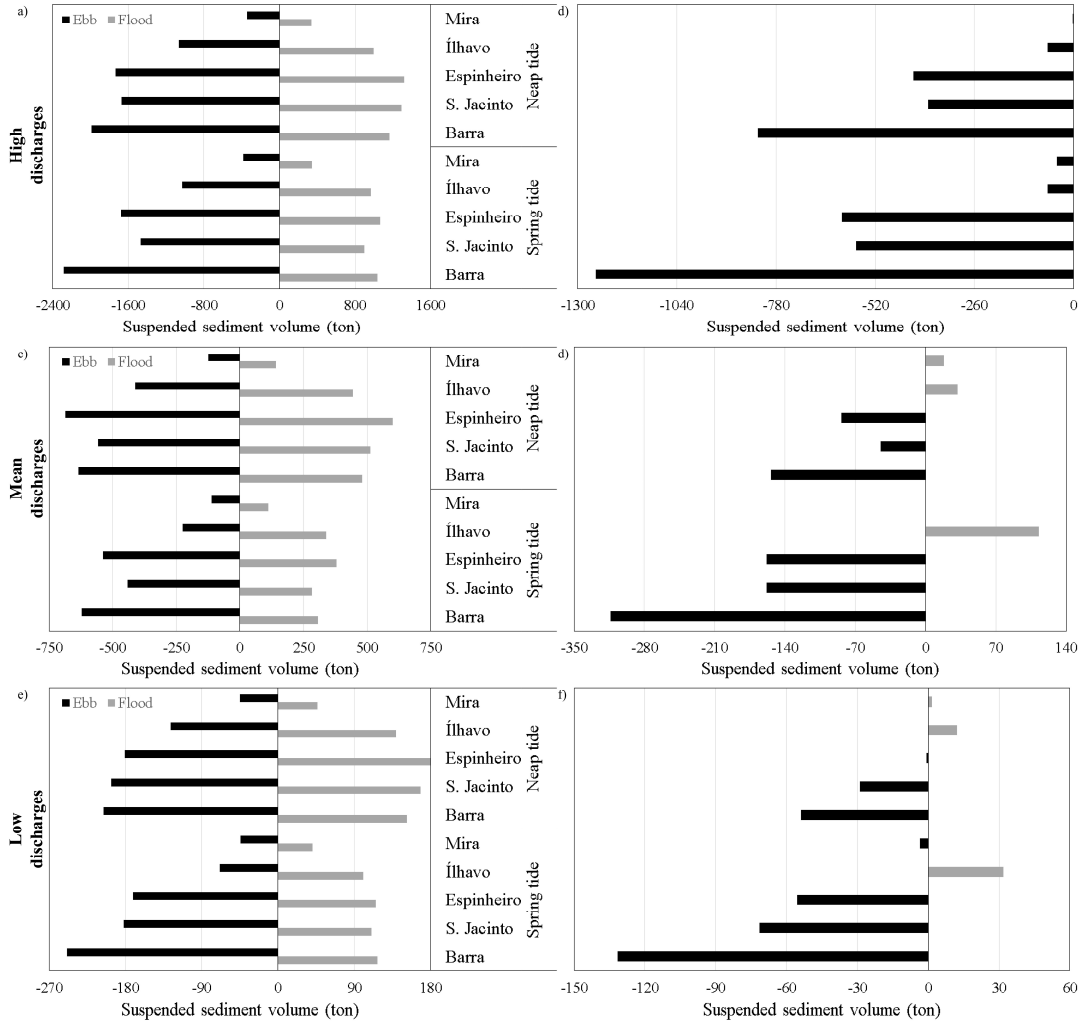

Figure 7.24: Total suspended sediment transport for scenario #5B at Barra, S. Jacinto, Espinheiro, Ílhavo and Mira channels cross sections, for high (a, b), mean (c, d) and low fluvial discharge conditions (e, f), in the flood and ebb periods (a, c, e) and tidal cycle balance (b, d, f).

Spatial SSC differences for low fluvial discharge conditions are expected to be similar to those predicted for the MSLR scenarios. This shows that fluvial discharges reduction due to climate change effects for low fluvial discharge conditions have a low impact in the lagoon SSC distribution, as previous verified for scenario #3 (Figures 7.27 and 7.30).

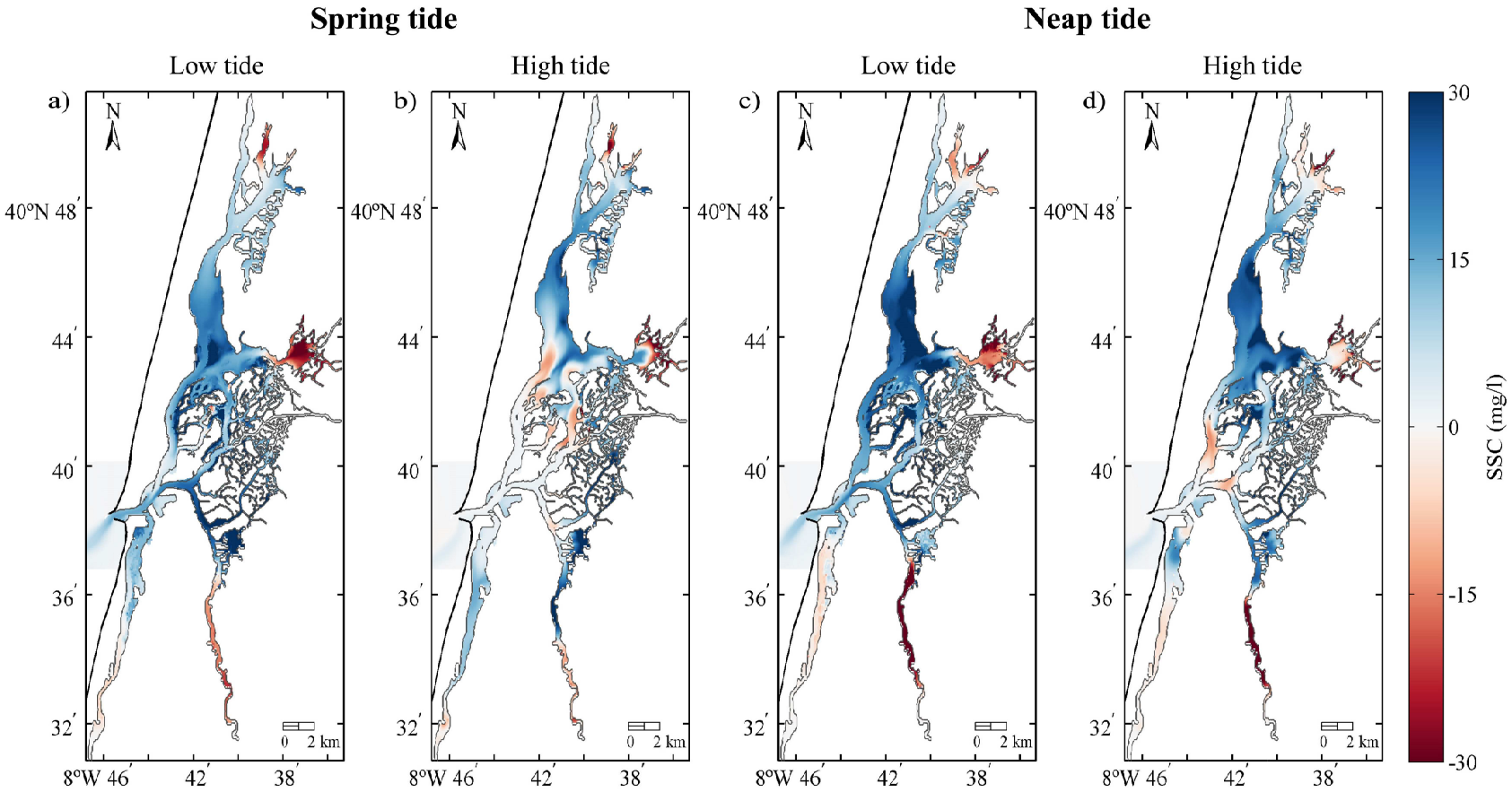

Figure 7.25: Spatial SSC differences between reference scenario and scenario #5A for high fluvial discharges, in spring (a, b) and neap (c, d) tide, at low (a, c) and high (b, d) tide at the inlet.

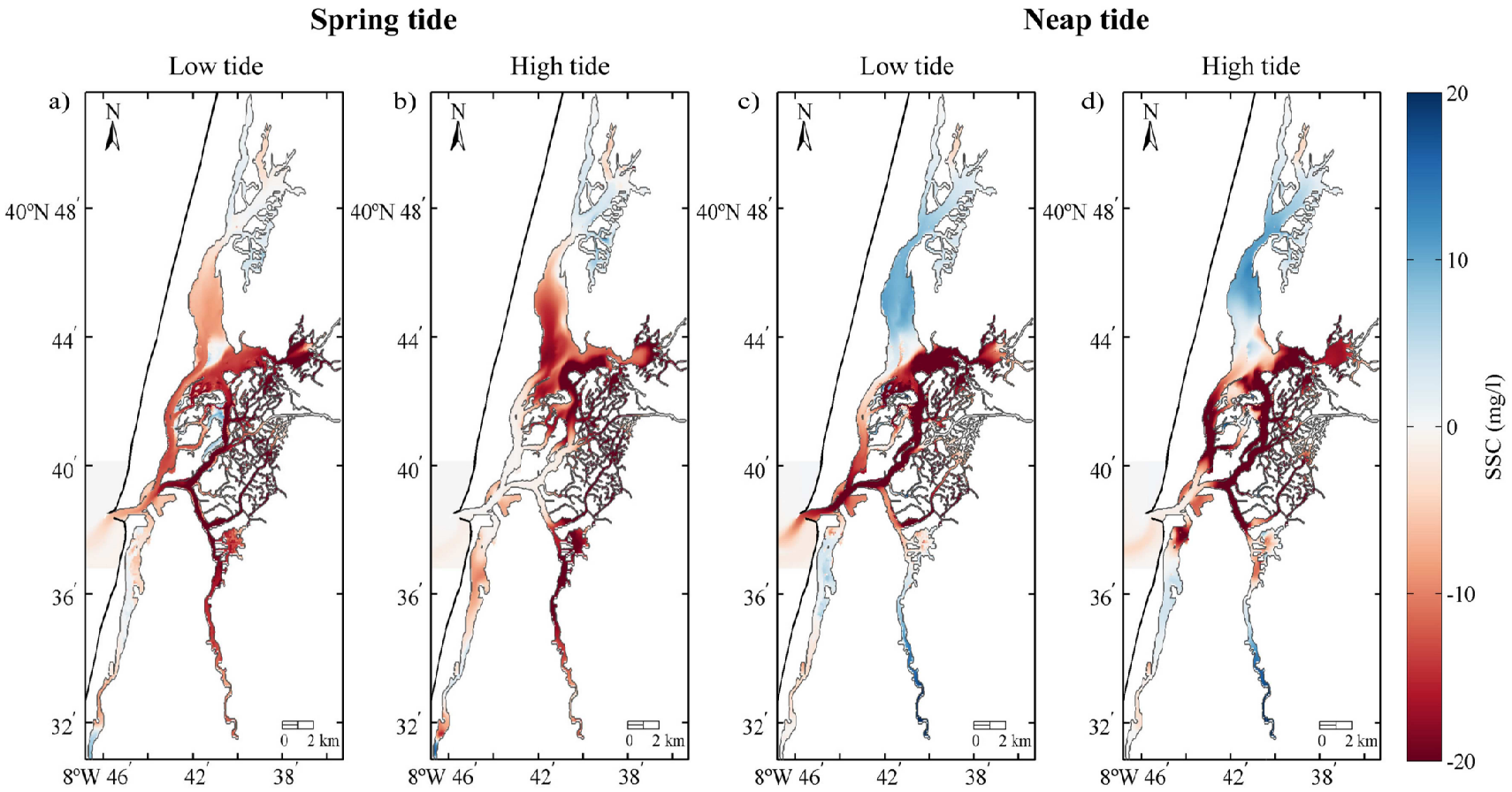

Figure 7.26: Spatial SSC differences between reference scenario and scenario #5A for mean fluvial discharge conditions, in spring (a, b) and neap (c, d) tide, at low (a, c) and high (b, d) tide at the inlet.

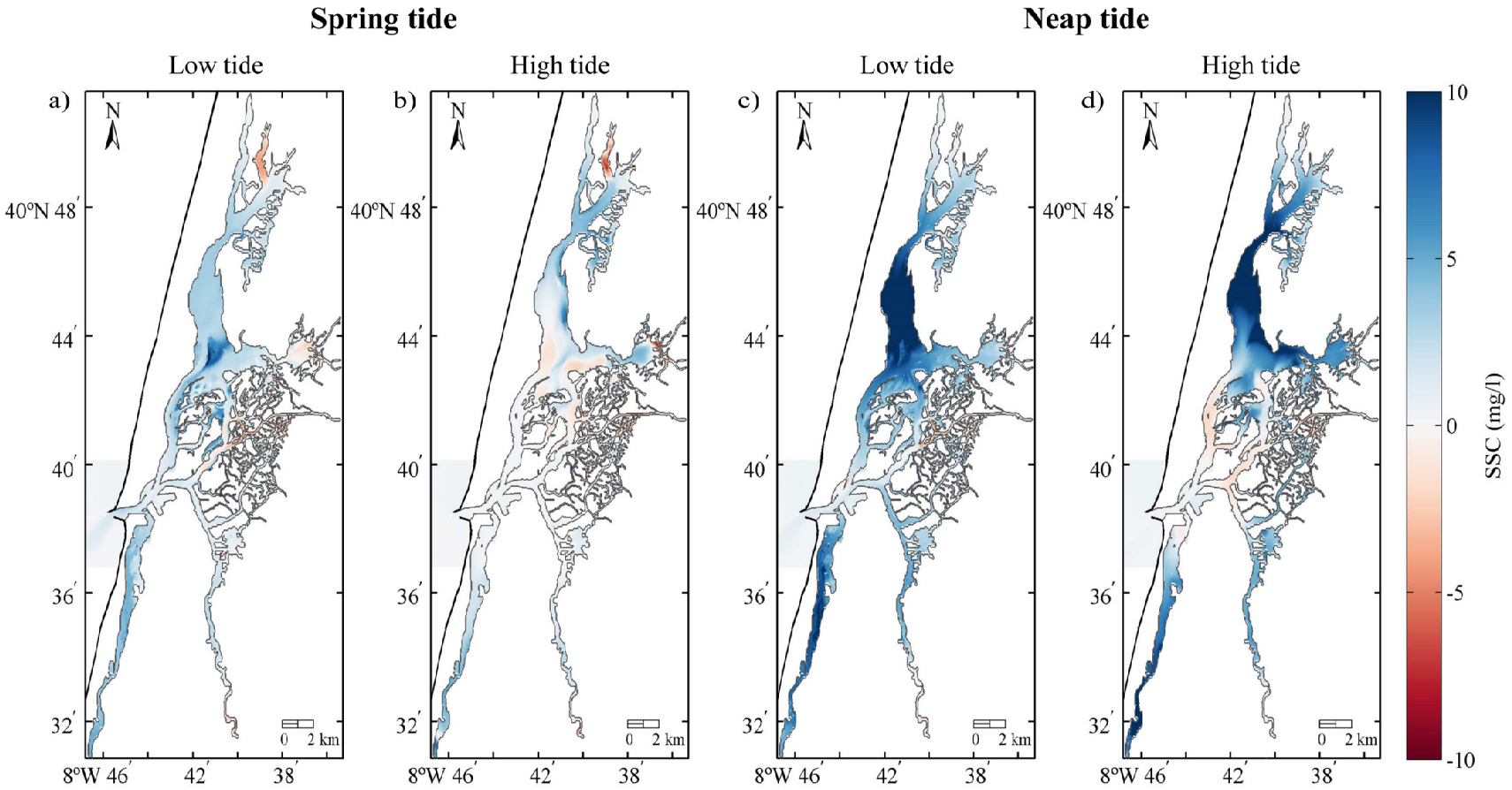

Figure 7.27: Spatial SSC differences between reference scenario and scenario #5A for low fluvial discharge conditions, in spring (a, b) and neap (c, d) tide, at low (a, c) and high (b, d) tide at the inlet.

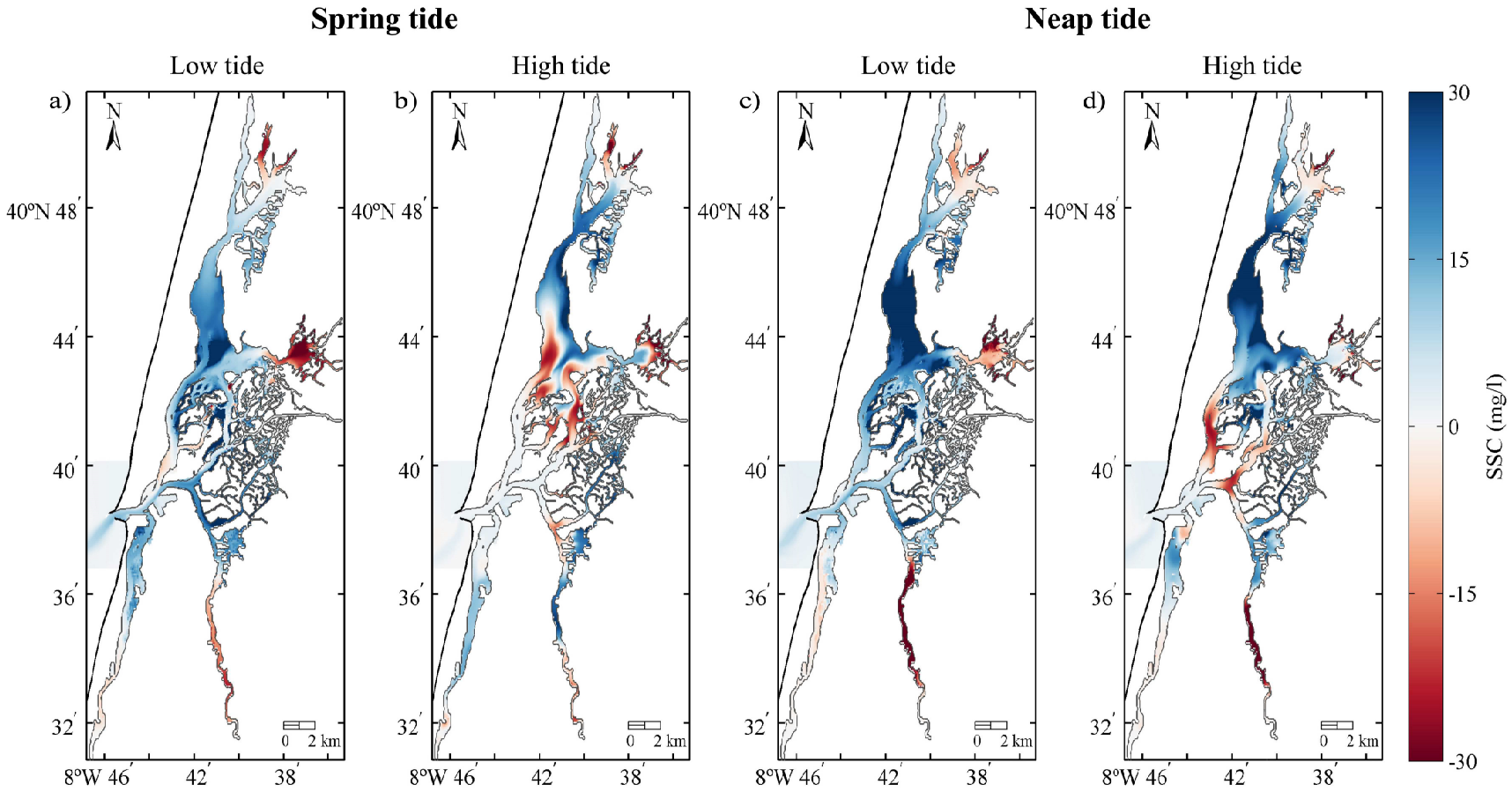

Figure 7.28: Spatial SSC differences between reference scenario and scenario #5B for high fluvial discharges, in spring (a, b) and neap (c, d) tide, at low (a, c) and high (b, d) tide at the inlet.

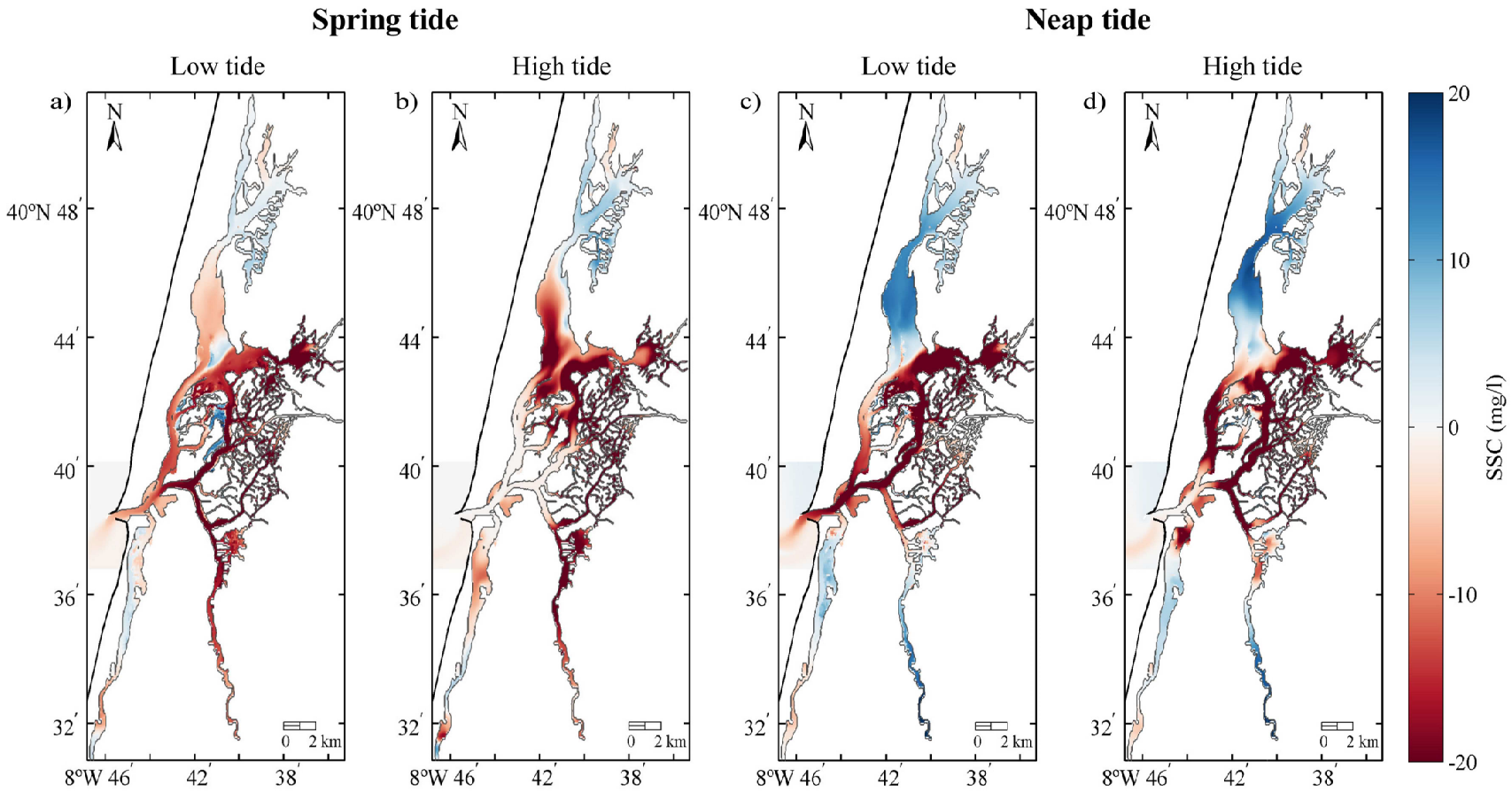

Figure 7.29: Spatial SSC differences between reference scenario and scenario #5B for mean fluvial discharge conditions, in spring (a, b) and neap (c, d) tide, at low (a, c) and high (b, d) tide at the inlet.

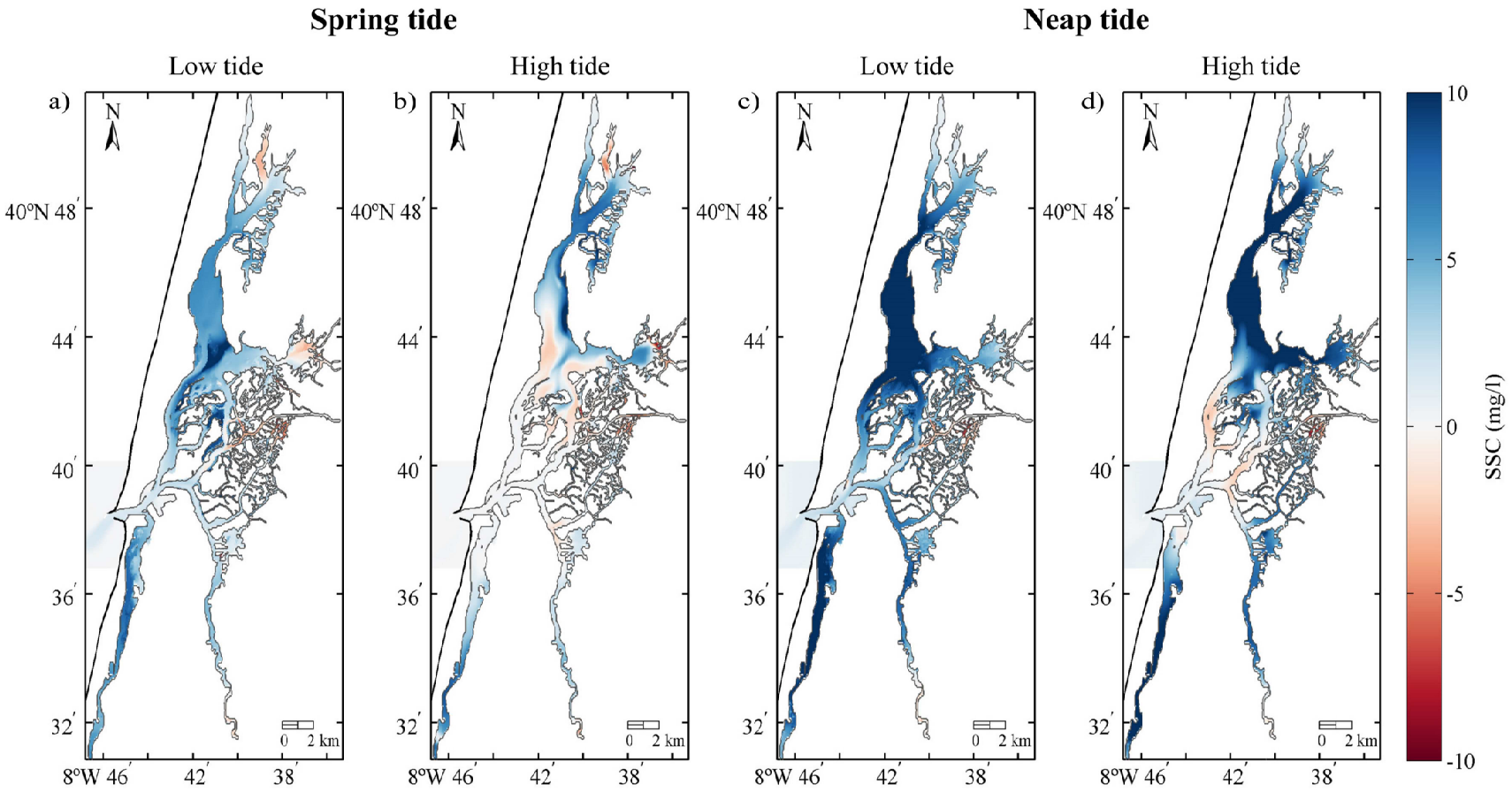

Figure 7.30: Spatial SSC differences between reference scenario and scenario #5B for low fluvial discharge conditions, in spring (a, b) and neap (c, d) tide, at low (a, c) and high (b, d) tide at the inlet.

7.4 Conclusions

The evaluation of the future anthropogenic actions and natural change effects influence on Ria de Aveiro suspended sediment dynamics was performed in this chapter by numerical simulation of different scenarios. Simulations were performed for high, mean and low fluvial discharge conditions, at spring and neap tides. Analysis of results was performed by establishing a comparison with a reference scenario (set to simulate the suspended sediment dynamics for the present conditions, using 2012 bathymetry and fluvial discharges for present climate). From the comparative analysis between the different studied scenarios and the reference scenario, the following conclusions were draw:

- Overall, future dredging operations (scenario #1) will have a low impact on the main lagoon channels, being expected the major changes at the channels with higher intervention area and volumes. Indeed, a velocity amplification of 14% at Mira channel and 50% increase of sediment fluxes at Ílhavo channel was identified. Additionally, an opposite pattern to the expected to reference scenario is predicted at Ílhavo channel, with higher sediment fluxes during the ebb comparing to flood, for high and mean fluvial discharge conditions, leading to less situations of sediment retention;
- Ribeiradio-Ermida dam (scenario #2) will lead to Vouga river discharges reduction, which can induce a decrease in velocities and water fluxes during ebb and their increase during flood at main lagoon channels. However, the differences comparing to reference scenario are low. In opposition, for SSC and sediment fluxes a significant decrease (350% on average) is expected, with higher differences for mean fluvial discharge conditions (approximately 700%). Moreover, at Espinheiro channel was predicted SSC and sediment fluxes decrease from flood to ebb in neap tide conditions, leading to suspended sediment retention at tidal cycle. Spatial SSC along the lagoon highlights the Vouga river importance as the main sediment source, being expected SSC decrease not only at Espinheiro channel, but at all central area which may lead to intertidal areas erosion, and S. Jacinto and Ílhavo channels downstream areas, for high and mean fluvial discharge conditions;
- The impact of climate change effects on fluvial discharges is predicted to lead to an amplification of the seasonal asymmetry. Although, no significant differences in the

velocities and water fluxes at main lagoon channels were found to scenario #3 comparing to reference scenario. However, for SSC and sediment fluxes is expected to follow the fluvial discharges variations, with higher values than reference scenario for high fluvial discharge conditions (approximately 33 and 35%, respectively), and lower for mean (44 and 48%, respectively) and low fluvial discharge conditions (5 and 8%, respectively). Therefore, are expected lower suspended sediment volumes transported, except for high fluvial discharge conditions;

- MSLR (scenarios #4A and #4B) can induce higher velocities and water fluxes (23 and 30%, respectively) at main lagoon channels, comparing to reference scenario. Thus, are expected lower SSC, but in opposition higher sediment fluxes, for high and mean fluvial conditions. However, for low fluvial discharges are predicted higher SSC and sediment fluxes. Therefore, MSLR induce higher transported suspended sediment volumes during the tidal cycle, being predicted more situations of suspended sediment exportation at Ílhavo and Mira channels. Spatial SSC distribution along the lagoon highlight these findings, being found lower SSC at lagoon central area and higher at upstream areas, for high and mean fluvial discharges. For low discharges, the SSC differences comparing to reference scenario at central area are approximately null;
- Scenarios #5A and #5B, that combine climate change effects on fluvial discharges and MSL, present similar patterns to those found for MSLR scenarios (scenarios #4A and #4B), with the velocities and water fluxes increase at the main lagoon channels, with significant differences (22 and 36%. respectively) comparing to the reference scenario. Regarding SSC and sediment fluxes, the trends are similar to those found for climate change effects on fluvial discharges (scenario #3), with SSC and sediment fluxes increase (21 and 68%, respectively), for high fluvial discharges and its decrease (40 and 24%, respectively) for mean fluvial discharge conditions. However, for low fluvial discharges is predicted SSC and sediment fluxes increase (29 and 71%, respectively), as found for MSLR scenarios. Spatial SSC along the lagoon, for high and mean fluvial discharges, present the same patterns found for scenario #3, being only reduced. On the other hand, for low fluvial discharges, are predicted the same patterns found for MSLR scenarios, but the differences are enhanced.

In summary, the obtained results indicated that only significant impact at hydrodynamic parameters is expected for scenarios with MSL changes. However, at all analysed scenarios are predicted significant changes at SSC and sediment fluxes, being the Vouga discharge and suspended sediment load reduction due to Ribeiradio-Ermida dam construction, the scenario where is expected a higher impact.

The combination of the climate change effects on fluvial discharges and MSL is expected to have a lower impact on the SSC and sediment fluxes, except for low fluvial discharge conditions, comparing to the scenario of only climate change effects on fluvial discharges. In opposition, comparing to the MSLR scenarios, the combination of the climate change effects is expected to have a higher impact.

8 Final remarks

8.1 Conclusions

The influence of anthropogenic activities and climate change effects in the suspended sediment dynamics of the Ria de Aveiro has received limited attention in previous studies. Therefore, the aim of this work was to contribute to improve the knowledge about the impact of those changes on the Ria de Aveiro suspended sediment dynamics and on the lagoon potential to export sediments. To achieve the proposed goal, the methodology adopted included data analysis, experimental work and numerical modelling.

Suspended sediment transport at Ria de Aveiro is governed by the tide, but also influenced by the river discharges and other forcing agents, with concentrations decreasing from the river and the main channels towards the inlet. In Chapter 2, analysis of bottom sediment samples from the inlet area and main lagoon channels showed an increase of the silt-clay fraction at bottom sediments from summer to winter conditions, especially at Espinheiro and Ílhavo channels, highlighting the channel's upstream areas contribution. Additionally, at channels closer to the inlet (Barra and S. Jacinto) an increase in gravel fraction was observed. Moreover, water samples collected at the main lagoon channels were also analysed, showing higher SSC for samples with lower salinities, which suggests that suspended sediment supply is done mainly by channels upstream areas.

As Vouga river represents the major freshwater contribution to the Ria de Aveiro, an evaluation of the suspended sediment loads evolution from this river and its main tributary, the Águeda river, was performed. Firstly, an analysis of the discharge and SSC data was performed. The considered data, obtained from SNIRH, was acquired at stations located ~60 and 20 km upstream of Ria de Aveiro, at Vouga and Águeda rivers, respectively. Results indicated that Vouga and Águeda river discharges are directly related to rainfall, with lower values in the dry season months and higher in winter months. Frequency analysis showed that for Vouga river most of the discharges present values lower than 100 m^3/s, but in winter they can reach higher values, in the range of 300-400 m^3/s. Moreover, analysis of its evolution showed a frequency decrease for high discharges (>200 m^3/s) from 1980 to 2010. A similar behaviour was observed for Águeda river, where most of discharges present values lower than 55 m^3/s, with a decrease between 1980 and 2010 of the frequency of discharges higher than 110 m^3/s. This decrease can be related with the dams implemented at both rivers drainage basins. Regarding SSC, Vouga river presented most of the values between 10 and 20 mg/l and in Águeda were observed lower values, in the range 3-3.5 mg/l. However, at both stations higher values were registered in the 50-150 mg/l interval. Additionally, a comparison between discharges and SSC indicated that for Vouga river, peak discharges can have different SSC magnitudes. Suspended sediment loads of Vouga and Águeda rivers were determined through SRC considering past data, with the obtained results showing a decrease in the suspended sediment loads at both rivers. Moreover, analysis of the monthly suspended sediment loads indicated extreme values in February and in August/September. Considering that the suspended sediment flux into the Ria de Aveiro corresponds to the sum of the Vouga and Águeda rivers suspended sediment loads, the higher and lower values should be observed in February and August. Vouga river suspended sediment load seasonal variation is notice at Ria de Aveiro SSC, as verified by Abrantes (2005). Therefore, in Chapter 6, in order to evaluate the extreme fluvial discharges effects these months were considered representative of wet and dry seasons.

In Chapter 3, bathymetric data collected between 2001 and 2012 at the lagoon inlet and harbour area, which includes the main lagoon channels downstream areas, was used to evaluate their morphological trend and relate it to the dredging operations and performed harbour engineering works, in order to identify a morphological trend. This analysis showed that the main lagoon channels and inlet have been deepening between 2001 and 2012, being

observed an increase of the area with depths higher than 15 m and in the range 10/15 m. This depth increase was associated mainly to dredging operations performed between 2001 and 2006. Overall, the harbour terminals morphological trend is deposition, which is consistent with the need to perform dredging operations annually. However, deposition rates are not equal, with higher values at NT of 40 cm/year, followed by ST with 20 cm/year. LBT, CFP and HFP sub-areas present the lower deposition rates of approximately 6 cm/year. Noteworthy is the opposite morphological behaviour, from erosion to deposition at LBT after 2006, following the construction of the docking piers. Regarding the navigation channels, the identification of a morphological trend was more difficult, since dredged volumes location was not known. Moreover, results have shown that negative elevation differences higher than 3 m between surveys are due to dredging operations, significant deposition being observed in the following year, with positive elevation differences in the interval 0.5 to 3 m.

In Chapter 4, the effect of salinity and initial sediment concentration on the Ria de Aveiro fine sediments settling velocity was evaluated in settling column experiments, providing new insights into deposition properties. The influence of salinity was observed for low salinity values (3.3‰). Additionally, it was observed that for salinity values of 15 and 30‰, the median settling velocity stabilizes, indicating that there can be a salinity limit, already observed by other authors (Krone, 1962; Al Ani *et al.*, 1991; van Leussen, 1999; Wan *et al.*, 2015). Initial sediment concentration influence on settling velocity was also observed, with 12, 9 and 6% of the initial sediment remaining in suspension at the end of the experiment, for initial concentrations of 0.15, 0.6 and 1.5 g/l, respectively. Median settling velocity ranged from 0.40 mm/s for fresh water conditions to 1.21 mm/s under brackish-marine conditions (S=30‰) and from 0.37 to 1.03 mm/s, for initial sediment concentrations of 0.15 and 0.90 g/l. Analysis of the evolution of d_{10}, d_{50} and d_{90} parameters along the experiments showed slower variations for fresh water conditions and the lower initial concentration of 0.15 g/l. Moreover, a particle size decrease over time was observed. In summary, settling column experiments showed that the settling velocity of fine sediments from the Ria de Aveiro is influenced by salinity, initial concentration and particle size.

In order to study the suspended sediment dynamics in the Ria de Aveiro, the numerical model MOHID was implemented in Chapter 5. Numerical model validation showed that daily variation observed in the SSC data at three stations located at Mira, Ílhavo and S. Jacinto

channels, is reproduced by the numerical model. Moreover, comparison between average historical observations and SSC predictions for more stations located along the lagoon showed reasonable agreement, with differences lower than 20 mg/l in most stations. Best fitting was obtained in July and at stations located nearby the inlet, with relative error of 47%. In opposition, higher errors were observed for high river discharges and at stations close to the river mouth, due to uncertainty on SSC associated to high fluvial discharges.

In Chapter 6 an analysis of the Ria de Aveiro suspended sediment dynamics evolution from the past to present conditions at main channels cross sections was performed, through numerical simulation applying the numerical model MOHID previously validated. Numerical results showed that channels deepening observed between 1987/88 and the present (2012) has led to the SSC decrease and sediment fluxes increase, due to higher tidal prism. However, tidal currents increase at the central area has led to higher sediment fluxes, with major differences at S. Jacinto and Ílhavo channels. Therefore, lower concentrations were found at the central area. However, at upstream areas, especially at S. Jacinto and Laranjo bay, higher SSC are predicted, due to combination of high currents and shallow areas. The obtained results are in agreement with morphological trends found for the main lagoon channels and harbour area in Chapter 3, being observed deposition at the downstream areas of Mira and Ílhavo channels.

In Chapter 7, the influence of future anthropogenic and climate change effects on the suspended sediment transport was evaluated, through numerical simulation of different scenarios, applying the numerical model MOHID. Analysis of dredging operations proposed in the frame of Polis Litoral Ria de Aveiro/CIRA Actions indicates that this intervention will lead in general to SSC and sediment fluxes decrease at main channels, although with low differences comparing to present conditions. Exceptions are found in the channels with major intervention area, namely Ílhavo and Mira, where sediment fluxes are predicted to increase by 50 and 16%, respectively. Additionally, an opposite pattern at Ílhavo channel is expected comparing to the present conditions, with higher sediment fluxes during ebb than during flood, for high and mean fluvial discharge conditions. The construction of the Ribeiradio-Ermida dam will affect the Vouga river discharge, the lagoon main fluvial tributary. However, major changes in the velocities and water fluxes at the main lagoon channels are not expected. The major impact could occur for SSC and sediment fluxes at the lagoon central area, where low SSC were found, with suspended sediment retention at

Espinheiro channel at tidal cycle for neap tide conditions. Therefore, a decrease of the sediment volume exported by the lagoon to the ocean is expected and erosion of the intertidal areas is possible at the central area.

The impact of climate change effects on lagoon fluvial tributaries will accentuate the seasonal asymmetry, with higher/lower discharges for wet and dry seasons. However, significant changes in time-averaged velocities and water fluxes at the main lagoon channels were not found. Major changes were predicted in the SSC and sediment fluxes, with an increase for high fluvial discharges and a decrease for mean fluvial discharges. For minimum fluvial discharge conditions, the differences comparing to reference scenario are minor.

MSLR induces higher velocities and water fluxes at the main lagoon channels. Therefore, SSC is expected to decrease and sediment fluxes to increase, with higher differences comparing to reference scenario found for high MSLR of 0.64 m. However, for low fluvial discharge conditions it is expected both SSC and sediment fluxes increase.

Combination of climate change effects on fluvial discharges and MSL present the same trends found for climate change effects only on fluvial discharges, for high and mean fluvial discharge conditions. Indeed, it is predicted that SSC and sediment fluxes increase/decrease for high/mean fluvial discharge conditions. For low fluvial discharge, higher values are expected comparing to the reference scenario, as predicted for MSLR scenarios. The combination of the climate change effects is expected to have a lower impact on the SSC and sediment fluxes comparing to only climate change effects on fluvial discharges, except for low discharge conditions. In opposition, comparing to the MSLR scenarios are predicted to have a higher impact.

In summary and considering the main research questions of this work (Section 1.1), the modelling results revealed that the lagoon suspended sediment transport has changed from the past to present lagoon conditions. The several works and dredging operations that were performed at Aveiro harbour, contributed to a general lagoon deepening at the inlet and harbour area. This could lead to lower SSC and higher sediment fluxes at main lagoon channels. Regarding the sediment fluxes direction, the results suggest that no differences from the past to present conditions are expected to have occur, being mainly towards the ocean, except at Ílhavo and Mira channels. Dredging operations planned in the frame of Polis Litoral Ria de Aveiro/CIRA Actions are expected to have a larger impact at Mira and Ílhavo

channels, where larger volumes will be dredged. Ribeiradio-Ermida dam construction at Vouga river implies suspended sediment fluxes decrease at the lagoon central area, particularly at Espinheiro channel. Climate change effects will influence the sediment fluxes at the main lagoon channels, being expected its increase under MSLR scenarios. However, for climate change effects on fluvial discharges, sediment fluxes decrease is expected, but not for high fluvial discharge conditions. Regarding the sediment fluxes direction at main lagoon channels, the results suggests that they will be towards the ocean, being also possible to occur this flux direction at Ílhavo and Mira channels. Climate change effects are expected to have a higher impact comparing to lagoon present conditions for the scenario of changes on fluvial discharges. However, for low fluvial discharge conditions, higher impact is expected under MSLR scenarios.

Considering the modelling results and despite its limitations, a conceptual model for the possible future Ria de Aveiro suspended sediment transport trends, highlighting the erosion and deposition areas, for mean fluvial discharge conditions, is presented in Figure 8.1.

SSC are expected to decrease at lagoon central area, due to sediment reduction from the lagoon major sediment source, the Vouga river, consequence of Ribeiradio-Ermida dam construction. Furthermore, the climate change effects on fluvial discharges and MSL will contribute to the SSC decrease at lagoon, especially at central area. Moreover, the sediment fluxes at main channels are expected to be intensified, being directly towards the ocean, except at Mira and Ílhavo channels. In these channels the sediments from upstream areas are expected to deposit, and this can only be changed at Ílhavo channel if the planned dredging operations are carried out. At S. Jacinto channel upstream area is also predicted the retention of the suspended sediment from upper reach.

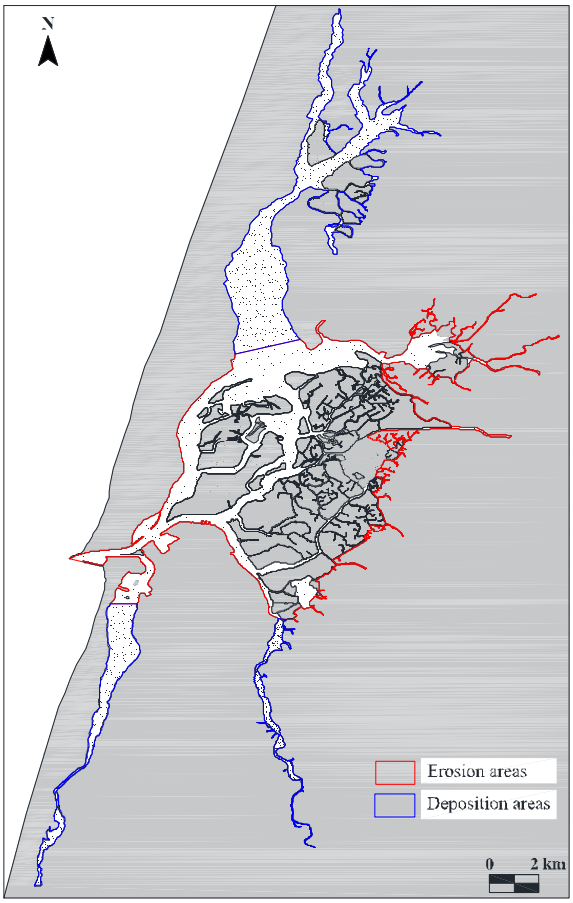

Figure 8.1: Ria de Aveiro future suspended sediment dynamics conceptual model.

8.2 Future developments

The conclusions presented in this work are restricted by the limitations of the work itself, namely the amount and quality of the available data. In fact, the basis of an accurate numerical modelling study lies in the availability of good quality data, in order to define the initial conditions and to calibrate the numerical predictions.

Firstly, the performed work will benefit of sediment fluxes measurements between the different fluvial tributaries and the lagoon. This implies the implementation of a sediment monitoring program for the lagoon fluvial tributaries, with continuous measurements of discharges and SSC. Moreover, monitoring the suspended sediment fluxes between the lagoon and the ocean is important and must have particular emphasis in future developments. Secondly, the suspended sediment transport model would benefit from more SSC data. Therefore, more field campaigns must be considered or even continuous monitoring.

Additionally, a denser sampling network, with more stations along the lagoon will allow to model specific patterns, especially at upstream areas where the tidal influence is weak.

Thirdly, the numerical model will benefit from a hydrodynamic calibration based in more velocity data, since the sediment transport is directly dependent on the bottom shear stress that is related to the flow velocity. Moreover, the combination of the SSC monitoring with hydrological parameters, namely velocity, salinity, water temperature and suspended sediment particle size, will make possible a better understanding of the Ria de Aveiro suspended sediment transport.

Other questions are related with a more profound knowledge about the physical processes of deposition and erosion of the lagoon fine sediments. The developed work has contributed to gain more insight into deposition processes, namely the settling velocity. However, some fine sediment transport parameters, namely the critical shear stresses for erosion and deposition, require more experiments *in situ* or in laboratory. Additionally, settling column experiments were performed using fine sediments collected only at Ílhavo channel. Therefore, experiments with samples collected at other lagoon locations should provide more insight into the settling behaviour of fine sediments along the lagoon.

Appendix

Appendix A1: Timetable of water samples collection in the surveys.

Station	Summer/Autumn	Winter/Spring
	07.10.2013	**17.03.2014**
	LT: 10:56>0.57 m (CD) HT: 17:31>3.30 m (CD)	LT: 09:20>0.56 m (CD) HT: 15:26>3.38 m (CD)
Barra	08:50	09:07
	12:02	10:33
	13:56	13:10
	15:37	13:51
	16:21	15:26
S. Jacinto	09:10	09:17
	11:52	10:44
	14:03	13:16
	15:27	13:56
	16:13	15:15
Espinheiro	09:35	09:33
	11:19	10:50
	14:16	13:26
	15:10	14:06
	15:58	15:00
Ílhavo	09:43	09:44
	10:53	10:55
	14:23	13:32
	15:04	14:12
	15:49	14:54

LT: Low tide; HT: High tide

Appendix A2: Monitoring periods of discharges and SSC data at Ponte Vouzela and Ponte Águeda stations.

	Ponte Vouzela	Ponte Águeda
Discharges	09/1917–02/1919 05/1919–01/1928 05/1928–11/1935 01/1936–01/1956 04/1956 09/1956–09/1979 02/1980–04/1999 10/1999–07/2003 12/2003–10/2007 12/2007–12/2008 02/2009–12/2009	06/1935–09/1990 10/2004–09/2007 11/2007 01/2008–11/2011 01/2012–07/2012 11/2012–12/2012 01/2013 03/2013–10/2013
SSC	04/1989–11/1994 01/1995–11/1995 01/1996–09/1996 01/1997–11/1997 01/1998–12/1998 02/1999–12/2001 02/2002–11/2003 01/2004–06/2004 04/2005–11/2005 02/2007–12/2007 02/2008–12/2008 02/2009–12/2009 02/2010–12/2010 02/2011–10/2012	06/1989–11/1994 01/1995–11/1995 01/1996–09/1996 01/1997–11/1997 01/1998–12/2001 02/2002–12/2003 02/2004–06/2004 01/2005–10/2005 02/2007–12/2007 02/2008–12/2008 02/2009–11/2009 02/2010–12/2010 02/2011–11/2011 01/2012–09/2012

Appendix B1: Depths distribution maps: a) 2001; b) 2003; c) 2004; d) 2005; e) 2006; f) 2007; g) 2008; h) 2010; i) 2012.

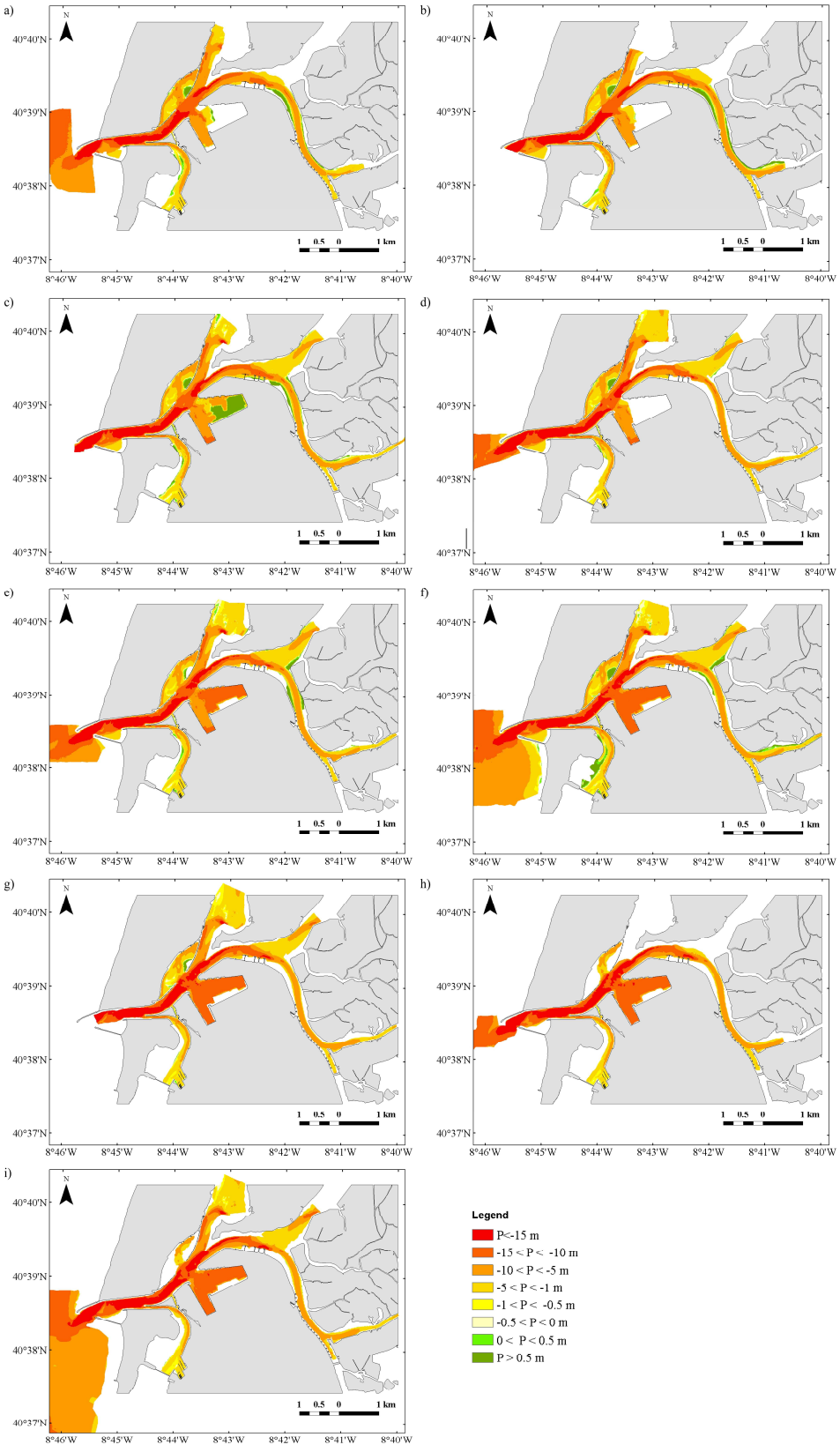

Appendix B2: Elevation differences distribution (minus sign indicates erosion): a) 2001/03; b) 2003/04; c) 2004/05; d) 2005/06; e) 2006/07; f) 2007/08; g) 2008/10; h) 2010/12.

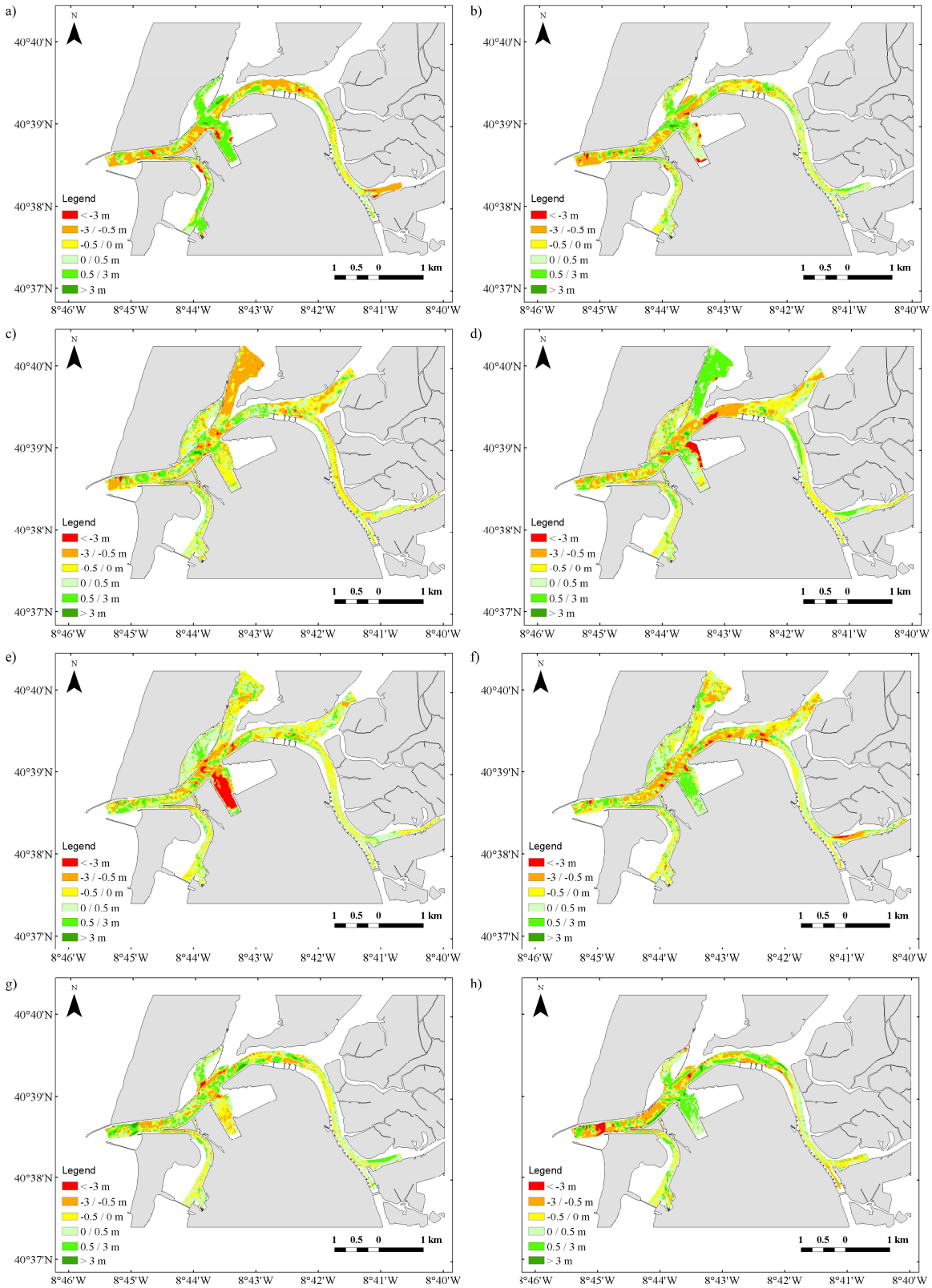

Appendix C1: Normalized vertically average suspended sediment concentrations of experiments with different salinities.

Time (min)	C/C_{ref} (adimensional)					
	Experiment					
	S=0‰	S=3.3‰	S=6.7‰	S=10‰	S=15‰	S=30‰
0	1.009	1.025	0.988	0.883	1.013	0.944
1	0.991	0.975	1.012	1.117	0.987	1.056
6	1.006	0.906	0.916	1.022	0.954	1.016
16	0.768	0.697	0.668	0.618	0.498	0.645
36	0.511	0.384	0.326	0.315	0.212	0.192
66	0.347	0.279	0.270	0.247	0.154	0.124
106	0.304	0.236	0.224	0.207	0.135	0.103
156	0.267	0.178	0.196	0.178	0.106	0.077
216	0.226	0.174	0.169	0.145	0.085	0.065
306	0.201	0.149	0.142	0.124	0.062	0.044

Appendix C2: Normalized vertically average suspended sediment concentrations of experiments with different initial suspended sediment concentrations.

Time (min)	C/C_{ref} (adimensional)			
	Experiment			
	C=0.15 g/l	C=0.30 g/l	C=0.60 g/l	C=0.90 g/l
0	1.000	0.974	0.986	0.984
1	1.000	1.026	1.014	1.016
6	0.918	0.927	0.975	0.971
16	0.949	0.804	0.622	0.534
36	0.587	0.456	0.315	0.260
66	0.385	0.333	0.224	0.199
106	0.274	0.256	0.182	0.141
156	0.211	0.201	0.143	0.106
216	0.167	0.169	0.118	0.089
306	0.103	0.169	0.088	0.064

Appendix C3: Obscuration of experiments with different salinities.

Time (min)	Experiment					
	S=0‰	S=3.3‰	S=6.7‰	S=10‰	S=15‰	S=30‰
0	14.47	15.05	15.70	15.17	15.97	15.07
1	14.93	15.57	15.60	14.67	14.57	14.77
6	15.30	15.27	14.80	14.63	14.27	15.00
16	13.63	14.90	14.00	13.67	12.67	12.37
36	12.67	12.30	12.50	11.27	8.50	6.77
66	13.63	11.27	10.83	9.83	6.13	5.80
106	11.33	10.50	9.63	8.53	6.57	3.73
156	11.23	8.70	7.57	7.27	4.97	3.63
216	10.63	8.33	7.30	5.70	4.90	2.60
306	10.30	7.57	6.70	4.77	4.03	1.80

Appendix C4: Obscuration of experiments with different initial suspended sediment concentrations.

Time (min)	Experiment			
	C=0.15 g/l	C=0.30 g/l	C=0.60 g/l	C=0.90 g/l
0	1.50	5.65	10.65	16.05
1	2.10	4.40	7.87	10.27
6	2.20	2.90	5.90	9.83
16	0.97	3.47	5.50	7.33
36	1.53	2.67	4.03	4.83
66	1.47	2.10	3.17	4.30
106	1.20	1.20	2.57	3.87
156	0.93	1.40	2.57	2.77
216	1.00	1.27	1.80	2.53
306	0.90	1.60	1.60	2.17

Bibliography

Abrantes, M.I. (2005). *Os sedimentos da margem continental, sector Espinho-Cabo Mondego*. PhD Thesis, Universidade de Aveiro, 289 p.

Abrantes, I., Dias, J.M., Rocha, F. (2006). Spatial and temporal variability of suspended sediments concentration in Ria de Aveiro lagoon and fluxes between the lagoon and the ocean. *Journal of Coastal Research*, SI39: 718-723.

Administração do Porto de Aveiro (2012). *Dragagem de inertes no Porto de Aveiro*.

Al Ani, S., Dyer, K.R. and Huntley, D.A (1991). Measurement of the influence of salinity on floc density and strength. *Geo-Marine Letters*, 11(3-4): 154-158.

Andersen, T.J., Fredsoe, J. and Pejrup, M. (2007). In situ estimation of erosion and deposition thresholds by Acoustic Doppler Velocimeter (ADV). *Estuarine, Coastal and Shelf Science*, 75(3): 327-336.

Andrade, C., Pires, H.O., Taborda, R. and Freitas, M.C. (2006). Zonas Costeiras. In: Santos, F.D. and Miranda, P. (Eds.), *Alterações Climáticas em Portugal: Cenários, Impactos e Medidas de Adaptação, Projecto SIAM II*. Lisboa, Gradiva.

Araújo, I.B., Dias, J.M. and Pugh, D.T. (2008). Model simulations of tidal changes in a coastal lagoon, the Ria de Aveiro (Portugal). *Continental Shelf Research*, 28(8): 1010-1025.

ARH Centro (2009). *Águas Superficiais de amostras da Ria de Aveiro*. Tecnical Report Nº342 to 380.

Asselman, N.E.M. (2000). Fitting and interpretation of sediment rating curves. *Journal of Hidrology*, 34(3-4): 228-248.

Baugh J.V. and Manning, A.J. (2007). An assessment of a new settling velocity parameterisation for cohesive sediment transport modeling. *Continental Shelf Research*, 27(13): 1835-1855.

Beer, N. and Joyce, C. (2013). North Atlantic coastal lagoons: conservation, management and research challenges in the twenty-first century. *Hydrobiologia*, 701(1): 1-11.

Benkhaldoun, F., Daoudi, S., Elmahi, I. and Seaid, M. (2012). Numerical modelling of sediment transport in the Nador lagoon (Morocco). *Applied Numerical Mathematics*, 62(12): 1749-1766.

Berhane, I., Sternberg, R.W., Kineke, G.C., Milligan, T.G. and Kranck, K. (1997). The variability of suspended aggregates on the Amazon Continental Shelf. *Continental Shelf Research*, 17(3): 267-285.

Berlamont, J., Ockenden, M., Toorman, E. and Winterwerp, J. (1993). The characterisation of cohesive sediment properties. *Coastal Engineering*, 21(1-3): 105-128.

Boateng, I., Bray, M. and Hooke, J. (2012). Estimating the fluvial sediment input to the coastal sediment budget: a case study of Ghana. *Geomorphology*, 138(1): 100-110.

Burban, P, Lick, W. and Lick, J. (1989). The flocculation of fine-grained sediments in estuarine waters. *Journal of Geophysical Research*, 94(C6): 8323-8330.

Burban, P.Y., Xu ,Y.U., McNeil, J. and Lick, W. (1990). Settling speeds of flocs in fresh water and seawater. *Journal of Geophysics Research*, 95(10): 18200-18213.

Burt, T.N. (1986). Field settling velocities of estuary muds. In: Metha, A.J. (Ed.), *Estuarine Cohesive Sediment Dynamics - Lecture Notes on Coastal and Estuarine Studies*. Berlin, Springer-Verlag, Vol. 14, 126-150.

Cancino, L. and Neves, R. (1994). 3D-numerical modelling of cohesive suspended sediment in the Western Scheldt estuary (The Netherlands). *Netherland Journal of Aquatic Ecology*, 28(3): 337-345.

Cancino, L. and Neves, R. (1999). Hydrodynamic and sediment suspension modelling in estuarine systems. Part I: Description of the numerical models. *Journal of Marine Systems*, 22(2-3): 105-116.

Chao, X., Jia, Y., Shields, J.R.D., Wang, S.S.W. and Cooper, C.M. (2008). Three dimensional numerical modeling of cohesive sediment transport and wind wave impact in a shallow oxbow lake. *Advances in Water Resources*, 31(7): 1004-1014.

Chapra, S.C. (1997). *Surface water quality modeling*. Waveland Press Inc. Illinois, 835 p.

Chen, S., Eisma, D. and Kalf, J. (1994). In situ distribution of suspended matter during the tidal cycle in the Elbe estuary. *Journal of Sea Research*, 32(1): 37-48.

Chen, W.B., Liu, W.C., Hsu, M.H. and Hwang, C.C. (2015). Modeling investigation of suspended sediment transport in a tidal estuary using a three-dimensional model. *Applied Mathematical Modelling*, 39(9): 2570-2586.

Church, J.A. and White, N.J. (2006). A 20th century acceleration in global sea-level rise. *Geophysical Research Letters*, 33(1): L01602.

COBA (2008). *Aproveitamento Hidroeléctrico de Ribeiradio-Ermida, F- Estudo de Impacto Ambiental*, Volume I – Relatório Síntese.

Coelho, C., Costa, S., Portela, L., Ribeiro, F. and Cunha, R. (2015). Aveiro Lagoon Fine Sediment Laboratory Tests. In: Wang, P., Rosati, J.D., Cheng, J. (Eds.), *The Proceedings of Coastal Sediments 2015*. World Scientific Co. Pte. Ltd, Singapore, 14 p.

Costa, R.G. (1995). Three-dimensional modelling of cohesive sediment transport in estuarine environments. University of Liverpool, Liverpool, 393 p.

Costa, S. and Coelho, C. (2011). Concentração da matéria particulada em suspensão na estimativa da velocidade de queda de sedimentos coesivos. *Revista de Gestão Costeira Integrada*, 11(2): 171-185.

Cunha, L.V., Ribeiro, L., Oliveira, R.P. and Nascimento, J. (2006). Recursos hídricos. In: Santos, F.D. and Miranda, P. (Eds.), *Alterações Climáticas em Portugal – Cenários, Impactos e Medidas de Adaptação, Projecto SIAM II*. Lisboa, Gradiva.

Cuthbertson, A., Dong, P., King, S. and Daves, P. (2008). Hindered settling velocity of cohesive/non cohesive sediment mixtures. *Coastal Engineering*, 55(12): 1197-1208.

Dankers, P.J.T. and Winterwerp, J.C. (2007). Hindered settling of mud flocs: theory and validation. *Continental Shelf Research*, 27(14): 1893–1907.

Dias, J.A., Ferreira, O. and Pereira, A. (1994). *Estudo sintético da geomorfologia e da dinâmica sedimentar dos troços costeiros entre Espinho e a Nazaré*. Estudos de Ambiente e Informática, Lda, 261 p.

Dias, J.M. (2001). *Contribution to the study of the Ria deAveiro hydrodynamics*. PhD Thesis, Universidade de Aveiro, 288 p.

Dias, J.M., Lopes, J.F. and Dekeyser, I. (1999). Hydrological characterization of Ria de Aveiro, Portugal, in early summer. *Oceanologica Acta*, 22(5): 473-485.

Dias, J.M., Lopes, J.F. and Dekeyser, I. (2000). Tidal propagation in Ria de Aveiro Lagoon, Portugal. *Physics and Chemistry of the Earth, Part B: Hydrology, Oceans and Atmosphere*, 25(4): 369-374.

Dias, J.M., Lopes, J.F. and Dekeyser, I. (2001). Lagrangian transport of particles in Ria de Aveiro lagoon, Portugal. *Physics and Chemistry of the Earth, Part B: Hydrology, Oceans and Atmosphere*, 26(9): 721-727.

Dias, J.M., Lopes, J.F. and Dekeyser, I. (2003). A numerical model system application to the study of the transport properties in Ria de Aveiro lagoon. *Ocean Dynamics*, 53(3): 220–231.

Dias, J.M., Abrantes, I. and Rocha, F. (2007). Suspended particulate matter sources and residence time in a mesotidal lagoon. *Journal of Coastal Research*, SI50: 1034-1039.

Dias, J.M., Araújo, I.B. and Picado, A. (2011). Dinâmica da maré na Ria de Aveiro. In: Almeida, A., Alves, F., Bernardes, C., Dias, J., Gomes, N., Pereira, E., Queiroga, H., Serôdio, J., Vaz, N. (Eds.), *Actas das Jornadas da Ria de Aveiro 2011*. Aveiro, Universidade de Aveiro, CESAM – Centro de Estudos do Ambiente e do Mar. Aveiro, 169-177.

Dias, J.M. and Mariano, S. (2011). Numerical modeling of hydrodynamic changes induced by a jetty extension – the case of Ria de Aveiro (Portugal). *Journal of Coastal Research*, SI64: 1008-1012.

Dias, J.M. and Picado, A. (2011). Impact of morphologic antrophogenic and natural changes in estuarine tidal dynamics. *Journal of Coastal Research*, SI64: 1490-1494.

Doulliet, P., Ouillon, S. and Courdier, E. (2001). A numerical model for fine suspended sediment transport in the southwest lagoon of New Caledonia. *Coral Reefs*, 20(4): 361-372.

Dyer, K.R. and Manning, A.J. (1999). Observation of the size, settling velocity and effective density of flocs, and their fractal dimensions. *Journal of Sea Research*, 41(1-2): 87-95.

EIA Vouga (2001). *Estudo de impacte ambiental, Projeto de desenvolvimento agrícola do Vouga, Bloco do Baixo Vouga Lagunar, Volume II – Situação de Referência*. Universidade de Aveiro, 361 p.

Etemad-Shahidi, A., Shahkolahi, A. and Liu, W.C. (2010). Modeling of hydrodynamics and cohesive sediment processes in an estuarine system: study case in Danshui River. *Environmental Modeling & Assessment*, 15(4): 261-271.

Fan, X., Shi, C., Shao, W. and Zhou, Y. (2013). The suspended sediment dynamics in the Inner-Mongolia reaches of the upper Yellow River. *Catena*, 109: 72-82.

Flemming, B. (2000). A revised textural classification of gravel-free muddy sediments on the basis of ternary diagrams. *Continental Shelf Research*, 20(10-11): 1125-1137.

Figueiredo, J.S., Duck, R., Hopkins, T. and Rodrigues, M. (2002). Evaluation of the nutrient inputs to a coastal lagoon: the case of the Ria de Aveiro, Portugal. In: Orive, E., Elliot, M., Jonge, V.N. (Eds.), *Developments in Hydrobiology. Nutrients and Eutrophication in Estuaries and Coastal Waters*, 164: 379-385.

Franz, G., Pinto, L., Ascione, I., Mateus, M., Fernandes, R., Leitão, P. and Neves, R. (2014). Modelling of cohesive sediment dynamics in tidal estuarine systems: case study of Tagus estuary, Portugal. *Estuarine, Coastal and Shelf Science*, 151: 34-44.

Freire, P. (2003). *Análise granulométrica por difração laser de sedimentos silto-argilosos. Procedimento de ensaio*. Technical Report 239/03-NEC, National Laboratory of Civil Engineering, LNEC, Lisboa, 47 p.

Ganju, N.K. and Schoellhamer, D.H. (2009). Calibration of an estuarine sediment transport model to sediment fluxes as an intermediate step for simulation of geomorphic evolution. *Continental Shelf Research*, 29(1): 148-158.

Génio, L., Sousa, A., Vaz, N., Dias, J.M. and Barroso, C.M. (2008). Effect of low salinity on the survival of recently hatched veliger of Nassarius reticulatus (L.) in estuarine habitats: a case study of Ria de Aveiro. *Journal of Sea Research*, 59(3): 133-143.

Girolamo, A.M., Pappagallo, P. and Lo Porto, A. (2015). Temporal variability of suspended sediment transport and rating curves in a Mediterranean river basin: the Celone (SE Italy). *Catena*, 128: 135-143.

Gonçalves, D.S., Pinheiro, L.M., Silva, P.A., Rosa, J., Rebelo, L., Bertin, X., Teixeira, S.B. and Esteves, R. (2014). Morphodynamic evolution of a sand extraction excavation offshore Vale do Lobo, Algarve, Portugal. *Coastal Engineering*, 88: 75-87.

Gray, A.B., Warrick, J.A., Pasternack, G.B., Watson, E.B. and Goñi, M.A. (2014). Suspended sediment behavior in a coastal dry-summer subtropical catchment: effects of hydrologic preconditions. *Geormophology*, 214: 485-501.

Gratiot, N., Michallet, H. and Mory, M. (2005). On the determination of the settling velocity flux of cohesive sediments in a turbulent fluid. *Journal of Geophysical Research*, 110(C06004), 10 p.

Harrington, S.T. and Harrington, J.R. (2013). An assessment of the suspended sediment rating curve approach for load estimation on Rivers Bandon and Owenabue, Ireland. *Geomorphology*, 185: 27-38.

Hill, P.S., Milligan, T.G. and Geyer, W.R. (2000). Controls on effective settling velocity in the Eel River flood plume. *Continental Shelf Research*, 20(16): 2095-2111.

Hu, J., Li, S. and Geng, B. (2011). Modeling the mass flux budgets of water and suspended sediments for the river network and estuary in the Pearl River Delta, China. *Journal of Marine Systems*, 88(2): 252-266.

Hunt, J.R. (1986). Particle aggregate breakup by fluid shear. In Mehta A.J. (Ed.), *Estuarine Cohesive Sediment Dynamics*. Berlin, Springer, 85-109.

Iadanza, C. and Napolitano, F. (2006). Sediment transport time series in the Tiber River. *Physics and Chemistry of the Earth*, 31(18): 1212-1227.

Jing, L. and Ridd, P.V. (1997). Modelling of suspended sediment transport in coastal areas under waves and currents. *Estuarine, Coastal and Shelf Science*, 45(1): 1-16.

Jiufa, L. and Zhang, C. (1998). Sediment resuspension and implications for turbidity maximum in the Changjiang Estuary. *Marine Geology,* 148(3-4): 117-124.

Johansen, C. and Larsen T. (1998). Measurement of settling velocity of fine sediment using a recirculated settling column. *Journal of Coastal Research*, 14(1): 132-139.

Karunaratha, H., Reeve, D. and Spivack, M. (2008). Long-term morphodynamic evolution of estuaries: an inverse problem. *Estuarine, Coastal and Shelf Science*, 77(3): 385-395.

Kitheka, J.U., Obiero, M. and Nthenge, P. (2005). River discharge, sediment transport and exchange in the Tana Estuary, Kenya. *Estuarine, Coastal and Shelf Science*, 63(3): 455-468.

Kranck, K. and Milligan, T.G. (1992). Characteristics of suspended particles at an 11-hour anchor station in San Francisco Bay, California. *Journal of Geophysical Research*, 97(C7): 11373-11382.

Krysanova, F., Wechsung, J., Arnold, R. and Williams, J. (2000). *SWIM - Soil and water integrated model - User manual*. PIK Report Nr. 69, 239 p.

Krone, R.B. (1962). *Flume studies of the transport of sediment in estuarial shoaling processes*. Hydraulic Engineering Laboratory and Sanitary Engineering Research Laboratory, University of California, Berkeley, 110 p.

Kumar, R.G., Strom, K.B. and Keyvani, A. (2010). Floc properties and settling velocity of San Jacinto estuary mud under variable shear and salinity conditions. *Continental Shelf Research*, 30(20): 2067-2081.

Leitão, P.C. (2003). *Integração de escalas e de processos na modelação do ambiente marinho*. PhD Thesis, Instituto Superior Técnico, Universidade Técnica de Lisboa, 466 p.

Leupi, C., Altinakar, M.S. and Deville, M.O. (2008). Numerical modeling of cohesive sediments dynamics in estuaries: Part I - Description of the model and simulations in the Po River Estuary. *International Journal for Numerical Methods in Fluids*, 57(3): 237-263.

Lin, B. and Namin, M. (2005). Modelling suspended sediment transport using an integrated numerical and ANNs model. *Journal of Hydraulic Research*, 43(5): 302-310.

Liu, W.C. (2005). Modeling the influence of settling velocity on cohesive sediment transport in Tanshui River estuary. *Environmental Geology*, 47(4): 535-546.

Liu, W.C. (2007). Modelling the effects of reservoir construction on tidal hydrodynamics and suspended sediment distribution in Danshuei River estuary. *Environmental Modelling & Software*, 22(11): 1588-1600.

Liu, W.C., Hsu, M.H and Kuo, A.Y. (2002). Modelling of hydrodynamics and cohesive sediment transport in Tanshui River estuarine system, Taiwan. *Marine Pollution Bulletin*, 44(10): 1076-1088.

Lillebø, A.I., Dias, J.M., Lencart e Silva, J.D., Alves, F.L., Stefanova, A. and Krysanova, V. (2013). Challenges for integrated catchment-to-coast modelling in the context of science-policy interface: the Ria de Aveiro coastal lagoon. *Proceedings of the TWAM2013 International Conference*, Aveiro, Portugal, 5 p.

Lopes, C. and Dias, J.M (2014). Influence of mean sea level rise on tidal dynamics of the Ria de Aveiro lagoon, Portugal. *Journal of Coastal Research*, SI70: 574-579.

Lopes, C. and Dias, J.M (2015). Tidal dynamics in a changing lagoon: Flooding or not floding the marginal regions. *Estuarine, Coastal and Shelf Science*, 167(Part A): 14-24.

Lopes, J.F. and Dias, J.M. (2007). Residual circulation and sediment distribution in the Ria de Aveiro lagoon, Portugal. *Journal of Marine Systems*, 68(3–4): 507-528.

Lopes, J.F., Dias, J.M. and Dekeyser, I. (2001). Influence of tides and river inputs on suspended sediment transport in the Ria de Aveiro lagoon, Portugal. *Physics and Chemistry of the Earth, Part B: Hydrology, Oceans and Atmosphere*, 26(9): 729-734.

Lopes, J.F., Dias, J.M. and Dekeyser, I. (2006). Numerical modelling of cohesive sediments transport in the Ria de Aveiro lagoon, Portugal. *Journal of Hydrology*, 319(1–4): 176-198.

Lopes, C.L., Silva, P.A., Dias, J.M., Rocha, A., Picado, A., Plecha, S. and Fortunato, A.B. (2011). Local sea level change scenarios for the end of the 21st and potential physical impacts in the lower Ria de Aveiro (Portugal). *Continental Shelf Research*, 31(14): 1515-1526.

Lopes, C.L., Azevedo, A. and Dias, J.M. (2013a). Flooding assessment under sea level rise scenarios: Ria de Aveiro case study. *Journal of Coastal Research*, SI65: 766-771.

Lopes, C.L., Plecha, S., Silva, P. and Dias, J.M. (2013b). Influence of morphological changes in a lagoon flooding extension: case study of Ria de Aveiro (Portugal). *Journal of Coastal Research*, SI65: 1158-1163.

Lumborg, U. and Windelin, A. (2003). Hydrography and cohesive sediment modelling: application to the Rømø Dyb tidal area. *Journal of Marine Systems*, 38(3-4): 287-303.

Manning, A.J. and Bass, S.J. (2006). Variability in cohesive sediment settling fluxes: observations under different estuarine tidal conditions. *Marine Geology*, 235(1-4): 177-192.

Manning, A. and Dyer, K. (2007). Mass settling flux of fine sediments in Northern European Estuaries: Measurements and predictions. *Marine Geology*, 245(1-4): 107-122.

Manning, A., Friend, P.L., Prowse, N. and Amos, C.L. (2007). Estuarine mud flocculation properties determined using an annular mini-flume and the LabSFLOC system. *Continental Shelf Research*, 27(8): 1080-1095.

Mantovanelli, A. and Ridd, P.V. (2006). Devices to measure settling velocity of cohesive sediment aggregates: a review of the in situ technology. *Journal of Sea Research*, 56(3): 199-226.

Mantovanelli, A. and Ridd, P.V. (2008). SEDVEL: An underwater balance for measuring in situ settling velocities and suspended cohesive sediment concentrations. *Journal of Sea Research*, 60(4): 235-245.

Marinheiro, J.M.S. (2008). *Assoreamento da Ria de Aveiro: Causas e Soluções*. MSc. Thesis, Universidade de Aveiro, 136p.

Markussen, T.N. and Andersen, T.J. (2013). A simple method for calculating in situ floc settling velocities based on effective density functions. *Marine Geology*, 344: 10-18.

Martins, F., Leitão, P., Silva, A. and Neves, R. (2001). 3D modelling in the Sado estuary using a new generic vertical discretization approach. *Oceanologica Acta*, 24(1): 51-62.

Martins, V., Dubert, J., Jouanneau, J.M., Weber, O., Silva, E.F., Patinha, C., Dias, J.A. and Rocha, F. (2007). A multiproxy approach of the Holocene evolution of shelf–slope circulation on the NW Iberian Continental Shelf. *Marine Geology*, 239(1-2): 1–18.

Martins, V., Jesus, C.C., Abrantes, I., Dias, J.M. and Rocha, F. (2009). Suspended particule matter vs bottom sediments in a mesotidal lagoon (Ria de Aveiro, Portugal). *Journal of Coastal Resarch*, SI 56: 1370-1374.

Martins, V., Grangeia, C., Jesus, C.C., Martins, P., Laut, L.M., Sequeira, C., Dias, J.M., Silva, P.A., Abrantes, I., Ferreira da Silva, E. and Rocha, F. (2011). Erosion and accretion in the Ria de Aveiro inlet (N Portugal) and exportation of the fine-grained sediments to the shelf. *Journal of Iberian Geology*, 37(2): 215-230.

Martins, V., Mane, M., Frontalini, F., Santos, J., Sobrinho da Silva, F., Terroso, D., Miranda, P., Figueira, R., Laut, L., Bernardes, C., Filho, J., Coccioni, R., Alveirinho Dias, J. and Rocha, F. (2015). Early diagenesis and clay mineral adsorption as driving factors of metal pollution in sediments: the case of Aveiro Lagoon (Portugal). *Environmental Science and Pollution Research*, 22(13): 10019-10033.

Mayerle, R., Narayanan, R., Etri, T. and Wahab, A. (2015). A case study of sediment transport in the Paranagua Estuary Complex in Brazil. *Ocean Engineering*, 106: 161-174.

Meehl, G., Stocker, T.F., Collins, W.D., Friedlingstein, P., Gaye, A.T., Gregory, J.M., Kitoh, A., Knutti, R., Murphy, J.M., Noda, A., Raper, S.C.B., Watterson, I.G., Weaver,A.J. and Zhao, Z.C. (2007). Global Climate Projections. In: Solomon, S., Qin, D., Manning, M., Chen, Z., Marquis, M., Averyt, K.B., Tignor, M. and Mille, H.L. (Eds.), *Climate change 2007: The Physical Science Basis: Contribution of working group I to the 4th Assessment Report of the Intergovernmental Panel on Climate Change*. Cambridge, 747-846.

Merwade, V., Maidment, D.R. and Goff, J.A. (2006). Anisotropic considerations while interpolating river channel bathymetry. *Journal of Hydrology*, 331(3-4): 731-741.

Metha, A.J., Hayter, E.J., Parker, W.R., Krone, R.B. and Teeter, A.M. (1989). Cohesive Sediment Transport. I: Process Description. *Journal of Hydraulic Engineering*, 115(8): 1076-1093.

Molinaroli, E., Guerzoni, S., Sarrreta, A., Masiol, M. and Pistolato, M. (2009). Thirty-year changes (1970 to 2000) in bathymetry and sediment texture recorded in the Lagoon of Venice sub-basins, Italy. *Marine Geology*, 258(1-4): 115-125.

Morehead, M.D., Syvitski, J.P., Hutton, E.W.H. and Peckham, S.D. (2003). Modeling the temporal variability in the flux of sediment from ungauged river basins. *Global and Planetary Change*, 39(1-2): 95-110.

Moreira, M.H., Queiroga, H., Machado, M.M. and Cunha, M.R. (1993). Environmental gradients in a southern Europe estuarine system: Ria de Aveiro, Portugal implications for soft bottom macrofauna colonization. *Netherland Journal of Aquatic Ecology*, 27(2): 465-482.

Morton, R., Ward, G. and White, W. (2000). Rates of sediment supply and sea-level rise in a large coastal lagoon. *Marine Geology*, 167(3-4): 261-284.

Moskalski, S. and Torres, R. (2012). Influences of tides, weather and discharge on suspended sediment concentration. *Continental Shelf Research*. 37: 36-45.

Nicholson, J., O'Connor, B.A. (1986). Cohesive sediment transport model. *Journal of Hydraulic Engineering*, 112(7): 621 -640.

Oliveira, A., Fortunato, A.B. and Dias, J.M. (2006). Numerical modeling of Ria de Aveiro inlet dynamics. In: Smith, J.D. (Ed.), *Proceedings of 30th International Conference on Coastal Engineering*, Vol. 4, 3282-3294.

Pawlowicz, R., Beardsley, B. and Lentz, S. (2002). Classical tidal harmonic analysis including error estimates in MATLAB using T TIDE. *Computers and Geosciences*, 28(8): 929–937.

Parchure, T.M. and Metha, A. (1985). Erosion of soft cohesive sediment deposits. *Journal of Hydraulic Engineering*, 11(10): 1308-1326.

Partheniades, E. (1965). Erosion and deposition of cohesive soils. *ASCE Journal of Hydraulic Division*, 91(1): 105-139.

PBV (2002). *Plano de bacia hidrográfica do Rio Vouga*. Relatório do Plano.

PBVML (2012). *Plano de gestão das bacias hidrográficas dos Rios Vouga, Mondego e Lis. Relatório técnico para efeitos de participação pública*. Administração Hidrográfica da Região Centro, 390 p.

Pereira, M.E., Duarte, A.C., Millward, G.E., Vale, C. and Abreu, S.N. (1998). Tidal export of particulate mercury from the most contaminated area of Aveiro's Lagoon, Portugal. *Science of The Total Environment*, 213(1-3): 157-163.

Pereira, M.E., Libellø, A.I., Pato, P., Válega, M., Coelho, J.P., Lopes, C.B., Rodrigues, S., Cachada, A., Otero, M., Pardal, M.A. and Duarte, A.C. (2009). Mercury pollution in Ria de Aveiro (Portugal): a review of the system assessment. *Environmental Monitoring and Assessment*, 155(1): 39-49.

Picado, A., Dias, J.M. and Fortunato, A.B. (2009). Effect of flooding the salt pans in the Ria de Aveiro. *Journal of Coastal Research*, SI56: 1395-1399.

Picado, A., Dias, J.M. and Fortunato, A.B. (2010). Tidal changes in estuarine systems induced by local geomorphologic modifications. *Continental Shelf Research*, 30(17): 1854-1864.

Picado, A., Silva, P. A., Fortunato, A.B. and Dias, J.M. (2011a). Particle tracking-modeling of morphologic changes in the Ria de Aveiro. *Journal of Coastal Resarch*, SI64: 1560-1564.

Picado, A., Lopes, C. and Dias, J.M. (2011b). Alterações hidrodinâmicas na Ria de Aveiro – Cenários futuros. In: Almeida, A., Alves, F., Bernardes, C., Dias, J., Gomes, N., Pereira, E., Queiroga, H., Serôdio, J., Vaz, N. (Eds.), *Actas das Jornadas da Ria de Aveiro 2011*. Aveiro, Universidade de Aveiro, CESAM – Centro de Estudos do Ambiente e do Mar, 115-122.

Picado, A., Lopes, C., Mendes, R., Vaz, N. and Dias, J.M. (2013). Storm surge impact in the hydrodynamics of a tidal lagoon: the case of Ria de Aveiro. *Journal of Coastal Research*, SI65: 796-801.

Plecha, S. (2011). *Contribution to the study of the Ria de Aveiro inlet morphodynamics*. PhD Thesis, Universidade de Aveiro, 195 p.

Plecha, S., Rodrigues, S., Silva, P., Dias, J.M., Oliveira, A. and Fortunato, A.B. (2007). Trends of bathymetric variations at a tidal inlet. In: Dohmen-Janssen, C.M., Hulscher, S.J.M.H, *River, Coastal and Estuarine Morphodynamics (RCEM2007)*. Netherlands, Taylor & Francis, 19-23.

Plecha, S., Picado, A., Chambel-Leitão, P., Dias, J.M. and Vaz, N. (2014). Study of suspended sediment dynamics in a temperate coastal lagoon: Ria de Aveiro (Portugal). *Journal of Coastal Research*, SI 70: 604-609.

Pont, D., Simmonet, J.P. and Walter, A.V. (2002). Medium-term changes in suspended sediment delivery to the ocean: consequences of catchment heterogeneity and river management (Rhône river, France). *Estuarine, Coastal and Shelf Science*, 54(1):1-18.

Portela, L. and Brito, F. (2009). *Coluna de sedimentação. Velocidade de queda de sedimentos do Esteiro dos Frades, Ria de Aveiro*. Techical Report 350/2009-NEC, National Laboratory of Civil Engineering, LNEC, Lisboa, 30 p.

Portela, L., Coelho, C., Costa, S. and Freire, P. (2011). Hydrodynamic and sedimentary characteristics of a small tidal channel in the Ria de Aveiro. *Journal of Coastal Research*, SI 64: 1629-1632.

Portela, L. and Neves, R. (1994). Numerical modelling of suspended sediment transport in tidal estuaries: a comparison between the Tagus (Portugal) and the Scheldt (Belgium-the Netherlands). *Netherland Journal of Aquatic Ecology*, 28(3): 329-335.

Portela, L., Ramos, S. and Trigo-Teixeira, A. (2013). Effect of salinity on the settling velocity of fine sediments of a harbour basin. *Journal of Coastal Research*, SI 65: 1188-1193.

Rao, V.P., Shynu, R., Kessarkar, P.M., Sundar, D., Michael, G.S., Narvekar, T., Blossom, V. and Mehra, P. (2011). Suspended sediment dynamics on a seasonal scale in the Mandovi and Zuari estuaries, central west coast of India. *Estuarine, Coastal and Shelf Science*, 91(1): 78-86.

Ravens, T. and Sindelar, M. (2008). Flume test section length and sediment erodibility. *Journal of Hydraulic Engineering*, 134(10): 1503-1506.

Rocha, F., Silva, E., Bernardes, C., Vidinha, J. and Patinha, C. (2005). Chemical and minerological characterization of the sediments from the Mira, Ílhavo and Ovar Channels of the Aveiro Lagoon. *Ciencias Marinas*, 1B(31): 253-263.

Roy, N.G. and Sinha, R. (2014). Effective discharge for suspended sediment transport of the Ganga river and its geomorphic implication. *Geomorphology*, 227: 18-30.

Sanchez, M. (2005). Settling velocity of the suspended sediment in three high-energy environments. *Ocean Engineering*, 33(5-6): 665-678.

Sarreta, A., Pillon, S., Molinarolli, E., Guerzoni, S. and Fontolan, G. (2010). Sediment budget in the Lagoon of Venice, Italy. *Continental Shelf Research*, 30(8): 934-949.

Schaff, E., Grenz, C., Pinazo, C. and Lansard, B. (2006). Field and laboratory measurements of sediment erodibility: a comparison. *Journal of Sea Research*, 55(1): 30-42.

Sener (2012). *Elaboração dos estudos da evolução e da dinâmica costeira e estuarina, de mobilidade e navegabilidade na laguna e de reforço de margens pela recuperação de diques e motas com vista à prevenção de riscos, Estudo 1 – Estudo da evolução e da dinâmica costeira e estuarina, Relatório 4 - Modelação da hidrodinâmica e da dinâmica sedimentar, cenários evolutivos*. Relatório para a Polis Litoral Ria de Aveiro, 1012 p.

Shen, X. and Maa, J.P.Y. (2015). Modeling floc size distribution of suspended cohesive sediments using quadrature method of moments. *Marine Geology*, 359: 106-119.

Shrestha, P.L. (1996). Aggregation of cohesive sediments by internal shear rates with application to sedimentation. *Environment International*, 22(6): 717-721.
Shrestha, P.L., Blumberg, A.L. (2005). Cohesive sediment transport. In: Shwartz, M.L. (Eds.), *Encyclopedia of Earth Science Series*. Netherlands, Springer, 327-330.

Silva, J.F (1994). *Circulação da água na Ria de Aveiro, contribuição para o estudo da qualidade da água*. PhD Thesis, Universidade de Aveiro, 167 p.

Silva, A. and Leitão, P. (2011). Simulação da evolução das condições hidromorfológicas da barra da Ria de Aveiro e respectivos impactes no prisma de maré. In: Almeida, A., Alves, F., Bernardes, C., Dias, J., Gomes, N., Pereira, E., Queiroga, H., Serôdio, J., Vaz, N. (Eds.), *Actas das Jornadas da Ria de Aveiro 2011*. Aveiro, Universidade de Aveiro, CESAM – Centro de Estudos do Ambiente e do Mar, 30-36.

Silva, J.F. and Duck, R.W. (2001). Historical changes of bottom topography and tidal amplitude in the Ria de Aveiro, Portugal - trends for future evolution. *Climate Research*, 18(1-2): 17-24.

Silva, J.F. and Oliveira, F. (2005). *The eutrophication in the river Vouga basin – impacts on the quality of water for public supply*. The 4th Inter-Celtic Colloquium in Hydrology and Management of Water Resources, Guimarães, Portugal, 11 p.

Son Le, V., Yamashita, T., Okunishi, T., Shinohara, R. and Miyatakei, M. (2006). Characteristics of suspended sediment material transport in the Ishikari Bay in snowmelt season. *Applied Ocean Research*, 28(4): 275-289.

Sousa, M.C. and Dias, J.M. (2007). Hydrodynamic model calibration for a mesotidal lagoon: the case of Ria de Aveiro (Portugal). *Journal of Coastal Resarch*, SI 50: 1075 - 1080.

Soulsby, R.L, Manning, A.J., Spearman, J. and Whitehouse, R.J.S. (2013). Settling velocity and mass settling flux of flocculated estuarine sediments. *Marine Geology*, 339: 1-12.

Stefanova, A., Krysanova, V., Hesse, C. and Lillebø, A.I. (2015). Climate change impact assessment on water inflow to a coastal lagoon: the Ria de Aveiro watershed, Portugal. *Hydrological Sciences Journal*, 60(5): 929-948.

Teisson, C. (1991). Cohesive suspended sediment transport: feasibility and limitations of numerical modeling. *Journal of Hydraulic Research*, 29(6): 755-769.

Teixeira, S. (1994). *Dinâmica morfosedimentar da Ria de Aveiro, Portugal*. PhD Thesis, Universidade de Lisboa, 396 p.

Temmerman, S., Goversa, G., Meireb, P. and Wartelc, S. (2003). Modelling long-term tidal marsh growth under changing tidal conditions and suspended sediment concentrations, Scheldt estuary, Belgium. *Marine Geology*, 193(1-2): 151-169.

Tóth B. and Bódis, E. (2015). Estimation of suspended loads in the Danube River at Göd (1668 river km), Hungary. *Journal of Hydrology*, 523: 139-146.

Valentim, J.M., Vaz, L., Vaz, N., Silva, H., Duarte, B., Caçador, I. and Dias, J.M. (2013). Sea level rise impact in residual circulation in Tagus estuary and Ria de Aveiro Lagoon. *Journal of Coastal Research*, SI65: 1981-1986.

Van Der Weijden, C.H. and Pacheco, F.A.L. (2006). Hydrogeochemistry in the Vouga River basin (central Portugal): pollution and chemical weathering. *Applied Geochemistry*, 21(4): 580–613.

Van Ledden, M., Kesteren, W. and Winterwerp, J. (2004). A conceptual framework for the erosion behaviour of sand-mud mixtures. *Continental Shelf Research*, 24(1): 1-11.

Van Leussen, W. (1999). The variability of settling velocities of suspended fine-grained sediment in the Ems estuary. *Journal of Sea Research*, 41(1-2): 109- 118.

Van Leussen, W. (2011). Macroflocs, fine-grained sediment transports, and their longitudinal variations in the Ems Estuary. *Ocean Dynamics*, 61(2): 387-401.

Vaz, N. (2007). *Study of heat and salt transport processes in the Espinheiro Channel (Ria de Aveiro)*. PhD Thesis, Universidade de Aveiro, 151 p.

Vaz, N. and Dias, J.M. (2008). Hydrographic characterization of an estuarine tidal channel. *Journal of Marine Systems*, 70(1-2): 168-181.

Vaz, N. and Dias, J.M. (2011). Cross sectional and stratification patterns induced by tidal and river discharge changes in a tidal channel: a modeling study. *Journal of Coastal Research*, SI 64: 1614-1618.

Vaz, N., Dias, J.M., Leitão, P.C. and Nolasco, R. (2007). Application of the Mohid-2D model to a mesotidal temperate coastal lagoon. *Computers and Geosciences*, 33: 1204-1209.

Vaz, N., Dias, J.M. and Leitão, P.C. (2009). Three-dimensional modelling of a tidal channel: The Espinheiro Channel (Portugal). *Continental Shelf Research*, 29(1): 29-41.

Volpe, V., Silvestri, S. and Marani, M. (2011). Remote sensing retrieval of suspended sediment concentration in shallow waters. *Remote Sensing of Environment*, 115(1): 44-54.

Walling, D.E. and Fang, D. (2003). Recent trends in the suspended sediment loads of the world's rivers. *Global and Planetary Change*, 39(1-2): 111-126.

Wan, Y., Wu, H., Roelvinkb, D. and Gua, F. (2015). Experimental study on fall velocity of fine sediment in the Yangtze Estuary, China. *Ocean Engineering*, 103: 180-187.

Wang, H, Bi, N., Saito, Y., Wang, Y., Sun, X., Zhang, J. and Yang, Z. (2010). Recent changes in sediment delivery by the Huanghe (Yellow river) to the sea: causes and environmental implications in its estuary. *Journal of Hydrology*, 391(3-4): 302-313.

Wass, P.D, Marksb, S.D., Finchc, J.W., Leeksc, G.J.L. and Ingramd, J.K. (1997). Monitoring and preliminary interpretation of in-river turbidity and remote sensed imagery for suspended sediment transport studies in the Humber catchment. *Science of the Total Environment*, 194-195: 263-283.

Wentworth, C. (1922). A scale of grade and class terms for clastic sediments. *The Journal of Geology*, 30(5): 377-392.

Whitehouse, R., Soulsby, R., Roberts, W. and Mitchener, H. (2000). *Dynamic of estuarine muds*. London, Thomas Telford, 210 p.

Wilkinson, S.N., Dougall, C., Kinsey-Henderson, A.E., Searle, R.D., Ellis, R.J. and Bartley, R. (2014). Development of a time-stepping sediment budget model for assessing land use impacts in large river basins. *Science of the Total Environment*, 468-469: 1210-1224.

Winterwerp, J.C. (2002). On the flocculation and settling velocity of estuarine mud. *Continental Shelf Research*, 22(9): 1339-1360.

Winterwerp, J.C., Manning, A.J., Martens, C, Mulder, T. and Vanlede, J. (2006). A heuristic formula for turbulence-induced flocculation of cohesive sediment. *Estuarine, Coastal and Shelf Science*, 68(1-2): 195-207.

Winterwerp, J.C and Van Kesteren, W.G.M. (2004). *Introduction to the physics of cohesive sediment in the marine environment*. Amesterdan, Elsevier, 576 p.

Worrall, F., Burt, T.P. and Howden, N.J.K. (2013). The flux of suspended sediment from the UK 1974 to 2010. *Journal of Hydrology*, 504(11): 29-39.

Xie, D.F., Gao, S., Wang, Z.B. and Pan, C.H. (2013). Numerical modeling of tidal currents, sediment transport and morphological evolution in Hangzhou Bay, China. *International Journal of Sediment Research*, 28(3): 316-328.

You, Z. (2004). The effect of suspended sediment concentration on the settling velocity of cohesive sediment in quiescent water. *Ocean Engineering*, 31(16): 1955-1965.